

**UCLA**

**UCLA Electronic Theses and Dissertations**

**Title**

Investigation and Characterization of Small Molecule Modulators for Mitochondrial Processing Peptidase

**Permalink**

<https://escholarship.org/uc/item/9th259gj>

**Author**

Douglas, Colin Joseph

**Publication Date**

2014

Peer reviewed|Thesis/dissertation

UNIVERSITY OF CALIFORNIA

Los Angeles

Investigation and Characterization of Small Molecule Modulators

For Mitochondrial Processing Peptidase

A dissertation submitted in partial satisfaction of the

requirements for the degree Doctor of Philosophy

in Biochemistry and Molecular Biology

by

Colin Joseph Douglas

2014

© Copyright by  
Colin Joseph Douglas  
2014

## ABSTRACT OF THE DISSERTATION

### Investigation and Characterization of Small Molecule Modulators For Mitochondrial Processing Peptidase

by

Colin Joseph Douglas

Doctor of Philosophy in Biochemistry and Molecular Biology

University of California, Los Angeles, 2014

Professor Carla M. Koehler, Chair

Mitochondria are an extremely complex organelle comprised of four discrete compartments and are vital for the proper functioning of key cellular pathways including, energy production, growth, differentiation, and cellular signaling. The mitochondrial genome encodes for 13 proteins, however the mitochondrial proteome is estimated to contain approximately 600–1000 proteins; most of these must be imported from the cytosol. Depending on a protein's intended location, there are host signals and import machinery that ensure the correct appropriate localization. Proteins destined for the mitochondrial matrix typically possess a mitochondrial targeting sequence (MTS) found at the N-terminus. These proteins are funneled through the translocon of the outer membrane (TOM complex), the translocon of the inner membrane

(TIM23 complex) into the matrix. Here, the MTS is cleaved off by mitochondrial processing peptidase (MPP), allowing the mature protein to fold into its native confirmation.

Many proteins, such as MPP, are essential for life, therefore it is difficult to study them using classical approaches or through methods such as RNAi as these may cause global side-effects and take a great deal of time for effect manifestation. As such, our lab devises ways to bypass these issues through the development of small molecule modulators for our proteins of interest. For MPP, this was accomplished through a high-throughput screen (HTS) of approximately 130,000 compounds at UCLA's CNSI screening center.

We focused on 2 molecules resulting from the screen, MitoBloCK-50 and -51, which were found to be inhibitors of MPP. Both compounds possess many similarities in the effects we see via MPP inhibition including cleavage of Su9-DHFR, import of Su9-DHFR, import of Cpn10, hPink1 import, and the import of CytB<sub>2</sub>-DHFR (1-167). Conversely, we also saw differences in their inhibition of MPP and their effect on downstream pathways including, the import of CytC<sub>1</sub>, the import of CytB<sub>2</sub>-DHFR (A63P), Parkin recruitment on the surface of mitochondria, and zebrafish development. These similarities and differences between the 2 MitoBloCK compounds could signify differences in their binding and inhibition of MPP, and these differences result in slightly different downstream effects. Overall, we have discovered and initiated the characterization of two MPP inhibitors and their respective analogs, potentially helping to elucidate the Pink1-Parkin mitochondrial degradation pathway and the pathways involved in copper metabolism, melanogenesis, and melanin formation.

The dissertation of Colin Joseph Douglas is approved.

Catherine F. Clarke

Alexander M. van der Blik

Carla M. Koehler, Committee Chair

University of California, Los Angeles

2014

## DEDICATION PAGE

This dissertation is dedicated to my family and Monkmonk for all of their support, love, encouragement, and guidance (if only through memory, my beloved Monkmonk). You instilled in me the belief I could accomplish anything I wanted, and because of that here we are today.

## TABLE OF CONTENTS

<b>CHAPTER 1: AN INTRODUCTION INTO MITOCHONDRIAL BIOLOGY, HIGH-THROUGHPUT SCREENING, AND THE ELUCIDATION OF SMALL MOLECULE MODULATORS .....</b>	<b>1</b>
<b>CHAPTER 2: DEVELOPMENT AND IMPLEMENTATION OF A HIGH-THROUGHPUT SCREEN FOR MITOCHONDRIAL PROCESSING PEPTIDASE.....</b>	<b>16</b>
<b>CHAPTER 3: CHARACTERIZATION OF MITOBLOCK-50 .....</b>	<b>68</b>
<b>CHAPTER 4: CHARACTERIZATION OF MITOBLOCK-51 .....</b>	<b>123</b>
<b>CHAPTER 5: COMPARISON OF MITOBLOCK-50 AND MITOBLOCK-51 .....</b>	<b>175</b>
<b>APPENDIX A: HIT COMPOUNDS FROM HTS.....</b>	<b>186</b>
<b>APPENDIX B: DATA MINED NEGATIVE SARS FOR MITOBLOCK-50.....</b>	<b>189</b>
<b>APPENDIX C: DATA MINED NEGATIVE SARS FOR MITOBLOCK-51.....</b>	<b>193</b>
<b>APPENDIX D: MB 50 NOMENCLATURE FOR PUBLISHED DATA .....</b>	<b>195</b>
<b>APPENDIX E: MB 51 NOMENCLATURE FOR PUBLISHED DATA.....</b>	<b>198</b>



## LIST OF FIGURES

Figure 1.1 The Respiratory Complexes of the Electron Transport Chain (ETC) in Mitochondria. .....	23
Figure 1.2 Mitochondrial Protein Import.....	25
Figure 1.3 Import of Precursor Proteins into the Mitochondrial Matrix.....	27
Figure 1.4 Examples of MPP and IMP Cleavage Motifs.....	29
Figure 1.5 Model for MPP Cleavage of Substrate within the Active Site Cavity. ....	31
Figure 1.6 Stages of Embryonic Development. ....	2
Figure 2.1 Overall schematic flow-chart for MPP HTS. ....	37
Figure 2.2 Examples of MPP and IMP Cleavage Motifs.....	39
Figure 2.3 MPP Cleavage of YDHA7 and PNPase Synthetic Peptides. ....	40
Figure 2.4 Model of JPT Fluorogenic Peptide Assay.....	41
Figure 2.5 Pre-Screen MPP/JPT Fluorogenic Peptide Assay. ....	42
Figure 2.6 Layout for HTS Plates & Sequence for Dispensing of Solutions and Compounds. ...	44
Figure 2.7 Statistics for HTS for MPP cleavage of JPT Fluorogenic Peptide.....	46
Figure 2.8 Small Molecules Ordered from MPP HTS.....	49
Figure 2.9 IC <sub>50</sub> Data for MPP inhibitors.....	50
Figure 2.10 DiS-C <sub>3</sub> Assay for MPP Small Molecule 199.....	51
Figure 2.11 MPP Cleavage of [ <sup>35</sup> S] Su9-DHFR with Drugs & EDTA. ....	53
Figure 2.12 [ <sup>35</sup> S] Su9-DHFR Import into Purified Yeast Mitochondria. ....	56
Figure 2.13 [ <sup>35</sup> S] AAC Import into Purified Yeast Mitochondria. ....	58
Figure 2.14 Recombinant MPP Cleavage of [ <sup>35</sup> S] PINK1.....	59
Figure 2.15 [ <sup>35</sup> S] hPink1 Import into Purified Yeast Mitochondria. ....	61

Figure 3.1 Parkin recruitment on the surface of EGFP-Parkin Expressing HeLa Cells. ....	91
Figure 3.2 MIC <sub>50</sub> of MB 50 in HEK Cells and Mitochondrial Morphology in HeLa Cells. ....	93
Figure 3.3 Structures of MB 50 and a Selection of its Analogs. ....	95
Figure 3.4 <i>In-Vitro</i> Cleavage of [ <sup>35</sup> S] Su9-DHFR by Recombinant MPP with MB 50 and Negative Analogs. ....	96
Figure 3.5 [ <sup>35</sup> S] Su9-DHFR import into GA74 Mitochondria with MB 50 and Analogs. ....	98
Figure 3.6 Titration of MB 50 with the Import of [ <sup>35</sup> S] Su9-DHFR into GA74 Mitochondria. ....	99
Figure 3.7 CytC <sub>1</sub> , CytB <sub>2</sub> -DHFR (1-167), and CytB <sub>2</sub> -DHFR (A63P) import into GA74 Mitochondria with MB 50. ....	101
Figure 3.8 Frataxin and Cpn10 Import into GA74 Mitochondria with MB 50 Treatment. ....	103
Figure 3.9 Import and Titration of hPink1 into GA74 Mitochondria and MB 50. ....	105
Figure 3.10 Parkin Recruitment in EGFP-Parkin Expressing MTS dsRed HeLa MTS with Quantification. ....	107
Figure 3.11 Comparison of [ <sup>35</sup> S] Su9-DHFR in GA74 and MAS1 ts Mitochondria with MB 50 Treatment. ....	108
Figure 3.12 Zebrafish Treatment with MB 50. ....	110
Figure 3.13 Zebrafish Treated with MB 50, Bathocuproine, and PTU for 3 Days and then Wash- out for 2 Days. ....	112
Figure 3.14 Zebrafish Treated with MB 50 and its analogs. ....	114
Figure 4.1 Pink1 Accumulation with Concurrent Treatment of CCCP and MB 51. ....	144
Figure 4.2 MIC <sub>50</sub> of MB 51 in HEK Cells and Mitochondrial Morphology in HeLa Cells. ....	146
Figure 4.3 Structures of MB 51 and a Selection of its Analogs. ....	148

Figure 4.4 In-Vitro Cleavage of [ <sup>35</sup> S] Su9-DHFR by Recombinant MPP with MB 51 and analogs. ....	149
Figure 4.5 [ <sup>35</sup> S] Su9-DHFR import into GA74 Mitochondria with MB 51 and Analogs. ....	151
Figure 4.6 Titration of MB 51 with the Import of [ <sup>35</sup> S] Su9-DHFR into GA74 Mitochondria..	152
Figure 4.7 CytC <sub>1</sub> , CytB <sub>2</sub> -DHFR (1-167), and CytB <sub>2</sub> -DHFR (A63P) import into GA74 Mitochondria with MB 51. ....	154
Figure 4.8 Frataxin and Cpn10 Import into GA74 Mitochondria with MB 51 Treatment. ....	156
Figure 4.9 Import and Titration of hPink1 into GA74 Mitochondria and MB 51. ....	158
Figure 4.10 Parkin Recruitment in EGFP-Parkin Expressing MTS dsRed HeLa MTS with Quantification. ....	160
Figure 4.11 Comparison of [ <sup>35</sup> S] Su9-DHFR in GA74 and MAS1 ts Mitochondria with MB 51 Treatment. ....	161
Figure 4.13 Zebrafish Treated with MB 50, Bathocuproine, and PTU for 3 Days and then Wash-out for 2 Days.....	165
Figure 4.14 Zebrafish Treated with MB 50 and its analogs. ....	167
Figure 5.1 Comparison of MB 50 and 51 with import of CytC <sub>1</sub> , CyB <sub>2</sub> -DHRF (1-167) and CytB <sub>2</sub> -DHFR (A63P). ....	180
Figure 5.2 Comparison of MB 50 and MB 51 with Pink1 Import in Conjunction with Carbonate Extraction.....	181
Figure 5.3 Comparison of MB 50 and MB 51 with Parkin Recruitment on EGFP Parkin Expressing HeLa Cells.....	182
Figure 5.4 Comparison of MB 50 & 51 Treatment with Zebrafish. ....	183

## ACKNOWLEDGMENTS

Firstly, I would like to especially thank my mentor, Carla M. Koehler for her guidance and support throughout my tenure as a graduate student. This project allow me to grow as a scientist and gain new knowledge in the areas of protein import, mitochondrial function, and high-throughput screening, while at the same utilizing my organic chemistry background. It has been a privilege to work under, and be trained by, her. I also extend my gratitude to the other members of my committee: Catherine F. Clarke, Michael A. Teitell, Alexander M. van der Blik, and Jorge Z. Torres, for their encouragement along the way.

I thank the Cell and Molecular Biology Training Grant (Ruth L. Kirschstein National Research Service Award GM007185) for funding and supporting this work. I also would like to extend my appreciation to Samuel A. Hasson, Deepa V. Dabir, Meghan E. Johnson, Non Miyata and Juwina Wijaya for their help, guidance, and teaching ability during various stages of my graduate project.

I would like to thank Meghan E Johnson, Non Miyata, Juwina Wijaya and Eric Torres for their contributions to the work presented in this dissertation. Chapter 1 contains Figure 1.6 that was used with permission from Meghan E. Johnson for reference purposes. Non Miyata helped provide preliminary data for MPP cleavage of Pink1, Parkin recruitment with MB 50 treatment and Pink1 accumulation following MB 51 treatment. Juwina Wijaya provided the data from the EGFP Parkin expressing HeLa cell experiment and Eric Torres provided the data from frataxin import and the MAS1 ts mitochondria experiment.

I would like to thank both the current and former members of the Koehler Nation: Deepa Dabir, Non Miyata, Esther Nuebel, Janos Steffen, Geng Wang, Yavuz Oktay, Samuel Hasson, Sonya Neal, Juwina Wijaya, Matthew Maland, Eriko Shimada, Moses Liao, Tanya Hioe, Justin

Hotter, Samuel Irving, Cennyanna Boon, Sravya Keremane, Eric Torres, Jisoo Han, Mike Conti, Jesmine Cheung, Christina Jayson, Fatimah Badran, Gary Shmorgon, and Jonathan Kwon.

Thank you for your assistance and technical knowledge during experiments, for your discussions of results, for providing materials, and most importantly your friendship. I would also like to thank Robert Damoiseaux and the rest of the CNSI screening lab for all your help and advice during the screening of MPP. Your expertise was invaluable and much appreciated.

I would like to give a special thanks to Arlene Russell for always providing an open door and a willingness to listen to a graduate student's problems and questions. I need to also extend a huge thank you to my close friends Tioga Martin, Courtney Thomas, Larissa Charnsangavej, Evan & Kim Martin (plus there two amazing children Caleb and Hayden) and Jason Nellis for always being there to provide motivation, support, and guidance through this entire process. An extra special thank you needs to be given to Meghan Johnson, without her this would have never been possible. She was there for me during all the ups and downs and always had my back even when I did not have it myself. Finally I need to thank my family: Sue Walker, Jeff Douglas, Meredith Douglas and Bob Walker – this is a culmination of everything you have done for me, with me, and poured your love into over all these years. I could not even begin to list all things you have done to make this possible (it would be a long list and this thesis is already long enough) but know that I would not be who I am, or have made it to this point, without your love and support.

## VITA

- 2006 B.S. in Biochemistry; B.A. in Psychology  
University of Carolina at Greensboro  
Greensboro, North Carolina
- 2007 M.S. in Nutrition  
Columbia University  
New York, New York
- 2008 M.S. in Organic Chemistry  
University of California, Los Angeles  
Los Angeles, California
- 2008 Teaching Assistant  
Department of Chemistry and Biochemistry  
University of California Los Angeles  
Los Angeles, California
- 2009 Diploma of Higher Education with Distinction in Medical  
Sciences  
St. George's University Medical School & Northumbria  
University  
Newcastle, England
- 2010-2012 Teaching Assistant  
Department of Chemistry and Biochemistry  
University of California Los Angeles  
Los Angeles, California

## PUBLICATIONS AND PRESENTATIONS

Dabir, D. V., Hasson, S. A., Setoguchi, K., Johnson, M. E., Wongkongkathep, P., **Douglas, C. J.**, Zimmerman, J., Damoiseaux, R., Teitell, M. A., and Koehler, C. M. (2013) *Developmental Cell* **25**, 81-92.

Tian, Xia, Alexander D. Hutters, **Colin J. Douglas**, Neil K. Garg. "Concise Synthesis of the Bicyclic Scaffold of N-Methylwelwitindolinone C Isothiocyanate via an Indolyne Cyclization" *Org. Lett.*, 2009; **11**: 2349-2351

**Douglas, C. J.**, Damoiseaux, R., Koehler, C. M. (April 19, 2013) "Identification of Small Molecule Modulators for Mitochondrial Proteases using a High-throughput Screening Method." Presented at *Tri-campus Symposium*. Los Angeles, CA.

**Douglas, C. J.**, Damoiseaux, R., Koehler, C. M. (January 17, 2013) “Identification of Small Molecule Modulators for Mitochondrial Proteases using a High-throughput Screening Method.” Presented at *2013 David S. Sigman Memorial Lecture & Symposium*. Los Angeles, CA.

**Douglas, C. J.**, Damoiseaux, R., Koehler, C. M. (March 11-16, 2012) “Identification of Small Molecule Modulators for Mitochondrial Proteases using a High-throughput Screening Method.” Presented at *Gordon Research Conference: Protein Transport Across Cell Membranes*. Galveston, TX.

**Douglas, C. J.** (January 31, 2012) “Use of a high-throughput screen to discover small molecule modulators of mitochondrial processing peptidase.” Presented at *Cell and Molecular Biology Seminar Series*. Los Angeles, CA.

**Douglas, C. J.**, Damoiseaux, R., Koehler, C. M. (October 16-18, 2011) “Identification of Small Molecule Modulators for Mitochondrial Proteases using a High-throughput Screening Method.” Presented at *Annual Molecular Biology Institute Lake Arrowhead Retreat*. Lake Arrowhead, CA.

**Douglas, C. J.**, Hasson, S. A., Koehler, C. M. (April 16-20, 2011) “Characterization of Small Molecule Inhibitors for the Tim22 Import Pathway.” Presented at *EMBO Conference Series; Protein Transport Systems: Structures, Mechanisms and Medical Aspects*. Santa Margherita di Pula, Italy.

**Douglas, C. J.** (March 2006) “Production of Optically Active Compounds by Enantioselective Protonation Using Lewis Acid-Assisted Chiral Brønsted Acids.” Presented at UNCG annual symposium for senior undergraduate chemistry students. Greensboro, NC.

## AWARDS

2006	UNCG Research Fellowship University of North Carolina at Greensboro Greensboro, North Carolina
2007–2013	University Fellowship University of California Los Angeles Los Angeles, California
2011	Hanson Dow Excellence in Teaching Award Department of Chemistry and Biochemistry University of California Los Angeles Los Angeles, California
2009–2012	Ruth L. Kirschstein National Research Service Award University of California Los Angeles Los Angeles, California

# **Chapter 1: An Introduction into Mitochondrial Biology, High-Throughput Screening, and the Elucidation of Small Molecule Modulators**

## **Abstract**

The mitochondrion is an organelle essential for the viability of most living things. While mitochondria do contain their own genome, it is limited, capable of encoding for only a few genes. As a result, mitochondria have devised pathways for importing the many other proteins required for function into the organelle, and subsequently sorting these proteins into their designated locations. Because the mitochondrion is so necessary for life, many of these proteins are essential, and as such cannot be studied via conical knockdown or knockout methods. To this end, other methods must be devised to transiently affect these proteins for study. Here we discuss these mitochondrial pathways, methods for identifying tools for the ephemeral inhibition of mitochondrial proteins, and the use of zebrafish as an *in vivo* platform for studying mitochondrial biology.



# Introduction

## The Mitochondrion

The mitochondrion is a dual membrane-bound organelle that is present in all vertebrate organisms. It consists of 4 respective compartments that include the outer membrane, the intermembrane space, the inner membrane and the matrix. (1) The mitochondrial proteome is estimated to contain 600–1000 proteins though only a small fraction of these proteins are translated from the mitochondrial genome; the rest are encoded in the nuclear genome and must be imported into the mitochondrion. (2-4)

### *The Mitochondrial Genome and Respiratory Complex*

Most animal mitochondrial genomes consist of approximately 16,000 base pairs and encode 37 genes. These genes products include: 22 tRNAs, 2 rRNAs, 13 proteins, and 1 untranslated region. (5) The mitochondrial human genome is 16,569 base pairs; similarly the mitochondrial genome of zebrafish is 16,596 bases pairs, while that of yeast is 85,779 base pairs. (6-8) All proteins encoded by the mitochondrial genome are subunits that comprise the respiratory chain complex, which is the most notable function of the mitochondrion. (5)

The role of the respiratory chain complex is to carry out oxidative phosphorylation by shuttling electrons generated via catabolic processes through the various protein complexes that encompass the chain. The energy generated from this movement of electrons is harnessed in the production of ATP; the energy source that is absolutely vital for the function of many biological processes (Figure 1.1). The first of these complexes is NADH dehydrogenase (Complex I),

which accepts electrons from NADH and is comprised of 45 polypeptide fragments and 8 iron-sulfur (Fe-S) clusters. (9, 10) Initially the electrons are transferred from NADH to a prosthetic FMN group via a chain of Fe-S clusters, culminating in the electrons being deposited on coenzyme Q. Concurrently, hydrogen ions are translocated from the matrix to the inner membrane; this process is necessary to set-up the proton gradient utilized for ATP production. (11, 12) The next enzyme in the electron transport chain is succinate dehydrogenase (Complex II), which also ultimately deposits its electrons on coenzyme Q. This protein complex consists of 4 subunits that transfer electrons from succinate using the co-factor FAD. (12) Coenzyme Q is fat soluble, making it extremely well suited to transfer electrons through in the inner membrane from the both complex I & II to the cytochrome  $bc_1$  complex (Complex III). Complex III utilizes a pathway know as Q-cycling to pass electrons from coenzyme Q to cytochrome  $c$ . Similar to Complex I, this process also pumps hydrogen ions across the inner membrane. (13) Cytochrome  $c$  then moves electrons through the inner membrane to cytochrome  $c$  oxidase (Complex IV); the next complex within the electron transport chain. (14) Within Complex IV, electrons are transferred from cytochrome  $c$  to molecule oxygen, the final electron acceptor. In this process the final hydrogen ions are transported across the inner membrane. (15) Ultimately, the transport of hydrogen ions back into the matrix is coupled to ATP synthesis via ATP synthase (Complex V). (16)

### *Protein Translocation into the Mitochondrion*

Though ATP production and the electron transport chain are the primary role for the mitochondrion there are many other processes that take place within this organelle, such as the citric acid cycle and lipid oxidation. (17, 18) The proteins required for these processes along

with most of the other proteins that are utilized within the mitochondrion are encoded by the nuclear genome, are translated in the cytosol, and must be transported into the mitochondrion and segregated to their respective compartments. Because there are many proteins requiring import into the mitochondrion, a complex system of translocation and assembly apparatuses are present within the various compartments of the mitochondrion to aid in sorting precursor proteins to the appropriate locations, and to help them fold into the proper conformations upon arrival (Figure 1.2). As pre-proteins are transported in the mitochondrion, the first protein complex that they encounter is the outer membrane translocase (TOM). (19, 20) The TOM complex is made-up of 7 integral membrane proteins (Tom70p, Tom40p, Tom22p, Tom20p, Tom7p, Tom6p, and Tom5p), all of which help pre-proteins cross the outer mitochondrial membrane. (19-22) Those proteins that are destined for the outer membrane or the intermembrane space are segregated and sorted through the sorting and assembly mechanism (SAM complex). This complex consists of 2 proteins, the Sam 50p and Mas37p (Figure 1.2: A). (23-25)

Those proteins destined for the inner membrane or the matrix must not only pass through the TOM complex but must also go through the translocase of the inner membrane (TIM complex). Within the mitochondrion there are 2 TIM complexes: the TIM23 and TIM22 complexes. Those proteins destined for the matrix, which also typically possess a positively charged N-terminal targeting sequence, are processed via the TIM23 complex (Figure 1.2: C). (19, 20) The TIM23 complex is composed of 3 integral membrane proteins: Tim50p, Tim17p, and Tim23p. (19, 20, 26) When examining the function of this complex, Tim50p acts as a guide for incoming precursors, while Tim17p and Tim23p comprise the complex pore. (27) For precursors to traverse the TIM23 complex a membrane potential is essential; Tim44p, Tim14p,

mHsp70 and mGrpE provide this potential. (28) Together these proteins function as the translocation motor and establish the electrophoretic effect required to attract the positively charged N-terminal targeting sequence and allow for precursor processing and integration into the matrix. (29)

Proteins destined for the inner membrane are processed via the TIM22 complex (Figure 1.2: B). (30, 31) The TIM22 complex is made up of 3 integral membrane proteins (Tim54p, Tim22p, and Tim18p), which form a channel that allows precursors to be inserted into the inner membrane. (31-33) Proteins destined for the inner membrane are hydrophobic, lack an N-terminal targeting sequence and require assistance crossing the intermembrane space. (34) These chaperones, the “small Tims,” form 6-membered complexes made-up of 3 subunits of 2 different proteins, and aid inner membrane proteins in traversing the intermembrane space. One complex consists of Tim8p and Tim13p, while the other is comprised of Tim9p and Tim10p. (35-37) Within this family of small Tims, all proteins share a common CX<sub>3</sub>C motif. For import to occur, all 4 thiols must be conserved. (38, 39) If any of the cysteine side-chains are eliminated, import is impaired, and the small Tim complex is improperly assembled. (40)

Unlike the cytosol, which has an overall reducing character, the intermembrane space is an oxidizing environment and is quite redox sensitive. (41) A large percentage of proteins found in the intermembrane space contain disulfide bonds that are vital for their respective biological functions. Examples of such proteins include Cox17p and Cox19p (subunits of the cytochrome *c* oxidase complex), which contain twin CX<sub>9</sub>C motifs. (42, 43) Similar to the small Tims, these proteins must be oxidized to their native state after being imported via the TOM complex before they function properly. In order to keep cysteine-rich proteins in the intermembrane space (like the small Tims) in their active oxidized state, a disulfide relay system exists. This relay (the

Mia40p-Erv1p pathway) is responsible for maintaining the activity of redox-active proteins. (44, 45)

Upon import via the TOM complex, precursors enter the intermembrane space where they encounter Mia40p, which contains 3 disulfide bonds. Two of the disulfide bonds are in the CX<sub>9</sub>C motif and appear to play a structural role, and the other disulfide bonds exists as a CPC triad and is located near the N-terminus. (46) Imported proteins destined for the intermembrane space initially form a transient disulfide exchange with Mia40p, thereby becoming oxidized and folding into their native conformation. (46) After undergoing this disulfide exchange, the redox-active cysteine of Mia40p must then be re-oxidized so that it can take part in the proper folding of additional precursor proteins. Erv1p, a sulfhydryl oxidase found in the mitochondrial intermembrane space, performs the re-oxidation of Mia40p. (41, 42, 47, 48) In addition to be required for the Mia40p-Erv1p pathway to remain functional, Erv1p itself is imported via this pathway and must be oxidized and folded into its active conformation. (49) Following the transfer of electrons from the substrate to Erv1p, the electrons are then shuttled to FAD. (47) Once the FAD has accepted the electrons they are passed to a number of electron acceptors, such as cytochrome *c* (which then donates the electrons to the electron transport chain) or molecular oxygen (which initially forms hydrogen peroxide but is ultimately converted to water using cytochrome *c* peroxidase). (41, 51)

As illustrated, the mitochondrial protein import pathways are of the utmost importance for mitochondrial homeostasis. Along similar lines, the mitochondrial proteolytic system, which functions to ensure the proper assembly and degradation of macromolecular complexes, is also vital for mitochondrial homeostasis. This complex system involves the general proteases Lon and Clp that are found in the matrix, a series of proteases responsible for ensuring the import and

processing of precursors, and a series of proteases required for import, assembly, and degradation of other general mitochondrial proteins. (52-54)

Precursor proteins that contain a targeting sequence, which is typically 20-60 amino acids long, are acted on by proteases that function in removing and degrading the targeting sequence. The first protease to interact with precursors containing the targeting sequence is the mitochondrial processing peptidase (MPP) (Figure 1.3). (53) For those precursors destined for the inter membrane space, a second cleavage of the targeting sequence is conducted by the inner membrane protease (IMP). For a small subset of precursor proteins that are mainly involved in iron-sulfur metabolism, eight additional amino acids are removed from the N-terminus by the mitochondrial intermediate processing peptidase (MIP). (53) Following these cleavages, the targeting sequence that has been removed from the precursor must be degraded; this is done by the processing protease/mammalian metallopeptidase 1 (Prep/MP1). (55-57)

## Mitochondrial Processing Peptidase

Based on its central role in mitochondrial precursor import, it is possible that MPP could play some part in mitochondrial disorders. In 2001, MPP was implicated in the pathogenesis of Friedreich ataxia (FRDA). FRDA is a fairly frequent (1:50,000 live births) autosomal recessive degenerative disorder caused by the dysfunction of frataxin. (58) Like so many mitochondrial proteins, frataxin is initially synthesized in the cytosol with an N-terminal targeting sequence and must be imported into the mitochondrial matrix. (59, 60) It was determined that the precursor of frataxin is cleaved by MPP in two sequential steps, which is extremely rare for MPP cleavage, before it can fold into its mature form in the matrix. (61, 62) When examining the presequence for both yeast and human frataxin, it was found that they are 51 and 55 amino acids respectively.

(63, 64) The presequence of yeast frataxin is cleaved between residues 20-21 and 51-52, while the presequence of human frataxin is cleaved between residues 41-42 and 55-56. (60-64) When examining the two cleavages for human frataxin, it was determined that the first cleavage happened very rapidly, while the second cleavage was much slower and was the rate-determining step for mature frataxin formation. The rate of this second cleavage is further reduced in FRDA patients. (62) The cleavage of frataxin by MPP was found to be inhibited by two of the most frequent point mutations observed in FRDA patients, I154F and G130V. (65)

MPP is a heterodimer that consists of an  $\alpha$  and a  $\beta$  subunit. It is a metalloendopeptidase within the pitrilysin family, which also includes the protease insulin-degrading enzyme. Unlike the typical metalloendopeptidase, MPP does not have the standard zinc-binding motif of HEXxH, but instead possesses an inverted zinc-binding motif, HxxEH. (66) Originally, it was purified from a number of different organisms by independent laboratories; therefore the two subunits have throughout the years been given a number of different names.  $\alpha$ -MPP has been known as MPP-1, MAS2, MIF2, P-55 and cytochrome *c* reductase subunit III, and  $\beta$ -MPP has been known as PEP, MAS1, MIF1, P-52 and cytochrome *c* reductase subunit I and II. (53, 67) As of 1993, the subunits of MPP have been referred to as  $\alpha$ -MPP (the larger subunit) and  $\beta$ -MPP (the smaller subunit). (67)

The original purifications of MPP were done from *Neurospora crassa*, *S. cerevisiae* and rat liver. MPP derived from yeast and mammals are soluble heterodimers that are 100 and 110 kDa respectively. (68, 69) Experimentation has concluded neither of the two subunits ( $\alpha$  or  $\beta$ ) is active by themselves. (70-72) The optimal pH range for purified MPP activity is pH 7-8, with inactivation at lower pH values. MPP is inhibited by EDTA and *o*-phenanthroline and activated by divalent cations ( $\text{Co}^{2+}$ ,  $\text{Mn}^{2+}$ ,  $\text{Zn}^{2+}$  and  $\text{Mg}^{2+}$ ). (73-76) At low metal concentrations the degree

of MPP activation follows this trend,  $Zn^{2+} > Mn^{2+} > Co^{2+}$ ; however unlike cobalt and manganese, excess zinc inhibits MPP activity. (77, 78)

Through the use of  $\alpha$ -MPP and  $\beta$ -MPP temperature-sensitive mutants it was determined that the two subunits of yeast MPP are coded by alleles MAS1/MIF1 and MAS2/MIF2. (68, 79-82) There is roughly 20-30% identity between the sequences of the  $\alpha$ -MPP and  $\beta$ -MPP subunits for any given species. (83, 84) Both MPP subunits are translated in the cytosol as larger precursor proteins with N-terminal targeting sequences that require the presence and function of MPP within the mitochondrial matrix to allow newly imported MPP to reach its native state. (53) In a study utilizing antisense RNA for  $\beta$ -MPP, it was found that the  $\beta$ -MPP protein was up-regulated 1.8 fold compared with wild-type; its mRNA increased 4.5 fold and both  $\alpha$ -MPP and Cox IV were induced. Inhibition of the  $\beta$ -MPP gene most likely acted through a retrograde signaling mechanism (informational relay pathway from mitochondrion to nucleus) to induce the expression of mitochondrial proteins. (85) MPP is quite different from other proteases as it does not recognize a specific sequence or position like exo-peptidases. MPP appears to have preferred recognition motifs and does not just cleave at random sites of polypeptide chains. (86)

### *MPP Cleavage Specificity*

Substrates of MPP typically contain an N-terminal targeting sequence of approximately 20-60 residues and carry a global positive charge. (87) These targeting sequences are both necessary and sufficient to target precursor proteins to their correct locations within the mitochondrion. A number of non-mitochondrial molecules, including cytosolic proteins and nucleic acids have been successfully targeted to the mitochondrion through the use of only an N-terminal matrix targeting sequence (Figure 1.3). (88, 89) The presequences that MPP recognizes



typically (but not universally) contain three key features: (1) a global positive charge, (2) an ability to form an amphiphilic  $\alpha$ -helix, and (3) an arginine residue usually at either the -2 or -3 position relative to the cleavage site. (87, 90-92) With regard to cleavage site motif sequence, there are currently four identified models, which include: (1) the R-2 motif (xRx↓x[S/s]), (2) the R-3 motif (xRx[Y/x]↓[S/A/x]x), (3) the R-10 motif (xRx↓[F/L/I]xx[S/T/G]xxxx↓; the first cleavage is done by MPP at the -2 position, following by an MIP cleavage at the -10 position), and (4) the R-none motif (xx↓x) (Figure: 1.4). (93) A common secondary structure of MPP substrates is the capability to form a helix-linker-helix orientation with the  $\alpha$ -helix disruptor being glycine and/or proline. (94, 95) In an examination of 71 yeast mitochondrial matrix targeting sequences, only 65% of those sequence fell into the categories of R-2, R-3 or R-10. As such, it is difficult to predict from the sequence whether a mitochondrial precursor protein is an MPP substrate. (92, 93, 96) The ability of MPP to interact with the targeting sequence of precursor proteins was found to be extremely sensitive to ionic strength. The  $K_m$  of MPP increases under high salt conditions, leading to the idea that this interaction occurs via electrostatic interactions. (97) However, alternative research endeavors argue against the necessity and importance of these parameters governing MPP cleavage and substrate specificity. Site-directed mutagenesis of the -2 or -3 arginine of different MPP substrates has shown mixed results. Depending on the precursor examined; partial or complete inhibition is observed, novel cleavage sites are discovered, or no effect is found. (98-101) When examining the necessity of the global positive charge for the targeting sequence, mild to severe effects were observed by substituting some or all of the arginine and lysine residues; however the substitution of the non-basic amino acids appeared to have no effect. (99, 100, 102) Experiments also showed that small deletions or point mutations on the C-terminal end of the cleavage site, both proximal and distal

from the MPP cleavage site, were capable of affecting the ability of MPP to act on a substrate.(94, 103) These findings suggest the structural features of both the targeting sequence and the mature portion of the substrate are likely important factors for whether MPP cleaves a particular target.

### *MPP Structural Analysis*

For MPP to function properly, both subunits ( $\alpha$  and  $\beta$ ) are necessary, but the two subunits perform different needs for cleavage of MPP substrates. (104) Regarding  $\beta$ -MPP, there are 2 areas within 200 residues at the N-terminal end that have a high overall degree of homology. The first area carries a high amount of negative charge and appears to interact with the positively charged amphiphilic  $\alpha$ -helix of the targeting sequence. (69) The second area (approximately 70 residues) contains the inverted zinc-binding domain (H-x-x-E-H-x<sub>76</sub>-E), and is responsible for MPP's catalytic activity. (83, 105) Within this motif, the histidine and final glutamate residues are responsible for metal binding. The first glutamate residue is involved in the activation of water for the hydrolysis of the substrate peptide bond. (106) All residues within the inverted zinc-binding domain are absolutely required for function; any replacements lead to the inability to bind zinc and the loss of MPP activity. (107) Mutations in the HxxEH zinc binding domain have little or no effect on the ability of the  $\alpha$  and  $\beta$  subunits to form a complex similar to that of wild-type MPP, therefore mutations in this domain do not significantly change the 3-D structure of  $\beta$ -MPP. (105) Conversely,  $\alpha$ -MPP has no catalytic activity but seems to play a role in substrate specificity and recognition via a highly conserved glycine-rich loop. (66)

From the crystal structure of yeast MPP, it appears the active site is located in a central, negatively charged cavity, and has a glycine-rich loop that blocks accessibility to the cavity.

When this loop is deleted, both the enzyme's substrate affinity and catalytic activity are decreased (Figure 1.5). (108, 109) Both subunits of MPP cooperatively form the substrate-binding pocket and each subunit is responsible for recognizing different aspects of the precursor. The subunits alone were found to have low affinity towards elements of presequence; the full native conformation is necessary for high substrate binding affinity. (110) The crystal structures found of MPP with synthetic signal peptides show the presequence interacts with the polar cavity of MPP in an extended conformation. These structures suggest the helical conformation taken by many mitochondrial targeting sequences is important for recognition by the mitochondrial import machinery, and this extended conformation is required for the cleavage by MPP (Figure 1.5).

(108) Through mutagenesis, it was concluded the zinc-binding domain (HxxEHx<sub>76</sub>H) of  $\beta$ -MPP is vital for the proper formation of active protein, and may be in contact with  $\alpha$ -MPP. Also, the central region around Lys215 of  $\beta$ -MPP, which is not highly conserved, plays a role in interacting with  $\alpha$ -MPP. Finally, the C-terminal region that surrounds Ser314 of  $\beta$ -MPP is needed for catalytic activity. (111) Using both cross-linking analysis and surface plasmon resonance,  $\alpha$ -MPP was found to bind a precursor protein in the absence of  $\beta$ -MPP and was able to bind the precursor as effectively as MPP. From this, it appears that  $\alpha$ -MPP is responsible for binding the mitochondrial targeting sequence before it is presented to the catalytic domain. (111) All of these factors come together to provide strict specificity and high affinity for MPP and its substrates.

## High-throughput Screening

A major shortcoming in studying mitochondrial activity in biological systems is the lack of tools. Classic genetic approaches used in mitochondrial biology in yeast and worms, rely on conditional mutants such as temperature-sensitive (ts) and overexpression mutants to induce changes in pathways, an approach that is not easily accomplished in mammalian cells. This approach often requires hours to switch from a permissive condition to a lethal condition and results in secondary perturbations, leading to global side effects. The goal is to generate small molecule modulators that alter activity of the mitochondrial proteases within minutes, with the aim of determining the role of mitochondria in diverse cellular pathways from fungi to plants and animals. These tools will be important for altering regulated proteolysis *in vivo*. An ultimate goal is to develop a “toolbox” of small molecules to study the roles of these proteases by eliminating their immediate function. Modulating the quality control system will affect a broad range of mitochondrial functions and provide insight into how the mitochondrion controls diverse cellular processes.

In the discovery and development of therapeutic drugs and biological probes, the benchmark methodology is conducting a high-throughput screen (HTS) with small molecule libraries. When using HTS to find drug-like compounds that have bioactivity, one of most vital aspects to ensure reliability and specificity is the use of a finely tuned assay. (112) Through the use of HTS, a researcher is capable of quickly conducting a plethora of chemical, genetic, or pharmacological tests that can rapidly identify active compounds, antibodies or genes that affect a particular biologic pathway. These reactions are typically conducted in microplates that contain 384, 1,536, or 3,465 wells. The researcher sets up the assay by first placing the desired entity into each well; this could be biological material such as a protein, cells, or animal

embryos. Typically, with use of the screening facility's automated system, each well is pinned with its corresponding vehicle control (such as DMSO) or small molecule. The reaction is then allowed to incubate for a specified amount of time to allow for the reaction to proceed. After the incubation period, measurements are conducted across the plate; this could consist of shining polarized light into each well and measuring reflectivity, measuring fluorescence from each well, microscopy, or measuring cell death. Data are collected from these experiments; with the aid of automation and robotics, hundreds of thousands of reactions can be analyzed fairly quickly. The typical HTS system consists of one or more robots that transport the assay plates from station to station, which include, sample and reagent addition, mixing, incubation, and readout or detection. Those small molecules that exceed the predetermined threshold for inhibition or activation are then re-screened (known as cherry-picking, this describes the transfer of the hit compounds from their original sample plate to a new assay plate) in the original assay to confirm their activity.

### *Quality Control*

Due to the speed at which data can be collected, HTS has led to an explosion in the rate of generated data in recent years. (112) This idea then leads to fundamental challenges that face HTS: how to determine biochemical significance from all of this data. Significance from HTS can only be found through the development and use of appropriate experimental designs and analytic methods regarding both hit selection and quality control. (113, 114)

High-quality assays are paramount for HTS experiments. Achieving a high degree of quality control (QC) when developing these types of assays requires the integration of both experimental and computational approaches. Good QC relies on three important factors: (1)

appropriate plate design, (2) use of effective positive and negative controls, and (3) development of a useful QC metric capable of differentiating viable data from inferior data. (115) High quality HTS assays are typified by a clear distinction between the positive control and the negative reference, therefore there have been a number of quality-assessment measurements utilized to gauge this difference when assessing data quality. These measurements include signal-to-background ratio, signal-to-noise ratio, signal window, assay variability ratio and Z-factor. (114, 116) We utilize the Z-factor in our lab, which is a measure of statistical effect size that judges if the effect observed in the assay is large enough to warrant further investigation. (116) There are four parameters that go in to defining the Z-factor, the means and standard deviations of both the positive and negative controls. This produced the following equation:  $Z\text{-factor} = 1 - ((3(\sigma_p + \sigma_n)/(|\mu_p - \mu_n|))$  where p and n represent the positive and negative controls, respectively. (116) Four ranges that describe the quality of the HTS assay have been implemented for the Z-factor measurement: (1) Z-factor equals 1 and the assay is described as being ideal (a Z-factor can not exceed 1), (2) Z-factor is between 0.5-1 and the assay is described as being an excellent assay, (3) Z-factor is between 0-0.5 and the assay is described as being a marginal assay, and (4) Z-factor is less than 0 and the assay is said to have to a large degree of overlap between the positive and negative controls, therefore it is not a useful assay. (116)

### *Hit Selection*

Once an HTS is completed, the next phase is hit selection, where compounds or other variables from the HTS are deemed a hit if they had the desired size of effect. Different statistical methods must be used to analyze screen data depending on whether the screen used replicates (usually done for confirmatory screens) or did not use replicates (typical seen in primary

screens). For those without replicates the Z-score is a sufficient method, while for those with replicates the t-statistic is suitable. (114) For primary screens without replicates, other values typically and easily investigated are average fold change, mean difference, percent inhibition and percent activity. (114)

## Zebrafish as a Model Organism

To a large extent the study of human disease pathways is examined through the use of animal model organisms. In the early 1980's the use of the mouse (*Mus musculus*) model was implemented to simulate human disease in a vertebrate system, as there is a high degree of homology between the species. (117)

Though mice are used worldwide as a model organism there are some significant drawbacks to their use in studying human biological processes, especially embryonic development. Several of these concerns when studying embryonic development include: large numbers of mice are needed to obtain enough material to conduct the study (a typical mating pair of mice can produce 50 offspring during their breeding span); embryonic development occurs internally, therefore surgery is required to examine early stages in development and finally the maintenance and testing of mouse colonies is both extremely time consuming and costly. (120)

Many of the drawbacks to studying embryonic development inherent with the mouse model are alleviated with the use of zebrafish as the model organism to study human disease pathways. Starting in the 1930's, zebrafish (*Danio rerio*) have been used to study development. (122) Zebrafish are fairly inexpensive to obtain from commercial sources, easy to maintain with the proper water filtration system, can yield hundreds of embryos per mating and the embryo

develops externally from the parental fish making it fast and simple to collect and manipulate the embryos once they have been fertilized. (122-125) Along with these benefits in the use of zebrafish as a model organism, zebrafish embryo development can also be monitored starting from the single-cell stage in real-time since their protective outer proteinaceous shell (the chorion) is optically clear. (126)

### *Zebrafish Embryonic Development*

The development of zebrafish has been thoroughly investigated, thereby allowing a particular research aim to be directed towards the most relevant stage of zebrafish development. Approximately 45 minutes after fertilization the zebrafish embryo initially passes through both the zygote and cleavage stages of development, which are exemplified by a few rapid rounds of synchronous division (Figure 1.6:A-F). (127) After these stages, the embryo transitions through the blastula and gastrula phases that are periods of long asynchronous divisions (approximately 3 hrs post fertilization) (Figure 1.6: G-N). These epibolic phases are points at which involution, convergence, extension of the epiblast and embryonic axis formation are seen. Segmentation starts ten hours post fertilization; this gives rise to 30-34 somites that ultimately develop into mostly skeletal muscle and, to some extent, vertebrae. (128, 129) The pharyngula phase follows segmentation; at this point the body axis straightens, pigmentation appears and blood circulation starts (begins 24 hrs post fertilization and lasts another 24 hrs) (Figure 1.6: Q-R). (127) Roughly 5 hours post fertilization the heart begins to form; this gives rise to the premature heart (cardiac disc) at approximately 22 hours post fertilization (Figure 1.6: R, arrow). (130) After 48 hours post fertilization a majority of the embryos hatch from the chorion (now defined as larvae); developmentally this period shows rapid formation of organ systems, along with cartilage



formation in the head and tail. Between the range of 48 and 60 hours post fertilization the pectoral fins begin to protrude and expand and the mouth begins to form. At 72 hours post fertilization, the mouth of the larvae start protruding, gill slits and filaments are seen, and the first bones become visible (Figure 1.6: S, arrow). (127) Between 72 and 96 hours post fertilization the swim bladder inflates, the gut tube moves ventrally, and the larvae starts to actively swim more and respond to external stimuli with precise movements. (127) From 5 to 7 days post fertilization the yolk sac is fully consumed and exogenous feeding is necessary. (131) In the range of 21 days to 3 months post fertilization zebrafish are considered adolescents; after 3 months they reach sexual maturity and are capable of producing offspring. (132)

Much like mice, the zebrafish genome has a great deal of homology with the human genome though their sizes are quite different from each other (1.5 billion bases on 25 chromosomes and 2.9 billion bases on 23 chromosomes respectively). (133, 134) The use of zebrafish as a model for development has been conducted for decades, but is hasn't been until recently that they have been analyzed on both the genomic and proteomic level, along with being used in the study and identification of drug compounds. (122) As part of this project, our lab utilized the zebrafish model as a way to examine the effects of our small molecules *in vivo* on a vertebrate model organism.

### *Zebrafish Biochemistry and Drug Discovery*

Zebrafish are well suited for our work because DNA can be introduced fairly easily into the organism for expression. The two basic ways of introducing DNA into zebrafish is through a transient fashion, and via a germ line integration. (135, 136) When it is necessary for the genes to be pass along to their progeny then DNA integration is the correct course of action. This form of

genetic integration allows proteins to be investigated at all stages of development since synthesis is under cellular control and produced constantly. Gene integration is accomplished by introducing cDNA for the gene of interest onto a plasmid that is flanked between 2 Tol2 transposition sites. (137) The plasmid along with RNA for the transposase protein is then injected into the single-cell stage of the embryo. Upon injection, the cellular translation machinery translates the transposase protein. The transposase protein then integrates the gene into the genome via homologous recombination at the Tol2 sites. (137) The fluorescent heart line used for these experiments for these assays was constructed via this method.

A major advantage of using zebrafish in our studies is due to fluorescent imaging. The optical clarity of the embryos allows for proteins or cellular components to be fluorescently tagged and viewed in real-time using microscopic imaging. (142) The most common transgenic markers used with zebrafish are GFP and DsRed due to their high stability, resistance to photo-bleaching and ease by which they can be detected using a number of microscopic techniques. (142-144) One useful technique is to pair fluorescent markers with transgenic expression systems, similar to the technique discussed previously to generate zebrafish lines that express reporter fluorescence in specific cell types (e.g., *cmlc2* is placed in front of the DsRed protein then DsRed will be expressed in cardiac cells). (141)

A relatively new avenue of use for zebrafish is their utilization in high-throughput screening (HTS) assays. (124) Currently in the scientific community there is a large push towards small-molecule discovery, and zebrafish provide an excellent system to perform large-scale small-molecule screens on an *in vivo* system. (126, 145) Zebrafish allow for the testing of small-molecules on a vertebrate organism that more closely relates to the phenotypic response of humans than the more classic organisms (*D melanogaster* and *C elegans*) used in HTS. (126,

146, 147) Several factors make zebrafish an excellent organism for the study of small molecules. Firstly, zebrafish are capable of producing 200–300 embryos per mating pair, which allows for multiple drugs and concentrations to be tested together with an ample amount of replicas. (124, 148) The embryos are also capable of surviving in as little as 50  $\mu$ L of water, thereby making it possible to conduct experiments in either 96- or 384-well plates. (124) Another key feature of zebrafish embryos is that they are osmotically permeable, allowing small molecules to diffuse through the embryo and makes it possible to study adsorption, biodistribution, and tissue specificity of drug molecules. (124) Despite the fact that metabolic processes of zebrafish are not completely elucidated, it is still possible to use this model organism to determine the toxicity small molecules. (149, 150) Through the use of morpholino injection or an alternate means of protein knockdown it is possible to identify both off-target and on-target effects of a small molecule by comparing the phenotypes of zebrafish treated with drug and those treated with morpholino injection. (151) Though the homology between humans and zebrafish is not identical, zebrafish do appear to be an excellent model organism to study the intricacies of mitochondrial function as they relate to human disorders.

With its many functions ranging from protein translocation to oxidative phosphorylation, the mitochondrion is an extremely complex organelle that still remains vastly a mystery. One aspect of our lab is the development of small molecule modulators that can be used in the study of mitochondrial function. The use of small molecules is advantageous as they allow the study of synthetically lethal proteins that were previously un-assayable using classical genetic approaches. Using small molecule modulators, our lab is capable of temporally inhibiting a protein of interest, and observing the effects, without globally affecting the genome of the model organism. Much of our preliminary work with the small molecule modulators is done *in vitro* to

confirm and characterize their mode of action. Following this investigation our lab transitions to the zebrafish model organism to assess the *in vivo* actions of our small molecule modulators.

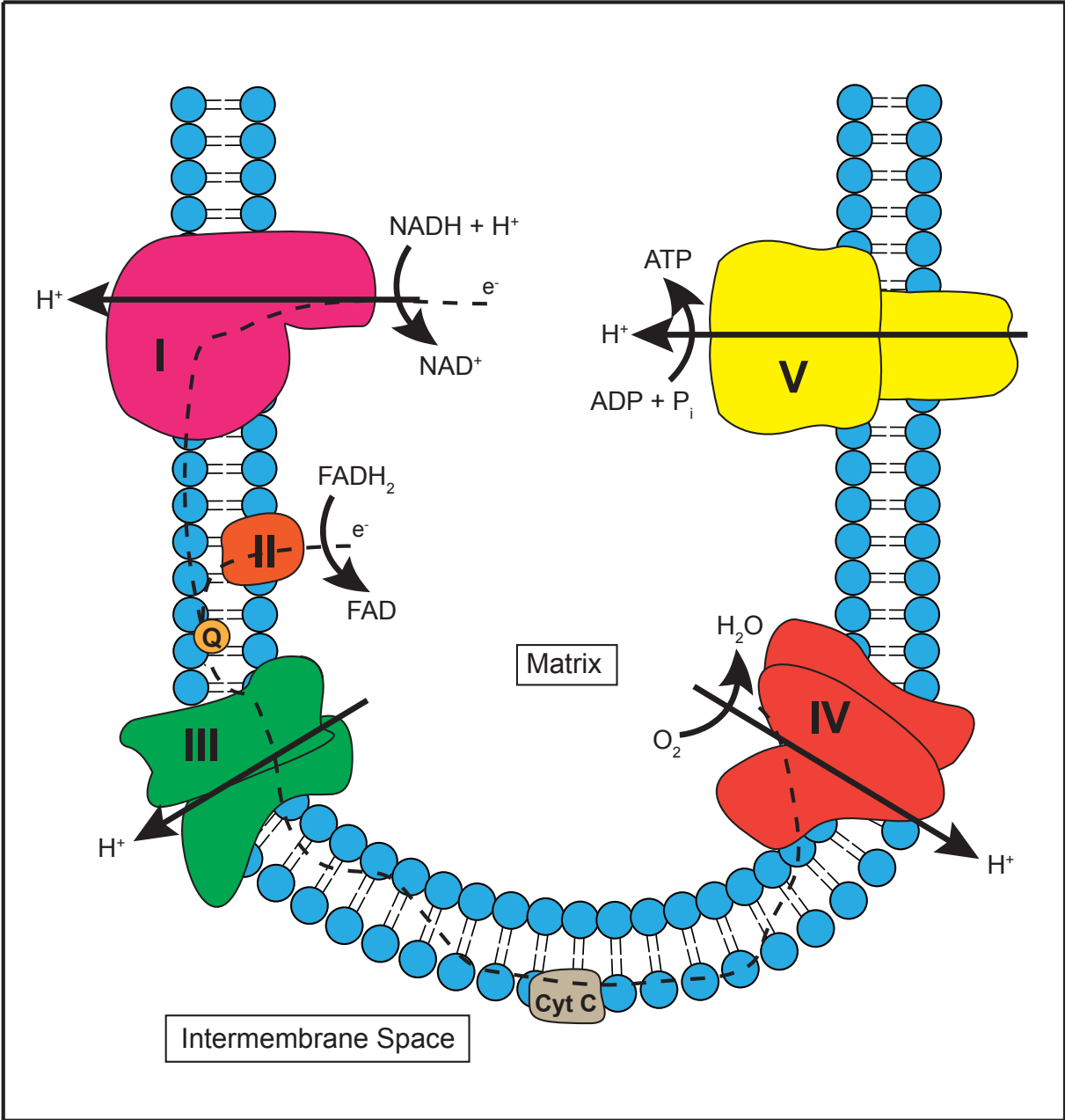
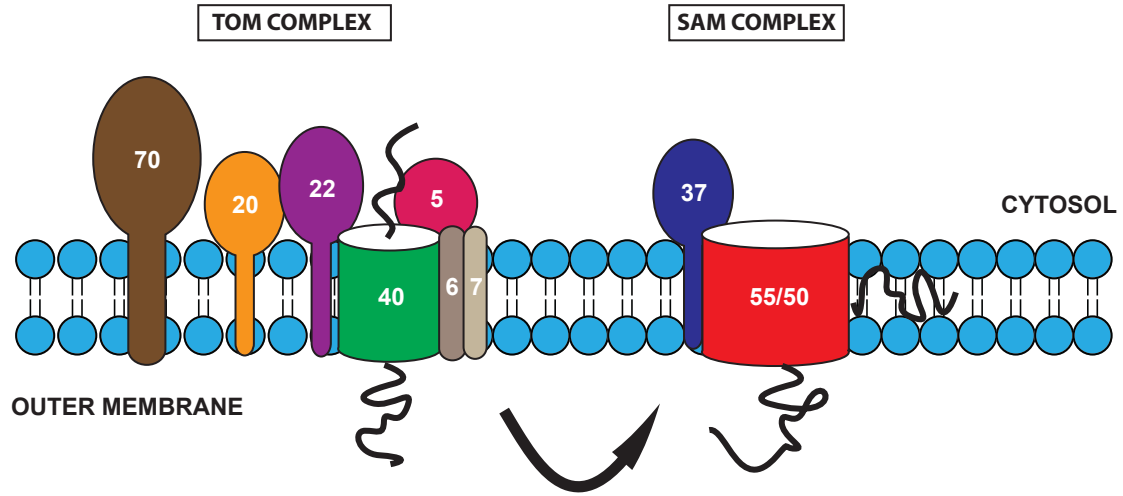


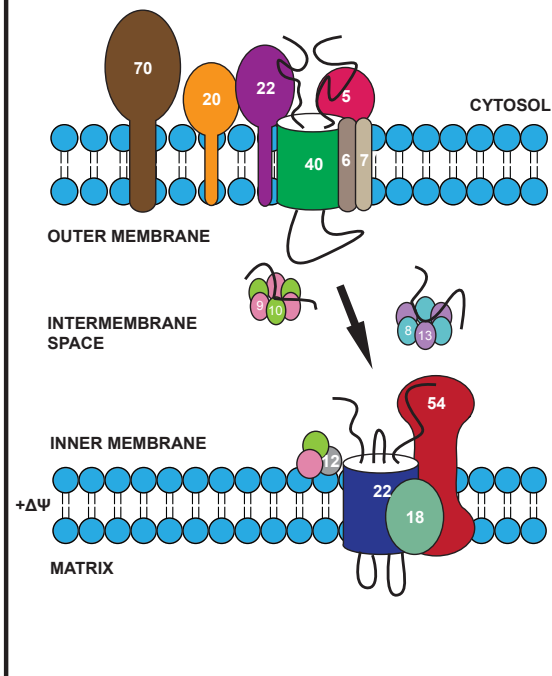
**Figure 1.1 The Respiratory Complexes of the Electron Transport Chain (ETC) in Mitochondria.**

Electrons from NADH enter the ETC at Complex I, which is located in the inner membrane. The electrons from NADH are shuttled to coenzyme Q (Q) via a series of iron-sulfur clusters within Complex I. This shuttling of electrons provides the energy to transport  $H^+$  ions from the matrix across the inner membrane to the intermembrane space, thereby helping to establish a proton gradient across the inner membrane. Electrons are also shuttled from  $FADH_2$  to Q within Complex II. Unlike Complex I this process does not translocate  $H^+$  across the inner membrane. Q is capable of traversing the inner membrane and takes electrons to Complex III. Electrons are then transferred to cytochrome *c*, similar to Complex I. This process is able to translocate more  $H^+$  ions through a method known as Q-cycling. The electrons from Cytochrome *c* are then passed to Complex IV and ultimately to the final electron acceptor,  $O_2$ . Complex IV is the final site in the ETC where  $H^+$  ions are pumped from the matrix to intermembrane space. The  $H^+$  ions are then pumped back across the inner membrane via Complex V. The energy generated from this process is harnessed to generate ATP from ADP and  $P_i$ .

## A. Import into Outer Membrane



## B. Import into Inner Membrane



## C. Import into Matrix

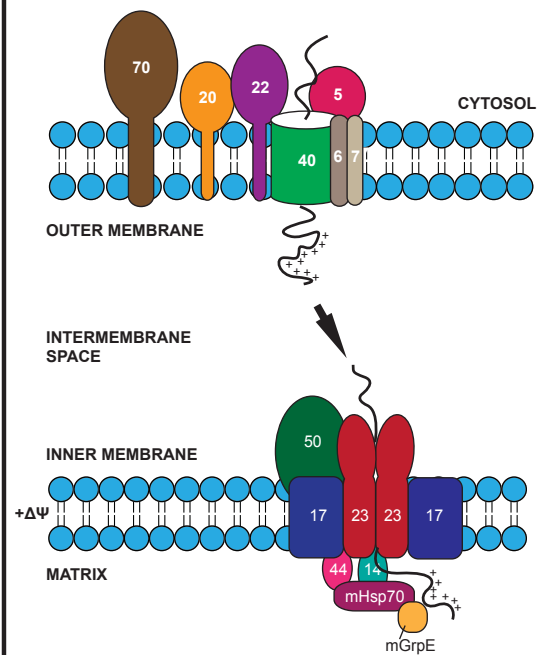


## **Figure 1.2 Mitochondrial Protein Import.**

Depending on where proteins are destined with the mitochondria (outer membrane, intermembrane space, inner membrane, or matrix) they follow different translocation pathways that ensure that the proper proteins are segregated to their appropriate compartment. Irrespective of what compartment a protein is destined, most proteins follow traditional pathways (as shown above) and first interact with the TOM complex. **A.** Following their interaction with the TOM complex, proteins staying in the outer membrane are shuttled to the SAM complex where they are inserted into the outer membrane. **B.** Proteins going to the inner membrane are aided across the intermembrane space by the small Tim complexes upon exit from the Tom40 pore. After being escorted by the small Tims the precursor proteins are transferred to the TIM22 complex for insertion into the inner membrane. **C.** Precursor proteins that are destined for the mitochondrial matrix typically possess a positively-charged N-terminal targeting sequence (MTS) that directs them to the TIM23 complex. The pore of the TIM23 complex consists of Tim23 and Tim17, which allow precursor proteins to traverse from the intermembrane space to the matrix. Once in the matrix the N-terminal targeting sequence of these precursor proteins must be cleaved off so the protein can fold into its native conformation. The MTS possessing precursor proteins are pulled into the matrix through the interaction of the positively-charged amino acids in the MTS and the translocation motor (Tim44, Tim14, mHsp70, and mGrpE) of the TIM23 complex. Translocation via the TIM22 and TIM23 complexes is dependent on a membrane potential ( $\Delta\Psi$ ) across the inner membrane.



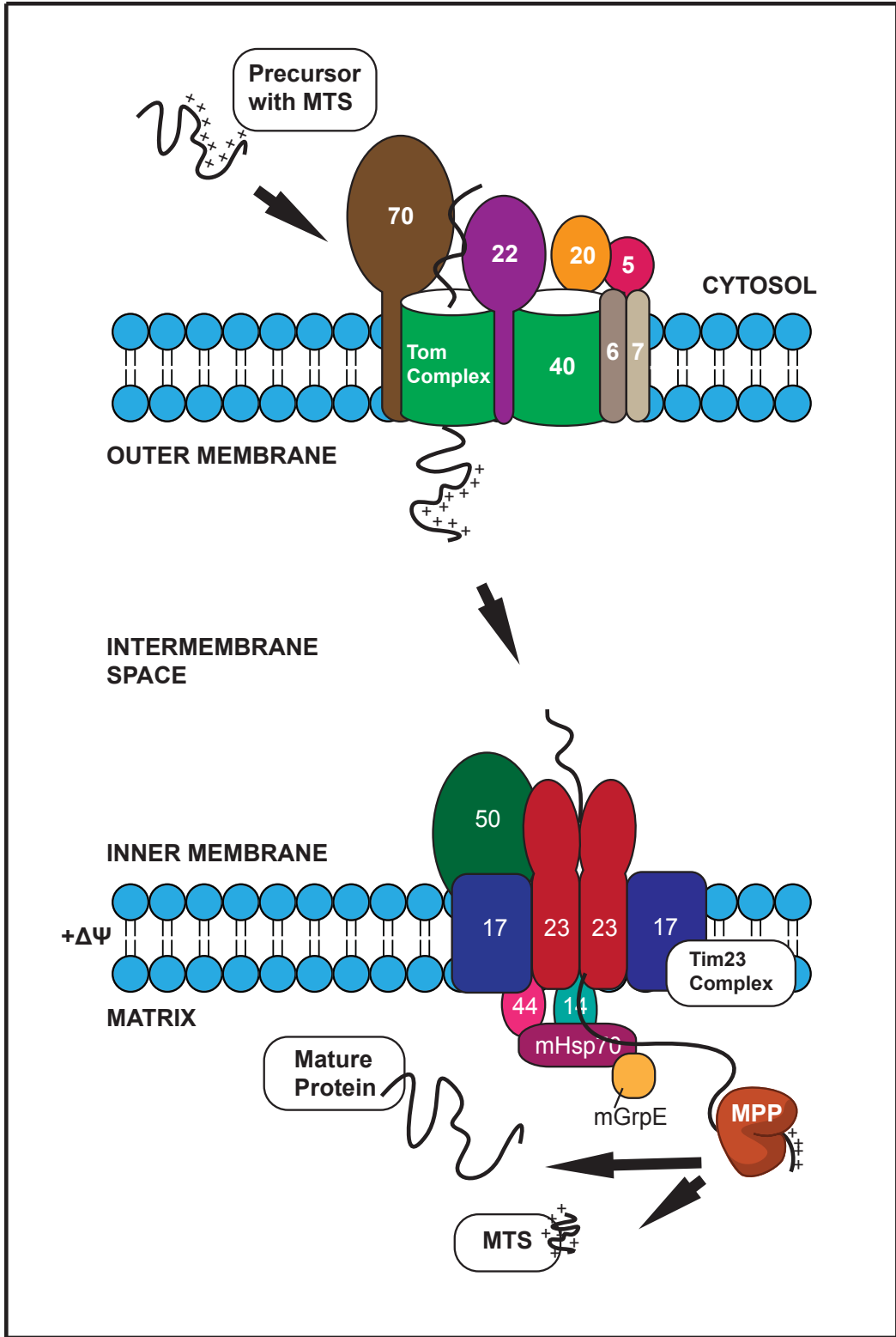


### **Figure 1.3 Import of Precursor Proteins into the Mitochondrial Matrix.**

Precursor proteins that possess a positively-charged mitochondrial targeting presequence (MTS) are typically destined to be imported into the mitochondrial matrix. Like many other precursor proteins that are imported into the mitochondria, these precursors first interact with the TOM complex in the outer mitochondrial membrane. Once across the intermembrane space, they interact with the TIM23 complex in the inner membrane; it is thought that these precursors traverse the intermembrane space while attached to both the TOM and TIM23 complex. As stated previously, the positively-charged amino acids within the MTS interact with translocation motor (Tim44, Tim14, mHsp70, and mGrpE) of the TIM23 complex, which aids in pulling the precursors into the matrix. Before the precursors are capable of folding into their mature and functional conformation the MTS must be cleaved off; this is accomplished by MPP. Currently, there is conflicting data as to whether the precursor protein completely passes through the TIM23 complex and into the matrix or only partially enters the matrix so the MTS is available before MPP acts, but in either instance, MPP is necessary for the proper import and processing of precursors with an MTS.

## R-2 or R-3 Motif

↓ MPP

HMUT	MLRAKNQLFLLSPHYLRQVKESSGSRLIQ <b>QRL</b>	LHQQ....
HPDHE3	MQSWSRVYCSLAKRGHFNRISHGLQGLSAVPL <b>R</b> TY	ADQP....
MAAT	MALLHSGRVLSGVSAFHPGLAAAAS <b>A</b> RA	SSWW....
RSCSA	MVSGSSGLAAARFFSRTFLLQQNG <b>I</b> RH	GSYT....
YCOX8	MLCQQMIRTTAKRSSNIMTRPIIM <b>K</b> RS	VHFK....
<b>YDHA7</b>	MFSRSTLCLKTSASSIGRL <b>Q</b> L <b>R</b> YF	SHLP....
YIDH1	MLNRTIA <b>K</b> RTL	ATAA....
YRM02	MWNPILLDTSSFSFQKHVSGVFL <b>Q</b> V <b>R</b> N	ATKR....

## R-10 Motif

↓ IMP

HOTC	MLFNLRILLNNAAFRNGHNF <b>M</b> V <b>R</b> N	<b>F</b> RC <b>G</b> QPLQ	NKVQ....
MMDH	MLSALARPVGAAL <b>R</b> S	<b>F</b> ST <b>S</b> AQNN	AKVA....
NCPB	MFGPRHFSVLKTTGSLVSSTFSSSLKPTATFSC <b>A</b> RA	<b>F</b> SQ <b>T</b> SSIM	SKVF....
YAT14	MFPIASRRILLNASVPLRLC <b>N</b> R <b>N</b>	<b>F</b> TT <b>T</b> RISY	NVIQ....
YCOXIV	MLSLRQSIRFFK <b>P</b> AT <b>T</b>	<b>L</b> CS <b>S</b> RYLL	QKQP....
YDLDH	MLRIRSLLN <b>N</b> K <b>R</b> A	<b>F</b> SH <b>S</b> TVRTL	TINK....
YFe/S	MLGIRSSVKT <b>C</b> FK <b>P</b> MSLT <b>S</b> K <b>R</b> L	<b>I</b> S <b>Q</b> SLLAS	KSTY....
YRM07	MQRFSLV <b>T</b> H <b>R</b> S	<b>F</b> SH <b>S</b> CVKP	KSAC....

## No R-2, R-3, or R-10 Motif

BMPC	....NAPHLQLVHDGLAGPRSDPAGPPGPPRRSRNLAAA	AVEE....
HF0A	....GALRRLTPSAALPPAQLLLRAVRRRSHPVRDYAAQ	TSPS....
NATP2	....GLISRSLGNSIPKSASRASSRASPGRLLNRAVQY	ATSA....
PCS	....MALLTAAARLFGAKNASCLVLAARHAS	ASST....
YATP6	....MFNLLNTYIT	SPLD....
YADH3	....MLRTSTLFTQRVQPSLFSRNILRLQST	AAIP..
YDHA1	....MLATRNLVPIIRASIKWRIKL	SALH....
YNDI1	....MLSKNLYSNKRLTSTNTLVRFASTR	STGV....
YRM04	....MWKRSFHSQGGPLR	ARTK....

#### Figure 1.4 Examples of MPP and IMP Cleavage Motifs.

Common cleavage sites for MPP consist of an Arg residue position at the -2, -3, or -10 positions relative to the site of cleavage. As illustrated, this is not always the case because there are a number of MPP substrates that possess none of these common motifs. The space between different fragments of each MPP substrate signifies the cleavage site of either MPP or IMP as indicated by the arrow.

BMPC – bovine mitochondrial phosphate carrier; HF0A – human F<sub>0</sub>-ATPase proteolipid subunit; HMUT – human methylmalonyl-CoA mutase; HOTC – human ornithine transcarbamylase; HPDHE3 – human pyruvate dehydrogenase E3 subunit; MAAT – mouse aspartate amino transferase; MMDH – mouse malate dehydrogenase; NATP2 – *Nicotiana plumboginifolia* ATP synthase beta chain; NCPB – *N. crassa* cyclosporin-binding protein; PCS – pig citrate synthase; RSCSA – rat succinyl-CoA synthetase  $\alpha$  subunit; YADH3 – *S. cerevisiae* alcohol dehydrogenase III; YAT14 – *S. cerevisiae* ATP synthase H chain; YATP6 – *S. cerevisiae* ATP synthase A chain; YCOX4 – *S. cerevisiae* cytochrome *c* oxidase subunit IV; YCOX8 – *S. cerevisiae* cytochrome *c* oxidase subunit VIII; YDHA1 – *S. cerevisiae* aldehyde dehydrogenase; YDHA7 – *S. cerevisiae* potassium-activated aldehyde dehydrogenase; YDLDH – *S. cerevisiae* dihydrolipoamide dehydrogenase; YFe/S – *S. cerevisiae* ubiquinol–cytochrome *c* reductase Rieske iron–sulfur protein; YIDH1 – *S. cerevisiae* isocitrate dehydrogenase subunit 1; YNDI1 – *S. cerevisiae* rotenone-insensitive NADH-ubiquinone.

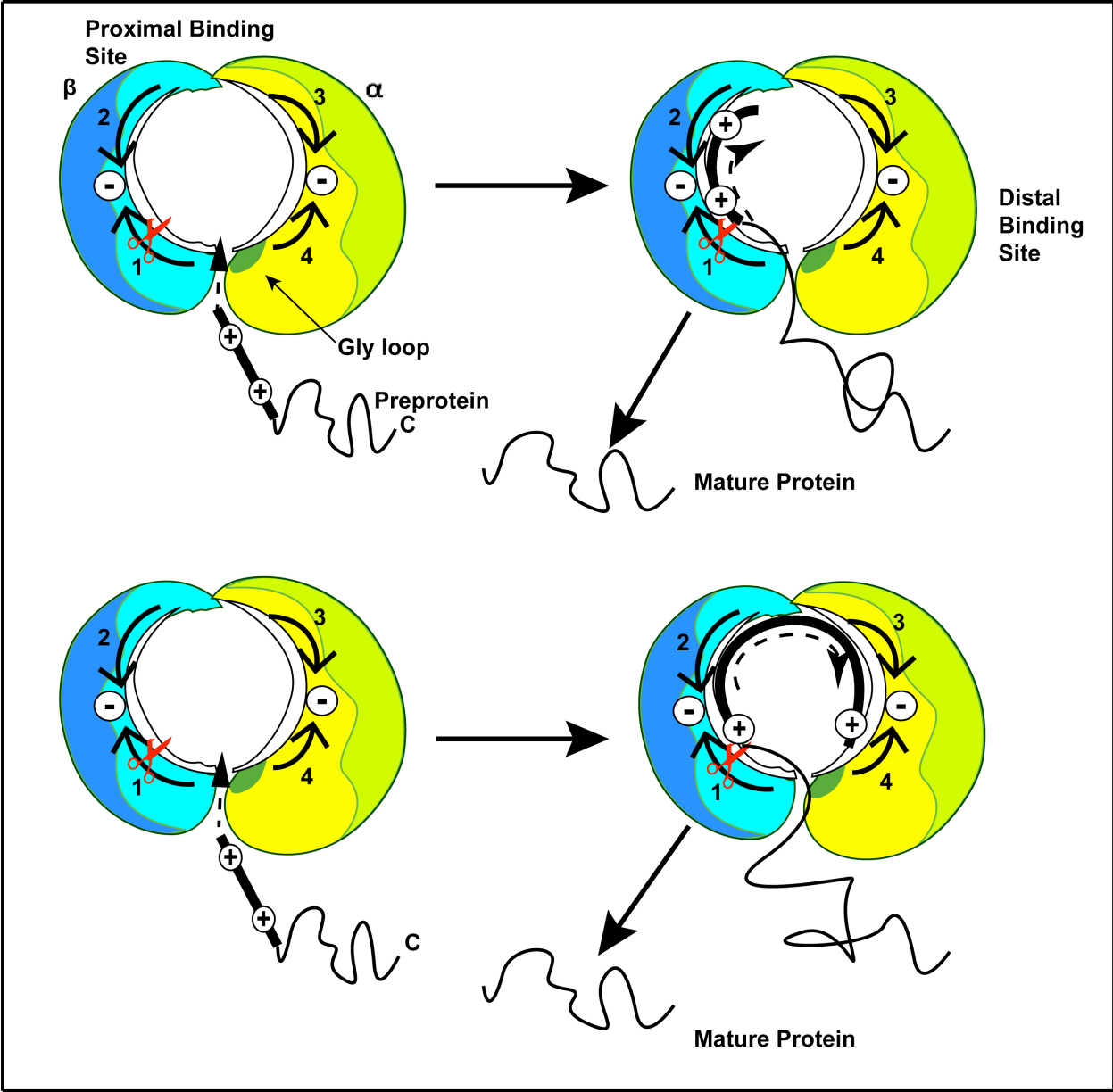


**Figure 1.5 Model for MPP Cleavage of Substrate within the Active Site Cavity.**

The model shows the differential ability of MPP to recognize short (upper pair) and long (lower pair) presequences.  $\alpha$ - and  $\beta$ -MPP subunits are represented in yellow and blue, respectively. 4 black arrows depict the substrate-binding scaffold, and the scissors show where the active site is located within the  $\beta$ -MPP subunit. For the precursor, the bold line indicates the presequence and the narrow line the rest of the protein. The plus symbols depict the basic amino acids that are present in the presequence and the negative symbols represent the binding site area for both the proximal (2) and distal (3,4) presequence binding regions. Model is based on the idea that for MPP to cleave its substrate, the presequence must enter the active site cavity of MPP in an extended conformation. It appears that electrostatic interactions are capable of capturing the positively-charged MTS and bringing it into the negatively-charged MPP cavity. MPP is capable of scanning the presequence as it threads through the cavity along the negatively-charged walls of both subunits and determine the correct site of cleavage. From this model, MPP would be capable of distinguishing different length presequences as they travel from the  $\beta$  subunit to the  $\alpha$  subunits, and thereby effectively and reproducibly cleave the correct site and release the mature protein. The process of directional insertion by which the precursor is allowed past the glycine-rich loop at the opening of the cavity, and the process of presequence scanning, are not yet completely understood. Deletion of the glycine-rich loop was found to significantly reduce the activity of MPP, but the exact mechanism of action is still unknown.

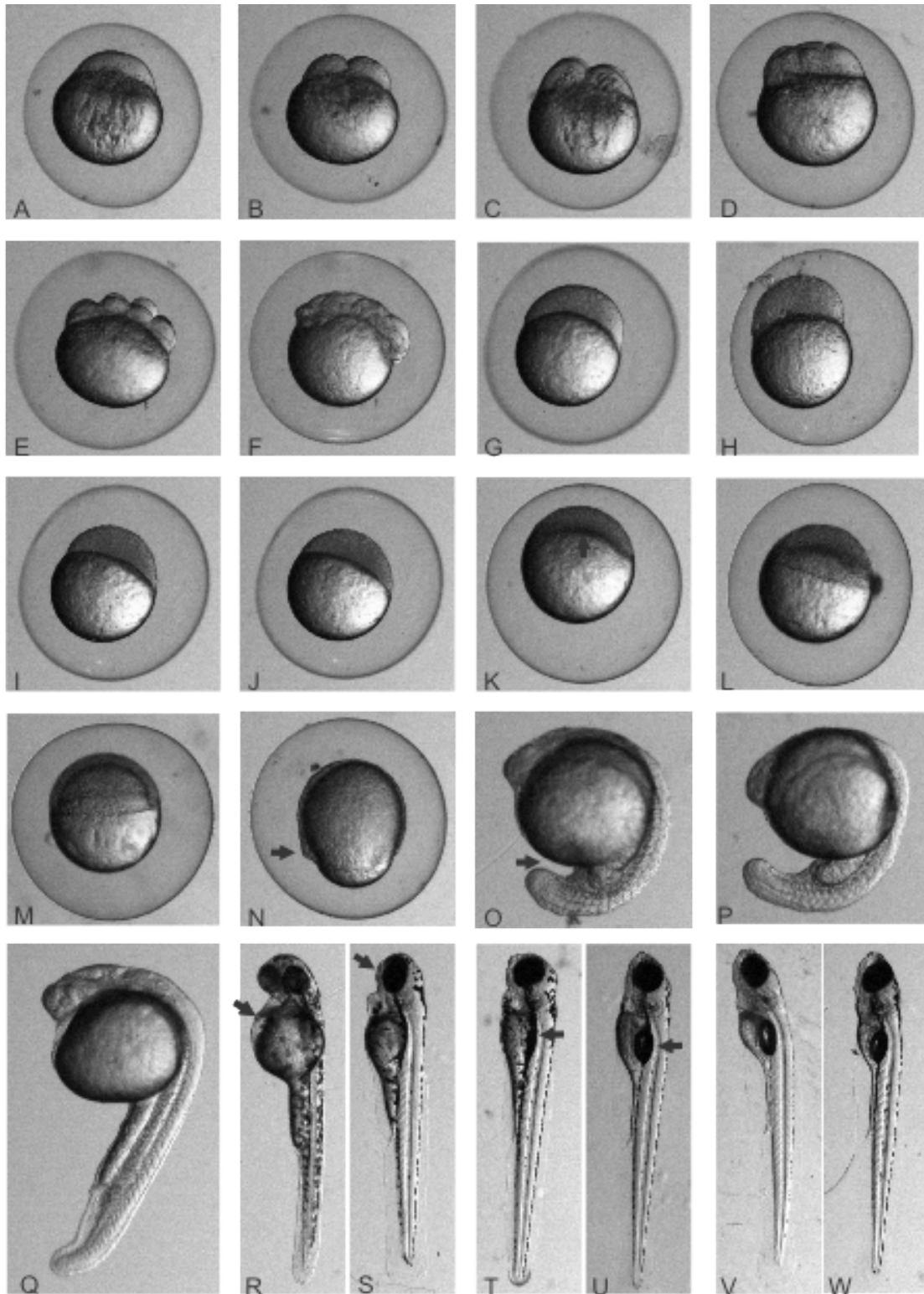


**Figure 1.6 Stages of Embryonic Development.**

A-M are face views; remaining are left-side views unless where noted, anterior up and dorsal to the left. A. 1-cell stage (0.2 hr) embryo resides at animal pole (top) and yolk migrates to vegetal pole (bottom) B. 2-cell stage (0.75 hr) C. 4-cell stage (1 hr) Blastomeres exist as a planar 2x2 array. D. 8-cell stage (1.25 hr) Blastomeres exist as a planar 2x4 array. E. 16-cell stage (1.5 hr) Blastomeres exist as a planar 4x4 array. F. 64-cell stage (2 hr) Blastomeres exist as three regular tiers of cells. G. 1000 cell stage (3 hr) Blastula period. The blastodisk appears ball-like and blastomeres reside in 11 tiers. H. High stage (3.3 hr) Beginning of blastodisc flattening. I. Oblong stage (3.7 hr) Flattening becomes elliptical in nature. J. Sphere stage (4 hr) A flat border exists between yolk and blastodisc, and embryo appears spherical. K. Dome stage (4.3 hr) Embryo stays spherical but yolk cells bulge inward towards animal pole as epiboly begins. (arrow) L. 30% epiboly stage (4.7 hr) Blastodisc thins and spreads uniformly around yolk. M. 50% epiboly stage (5.3 hr) Blastodisc continues to spread around yolk, and remains uniform in thickness. N. Bud stage (10 hr) Right side view, with anterior up and dorsal right. The tail bud becomes visible. (arrow) O. 16-18 somite stage (approx. 8 hr) Segmentation period. Extension of the tail begins, P. 21-24 somite stage (approx. 20 hr) Yolk begins to straighten out the posterior of the embryo. Q. Prim-5 (24 hr) Pharyngula period. There are approx. 30 somites, and length of yolk extension equals diameter of yolk ball. R. Long-pec stage (48 hr) Hatching period. Embryo begins to hatch from chorion. Pectoral fins have elongated and heart is clearly visible (arrow) S. Protruding-mouth stage (72 hr) The mouth is wide open (arrow) and gills are forming. T. Day 4 (96 hr) Swim bladder begins to inflate.(arrow) U. Day 5 (120 hr) Swim bladder is fully inflated. (arrow) V. 6 day (144 hr) W. 7 day (168 hr) A-Q and R-W imaged at 25x and 16x magnification, respectively (Leica MZ16F stereoscope). *Figure included with permission from Meghan E.*

*Johnson.*



# References

1. Daum G, Bohni PC, & Schatz G (1982) Import of proteins into mitochondria. Cytochrome b2 and cytochrome c peroxidase are located in the intermembrane space of yeast mitochondria. *J Biol Chem* 257(21):13028-13033.
2. Sickmann A, *et al.* (2003) The proteome of *Saccharomyces cerevisiae* mitochondria. *Proc Natl Acad Sci U S A* 100(23):13207-13212.
3. Taylor SW, *et al.* (2003) Characterization of the human heart mitochondrial proteome. *Nat Biotechnol* 21(3):281-286.
4. Reinders J, Zahedi RP, Pfanner N, Meisinger C, & Sickmann A (2006) Toward the complete yeast mitochondrial proteome: multidimensional separation techniques for mitochondrial proteomics. *J Proteome Res* 5(7):1543-1554.
5. Anderson S, *et al.* (1981) Sequence and organization of the human mitochondrial genome. *Nature* 290(5806):457-465.
6. Alexeyev MF, Ledoux SP, & Wilson GL (2004) Mitochondrial DNA and aging. *Clin Sci (Lond)* 107(4):355-364.
7. Broughton RE, Milam JE, & Roe BA (2001) The complete sequence of the zebrafish (*Danio rerio*) mitochondrial genome and evolutionary patterns in vertebrate mitochondrial DNA. *Genome Res* 11(11):1958-1967.
8. Foury F, Roganti T, Lecrenier N, & Purnelle B (1998) The complete sequence of the mitochondrial genome of *Saccharomyces cerevisiae*. *FEBS Lett* 440(3):325-331.
9. Schultz BE & Chan SI (2001) Structures and proton-pumping strategies of mitochondrial respiratory enzymes. *Annu Rev Biophys Biomol Struct* 30:23-65.
10. Carroll J, *et al.* (2006) Bovine complex I is a complex of 45 different subunits. *J Biol Chem* 281(43):32724-32727.
11. Bourges I, *et al.* (2004) Structural organization of mitochondrial human complex I: role of the ND4 and ND5 mitochondria-encoded subunits and interaction with prohibitin. *Biochem J* 383(Pt. 3):491-499.
12. Tomitsuka E, *et al.* (2003) Direct evidence for two distinct forms of the flavoprotein subunit of human mitochondrial complex II (succinate-ubiquinone reductase). *J Biochem* 134(2):191-195.

13. Gao X, *et al.* (2003) Structural basis for the quinone reduction in the bc1 complex: a comparative analysis of crystal structures of mitochondrial cytochrome bc1 with bound substrate and inhibitors at the Qi site. *Biochemistry* 42(30):9067-9080.
14. Capaldi RA, Darley-USmar V, Fuller S, & Millett F (1982) Structural and functional features of the interaction of cytochrome c with complex III and cytochrome c oxidase. *FEBS Lett* 138(1):1-7.
15. Fernandez-Vizarra E, Tiranti V, & Zeviani M (2009) Assembly of the oxidative phosphorylation system in humans: what we have learned by studying its defects. *Biochim Biophys Acta* 1793(1):200-211.
16. Boyer PD (1997) The ATP synthase--a splendid molecular machine. *Annu Rev Biochem* 66:717-749.
17. Owen OE, Kalhan SC, & Hanson RW (2002) The key role of anaplerosis and cataplerosis for citric acid cycle function. *J Biol Chem* 277(34):30409-30412.
18. Di Mauro S, Trevisan C, & Hays A (1980) Disorders of lipid metabolism in muscle. *Muscle Nerve* 3(5):369-388.
19. Pfanner N, Craig EA, & Honlinger A (1997) Mitochondrial preprotein translocase. *Annu Rev Cell Dev Biol* 13:25-51.
20. Neupert W (1997) Protein import into mitochondria. *Annu Rev Biochem* 66:863-917.
21. Dietmeier K, *et al.* (1997) Tom5 functionally links mitochondrial preprotein receptors to the general import pore. *Nature* 388(6638):195-200.
22. Honlinger A, *et al.* (1996) Tom7 modulates the dynamics of the mitochondrial outer membrane translocase and plays a pathway-related role in protein import. *EMBO J* 15(9):2125-2137.
23. Kozjak V, *et al.* (2003) An essential role of Sam50 in the protein sorting and assembly machinery of the mitochondrial outer membrane. *J Biol Chem* 278(49):48520-48523.
24. Paschen SA, *et al.* (2003) Evolutionary conservation of biogenesis of beta-barrel membrane proteins. *Nature* 426(6968):862-866.
25. Wiedemann N, *et al.* (2003) Machinery for protein sorting and assembly in the mitochondrial outer membrane. *Nature* 424(6948):565-571.
26. Yamamoto H, *et al.* (2002) Tim50 is a subunit of the TIM23 complex that links protein translocation across the outer and inner mitochondrial membranes. *Cell* 111(4):519-528.
27. Geissler A, *et al.* (2002) The mitochondrial presequence translocase: an essential role of Tim50 in directing preproteins to the import channel. *Cell* 111(4):507-518.

28. Gaume B, *et al.* (1998) Unfolding of preproteins upon import into mitochondria. *EMBO J* 17(22):6497-6507.
29. Geissler A, *et al.* (2000) Membrane potential-driven protein import into mitochondria. The sorting sequence of cytochrome b(2) modulates the deltapsi-dependence of translocation of the matrix-targeting sequence. *Mol Biol Cell* 11(11):3977-3991.
30. Rehling P, *et al.* (2003) Protein insertion into the mitochondrial inner membrane by a twin-pore translocase. *Science* 299(5613):1747-1751.
31. Sirrenberg C, Bauer MF, Guiard B, Neupert W, & Brunner M (1996) Import of carrier proteins into the mitochondrial inner membrane mediated by Tim22. *Nature* 384(6609):582-585.
32. Kerscher O, Holder J, Srinivasan M, Leung RS, & Jensen RE (1997) The Tim54p-Tim22p complex mediates insertion of proteins into the mitochondrial inner membrane. *J Cell Biol* 139(7):1663-1675.
33. Kerscher O, Sepuri NB, & Jensen RE (2000) Tim18p is a new component of the Tim54p-Tim22p translocon in the mitochondrial inner membrane. *Mol Biol Cell* 11(1):103-116.
34. Koehler CM (2004) New developments in mitochondrial assembly. *Annu Rev Cell Dev Biol* 20:309-335.
35. Paschen SA, *et al.* (2000) The role of the TIM8-13 complex in the import of Tim23 into mitochondria. *EMBO J* 19(23):6392-6400.
36. Adam A, *et al.* (1999) Tim9, a new component of the TIM22.54 translocase in mitochondria. *EMBO J* 18(2):313-319.
37. Koehler CM, *et al.* (1998) Tim9p, an essential partner subunit of Tim10p for the import of mitochondrial carrier proteins. *EMBO J* 17(22):6477-6486.
38. Koehler CM, *et al.* (1999) Human deafness dystonia syndrome is a mitochondrial disease. *Proc Natl Acad Sci U S A* 96(5):2141-2146.
39. Lutz T, Neupert W, & Herrmann JM (2003) Import of small Tim proteins into the mitochondrial intermembrane space. *EMBO J* 22(17):4400-4408.
40. Roesch K, Curran SP, Tranebjaerg L, & Koehler CM (2002) Human deafness dystonia syndrome is caused by a defect in assembly of the DDP1/TIMM8a-TIMM13 complex. *Hum Mol Genet* 11(5):477-486.
41. Dabir DV, *et al.* (2007) A role for cytochrome c and cytochrome c peroxidase in electron shuttling from Erv1. *EMBO J* 26(23):4801-4811.

42. Allen S, Balabanidou V, Sideris DP, Lisowsky T, & Tokatlidis K (2005) Erv1 mediates the Mia40-dependent protein import pathway and provides a functional link to the respiratory chain by shuttling electrons to cytochrome c. *J Mol Biol* 353(5):937-944.
43. Mesecke N, *et al.* (2005) A disulfide relay system in the intermembrane space of mitochondria that mediates protein import. *Cell* 121(7):1059-1069.
44. Chacinska A, *et al.* (2004) Essential role of Mia40 in import and assembly of mitochondrial intermembrane space proteins. *EMBO J* 23(19):3735-3746.
45. Rissler M, *et al.* (2005) The essential mitochondrial protein Erv1 cooperates with Mia40 in biogenesis of intermembrane space proteins. *J Mol Biol* 353(3):485-492.
46. Grumbt B, Stroobant V, Terziyska N, Israel L, & Hell K (2007) Functional characterization of Mia40p, the central component of the disulfide relay system of the mitochondrial intermembrane space. *J Biol Chem* 282(52):37461-37470.
47. Fass D (2008) The Erv family of sulfhydryl oxidases. *Biochim Biophys Acta* 1783(4):557-566.
48. Lee J, Hofhaus G, & Lisowsky T (2000) Erv1p from *Saccharomyces cerevisiae* is a FAD-linked sulfhydryl oxidase. *FEBS Lett* 477(1-2):62-66.
49. Gabriel K, *et al.* (2007) Novel mitochondrial intermembrane space proteins as substrates of the MIA import pathway. *J Mol Biol* 365(3):612-620.
50. Hofhaus G, Lee JE, Tews I, Rosenberg B, & Lisowsky T (2003) The N-terminal cysteine pair of yeast sulfhydryl oxidase Erv1p is essential for in vivo activity and interacts with the primary redox centre. *Eur J Biochem* 270(7):1528-1535.
51. Bihlmaier K, *et al.* (2007) The disulfide relay system of mitochondria is connected to the respiratory chain. *J Cell Biol* 179(3):389-395.
52. Reddehase S, Grumbt B, Neupert W, & Hell K (2009) The disulfide relay system of mitochondria is required for the biogenesis of mitochondrial Ccs1 and Sod1. *J Mol Biol* 385(2):331-338.
53. Gakh O, Cavadini P, & Isaya G (2002) Mitochondrial processing peptidases. *Biochim Biophys Acta* 1592(1):63-77.
54. Endo T & Yamano K (2009) Multiple pathways for mitochondrial protein traffic. *Biol Chem* 390(8):723-730.
55. Chow KM, *et al.* (2009) Mammalian pitrilysin: substrate specificity and mitochondrial targeting. *Biochemistry* 48(13):2868-2877.

56. Falkevall A, *et al.* (2006) Degradation of the amyloid beta-protein by the novel mitochondrial peptidase, PreP. *J Biol Chem* 281(39):29096-29104.
57. Mokranjac D & Neupert W (2009) Thirty years of protein translocation into mitochondria: unexpectedly complex and still puzzling. *Biochim Biophys Acta* 1793(1):33-41.
58. Patel PI & Isaya G (2001) Friedreich ataxia: from GAA triplet-repeat expansion to frataxin deficiency. *Am J Hum Genet* 69(1):15-24.
59. Babcock M, *et al.* (1997) Regulation of mitochondrial iron accumulation by Yfh1p, a putative homolog of frataxin. *Science* 276(5319):1709-1712.
60. Knight SA, Sepuri NB, Pain D, & Dancis A (1998) Mt-Hsp70 homolog, Ssc2p, required for maturation of yeast frataxin and mitochondrial iron homeostasis. *J Biol Chem* 273(29):18389-18393.
61. Branda SS, *et al.* (1999) Yeast and human frataxin are processed to mature form in two sequential steps by the mitochondrial processing peptidase. *J Biol Chem* 274(32):22763-22769.
62. Cavadini P, Adamec J, Taroni F, Gakh O, & Isaya G (2000) Two-step processing of human frataxin by mitochondrial processing peptidase. Precursor and intermediate forms are cleaved at different rates. *J Biol Chem* 275(52):41469-41475.
63. Gordon DM, Kogan M, Knight SA, Dancis A, & Pain D (2001) Distinct roles for two N-terminal cleaved domains in mitochondrial import of the yeast frataxin homolog, Yfh1p. *Hum Mol Genet* 10(3):259-269.
64. Adamec J, *et al.* (2000) Iron-dependent self-assembly of recombinant yeast frataxin: implications for Friedreich ataxia. *Am J Hum Genet* 67(3):549-562.
65. Koutnikova H, Campuzano V, & Koenig M (1998) Maturation of wild-type and mutated frataxin by the mitochondrial processing peptidase. *Hum Mol Genet* 7(9):1485-1489.
66. Ito A (1999) Mitochondrial processing peptidase: multiple-site recognition of precursor proteins. *Biochem Biophys Res Commun* 265(3):611-616.
67. Kalousek F, Neupert W, Omura T, Schatz G, & Schmitz UK (1993) Uniform nomenclature for the mitochondrial peptidases cleaving precursors of mitochondrial proteins. *Trends Biochem Sci* 18(7):249.
68. Yang M, Jensen RE, Yaffe MP, Oppliger W, & Schatz G (1988) Import of proteins into yeast mitochondria: the purified matrix processing protease contains two subunits which are encoded by the nuclear MAS1 and MAS2 genes. *EMBO J* 7(12):3857-3862.

69. Kleiber J, Kalousek F, Swaroop M, & Rosenberg LE (1990) The general mitochondrial matrix processing protease from rat liver: structural characterization of the catalytic subunit. *Proc Natl Acad Sci U S A* 87(20):7978-7982.
70. Geli V (1993) Functional reconstitution in *Escherichia coli* of the yeast mitochondrial matrix peptidase from its two inactive subunits. *Proc Natl Acad Sci U S A* 90(13):6247-6251.
71. Saavedra-Alanis VM, Rysavy P, Rosenberg LE, & Kalousek F (1994) Rat liver mitochondrial processing peptidase. Both alpha- and beta-subunits are required for activity. *J Biol Chem* 269(12):9284-9288.
72. Adamec J, Gakh O, Spizek J, & Kalousek F (1999) Complementation between mitochondrial processing peptidase (MPP) subunits from different species. *Arch Biochem Biophys* 370(1):77-85.
73. McAda PC & Douglas MG (1982) A neutral metallo endoprotease involved in the processing of an F1-ATPase subunit precursor in mitochondria. *J Biol Chem* 257(6):3177-3182.
74. Miura S, Mori M, Amaya Y, & Tatibana M (1982) A mitochondrial protease that cleaves the precursor of ornithine carbamoyltransferase. Purification and properties. *Eur J Biochem* 122(3):641-647.
75. Conboy JG, Fenton WA, & Rosenberg LE (1982) Processing of pre-ornithine transcarbamylase requires a zinc-dependent protease localized to the mitochondrial matrix. *Biochem Biophys Res Commun* 105(1):1-7.
76. Schmidt B, Wachter E, Sebald W, & Neupert W (1984) Processing peptidase of *Neurospora* mitochondria. Two-step cleavage of imported ATPase subunit 9. *Eur J Biochem* 144(3):581-588.
77. Luciano P, Tokatlidis K, Chambre I, Germanique JC, & Geli V (1998) The mitochondrial processing peptidase behaves as a zinc-metallopeptidase. *J Mol Biol* 280(2):193-199.
78. Auld DS (1995) Removal and replacement of metal ions in metallopeptidases. *Methods Enzymol* 248:228-242.
79. Yaffe MP & Schatz G (1984) Two nuclear mutations that block mitochondrial protein import in yeast. *Proc Natl Acad Sci U S A* 81(15):4819-4823.
80. Yaffe MP, Ohta S, & Schatz G (1985) A yeast mutant temperature-sensitive for mitochondrial assembly is deficient in a mitochondrial protease activity that cleaves imported precursor polypeptides. *EMBO J* 4(8):2069-2074.

81. Witte C, Jensen RE, Yaffe MP, & Schatz G (1988) MAS1, a gene essential for yeast mitochondrial assembly, encodes a subunit of the mitochondrial processing protease. *EMBO J* 7(5):1439-1447.
82. Pollock RA, *et al.* (1988) The processing peptidase of yeast mitochondria: the two co-operating components MPP and PEP are structurally related. *EMBO J* 7(11):3493-3500.
83. Paces V, Rosenberg LE, Fenton WA, & Kalousek F (1993) The beta subunit of the mitochondrial processing peptidase from rat liver: cloning and sequencing of a cDNA and comparison with a proposed family of metallopeptidases. *Proc Natl Acad Sci U S A* 90(11):5355-5358.
84. Schulte U, *et al.* (1989) A family of mitochondrial proteins involved in bioenergetics and biogenesis. *Nature* 339(6220):147-149.
85. Nagayama K, *et al.* (2008) Antisense RNA inhibition of the beta subunit of the *Dictyostelium discoideum* mitochondrial processing peptidase induces the expression of mitochondrial proteins. *Biosci Biotechnol Biochem* 72(7):1836-1846.
86. Mukhopadhyay A, Hammen P, Waltner-Law M, & Weiner H (2002) Timing and structural consideration for the processing of mitochondrial matrix space proteins by the mitochondrial processing peptidase (MPP). *Protein Sci* 11(5):1026-1035.
87. von Heijne G, Steppuhn J, & Herrmann RG (1989) Domain structure of mitochondrial and chloroplast targeting peptides. *Eur J Biochem* 180(3):535-545.
88. Hurt EC, Allison DS, Muller U, & Schatz G (1987) Amino-terminal deletions in the presequence of an imported mitochondrial protein block the targeting function and proteolytic cleavage of the presequence at the carboxy terminus. *J Biol Chem* 262(3):1420-1424.
89. Vestweber D, Brunner J, Baker A, & Schatz G (1989) A 42K outer-membrane protein is a component of the yeast mitochondrial protein import site. *Nature* 341(6239):205-209.
90. Allison DS & Schatz G (1986) Artificial mitochondrial presequences. *Proc Natl Acad Sci U S A* 83(23):9011-9015.
91. Roise D & Schatz G (1988) Mitochondrial presequences. *J Biol Chem* 263(10):4509-4511.
92. Hendrick JP, Hodges PE, & Rosenberg LE (1989) Survey of amino-terminal proteolytic cleavage sites in mitochondrial precursor proteins: leader peptides cleaved by two matrix proteases share a three-amino acid motif. *Proc Natl Acad Sci U S A* 86(11):4056-4060.
93. Gavel Y & von Heijne G (1990) Cleavage-site motifs in mitochondrial targeting peptides. *Protein Eng* 4(1):33-37.

94. Song MC, Ogishima T, & Ito A (1998) Importance of residues carboxyl terminal relative to the cleavage site in substrates of mitochondrial processing peptidase for their specific recognition and cleavage. *J Biochem* 124(5):1045-1049.
95. Moriwaki K, Ogishima T, & Ito A (1999) Analysis of recognition elements for mitochondrial processing peptidase using artificial amino acids: roles of the intervening portion and proximal arginine. *J Biochem* 126(5):874-878.
96. Branda SS & Isaya G (1995) Prediction and identification of new natural substrates of the yeast mitochondrial intermediate peptidase. *J Biol Chem* 270(45):27366-27373.
97. Kitada S & Ito A (2001) Electrostatic recognition of matrix targeting signal by mitochondrial processing peptidase. *J Biochem* 129(1):155-161.
98. Horwich AL, Kalousek F, & Rosenberg LE (1985) Arginine in the leader peptide is required for both import and proteolytic cleavage of a mitochondrial precursor. *Proc Natl Acad Sci U S A* 82(15):4930-4933.
99. Horwich AL, Kalousek F, Fenton WA, Pollock RA, & Rosenberg LE (1986) Targeting of pre-ornithine transcarbamylase to mitochondria: definition of critical regions and residues in the leader peptide. *Cell* 44(3):451-459.
100. Nishi T, *et al.* (1989) Import and processing of precursor to mitochondrial aspartate aminotransferase. Structure-function relationships of the presequence. *J Biol Chem* 264(11):6044-6051.
101. Zhang XP, *et al.* (2001) Mutagenesis and computer modelling approach to study determinants for recognition of signal peptides by the mitochondrial processing peptidase. *Plant J* 27(5):427-438.
102. Horwich AL, *et al.* (1987) The ornithine transcarbamylase leader peptide directs mitochondrial import through both its midportion structure and net positive charge. *J Cell Biol* 105(2):669-677.
103. Cossee M, *et al.* (2000) Inactivation of the Friedreich ataxia mouse gene leads to early embryonic lethality without iron accumulation. *Hum Mol Genet* 9(8):1219-1226.
104. Shimokata K, Kitada S, Ogishima T, & Ito A (1998) Role of alpha-subunit of mitochondrial processing peptidase in substrate recognition. *J Biol Chem* 273(39):25158-25163.
105. Kitada S, Shimokata K, Niidome T, Ogishima T, & Ito A (1995) A putative metal-binding site in the beta subunit of rat mitochondrial processing peptidase is essential for its catalytic activity. *J Biochem* 117(6):1148-1150.



106. Kitada S, Yamasaki E, Kojima K, & Ito A (2003) Determination of the cleavage site of the presequence by mitochondrial processing peptidase on the substrate binding scaffold and the multiple subsites inside a molecular cavity. *J Biol Chem* 278(3):1879-1885.
107. Luciano P & Geli V (1996) The mitochondrial processing peptidase: function and specificity. *Experientia* 52(12):1077-1082.
108. Taylor AB, *et al.* (2001) Crystal structures of mitochondrial processing peptidase reveal the mode for specific cleavage of import signal sequences. *Structure* 9(7):615-625.
109. Nagao Y, *et al.* (2000) Glycine-rich region of mitochondrial processing peptidase alpha-subunit is essential for binding and cleavage of the precursor proteins. *J Biol Chem* 275(44):34552-34556.
110. Kojima K, Kitada S, Shimokata K, Ogishima T, & Ito A (1998) Cooperative formation of a substrate binding pocket by alpha- and beta-subunits of mitochondrial processing peptidase. *J Biol Chem* 273(49):32542-32546.
111. Luciano P, Geoffroy S, Brandt A, Hernandez JF, & Geli V (1997) Functional cooperation of the mitochondrial processing peptidase subunits. *J Mol Biol* 272(2):213-225.
112. Howe D, *et al.* (2008) Big data: The future of biocuration. *Nature* 455(7209):47-50.
113. Eisenstein M (2006) Microarrays: quality control. *Nature* 442(7106):1067-1070.
114. Zhang XHD (2011) *Optimal High-Throughput Screening: Practical Experimental Design and Data Analysis for Genome-scale RNAi Research* (Cambridge University Press).
115. Zhang XD, *et al.* (2008) Integrating experimental and analytic approaches to improve data quality in genome-wide RNAi screens. *J Biomol Screen* 13(5):378-389.
116. Zhang JH, Chung TD, & Oldenburg KR (1999) A Simple Statistical Parameter for Use in Evaluation and Validation of High Throughput Screening Assays. *J Biomol Screen* 4(2):67-73.
117. Hanahan D, Wagner EF, & Palmiter RD (2007) The origins of oncomice: a history of the first transgenic mice genetically engineered to develop cancer. *Genes Dev* 21(18):2258-2270.
118. Waterston RH, *et al.* (2002) Initial sequencing and comparative analysis of the mouse genome. *Nature* 420(6915):520-562.
119. Emes RD, Goodstadt L, Winter EE, & Ponting CP (2003) Comparison of the genomes of human and mouse lays the foundation of genome zoology. *Hum Mol Genet* 12(7):701-709.

120. Nagy A (2003) *Manipulating the mouse embryo: A laboratory manual* (Cold Spring Harbor Laboratory Press, Cold Spring Harbor, NY) 3rd Ed.
121. Davis K (2007) *Breeding Strategies for Maintaining Colonies of Laboratory Mice: A Jackson Laboratory Resource Manual* (The Jackson Laboratory, Bar Harbor, ME).
122. Lieschke GJ & Currie PD (2007) Animal models of human disease: zebrafish swim into view. *Nat Rev Genet* 8(5):353-367.
123. Koerber AS & Kalishman J (2009) Preparing for a semiannual IACUC inspection of a satellite zebrafish (*Danio rerio*) facility. *J Am Assoc Lab Anim Sci* 48(1):65-75.
124. Delvecchio C, Tiefenbach J, & Krause HM (2011) The zebrafish: a powerful platform for in vivo, HTS drug discovery. *Assay Drug Dev Technol* 9(4):354-361.
125. Laelle H (1977) The biology and use of zebrafish, *Brachydanio rerio* in fisheries research. *J Fish Biol* 10(2):121-174.
126. Zon LI & Peterson RT (2005) In vivo drug discovery in the zebrafish. *Nat Rev Drug Discov* 4(1):35-44.
127. Kimmel CB, Ballard WW, Kimmel SR, Ullmann B, & Schilling TF (1995) Stages of embryonic development of the zebrafish. *Dev Dyn* 203(3):253-310.
128. Stickney HL, Barresi MJ, & Devoto SH (2000) Somite development in zebrafish. *Dev Dyn* 219(3):287-303.
129. Westerfield M (2000) *The Zebrafish Book. A Guide for the Laboratory Use of Zebrafish (Danio rerio)* (University of Oregon Press, Eugene, Or) 4th Ed.
130. Tu S & Chi NC (2012) Zebrafish models in cardiac development and congenital heart birth defects. *Differentiation* 84(1):4-16.
131. Lawrence C (2007) The husbandry of zebrafish (*Danio rerio*): A review. *Aquaculture* 269(1-4):1-20.
132. Shafizadeh E, Huang H, & Lin S (2002) Transgenic zebrafish expressing green fluorescent protein. *Methods Mol Biol* 183:225-233.
133. Venter JC, *et al.* (2001) The sequence of the human genome. *Science* 291(5507):1304-1351.
134. Lu J, Peatman E, Tang H, Lewis J, & Liu Z (2012) Profiling of gene duplication patterns of sequenced teleost genomes: evidence for rapid lineage-specific genome expansion mediated by recent tandem duplications. *BMC Genomics* 13:246.

135. Lin F, *et al.* (2012) Transient and stable GFP expression in germ cells by the vasa regulatory sequences from the red seabream (*Pagrus major*). *Int J Biol Sci* 8(6):882-890.
136. Kennedy BN, Vihtelic TS, Checkley L, Vaughan KT, & Hyde DR (2001) Isolation of a zebrafish rod opsin promoter to generate a transgenic zebrafish line expressing enhanced green fluorescent protein in rod photoreceptors. *J Biol Chem* 276(17):14037-14043.
137. Clark KJ, Urban MD, Skuster KJ, & Ekker SC (2011) Transgenic zebrafish using transposable elements. *Methods Cell Biol* 104:137-149.
138. Kwan KM, *et al.* (2007) The Tol2kit: a multisite gateway-based construction kit for Tol2 transposon transgenesis constructs. *Dev Dyn* 236(11):3088-3099.
139. Fischer JA, Giniger E, Maniatis T, & Ptashne M (1988) GAL4 activates transcription in *Drosophila*. *Nature* 332(6167):853-856.
140. Scheer N & Campos-Ortega JA (1999) Use of the Gal4-UAS technique for targeted gene expression in the zebrafish. *Mech Dev* 80(2):153-158.
141. Huang CJ, Tu CT, Hsiao CD, Hsieh FJ, & Tsai HJ (2003) Germ-line transmission of a myocardium-specific GFP transgene reveals critical regulatory elements in the cardiac myosin light chain 2 promoter of zebrafish. *Dev Dyn* 228(1):30-40.
142. Finley KR, Davidson AE, & Ekker SC (2001) Three-color imaging using fluorescent proteins in living zebrafish embryos. *Biotechniques* 31(1):66-70, 72.
143. Amsterdam A, Lin S, & Hopkins N (1995) The *Aequorea victoria* green fluorescent protein can be used as a reporter in live zebrafish embryos. *Dev Biol* 171(1):123-129.
144. Zhu H & Zon LI (2004) Use of the DsRed fluorescent reporter in zebrafish. *Methods Cell Biol* 76:3-12.
145. Bowman TV & Zon LI (2010) Swimming into the future of drug discovery: in vivo chemical screens in zebrafish. *ACS Chem Biol* 5(2):159-161.
146. Chang S, *et al.* (2008) Identification of small molecules rescuing fragile X syndrome phenotypes in *Drosophila*. *Nat Chem Biol* 4(4):256-263.
147. Petrascheck M, Ye X, & Buck LB (2009) A high-throughput screen for chemicals that increase the lifespan of *Caenorhabditis elegans*. *Ann N Y Acad Sci* 1170:698-701.
148. Hong CC (2009) Large-scale small-molecule screen using zebrafish embryos. *Methods Mol Biol* 486:43-55.
149. Hill AJ, Teraoka H, Heideman W, & Peterson RE (2005) Zebrafish as a model vertebrate for investigating chemical toxicity. *Toxicol Sci* 86(1):6-19.

150. Wheeler GN & Brandli AW (2009) Simple vertebrate models for chemical genetics and drug discovery screens: lessons from zebrafish and *Xenopus*. *Dev Dyn* 238(6):1287-1308.
151. Ito T, *et al.* (2010) Identification of a primary target of thalidomide teratogenicity. *Science* 327(5971):1345-1350.

# **Chapter 2: Development and Implementation of a High-Throughput Screen for Mitochondrial Processing Peptidase**

## **Abstract**

Mitochondrial processing peptidase (MPP) is required for viability, and thus cannot be studied through traditional methods; alternative approaches must be utilized. To this end, high-throughput screening (HTS) allowed for the systematic and efficient identification of small molecule modulators that temporally affected protein function. We conducted an HTS assay utilizing recombinantly purified MPP, and a fluorescent probe with an MPP cleavage site from YDHA7, to screen over 130,000 compounds. From this screen, we identified a number of small molecules capable of modulating MPP activity. Here we present the details of the screening process, the identification and confirmation of the preliminary hit compounds, and the initial characterization conducted to identify the subset of molecules that appeared the most promising.

# Introduction

## Mitochondria & Mitochondrial Processing Peptidase

### *Mitochondrial Structure*

Mitochondria consist of four compartments: the outer membrane, the intermembrane space, the inner membrane and the matrix. (1) The mitochondrial genome is approximately 16,000 base pairs and encodes for 37 genes, which include: 22 tRNAs, 2 rRNAs, 13 proteins, and 1 untranslated region. (2) A majority of the proteins that are utilized in the mitochondria are encoded by the nuclear genome, translated in the cytosol and must be imported into the mitochondria. Depending on where these proteins are located within the mitochondria they follow a different protein translocation pathway.

### *Mitochondrial Import*

Proteins destined for the outer membrane or the intermembrane space first interact with the translocase of the outer membrane (TOM), which is comprised of 7 integral membrane proteins (Tom70p, Tom40p, Tom22p, Tom20p, Tom7p, Tom6p, and Tom5p). (3-6) Following this interaction, the imported proteins are segregated and sorted by the sorting and assembly mechanism (SAM complex), which consists of Sam50p and Mas37p. (7-9) For proteins that need to go to the inner membrane or the matrix, not only do they interact with the TOM complex, but they must also interact with one of the two translocases of the inner membrane (TIM complex). The two TIMs are TIM23, which is involved with proteins destined for the matrix and TIM22, which helps negotiate imported proteins to the inner membrane. (3, 4) The TIM23 is comprised

of 3 integral membrane proteins (Tim50p, Tim17p, and Tim23p), while TIM22 is composed 3 different integral membrane proteins (Tim54p, Tim22p, and Tim18p). (3, 4, 10-12)

Imported proteins functioning in the mitochondrial matrix typically possess a positively charged N-terminal mitochondrial targeting sequence (MTS) that directs them through the translocase machinery to the mitochondrial matrix. (4) Regarding the TIM23 complex, Tim17p and Tim23p make-up the pore of the complex, Tim50p acts as a guide for precursor proteins and Tim44p, Tim14p, mHsp70, and mGrpE function as the motor to attract the MTS to the complex and draw the precursor protein into the matrix for processing. (13-15) For precursor proteins imported into the mitochondrial matrix to fold and function properly, their MTS must first be cleaved off. This cleavage is accomplished by the matrix protease, mitochondrial processing peptidase (MPP). (16, 17)

### *Mitochondrial Processing Peptidase*

The MTS of precursor proteins is typically 20-60 amino acids long and MPP is the first of potentially several proteases responsible for cleaving and degrading the MTS. (16) MPP has been linked to the autosomal recessive degenerative disorder, Friedreich ataxia (FRDA), which affects 1:50,000 live births. (18) FRDA patients exhibit neurodegeneration of the spinal cord and hypertrophic cardiomyopathy, along with being plagued with muscle weakness in the extremities, loss of coordination, vision and hearing impairment, slurred speech, scoliosis, atrial fibrillation, and tachycardia. (19, 20) FRDA is caused by the dysfunction of a mitochondrial matrix protein, frataxin, which is cleaved in 2 sequential steps by MPP. (21-24)

MPP is a heterodimer of approximately 100 kDa, consisting of  $\alpha$  and  $\beta$  subunits. The proper functioning of MPP is reliant on both subunits, but only the  $\beta$  subunit contains the

metalloendopeptidase domain. (25) MPP is a member of the pitrilysin family of inverted zinc-binding proteases that include pitrilysin and 3 members of the insulin-degrading enzyme family. (25) The inverted zinc-binding domain is made up of the following structure; H-x-x-E-H-x<sub>76</sub>-E, with the zinc ion being coordinated via both His residues and the downstream Glu residue. The upstream Glu residue is responsible for the activation of water, which is necessary for cleavage of the precursor protein. (26-28) The optimal pH range for purified MPP activity is pH 7-8, with inactivation at lower pH. MPP is inhibited by EDTA and *o*-phenanthroline and activated by divalent cations (Co<sup>2+</sup>, Mn<sup>2+</sup>, Zn<sup>2+</sup> and Mg<sup>2+</sup>). (29-32) At low concentrations of metals the degree of MPP activation follows the following trend, Zn<sup>2+</sup> > Mn<sup>2+</sup> > Co<sup>2+</sup>; though unlike cobalt and manganese, excess zinc inhibits MPP activity. (33, 34)

The presequences MPP recognizes typically, but not universally, contain three key features: (1) a global positive charge, (2) an ability to form an amphiphilic  $\alpha$ -helix, and (3) an arginine residue typically at the -2, -3, or -10 position relative to the cleavage site. (35-38) Currently there are four identified cleavage motif models, which include: (1) the R-2 motif (xRx↓x[S/s]), (2) the R-3 motif (xRx[Y/x]↓[S/A/x]x), (3) the R-10 motif (xRx↓[F/L/I]xx[S/T/G]xxxx↓; the first cleavage is done by MPP at the -2 position, following by an MIP cleavage at the -10 position), and (4) the R-none motif (xx↓x). (39) Within the secondary structure of the MPP substrate, a common feature is the capability of forming a helix-linker-helix orientation, and typically this  $\alpha$ -helix disruptor is glycine and/or proline. (40, 41)



## Rational for High-Throughput Screen

This project represents a new direction in mitochondrial biogenesis studies. A major shortcoming in studying mitochondrial activity in biological systems is the lack of tools. Classic genetic approaches, used in mitochondrial biology in yeast and worms, rely on conditional mutants such as temperature-sensitive (ts) and overexpression mutants to induce changes in pathways, an approach that is not easily accomplished in mammalian cells. This approach often requires hours to switch from a permissive condition to a lethal condition and results in secondary perturbations, leading to global side effects. (42) Another method to study protein interaction pathways in organisms such as cultured cells, worms and flies is via down-regulation using RNAi, which alters gene expression. Similarly this method has a major drawback because its modulation can typically takes days to observe an effect and it causes significant global side effects. (43, 44) The goal of this project was to generate small molecule modulators for MPP that alter the proteolytic activity within minutes, with the aim of determining the role of MPP in the mitochondria in diverse cellular pathways from fungi to animals. (45) These tools will be important for altering regulated proteolysis *in vivo*. An ultimate goal is to develop a “toolbox” of small molecules to study the roles of these proteases by eliminating their immediate function. Modulating the quality control system will affect a broad range of mitochondrial functions and provide insight into how the mitochondrion controls diverse cellular processes. These small modulators will be discovered via a high-throughput screening (HTS) assay using purified recombinant MPP.

# Results

Obtaining purified MPP was the first necessity of this project. The MPP plasmid was expressed and purified using BL21 gold bacterial cells, auto-induction expression, and purified using Nickel beads against the His<sub>6</sub> tag on MPP. (46) Using BCA quantification, we determined the concentration of MPP was 33 mg/mL. The overall scheme of the HTS for purified recombinant MPP can be seen in Figure 2.1.

The essence of our high-throughput screening assay was to synthesize a small peptide around a known MPP cleavage site that also contained a flanking fluorophore and quencher moiety. From this, if the cleavage by MPP was inhibited, or stopped all together, the fluorescence would be minimal, while if MPP was able to cleave the peptide the fluorescence would increase significantly. Many of the known presequences of substrates for MPP are quite hydrophobic, but we set out to choose the most hydrophilic sequence, simply to increase the likelihood the peptide would be soluble in the HTS assay. We analyzed a number MTS amino acid sequences and settled on using a peptide modeled around the cleave site of YDHA7 (yeast potassium-activated aldehyde dehydrogenase) (Figure 2.2). Our lab is also interested in the study of polynucleotide phosphorylase (PNPase), which is a 3' → 5' exoribonuclease and poly-A polymerase located in the intermembrane space that regulates the import of RNA into mitochondria. (47) For this reason, we also obtained a synthesized peptide based on the proposed cleavage site of PNPase.

Using purified MPP, both synthetic peptides from JPT Peptide Technologies, and a flex station plate reader we set out to determine which of the peptides could be cleaved by MPP. MPP was found to only cleave the peptide modeled around YDHA7, therefore we moved forward with

this peptide for the rest of the pre-screening and the primary screen (Figure 2.3). The premise of the assay and the structure of the YDHA7 synthetic peptide can be seen in Figure 2.4. An assay was used to determine the optimal concentration of the purified recombinant MPP,  $2^+$  metal cation, synthetic peptide, and EDTA/*o*-phenanthroline concentration needed to completely inhibit MPP cleavage of the JPT peptide (Figure 2.5). From these results, we determined the optimal concentrations to use were: 128 nM MPP, 1 mM  $MnCl_2$ , and 12  $\mu M$  JPT synthetic peptide. Since MPP is a metalloendopeptidase, EDTA and *o*-phenanthroline were used to form the negative control for MPP. Their optimal concentrations were 4 mM and 0.04 mM, respectively. This assay was also used to determine if general protease inhibitors such as PMSF, STI, IAA, and a chymostatin/leupeptin/pepstatin cocktail were capable of inhibiting the cleavage of MPP and the JPT synthetic peptide; which were all negative. The  $K_m$  of the JPT synthetic peptide was found to be 13  $\mu M$ . Before the HTS could be conducted, we needed to determine the Z score for the MPP/JPT fluorogenic peptide assay so we could be confident with the HTS results. The Z score is calculated by examining a plate that consists of half positive and half negative control wells. Using the reading from the entire plate and Z score equation we determined that the Z score for this assay was 0.8. The maximum Z score is 1 and any value over 0.5 is believed to be a good HTS assay, therefore we were extremely confident that any hits we found from the primary screen and the “cherry-picked” re-screen would be indicative of compounds specific for modulating the MPP/JPT fluorogenic peptide assay.

Utilizing the robotic system screening system available at the Screening Center at the California Nanosystems Institute at UCLA, roughly 130,000 small molecules were investigated for their ability to modulate the cleavage activity of MPP on the JPT fluorogenic peptide (Figure 2.7). A sample of how each screening plate was laid out can be seen in Figure 2.6. Following the

re-screen of the “cherry-picked” compounds from the primary screen, we identified 88 inhibitor small molecules and no enhancer molecules. The fact that we failed to find any enhancer small molecules was not surprising as our assay only investigated the end-point fluorescence instead of looking at multiple points within the linear range of the JPT fluorogenic peptide cleavage assay. From these 88 inhibitors of MPP cleavage we roughly organized the compounds by central scaffolding (approximately 8-10 groups) and ordered approximately 30 compounds from the primary screen that did not possess moieties known to disrupt membrane integrity such as: nitro groups, halogen groups and other highly reactive groups. Figure 2.8 shows the compounds that we further investigated with non-automated JPT fluorogenic assays and Su9-DHFR cleavage assays, along with the groups each compound falls into.

Out of the compounds ordered, only one compound failed to inhibit the cleavage activity of MPP on the JPT fluorogenic peptide, compound 216 (F3257-0216). The non-automated fluorogenic assay was also used to determine the  $IC_{50}$  of these compounds; this data can be seen in Figure 2.9. Before moving further with these compounds we also wanted to make sure they did not cause general mitochondrial dysfunction, such as causing membrane depolarization, disrupting membrane integrity, or disrupting the electron transport chain and oxygen consumption. The ability of the compounds to elicit a depolarization in the outer mitochondrial membrane was assessed using the diS-C<sub>3</sub> assay. This assay uses the mitochondrial membrane potential sensitive probe 3,3'-dipropylthiadicarbocyanine iodide (diS-C<sub>3</sub>); under normal conditions of mitochondrial membrane polarization the diS-C<sub>3</sub> probe is taken up by the mitochondria and fluorescence signal in the solution is fairly low. If the membrane is depolarized, as seen when purified mitochondria are treated with CCCP, the probe is not within the mitochondria and the fluorescence signal in solution is significantly higher. (48-50) The

fluorescence difference between the test conditions (compound in 1% DMSO and 20  $\mu$ M CCCP [negative control]) was consistently greater than a 2-fold difference. All of the compounds were tested in this assay at both a concentration of 10 and 50  $\mu$ M. None of the small molecules caused a significant increase in the fluorescence signal as compared to DMSO only; a representative analysis of compound 199 (MB 50) can be seen in Figure 2.10.

Mitochondrial membrane integrity was assessed using purified wild-type GA74 mitochondria treated with either 25 or 100  $\mu$ M of each compound. Both supernatant and mitochondrial pellet fractions were then analyzed on a SDS-PAGE gel with coomassie staining. If proteins were seen in the supernatant lane then that drug was positive for disrupting mitochondrial membrane integrity. None of analyzed drugs were found to disrupt membrane integrity. The final test conducted on each drug to examine their ability to cause global mitochondrial dysfunction was an oxygen electrode test with purified mitochondria. Drugs that disrupted the ETC would have oxygen consumption rates similar to treatment with CCCP and not basal consumption like NADH treatment. Compound 993 was found to significantly increase the consumption of oxygen; therefore this compound was not further characterized.

The next aspect of characterizing these inhibitors of MPP activity was to test these compounds with other known substrates of MPP by non-fluorescence methods. Initially, the compounds were tested for their ability to inhibit the cleavage of [ $^{35}$ S] radiolabelled Su9-DHFR by purified recombinant MPP. Su9-DHFR is a fusion protein consisting of the MTS (Su9) of subunit 9 of mitochondria ATP synthase fused to mouse dihydrofolate reductase (DHFR). Under normal conditions, DHFR is located in the cytosol, but when fused to Su9 it is directed towards the mitochondrial matrix where it is processed by MPP, with 2 sequential cleavages. (51-54) Figure 2.11 shows a sample of some of the drugs (100  $\mu$ M) and their ability to inhibit the

protease activity of MPP (128 nM). According to this data all but one of the drugs (compound 160) were able to inhibit the cleavage of [<sup>35</sup>S] Su9-DHFR by MPP. The other drugs not displayed in this figure showed similar potency for inhibiting the activity of MPP. Following the cleavage of [<sup>35</sup>S] Su9-DHFR with purified recombinant MPP we investigated the ability of the drugs to inhibit the import of [<sup>35</sup>S] Su9-DHFR into purified wild-type GA74 mitochondria. This type of assay more closely exemplifies the natural state of MPP, since import is reliant on just the amount of endogenous MPP present in the purified mitochondria. Figure 2.12 shows a sample of some of the drugs (100 μM) and their ability to inhibit import of [<sup>35</sup>S] Su9-DHFR into purified GA74 mitochondria (50 μg/lane on the gel). A number of the compounds appeared to inhibit the import of [<sup>35</sup>S] Su9-DHFR: compounds 707, 546, 022, 113, 184, 247, 325, 132, 060, 515, 700, 004, and 238. Others did not appear to significantly inhibit the import of [<sup>35</sup>S] Su9-DHFR: compounds 589, 086, 051, 067, 146, 013, 340, 589, and 479.

To test whether the compounds were simply acting as a general import blocker, the drugs were examined for their ability to inhibit the import of ADP/ATP carrier protein (AAC). AAC is a 30 kD homodimeric protein responsible for importing ADP into the mitochondria, and exporting ATP out of the mitochondria into the cytosol following synthesis from oxidative phosphorylation. AAC is an integral membrane protein synthesized without a cleavage presequence. It instead contains internal targeting information. (55-57) The import and processing of AAC in the mitochondria is not contingent on the functioning of MPP, therefore we intended to use the import of AAC into purified GA74 mitochondria as a means to identify whether any of the small molecules were causing global import dysfunction (Figure 2.13). From the import of [<sup>35</sup>S] AAC it appears there are a number of compounds that did not appear to significantly inhibit the import of AAC: compounds 081, 100, 113, 546, 199, 707, 132, 060, 051,

067, 340, 819, 238, 515, and 700. There were several compounds that completely blocked the import of AAC: compounds 993, 247, 004, 160, 022, 325, and 184.

A protein of interest for our lab is PTEN induced putative kinase 1 (Pink1), which is synthesized as a 63 kDa protein that is cleaved by PARL between residues Ala103 and Phe104 resulting in a 43 kDa fragment. Within the topology of PINK1 there is an N-terminal mitochondrial localization sequence, a putative transmembrane sequence, a Ser/Thr kinase domain, and a C-terminal regulatory sequence. The protein has been found to localize to the outer membrane of mitochondria, but is found primarily in the cytosol. Experiments suggest the Ser/Thr kinase domain faces outward toward the cytosol, indicating a possible point of interaction with Parkin; which is believed to play a role in the clearance of dysfunctional mitochondria. (58-64) We determined recombinant MPP was capable of processing both human Pink1 (hPink1) and drosophila Pink1 (dPink1) (Figure 2.14). Following these results we examined the ability of small molecules to inhibit the import of hPink1 into GA74 mitochondria (Figure 2.15). The data showed a number of the compounds appeared to inhibit the import of [<sup>35</sup>S] hPink1 into the mitochondrion; compounds 184, 238, 004, 700, 199, 546, 707, 169, 819, 022, 132, 060, 325, 247, 113, 100, 340, 067, and 051. While several molecules did not appear to significantly inhibit the import of [<sup>35</sup>S] hPink1 into the mitochondrion: compounds 515, 003, 146, 479, and 081.

# Discussion

An HTS primary screen was conducted on recombinant MPP with the use of a JPT fluorogenic peptide modeled after the MPP cleavage site of YDHA7. Approximately 130,000 compounds were screened and out of those we identified 88 inhibitors of MPP (0.07%). When examining any re-screen data, one is looking for less than 0.1% of hits, which signifies that the relationship between the hit compounds and the molecule (purified MPP) of interest are not hugely promiscuous. Typically this type of assay, one wants to use a control protein to rule out general protease inhibitors, metal chelators or general oxidative compounds. We accomplished this by concurrently screening Prep (same general family as MPP), Erv1, and several yeast cell viability screens. Any overlapping compounds between the screens were omitted from further investigation. The lack of confirmation for the enhancers was not surprising since the assay was based on an end-point determination; it would be difficult to determine enhancers since the final fluorescence reading was done fairly close the maximum fluorescence reading for the peptide. For this primary screen to yield legitimate activators of MPP the screen would have had to been done at multiple time points within the linear region of the assay, but this was not feasible at the UCLA screening center.

After analyzing these molecules and grouping them based on general scaffolding, we ordered 28 compounds to be characterized further. Within these compounds, two main groups presented themselves: one centered on compounds containing a quinone/hydroquinone moiety, while the common substituent of the other group was a *para*-*t*-butyl phenol connected to a substituted benzene ring via a methyl imine moiety. We were able to confirm all 28 compounds using a non-automated version of the fluorogenic peptide assay, and a majority of the



compounds tested were capable of inhibiting the cleavage of [<sup>35</sup>S] Su9-DHFR as well as its import into GA74 mitochondria.

Parkinson's disease is a neurodegenerative disorder of the central nervous system, typified by movement-related symptoms resulting from the loss of dopamine-generating cells in the substantia nigra. (65) Recently two genes have been linked to familial forms of this disease, Pink1 and Parkin. (60) Drosophila studies revealed the two proteins function in the same pathway and that Pink1 is upstream of Parkin. (66-68) Under normal conditions Pink1 is quickly degraded, but under conditions where the mitochondrial membrane is depolarized Pink1 is stabilized. Once stabilized, Pink1 goes to the outer mitochondrial membrane where it recruits Parkin via its Ser/Thr kinase domain and results in the ubiquitination and degradation of senescent or damaged mitochondria. (60, 64) We were able to show MPP is capable of cleaving both human and drosophila Pink1. Previous work using RNAi has showed that decreasing the amount of MPP caused an increase in the accumulation of Pink1 on the mitochondrial surface. This increase in Pink1 accumulation caused an increase in Parkin recruitment and mitochondrial degradation. (69) Because of these results, we wanted to examine if our small molecule inhibitors of MPP could inhibit the mitochondrial import of hPink1. We found the following compounds were capable of inhibiting the import of Pink1: 184, 238, 004, 700, 199, 546, 707, 169, 819, 022, 132, 060, 325, 247, 113, 100, 340, 067, and 051; the majority of which fell into the two main scaffolds mentioned previously. From these groups we identified two candidate molecules for further study. The next phase of our characterization of MPP inhibitors was aimed primarily at compounds 819 (MitoBloCK-50) and 199 (MitoBloCK-51).

# Materials and Methods

**Reagents.** Chemical libraries and investigated compounds were obtained from Chembridge Corporation (San Diego, CA), Asinex Ltd (Moscow, Russia) and Life Chemicals (Burlington, Canada). All other reagents were purchased from Sigma-Aldrich, EMD Biosciences, MB Biomedicals, US Biological and JPT innovative peptide solutions. For the expression of MPP the following solutions were used: ZY media (10 g tryptone and 5 g yeast extract per 1 L), 20X NPS (0.5 M  $(\text{NH}_4)_2\text{SO}_4$ , 1 M  $\text{KH}_2\text{PO}_4$ , and 1 M  $\text{Na}_2\text{HPO}_4$ ), 50X 5052 (25 g glycerol, 2.5 g glucose, and 10 g  $\alpha$ -lactose per 100 mL), and 40% glucose (all solutions were autoclaved). For the purification of MPP the following solutions were used: 0.5 M Sodium phosphate pH 7.0, 4 M NaCl, 1X Equilibration/Wash buffer pH 7.0 (50 mM sodium phosphate buffer, 300 mM NaCl, and sterile filtered), 1X Wash Buffer pH 7.0 (50 mM sodium phosphate, 300 mM NaCl, 7.5 mM imidazole, and sterile filtered), and 1X Elution buffer pH 7.0 (50 mM sodium phosphate, 300 mM NaCl, 150 mM imidazole, and sterile filtered). For trypan blue assays, cultured HeLa cells were grown in DMEM high glucose medium (Invitrogen) with glutamine, sodium pyruvate, 10% FBS, and penicillin-streptomycin (complete medium).

**Expression and Purification of MPP.** The MPP plasmid (46) was transformed into BL21 gold bacterial cells for expression. A starter culture of MPP/BL21 gold was grown overnight at 37°C in ZYP-0.8G media (ZY media, 1 mM  $\text{MgSO}_4$ , 0.8% glucose, 1X NPS, and 1X of both ampicillin and chloramphenicol). The following day 500  $\mu\text{L}$  of starter culture was transferred to each 1 L flask of ZYP-5052 (1 mL  $\text{MgSO}_4$ , 1X 5052, 1X NPS, and 1X each of ampicillin and chloramphenicol) to initiate the auto-induction of MPP expression. Protein expression was conducted for 24 hours at 37°C, while shaking at 200 rpm. At the conclusion of protein

expression, the bacterial cells were collected by centrifugation (10 min., 7,000 xg, at 4°C) and cleansed with 0.9% NaCl. The pellet was then resuspended in 50 mL of cold equilibration/wash buffer. Once resuspended the bacteria cells were lysed using a microfluidizer (Microfluidics M-110P). The cell lysate was collected by centrifugation (10,000 xg, 30 min, 4°C) and then the supernatant was incubated with Nickel beads for 1 hour at 4°C. Following the incubation, the resin was washed 3 times with approximately 10-20 mL of 1X Wash buffer, transferred to a gravity-flow column, and eluted with 1X Elution buffer into 1 mL aliquots. A bicinchoninic acid (BCA) assay was conducted on each aliquot and the samples that contained the highest protein concentration were pooled and glycerol (20% final) was added. A final BCA assay was done on the pooled protein sample to determine the final protein concentration. Small aliquots were flash frozen with liquid nitrogen and stored at -80°C for later use. All steps of both expression and purification were examined via coomassie staining of a SDS-PAGE gel and western blot analysis (His<sub>6</sub> antibody).

**MPP/JPT Fluorogenic Peptide Assay.** Purified MPP was tested against a small synthetic peptide flanked on opposite sides by both a fluorophore and quencher from JPT. The synthetic peptide was modeled after the cleavage site of the presequence of the known MPP precursor YDHA7 (yeast potassium-activated aldehyde dehydrogenase). The synthetic peptide contained the following groups and amino acid sequence: 7-Methoxycoumarinyl-acetyl-LQLRYRFSHLPM-Lys (JPT)-NH<sub>2</sub>. The peptide has a molecular weight of 1,912.25 g/mol, was >80% pure based on HPLC, was supplied to use as a trifluoroacetate salt, stored at -20°C. All assays were monitored using a FlexStation Plate Reader (Molecular Devices) with constant shaking, for 90 min (at 2 min. intervals) at an excitation of 330 nm, an emission of 405 nm, and an auto cutoff of 325 nm (these values were determined based the literature provided by JPT for

their fluorophore/quencher combination). Different iterations of this assay were used to determine the optimal values for the following parameters that would be utilized in the HTS primary screen: MPP concentration, MnCl<sub>2</sub> concentration, EDTA concentration, *o*-phenanthroline concentration, and JPT fluorogenic peptide Km and concentration. Along with these values the assay was used to determine which divalent cation (Zn<sup>2+</sup>, Mg<sup>2+</sup>, or Mn<sup>2+</sup>) worked best for the MPP/JPT fluorogenic peptide assay, the Z-score of the assay (the difference between positive [DMSO only] and negative [with EDTA and *o*-phenanthroline] controls; a score of 1 indicating an ideal, and reliable assay), whether any common protease inhibitors were capable of inhibiting the cleavage of the fluorogenic peptide by MPP (e.g., PMSF, STI, IAA, and a chymostatin/leupeptin/pepstatin cocktail).

**High-Throughput Screening (HTS).** A primary screen of approximately 130,000 drug-like small molecules was conducted against purified recombinant matrix processing protease (MPP) in 384-well plates. All screening was performed with an integrated robotic screening platform with dynamic plate scheduling. Each plate was handled in a consistent pattern by robotics and timing of each step was tightly controlled. The primary chemical screen used fresh recombinant MPP (in buffer: 10 mM Hepes, pH 7.4, 50 mM NaCl, 0.01% BSA, and 1 mM MnCl) at a concentration of 128 nM. A Titertek multidrop (Beckman Coulter) was used to dispense 25 μL of MPP or 25 μL of MPP with 4 mM EDTA and 0.04 mM of *o*-phenanthroline (inactivated MPP due to metal chelation) into wells of a clear bottom 384-well plate (Greiner Bio One). A Biomek FX (Beckman Coulter) was used to pin transfer 0.5 μL of each drug compound (1 mM stock) or DMSO vehicle to their respective wells. The concentration of each drug compound was approximately 10 μM. After compound transfer to all plates they were allowed to incubate at 25°C in a humidified incubator for 1 hr. A Titertek mulidrop was used to dispense 15 μL of

fluorogenic peptide (7-Methoxycoumarinyl-acetyl-LQLRYRFSHLPM-Lys (JPT)-NH<sub>2</sub>, cleavage site modeled after the presequence of the known MPP precursor YDHA7) to each well; the final concentration of peptide was 12  $\mu$ M. Plates were incubated at 25°C in a humidified incubator for an additional 25 minutes. Following incubation the end-point fluorescence reading was conducted with an excitation of 330 nm, an emission of 405 nm, and an auto cutoff of 325 nm. An automated plate scheduler conducted all operations throughout the screening process to ensure consistency. MPP inhibitor compounds were chosen based on a cutoff of greater than 50% inhibition as compared to DMSO only treated controls; while MPP activator compounds were chosen based on a cutoff of greater than 130% activation as compared to DMSO only treated controls. Compounds that fit either of these conditions were then “cherry-picked,” pinned from their stock plates into new drugs plates that contained only the selected compounds, and re-screened against the same MPP/JPT fluorogenic peptide assay as used in the primary screen.

**Confirmation of Selected Small Molecules via Non-automation.** Compounds that were confirmed via the “cherry picked” screen were analyzed and placed in approximate groups based on common scaffold moieties. Using Lipinski’s rule of 5 and attempting to avoid compounds that contained functional groups that could potentially cause membrane disruption or ETC disruption, roughly 30-35 compounds were ordered from their respective companies. Using a non-automated version of the MPP/JPT fluorogenic peptide assay, all of the ordered compounds were tested for their ability to inhibit or activate MPP. A solution of MPP was made using the exact concentrations of protein, MnCl<sub>2</sub>, buffer components along with the exact same solution plus EDTA and *o*-phenanthroline. 1  $\mu$ L of JPT synthetic peptide was pipetted into each well (final concentration of 12  $\mu$ M). 10  $\mu$ M of drug or the corresponding amount of DMSO was added to separate aliquots of the MPP buffer solution. EDTA/*o*-phenanthroline was added in a separate

aliquot of MPP buffer solution with final concentrations of 4 mM and 0.04 mM, respectively. All samples were allowed to incubate for 1 hour in the dark with gentle shaking. 50  $\mu$ L of MPP with drug or DMSO only or MPP plus EDTA/*o*-phenanthroline solution was added to each well. Once the MPP solution was added the reaction was initiated, and the plate was transferred to the FlexStation. The fluorescence was monitored over an hour and a half (2 min. interval readings) using a FlexStation Plate Reader (Molecular Devices) with constant shaking at an excitation of 330 nm, an emission of 405 nm, and an auto cutoff of 325 nm. All samples were done in triplicate and analyzed with GraphPad Prism 5.

**Drug IC<sub>50</sub>.** The IC<sub>50</sub> for each compound was assessed using the MPP/JPT fluorogenic peptide assay. These assays were conducted in the same manner as described for the non-automated confirmation of each compound with one alteration. For each small molecule the concentration was varied from 0.01  $\mu$ M to 20  $\mu$ M. All small molecule concentrations were done in triplicate and analyzed with GraphPad Prism 5. The fluorescence was monitored over 90 min using a FlexStation Plate Reader (Molecular Devices) with constant shaking at an excitation of 330 nm, an emission of 405 nm, and an auto cutoff of 325 nm.

**diS-C<sub>3</sub> Membrane Depolarization Assay.** The ability for the small molecule modulators to affect the depolarization of the mitochondrial membrane was assessed using the mitochondrial membrane potential sensitive probe 3,3'-dipropylthiadicarbocyanine iodide (diS-C<sub>3</sub>) as previously described. (48, 49) Each compound (10 & 50  $\mu$ M) and CCCP (20  $\mu$ M) plus oligomycin (2  $\mu$ g/mL) was tested with the diS-C<sub>3</sub> compound on purified wild-type GA74 mitochondria.

**Mitochondrial integrity assays.** Frozen aliquots of yeast mitochondria were quickly thawed and then diluted to a concentration of 100 µg/mL in import buffer (0.6 M sorbitol, 2 mM KH<sub>2</sub>PO<sub>4</sub>, 60 mM KCl, 50 mM HEPES-KOH, 5 mM MgCl<sub>2</sub>, 2.5 mM EDTA, 5 mM L-methionine, pH 7.1) and incubated at 25°C for 5 minutes. Reactions were treated with DMSO (1% final concentration), drug, or CCCP and incubated for 30 minutes at 25°C. After 8,000 x g centrifugation for 5 minutes (mitochondrial reactions) or 100,000 x g centrifugation for 15 minutes (microsomal reactions), supernatants were collected and released proteins were subsequently TCA precipitated and suspended in reducing SDS sample buffer (2% SDS, 80 mM Tris-HCl pH 6.8, 10% glycerol, 0.002% bromphenol blue, and 5% BME. The pellets from each reaction after 8,000 or 100,000 x g spin were gently rinsed with BB7.4 buffer. The wash buffer was aspirated and pellets were resuspended in reducing SDS sample buffer. Aliquots from all samples were boiled for 10 minutes and resolved on SDS-PAGE gels. Gels were coomassie stained.

**Oxygen consumption assays.** Oxygen consumption of purified wild-type yeast mitochondria was measured using a Clark-type oxygen electrode as described previously. (70) Briefly, state II respiration was induced to a suspension of 100 mg/ml mitochondria in 0.23 M sucrose, 20 mM KCl, 20 mM Tris-HCl, 0.5 mM EDTA, 4 mM KH<sub>2</sub>PO<sub>4</sub> and 3 mM MgCl<sub>2</sub>, pH 7.2 by adding 2 mM NADH. The consumption rate was monitored for approximately 2 min. Small molecule or DMSO was added to a final vehicle concentration of 1% and respiration was measured for another approximately 2 min. Uncoupled respiration was achieved by adding 20 mM CCCP to the chamber.

***In-vitro* Su9-DHFR Cleavage Assay.** Before the cleavage assay with purified recombinant MPP, [<sup>35</sup>S]-methionine and cysteine labeled Su9-DHFR was made with the TNT Quick Coupled

Transcription/Translation kit (Promega). Each sample consisted of 8  $\mu\text{L}$  of Su9-DHFR/[ $^{35}\text{S}$ ] added to 12  $\mu\text{L}$  of MPP solution (solution included purified recombinant MPP at 128 nM final concentration, drug at 100  $\mu\text{M}$  final concentration (if added), 4 mM EDTA with 0.04 mM *o*-phenanthroline [final concentration; negative control], 1% DMSO [final concentration], and 1 mM  $\text{MnCl}_2$  [final concentration]). DMSO only, drugs, or EDTA/*o*-phenanthroline were incubated with MPP for an hour at room temperature before the addition of Su9-DHFR. 20  $\mu\text{L}$  aliquots were taken at 2, 5, and 10-minute time points; the reactions were quenched with the addition of Laemmli sample buffer and all samples were analyzed by SDS-PAGE and autoradiography.

**Mitochondria Purification.** Mitochondria were purified from GA74 or MAS1 ts yeast cells grown in YPEG as described in previous studies. (71, 72) After purification, the concentration was measured by BCA assay and mitochondria were stored at  $-80^\circ\text{C}$ . Mammalian mitochondria were purified from HeLA cells grown in DMEM as previously described in studies(73). After purification, the concentration was measured by BCA assay and the mitochondria were purified and used fresh for each import assay.

**Import of radiolabeled proteins into mitochondria.** Before import into purified mitochondria, [ $^{35}\text{S}$ ]-methionine and cysteine labeled precursor proteins were made with the TNT Quick Coupled Transcription/Translation kit (Promega). Imports of precursor proteins into purified yeast mitochondria were conducted based on established protocols. (71, 74) As the drug compounds were primarily only soluble in DMSO, a final concentration in each import reaction of 1% was used. Drugs in DMSO or DMSO vehicle only was added to the mitochondria (25-50  $\mu\text{g}/\text{mL}$ ) in import buffer and incubated for 15 min at  $25^\circ\text{C}$ . Imports were initiated with the addition of radio-labeled precursor and aliquots were removed at intervals during the reaction



time-course. Import was terminated with the addition of 25 µg/mL of trypsin or just placed on ice for those import reactions where carbonate extraction was performed. After 15 min, 200 µg/mL of soybean trypsin inhibitor was added to deactivate trypsin. Mitochondria were pelleted by centrifugation at 8,000 x g for 5 min. To investigate proteins that had not been inserted into the membrane a carbonate extraction step was performed without the use of trypsin as described previously. (75) For all imports, the mitochondria were disrupted in Laemmli sample buffer after the final centrifugation and analyzed by SDS-PAGE and autoradiography.

**Analysis and Statistics.** Unless otherwise stated, all results reported are representative of three experimental replicates. Quantitative analysis was performed in GraphPad Prism 5 software (GraphPad Software, Inc.) unless otherwise stated.

**Miscellaneous.** Western blotting was performed using standard protocols with polyclonal antibodies raised towards highly purified antigens. The PDI antibody was a mouse monoclonal antibody purchased from Abcam Inc. (Cambridge, MA). Proteins were transferred to nitrocellulose membranes and immune complexes were visualized with HRP labeled Protein A in a chemiluminescence assay (Pierce). Chemiluminescent imaging was performed on an Alpha Innotech (Santa Clara, CA) FluorChem FC2 workstation unless otherwise noted. Autoradiographic imaging was performed on film.

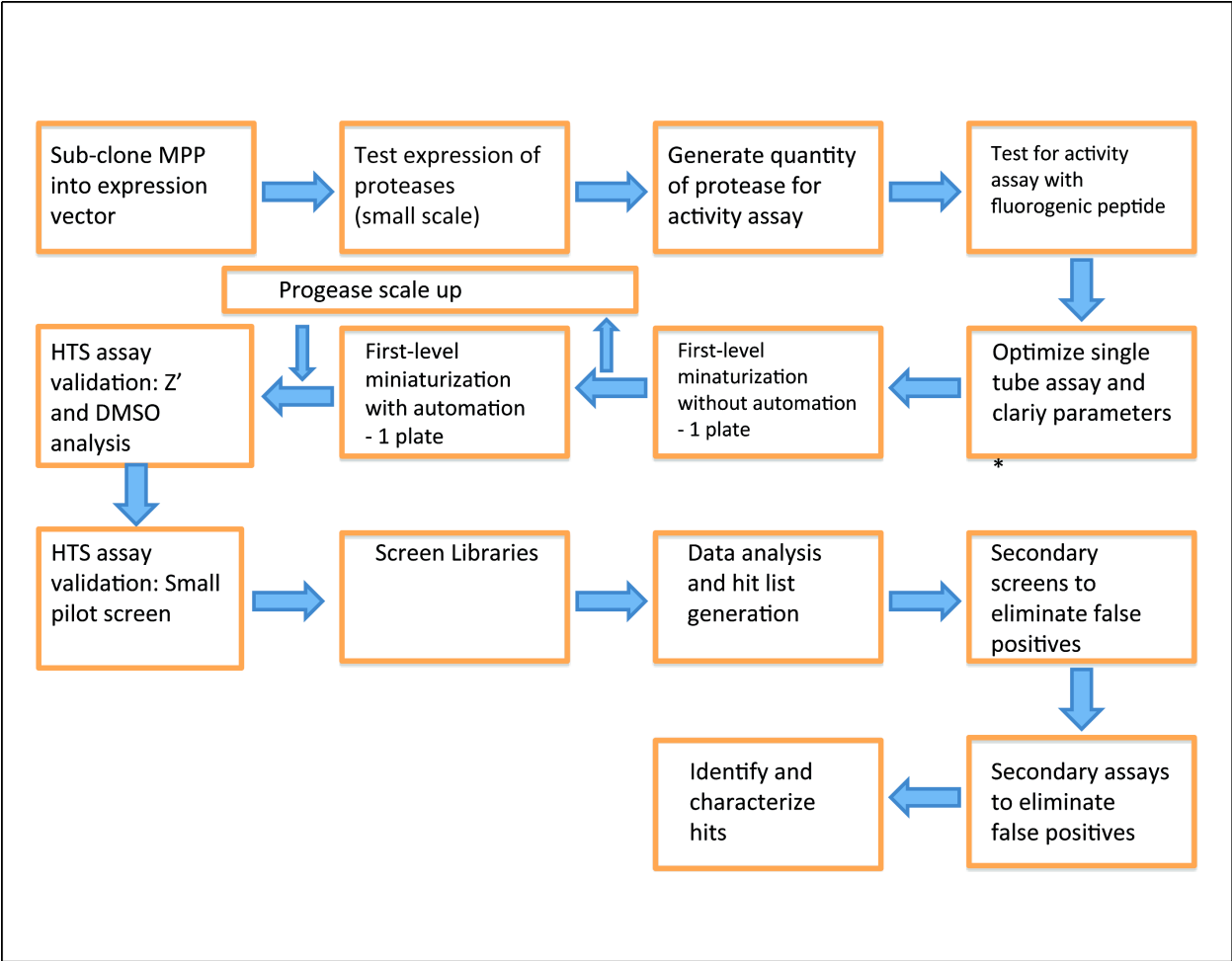


**Figure 2.1 Overall schematic flow-chart for MPP HTS.**

Step by step outline of the HTS to identify and characterize small molecule modulators of purified recombinant MPP.

## R-2 or R-3 Motif

		↓ MPP	
HMUT	MLRAKNQLFLLSPHYLRQVKESGSRLIQQRL		LHQQ....
HPDHE3	MQSWSRVYCSLAKRGHFNRIHGLQGLSAVPLRTY		ADQP....
MAAT	MALLHSGRVLGVSFAHPGLAAAASARA		SSWW....
RSCSA	MVSGSSGLAAARFFSRTFLLQQNGIRH		GSYT....
YCOX8	MLCQQMIRTTAKRSSNIMTRPIIMKRS		VHFK....
<b>YDHA7</b>	MFSRSTLCLKTSASSIGRLQLRYF		SHLP.... ← Used for assay
YIDH1	MLNRTIAKRTL		ATAA....
YRM02	MWNPILLDTSSFSFQKHVSGVFLQVRN		ATKR....

## R-10 Motif

		↓ IMP	
HOTC	MLFNLRILLNNAAFRNHGFNFMVRN	FRCGQPLQ	NKVQ....
MMDH	MLSALARPVGAALRRS	FSTSAQNN	AKVA....
NCPB	MFGPRHFSVLKTTGSLVSTFSSSLKPTATFSCARA	FSQTSSIM	SKVF....
YAT14	MFPIASRRILLNASVPLRLCNRN	FTTTRISY	NVIQ....
YCOXIV	MLSLRQSIREFFKPATRT	LCSSRYLL	QQKP....
YDLDH	MLRIRLLNKKRA	FSHSTVRTL	TINK....
YFe/S	MLGIRSSVKTCFKPMSLTSKRL	ISQSLLAS	KSTY....
YRM07	MQRFSVLVTHRS	FSHSCVKP	KSAC....

## No R-2, R-3, or R-10 Motif

BMPC	....NAPHLQLVHDGLAGPRSDPAGPPGPPRRSRNLAAA	AVEE....
HF0A	....GALRRLTPSAALPPAQLLLRAVRRRSHPVRYAAQ	TSPS....
NATP2	....GLISRSLGNSIPKSASRASSRASPGRLLNRAVQY	ATSA....
PCS	....MALLTAAARLFGAKNASCLVLAARHAS	ASST....
YATP6	....MFNLLNTYIT	SPLD....
YADH3	....MLRTSTLFTQRVQPSLFSRNILRLQST	AAIP..
YDHA1	....MLATRNLVPIIRASIKWRIKL	SALH....
YNDI1	....MLSKNLYSNKRLTSTNTLVRFASTR	STGV....
YRM04	....MWKRSFHSQGGPLR	ARTK....

## Figure 2.2 Examples of MPP and IMP Cleavage Motifs.

Common cleavage sites for MPP consist of an Arg residue at the -2, -3, or -10 positions relative to the cleavage site. As illustrated, this is not always the case as there are a number of MPP substrates that possess none of these common motifs. The space between different fragments of each MPP substrate signifies the cleavage site of either MPP or IMP as indicated by the arrow. A black horizontal arrow notes the MPP substrate we modeled our JPT synthetic peptide around. We chose YDHA7 due to the presence of more hydrophilic amino acids (both up- and downstream of the cleavage site) than the other sequences investigated.

BMPC – bovine mitochondrial phosphate carrier; HF0A – human F<sub>0</sub>-ATPase proteolipid subunit; HMUT – human methylmalonyl-CoA mutase; HOTC – human ornithine transcarbamylase; HPDHE3 – human pyruvate dehydrogenase E3 subunit; MAAT – mouse aspartate amino transferase; MMDH – mouse malate dehydrogenase; NATP2 – *Nicotiana plumbaginifolia* ATP synthase beta chain; NCPB – *N. crassa* cyclosporin-binding protein; PCS – pig citrate synthase; RSCSA – rat succinyl-CoA synthetase  $\alpha$  subunit; YADH3 – *S. cerevisiae* alcohol dehydrogenase III; YAT14 – *S. cerevisiae* ATP synthase H chain; YATP6 – *S. cerevisiae* ATP synthase A chain; YCOX4 – *S. cerevisiae* cytochrome *c* oxidase subunit IV; YCOX8 – *S. cerevisiae* cytochrome *c* oxidase subunit VIII; YDHA1 – *S. cerevisiae* aldehyde dehydrogenase; YDHA7 – *S. cerevisiae* potassium-activated aldehyde dehydrogenase; YDLDH – *S. cerevisiae* dihydrolipoamide dehydrogenase; YFe/S – *S. cerevisiae* ubiquinol–cytochrome *c* reductase Rieske iron–sulfur protein; YIDH1 – *S. cerevisiae* isocitrate dehydrogenase subunit 1; YNDI1 – *S. cerevisiae* rotenone-insensitive NADH-ubiquinone.

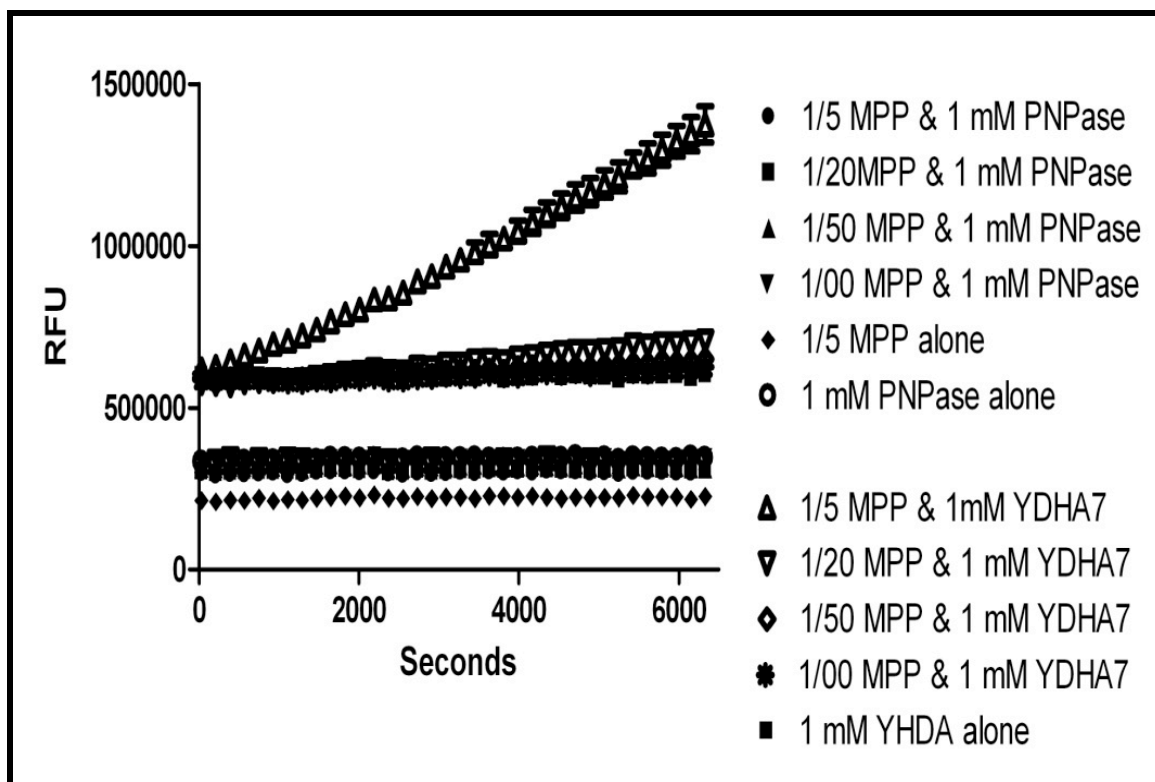


**Figure 2.3 MPP Cleavage of YDHA7 and PNPase Synthetic Peptides.**

1 mM of JPT peptide (YDHA7 or PNPase) was incubated with varying concentrations of purified recombinant MPP in screening buffer (10 mM Hepes, pH 7.4, 50 mM NaCl, 0.01% BSA) at 25°C with gentle shaking for 2 hrs. Individual readings were taken at 2 min intervals and the fluorescence signal was monitored at an excitation of 330 nm, an emission of 405 nm, and an auto cutoff of 325 nm. These values were chosen from the data provided by JPT to correspond to their fluorophore-quencher combination. Only the YDHA7 synthetic peptide was cleaved by MPP.

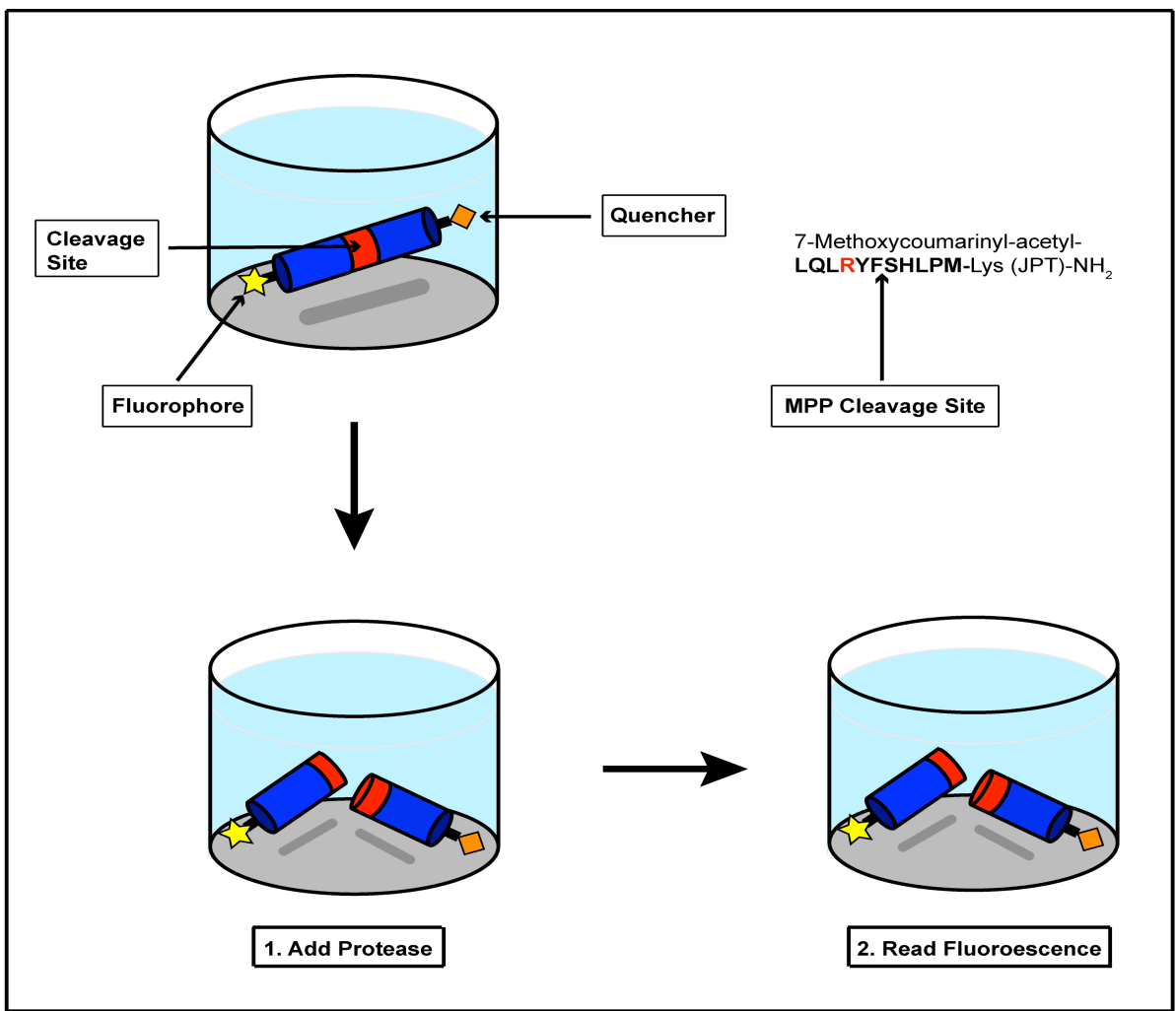


**Figure 2.4 Model of JPT Fluorogenic Peptide Assay.**

The fluorogenic peptide assay was design around evaluating the significant signal difference between the fluorescence of the un-cleaved verse the cleave JPT fluorogenic synthetic peptide. From the modeled cleavage of MPP and YDHA7, MPP was thought to cleave the synthetic peptide between phenylalanine and serine, with an arginine at the -2 position compared to the cleavage site. The JPT moiety in the synthetic peptide is proprietary therefore we are not aware of the exact structure of the quenching moiety of this peptide. The fluorophore/quencher pair of the JPT synthetic peptide has an excitation of 330 nm, an emission of 405 nm, and an auto cutoff of 325 nm.

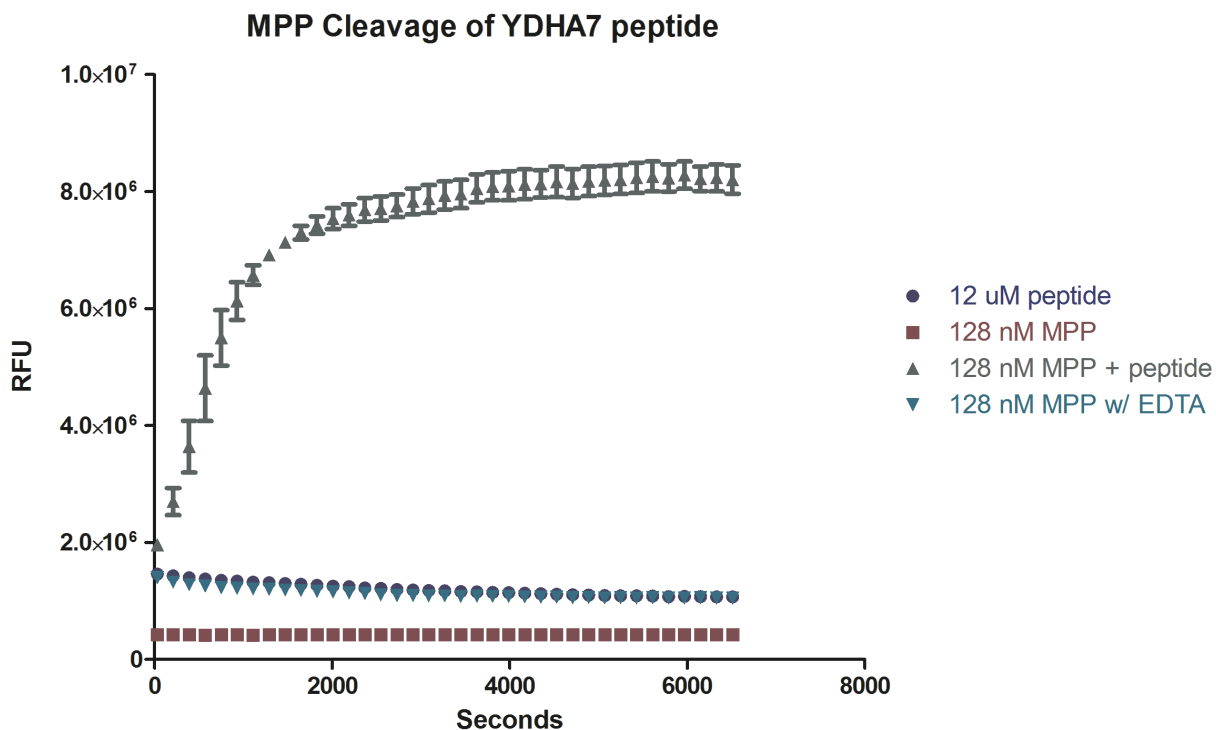


**Figure 2.5 Pre-Screen MPP/JPT Fluorogenic Peptide Assay.**

From the pre-screen data done for the HTS primary screen the optimal concentration of MPP was determined to be 128 nM, 1 mM  $\text{MnCl}_2$ , 12  $\mu\text{M}$  JPT peptide. Inhibition of MPP was achieved with 4 mM and 0.04 mM of EDTA and o-phenanthroline, respectively. This assay determined the Z-score for the assay was 0.8, signifying the assay has a high degree of confidence. The  $K_m$  of the JPT synthetic peptide was determined to be 13  $\mu\text{M}$ .

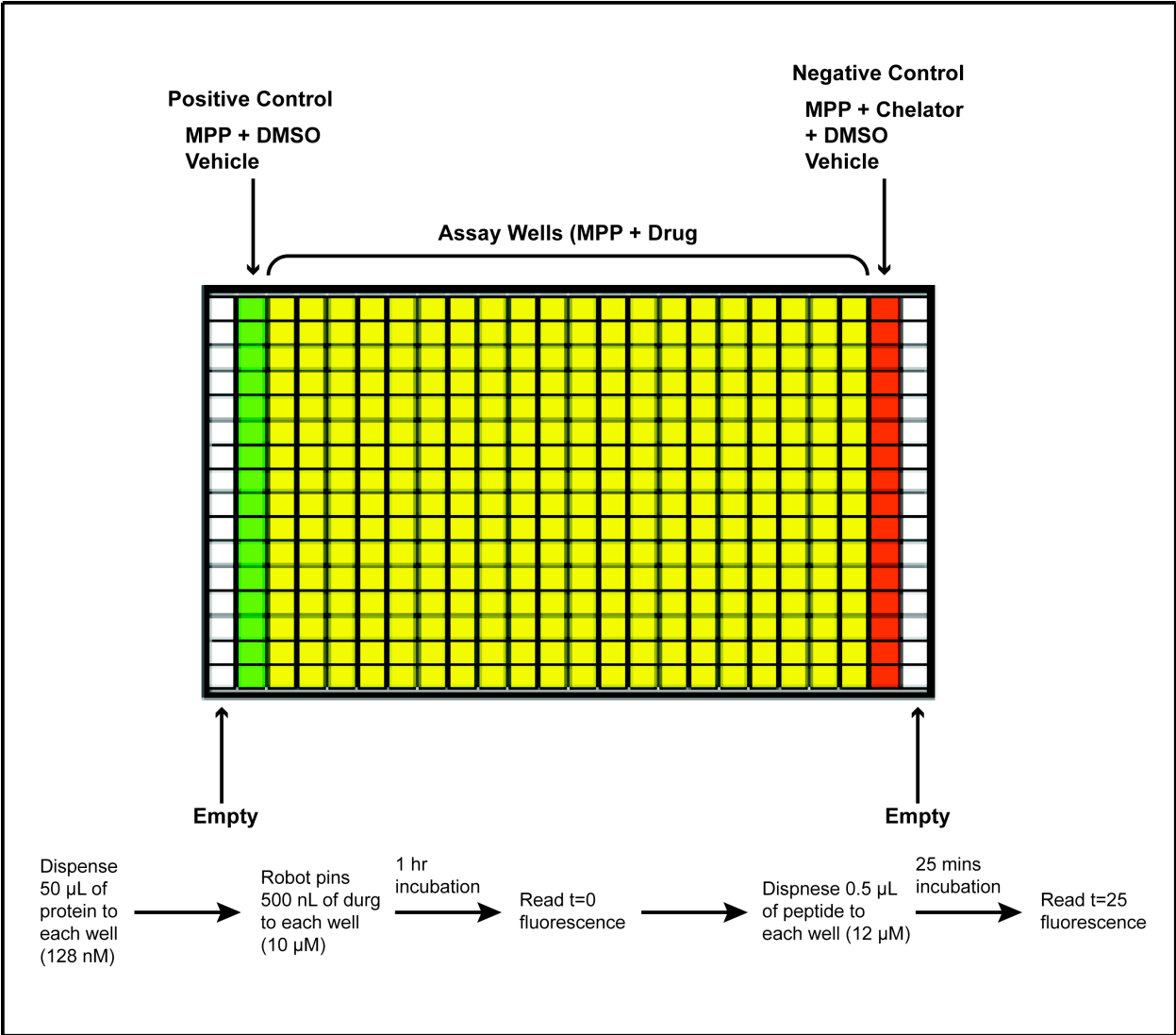




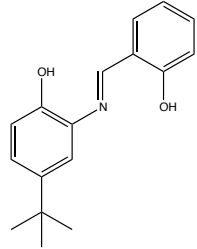
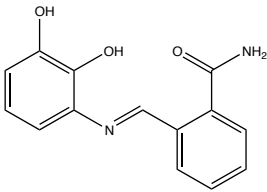
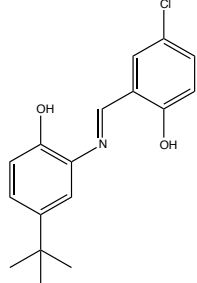
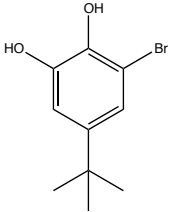
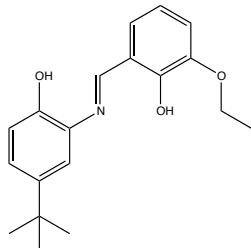
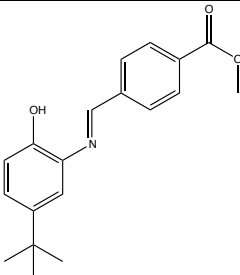
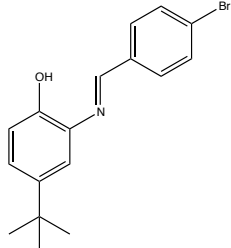
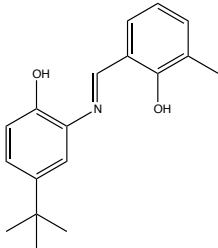
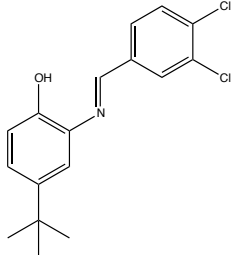
**Figure 2.6 Layout for HTS Plates & Sequence for Dispensing of Solutions and Compounds.**

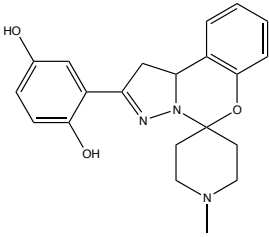
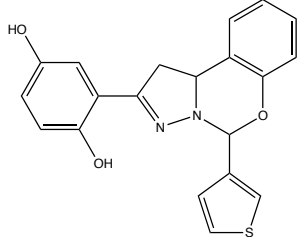
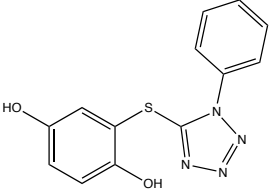
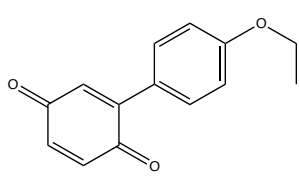
Due to edge effects no samples were placed in the first or the last column of the plate. The positive control (MPP + DMSO vehicle) was placed in the second column and the negative control (MPP + EDTA & *o*-phenanthroline + DMSO vehicle) was placed in the second to last column. Each drug was pinned into the remaining wells. 128 nM solution of MPP was initially incubated at 25°C in an incubator for 1 hour with drug, DMSO only, or EDTA & *o*-phenanthroline. A  $\text{time}_0$  fluorescence reading was taken after the hour incubation and then the JPT synthetic peptide was dispensed into each well. Once the peptide was added the reaction was started and allowed to incubate at 25°C in an incubator for 25 minutes, after which point the  $\text{time}_{25}$  fluorescence reading was acquired. This data was analyzed for each plate using Excel to identify MPP modulators.

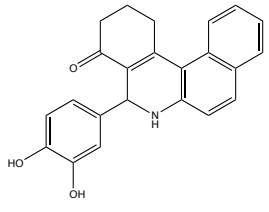
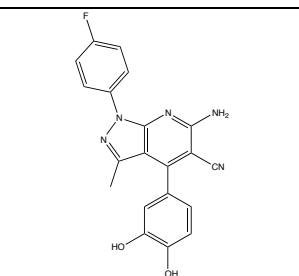
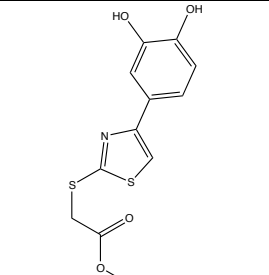
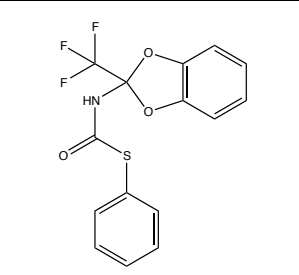
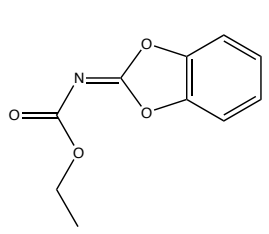
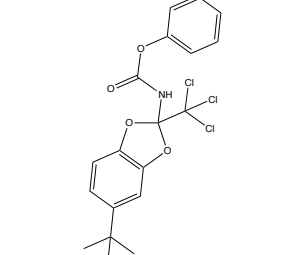
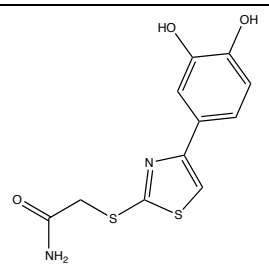
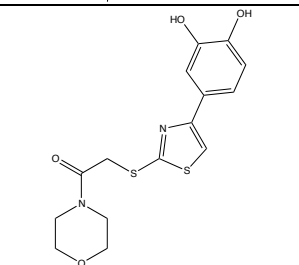
Library	# of Plates/ Compounds	Enhancers	Inhibitors	Confirmed Enhancers	Confirmed Inhibitors
TAR	27 / 8,640	0	3	0	0
DL	62 / 19,840	8	7	0	1
MS	7 / 2,240	0	5	0	5
PW	4 / 1,280	1	3	0	3
SS	8 / 2,560	1	1	0	1
NIH	2 / 640	0	0	0	0
ESI	6 / 1,920	0	1	0	0
UCLA	94 / 29,760	27	49	0	39
EAM	64 / 20,480	4	17	0	1
NEW	125 / 40,000	5	72	0	38
<b>Total</b>	<b>127,360</b>	<b>46</b>	<b>158</b>	<b>0</b>	<b>88</b>
<b>Hit rate (%)</b>		<b>0.036</b>	<b>0.12</b>	<b>0.0</b>	<b>0.07</b>

**Figure 2.7 Statistics for HTS for MPP cleavage of JPT Fluorogenic Peptide.**

Using the MPP/JPT fluorogenic peptide assay, approximately 130,000 small molecules were assayed for their ability to modulate the activity of MPP cleavage. According to the primary screen, 46 enhancers and 158 inhibitors were discovered. After the compounds were “cherry-picked” and rescreened using the same fluorogenic assay, none of the enhancers were confirmed and 88 (0.07%) of the inhibitors were confirmed.

Group	Structure	Order Number	pKa	Structure	Order Number	pKa
MB50		5309819	8.35		5320340	8.65
MB50		5302993	8.09		5216515	8.46
MB50		5311238	8.46		5302700	8.53
MB50		5305051	8.50		5488067	8.44
MB50		5305930	8.53			

MB51		F2801-0199	8.27		F2804-0325	9.04
MB51		5406184	8.80		5406172	-4.85

other		5213707	8.86		F3225-8247	8.28
other		F3358-0060	-5.74		F1023-0100	14.00
other		F1023-0086	8.86		F1023-0022	13.00
other		F3328-0146	8.66		F3328-0132	8.86

other		F1023-0113	7.62		F1798-0479	9.26
other		F2359-0160	2.75		5213721	9.23
other		T5902004	9.20		F3257-0216	6.78
other		F3282-0003	9.2			

**Figure 2.8 Small Molecules Ordered from MPP HTS.**

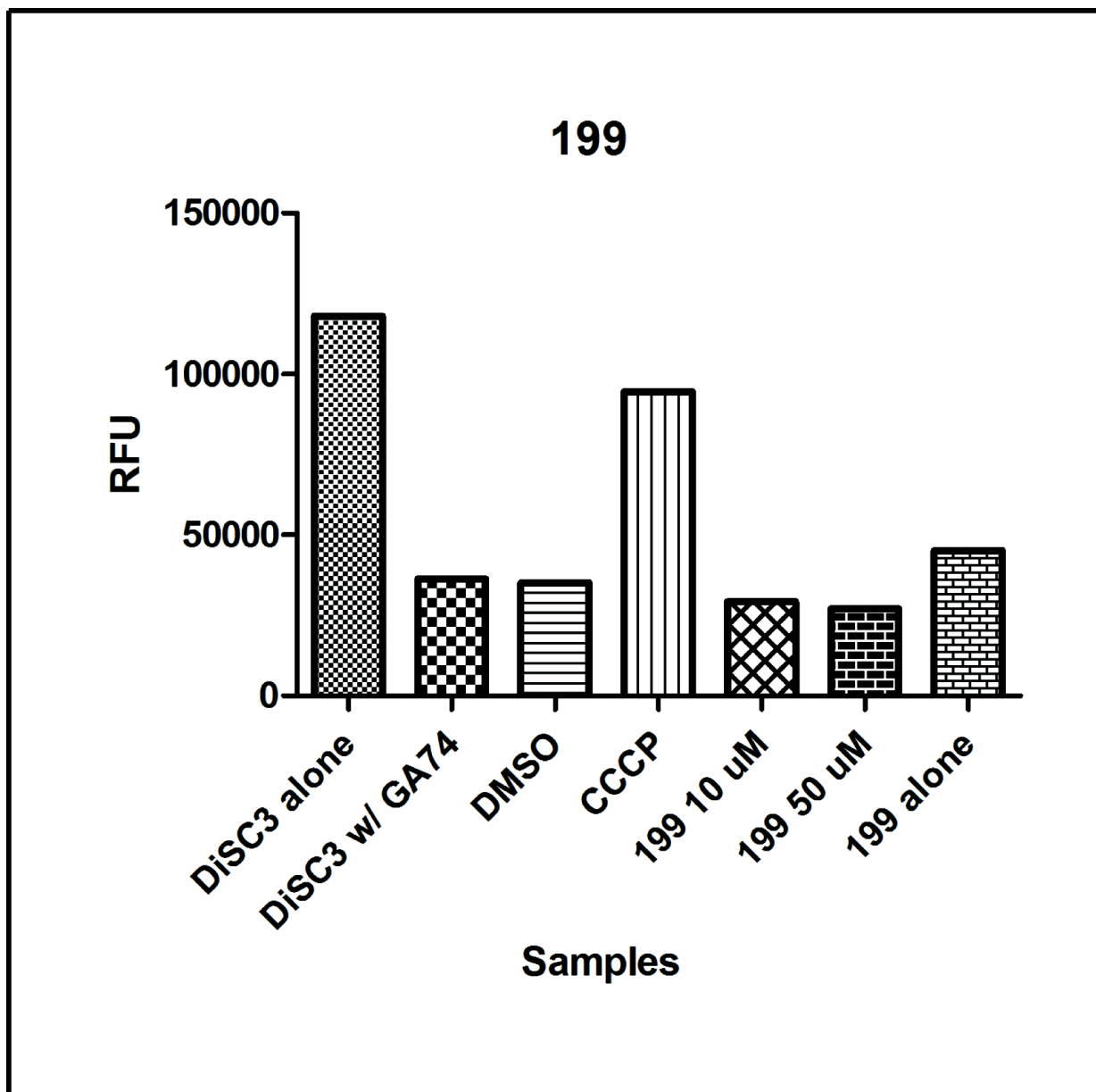
These are the structures of the small molecules that were ordered and further characterized.

Compounds within table are grouped into 3 broad categories based on scaffold structure. These categories consisted of those compounds similar to MB 50, MB 51, and the others ordered. The table also includes the order number and pKa for each compound.

Compound Number	IC <sub>50</sub> (μM)	Compound Number	IC <sub>50</sub> (μM)	Compound Number	IC <sub>50</sub> (μM)
819	1.3	340	0.13	993	0.05
515	1.9	238	0.83	700	0.95
051	3.4	067	2.1	930	1.1
199	0.54	325	0.33	184	2.6
172	4.5	707	0.54	247	7.9
060	3.2	100	1.4	086	5.5
022	1.7	146	6.3	132	2.8
113	1.6	479	4.5	160	8.4
721	4.8	004	2.9	216	5.1
003	9.7				

**Figure 2.9 IC<sub>50</sub> Data for MPP inhibitors.**

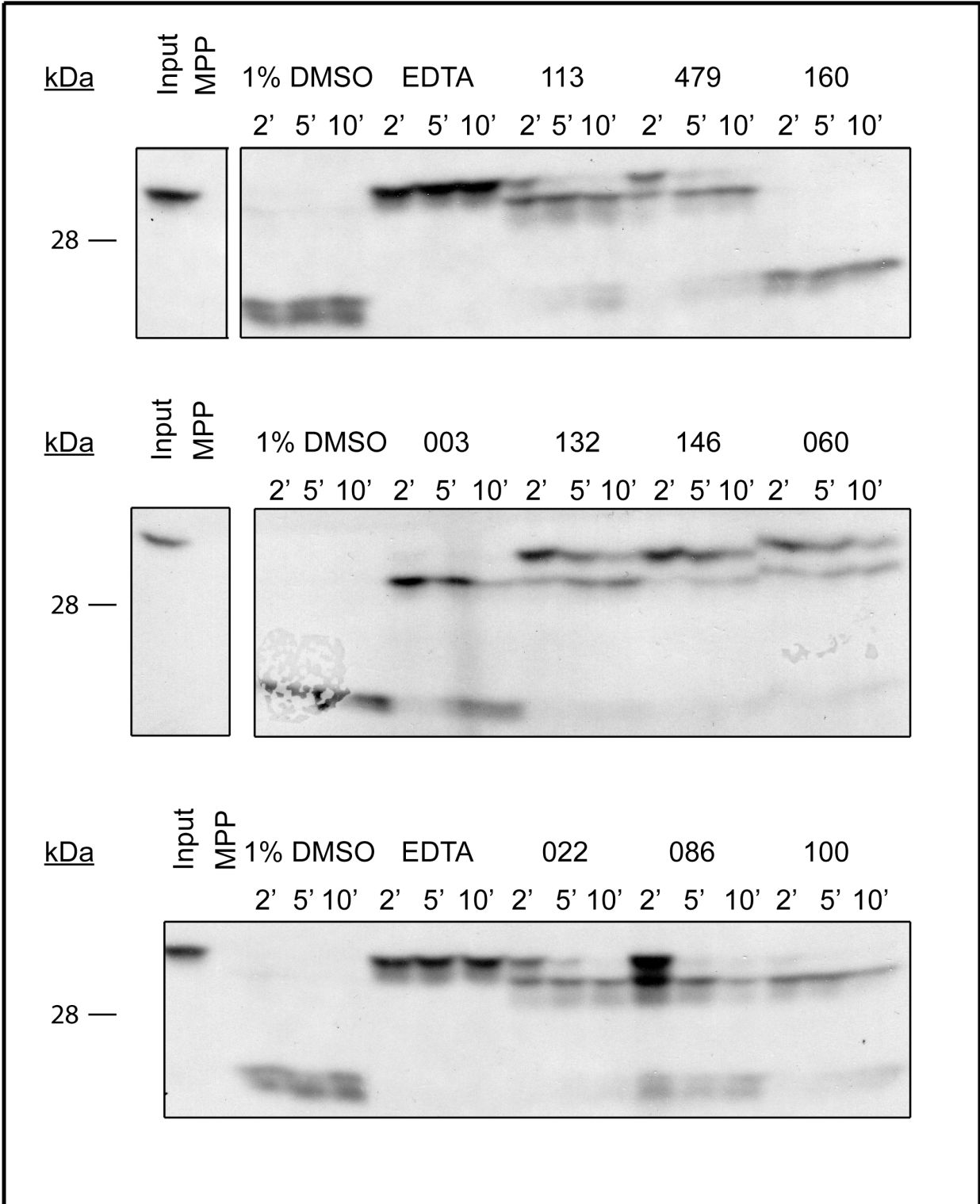
Using the parameters from the HTS assay as a baseline, the IC<sub>50</sub> for each drug was determined using 128 nM MPP (in screening buffer), 1mM MnCl<sub>2</sub>, 12 μM JPT peptide, and varying drug concentrations. All of the IC<sub>50</sub> values were determined to be in the low micromolar to submicromolar range.



**Figure 2.10 DiS-C<sub>3</sub> Assay for MPP Small Molecule 199.**

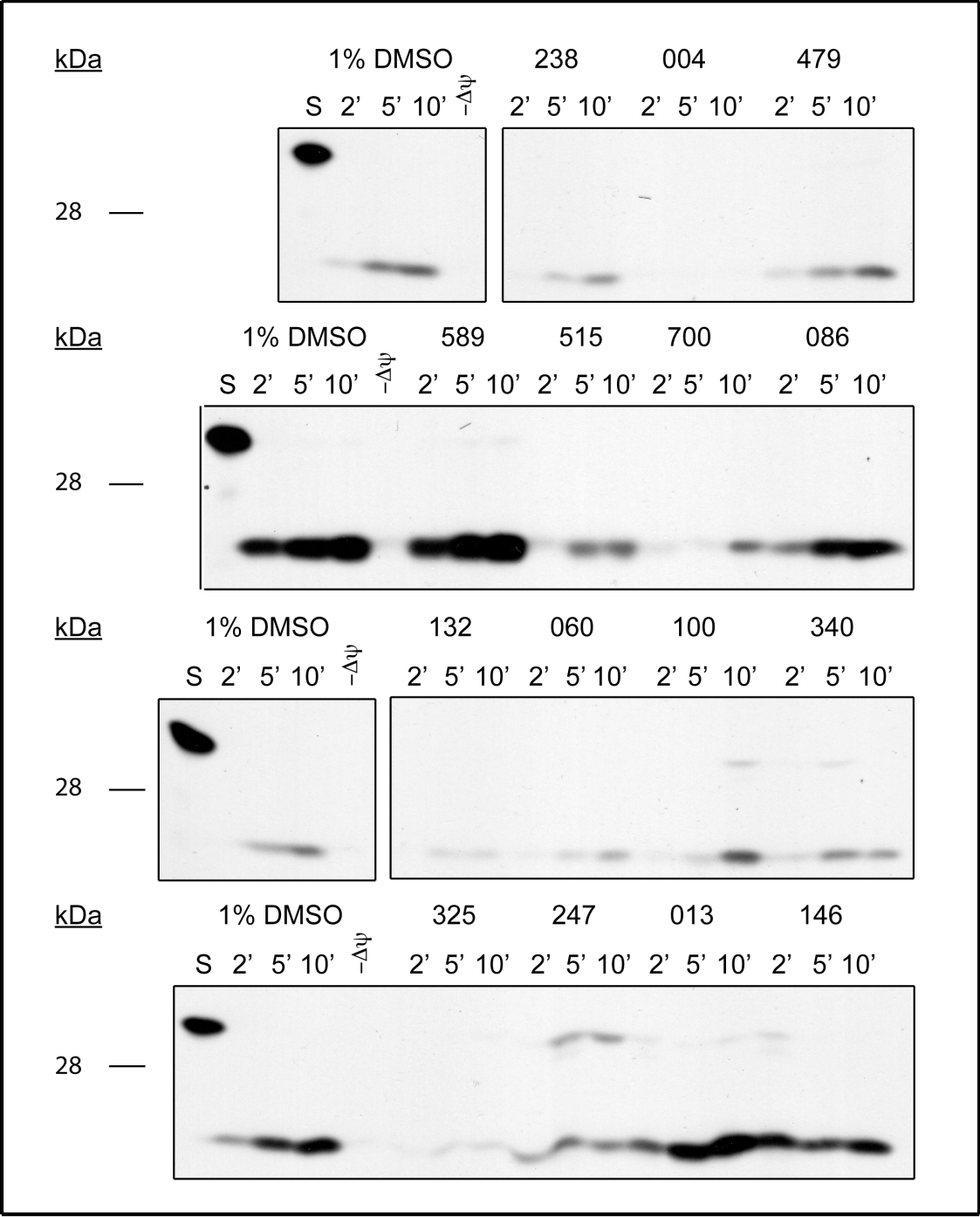
Purified wild-type GA74 yeast mitochondria were treated with diS-C<sub>3</sub> probe alone, diS-C<sub>3</sub> plus DMSO, 20  $\mu$ M CCCP and 2  $\mu$ g/mL oligomycin, or 10 or 50  $\mu$ M of compound 199. The fluorescent signals of the diS-C<sub>3</sub> probe and compound 199 were also investigated. The diS-C<sub>3</sub> probe absorbs at 651 nm, and emits at 675 nm. All conditions were repeated in triplicate and GraphPad Prism 5 was used to analyze the data.





**Figure 2.11 MPP Cleavage of [<sup>35</sup>S] Su9-DHFR with Drugs & EDTA.**

[<sup>35</sup>S] Su9-DHFR was synthesized using a TNT Quick Coupled Transcription/Translation kit. MPP (128 nM [screening buffer], 1 mM MnCl<sub>2</sub>) was incubated for 1 hr in the dark with 1% DMSO, 4 mM EDTA & 0.04 mM *o*-phenanthroline, or 100 μM of drug. Each reaction consisted of a ratio of 8 μL of [<sup>35</sup>S] Su9-DHFR solution to 12 μL of MPP solution with DMSO, drug, or EDTA. 2, 5, and 10-minute time points were taken for each condition. All drugs except compound 160 appeared to significantly inhibit the cleavage of [<sup>35</sup>S] Su9-DHFR by MPP. Compound 086 appeared to inhibit this cleavage but not as severely as the other drugs. Su9-DHFR is cleaved twice by MPP; EDTA appeared to inhibit any processing of [<sup>35</sup>S] Su9-DHFR by MPP, while the drugs appeared to primarily work by inhibiting the second site of processing for Su9-DHFR.



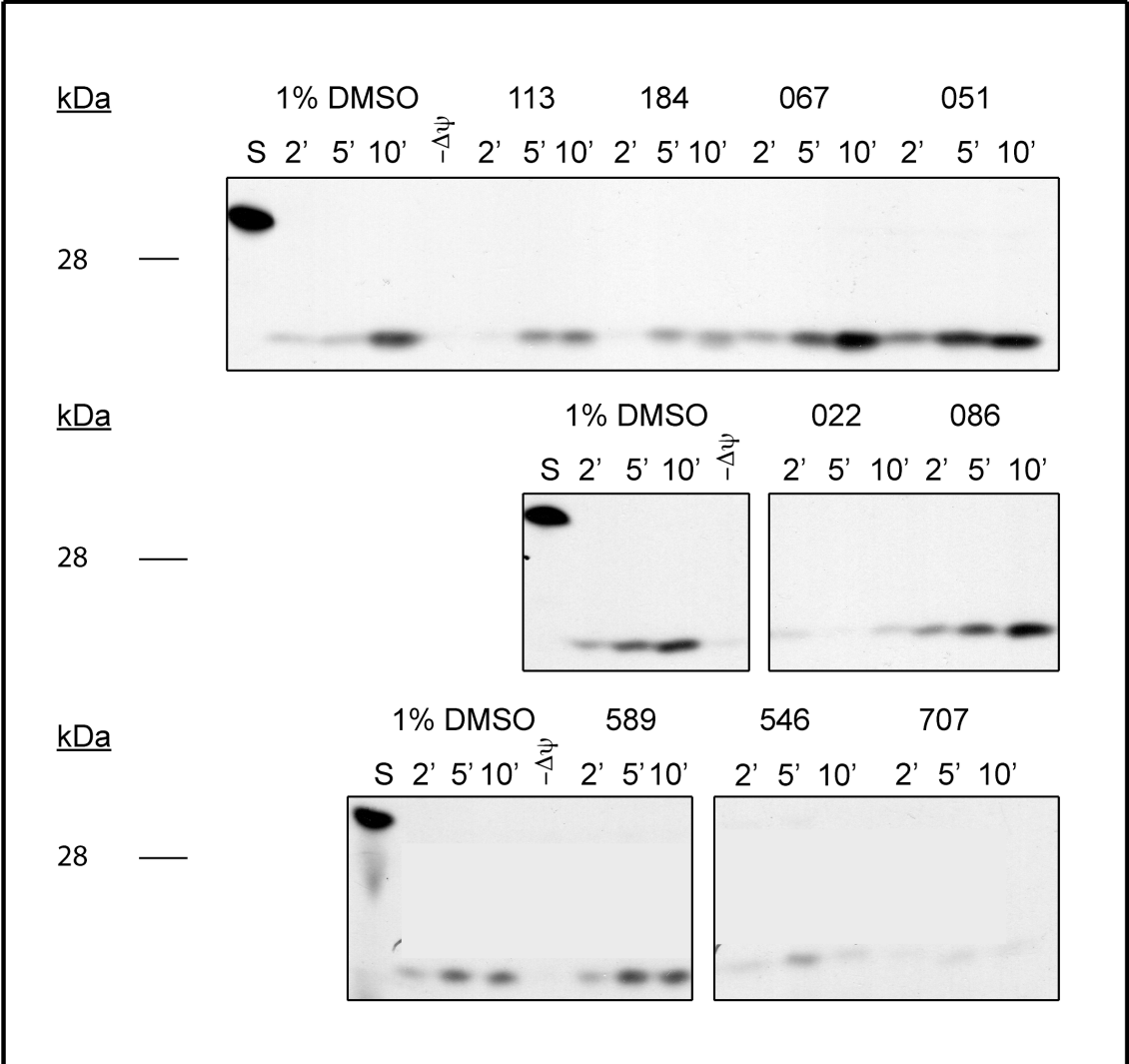


**Figure 2.12 [<sup>35</sup>S] Su9-DHFR Import into Purified Yeast Mitochondria.**

[<sup>35</sup>S] Su9-DHFR was synthesized using a TNT Quick Coupled Transcription/Translation kit. GA74 yeast mitochondria were treated with 1% DMSO, 50 μM CCCP & 1 mg/mL valinomycin, or 100 μM of Drug for 15 minutes at 25°C. 10 μL of [<sup>35</sup>S] Su9-DHFR solution/reaction time point was added to each condition and 250 μL aliquots were taken at each of 3 time points (2, 5, and 10 minutes). Reactions were quenched on ice by adding 50 μg/mL of trypsin. All imports were disrupted in Laemmli sample buffer and analyzed by SDS-PAGE and autoradiography. A number of the compounds appeared to inhibit the import of [<sup>35</sup>S] Su9-DHFR (compounds 707, 546, 022, 113, 184, 247, 325, 132, 060, 515, 700, 004, and 238), while others did not appear to significantly inhibit the import of [<sup>35</sup>S] Su9-DHFR (compounds 589, 086, 051, 067, 146, 013, 340, 589, and 479).

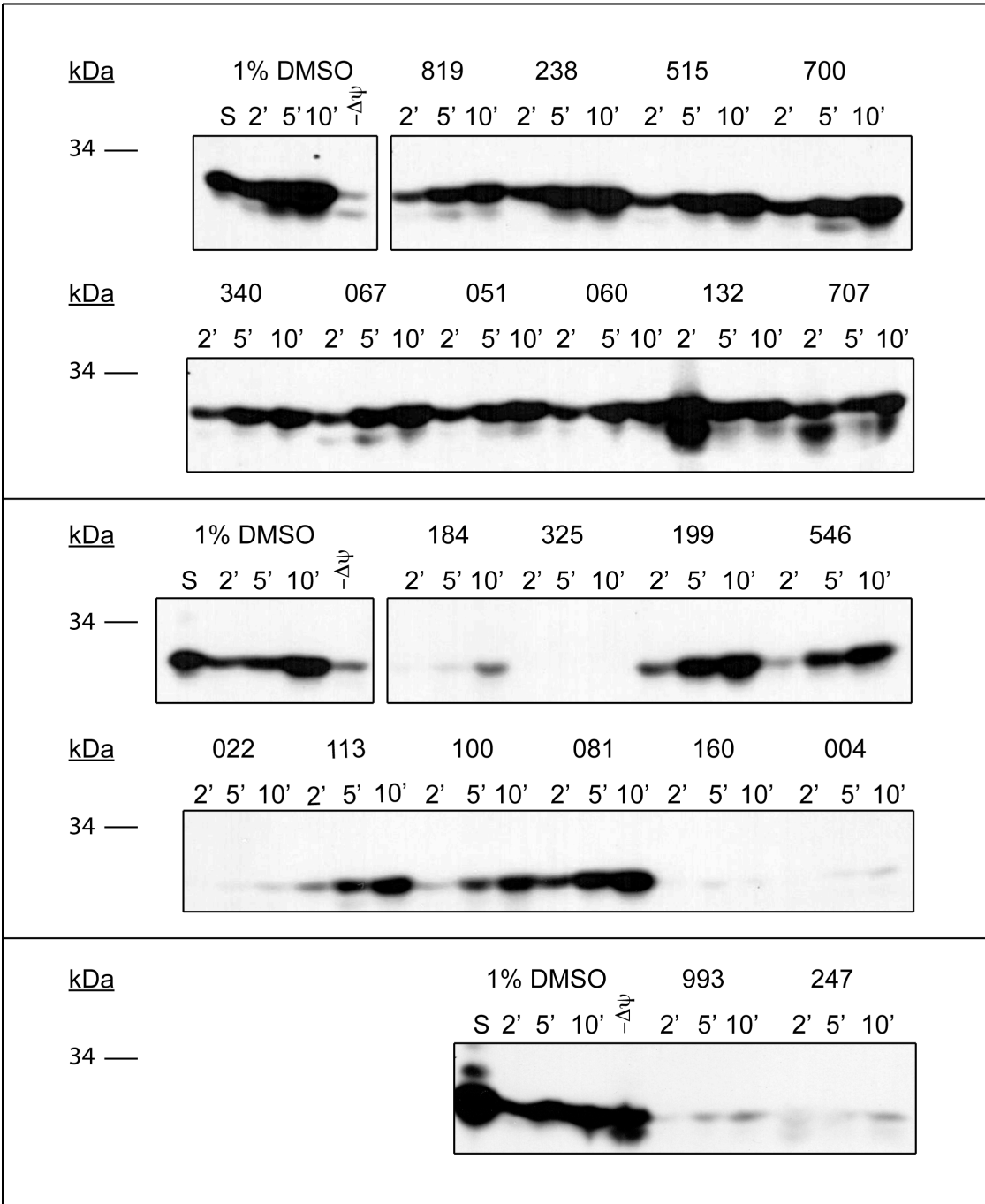


**Figure 2.13 [<sup>35</sup>S] AAC Import into Purified Yeast Mitochondria.**

[<sup>35</sup>S] AAC was synthesized using a TNT Quick Coupled Transcription/Translation kit. GA74 yeast mitochondria were treated with 1% DMSO, 50 μM CCCP & 1 mg/mL valinomycin, or 100 μM of Drug for 15 minutes at 25°C. 10 μL of [<sup>35</sup>S] AAC solution/reaction time point was added to each condition and 250 μL aliquots were taken at each of 3 time points (2, 5, and 10 minutes). Reactions were quenched on ice by adding 50 μg/mL of trypsin. All imports were disrupted in Laemmli sample buffer and analyzed by SDS-PAGE and autoradiography. A number of compounds did not appear to significantly inhibit the import of AAC (compounds 081, 100, 113, 546, 199, 707, 132, 060, 051, 067, 340, 819, 238, 515, and 700), while there were several compounds that completely blocked the import of AAC (compounds 993, 247, 004, 160, 022, 325, and 184).

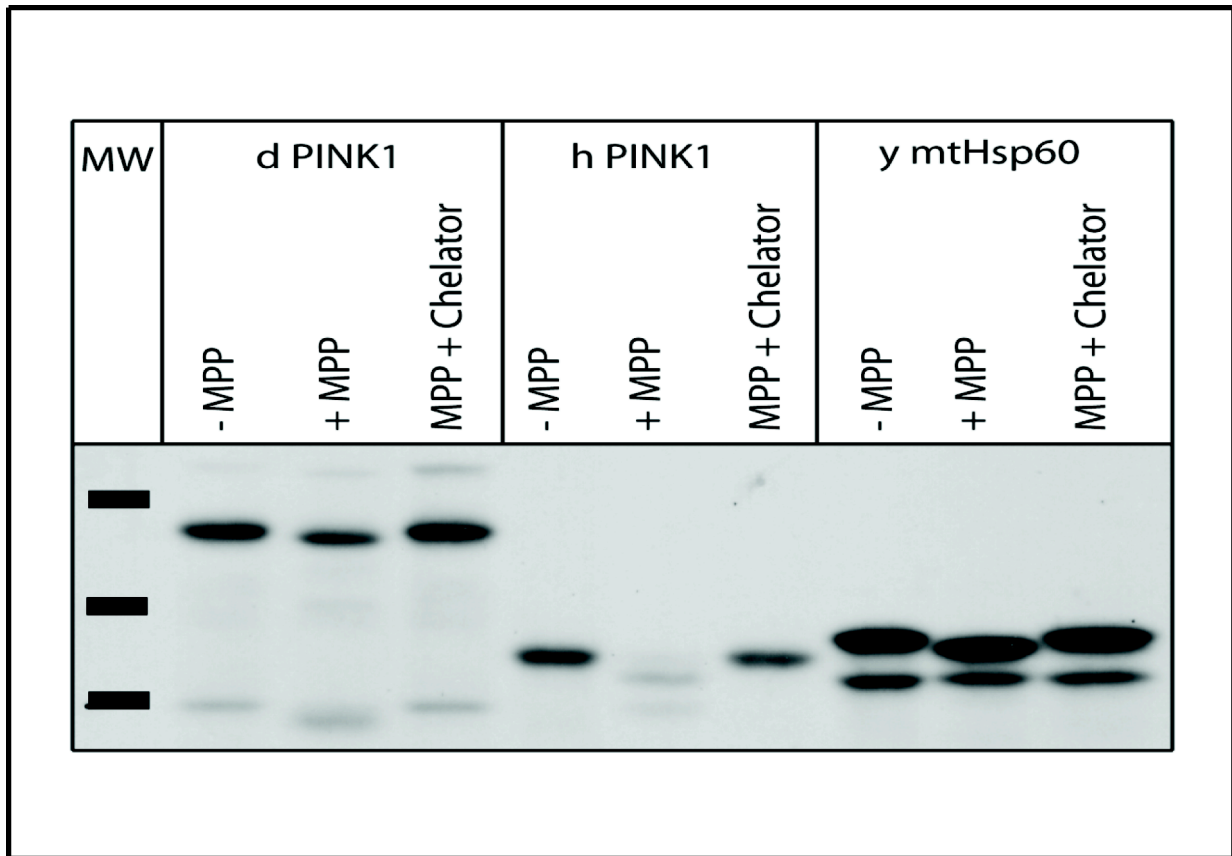


**Figure 2.14 Recombinant MPP Cleavage of [<sup>35</sup>S] PINK1**

[<sup>35</sup>S] PINK1 was synthesized using a TNT Quick Coupled Transcription/Translation kit. MPP (128 nM [screening buffer], 1 mM MnCl<sub>2</sub>, with or without 4 mM EDTA & 0.04 mM *o*-phenanthroline) was incubated with Pink1 (drosophila, human, and the yeast homolog mtHsp60). Purified recombinant MPP was found to be able to process both drosophila and human Pink1.



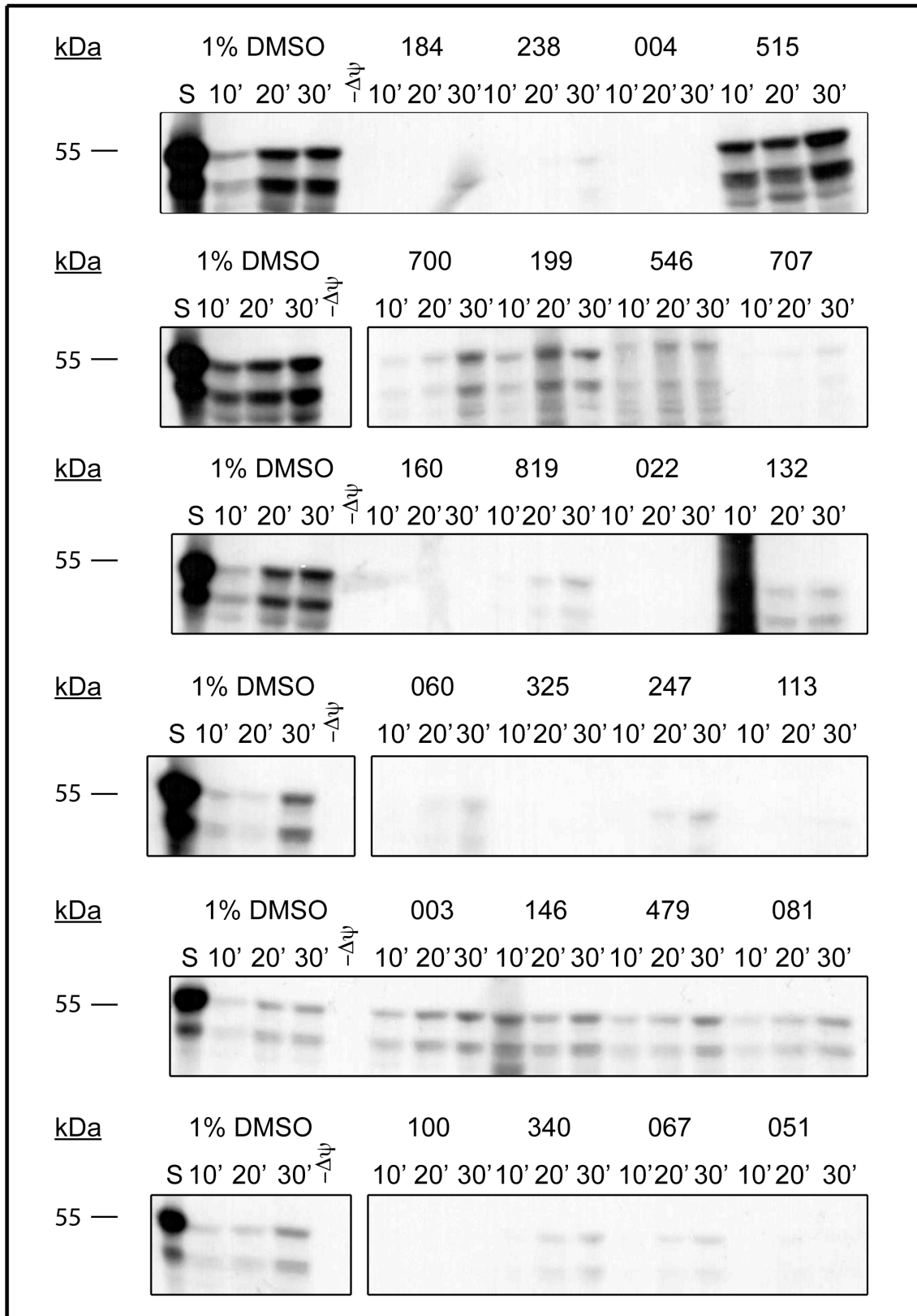


**Figure 2.15 [<sup>35</sup>S] hPink1 Import into Purified Yeast Mitochondria.**

[<sup>35</sup>S] hPink1 was synthesized using a TNT Quick Coupled Transcription/Translation kit. GA74 yeast mitochondria were treated with 1% DMSO, 50 μM CCCP & 1 mg/mL valinomycin, or 100 μM of Drug for 15 minutes at 25°C. 10 μL of [<sup>35</sup>S] hPink1 solution/reaction time point was added to each condition and 250 μL aliquots were taken at each of 3 time points (10, 20, and 30-minutes). Reactions were quenched on ice by adding 50 μg/mL of trypsin. All imports were disrupted in Laemmli sample buffer and analyzed by SDS-PAGE and autoradiography. A number of the compounds appeared to inhibit the import of [<sup>35</sup>S] hPink1 (compounds 184, 238, 004, 700, 199, 546, 707, 169, 819, 022, 132, 060, 325, 247, 113, 100, 340, 067, and 051), while others did not appear to significantly inhibit the import of [<sup>35</sup>S] hPink1 (compounds 515, 003, 146, 479, and 081).

# References

1. Daum G, Bohni PC, & Schatz G (1982) Import of proteins into mitochondria. Cytochrome b2 and cytochrome c peroxidase are located in the intermembrane space of yeast mitochondria. (Translated from eng) *J Biol Chem* 257(21):13028-13033 (in eng).
2. Anderson S, *et al.* (1981) Sequence and organization of the human mitochondrial genome. (Translated from eng) *Nature* 290(5806):457-465 (in eng).
3. Pfanner N, Craig EA, & Honlinger A (1997) Mitochondrial preprotein translocase. (Translated from eng) *Annu Rev Cell Dev Biol* 13:25-51 (in eng).
4. Neupert W (1997) Protein import into mitochondria. (Translated from eng) *Annu Rev Biochem* 66:863-917 (in eng).
5. Dietmeier K, *et al.* (1997) Tom5 functionally links mitochondrial preprotein receptors to the general import pore. (Translated from eng) *Nature* 388(6638):195-200 (in eng).
6. Honlinger A, *et al.* (1996) Tom7 modulates the dynamics of the mitochondrial outer membrane translocase and plays a pathway-related role in protein import. (Translated from eng) *EMBO J* 15(9):2125-2137 (in eng).
7. Kozjak V, *et al.* (2003) An essential role of Sam50 in the protein sorting and assembly machinery of the mitochondrial outer membrane. (Translated from eng) *J Biol Chem* 278(49):48520-48523 (in eng).
8. Paschen SA, *et al.* (2003) Evolutionary conservation of biogenesis of beta-barrel membrane proteins. (Translated from eng) *Nature* 426(6968):862-866 (in eng).
9. Wiedemann N, *et al.* (2003) Machinery for protein sorting and assembly in the mitochondrial outer membrane. (Translated from eng) *Nature* 424(6948):565-571 (in eng).
10. Yamamoto H, *et al.* (2002) Tim50 is a subunit of the TIM23 complex that links protein translocation across the outer and inner mitochondrial membranes. (Translated from eng) *Cell* 111(4):519-528 (in eng).
11. Rehling P, *et al.* (2003) Protein insertion into the mitochondrial inner membrane by a twin-pore translocase. (Translated from eng) *Science* 299(5613):1747-1751 (in eng).
12. Sirrenberg C, Bauer MF, Guiard B, Neupert W, & Brunner M (1996) Import of carrier proteins into the mitochondrial inner membrane mediated by Tim22. (Translated from eng) *Nature* 384(6609):582-585 (in eng).

13. Geissler A, *et al.* (2002) The mitochondrial presequence translocase: an essential role of Tim50 in directing preproteins to the import channel. (Translated from eng) *Cell* 111(4):507-518 (in eng).
14. Gaume B, *et al.* (1998) Unfolding of preproteins upon import into mitochondria. (Translated from eng) *EMBO J* 17(22):6497-6507 (in eng).
15. Geissler A, *et al.* (2000) Membrane potential-driven protein import into mitochondria. The sorting sequence of cytochrome b(2) modulates the  $\Delta\psi$ -dependence of translocation of the matrix-targeting sequence. (Translated from eng) *Mol Biol Cell* 11(11):3977-3991 (in eng).
16. Gakh O, Cavadini P, & Isaya G (2002) Mitochondrial processing peptidases. (Translated from eng) *Biochim Biophys Acta* 1592(1):63-77 (in eng).
17. Endo T & Yamano K (2009) Multiple pathways for mitochondrial protein traffic. (Translated from eng) *Biol Chem* 390(8):723-730 (in eng).
18. Patel PI & Isaya G (2001) Friedreich ataxia: from GAA triplet-repeat expansion to frataxin deficiency. (Translated from eng) *Am J Hum Genet* 69(1):15-24 (in eng).
19. Thoren C (1962) diabetes Mellitus in Friedreich's Ataxia. *Acta Paediatrica* 51:239-247.
20. Pandolfo M (2009) Friedreich ataxia: The clinical picture. *Journal of Neurology* 256:3-8.
21. Babcock M, *et al.* (1997) Regulation of mitochondrial iron accumulation by Yfh1p, a putative homolog of frataxin. (Translated from eng) *Science* 276(5319):1709-1712 (in eng).
22. Knight SA, Sepuri NB, Pain D, & Dancis A (1998) Mt-Hsp70 homolog, Ssc2p, required for maturation of yeast frataxin and mitochondrial iron homeostasis. (Translated from eng) *J Biol Chem* 273(29):18389-18393 (in eng).
23. Branda SS, *et al.* (1999) Yeast and human frataxin are processed to mature form in two sequential steps by the mitochondrial processing peptidase. (Translated from eng) *J Biol Chem* 274(32):22763-22769 (in eng).
24. Cavadini P, Adamec J, Taroni F, Gakh O, & Isaya G (2000) Two-step processing of human frataxin by mitochondrial processing peptidase. Precursor and intermediate forms are cleaved at different rates. (Translated from eng) *J Biol Chem* 275(52):41469-41475 (in eng).
25. Ito A (1999) Mitochondrial processing peptidase: multiple-site recognition of precursor proteins. (Translated from eng) *Biochem Biophys Res Commun* 265(3):611-616 (in eng).

26. Paces V, Rosenberg LE, Fenton WA, & Kalousek F (1993) The beta subunit of the mitochondrial processing peptidase from rat liver: cloning and sequencing of a cDNA and comparison with a proposed family of metallopeptidases. (Translated from eng) *Proc Natl Acad Sci U S A* 90(11):5355-5358 (in eng).
27. Kitada S, Shimokata K, Niidome T, Ogishima T, & Ito A (1995) A putative metal-binding site in the beta subunit of rat mitochondrial processing peptidase is essential for its catalytic activity. (Translated from eng) *J Biochem* 117(6):1148-1150 (in eng).
28. Kitada S, Yamasaki E, Kojima K, & Ito A (2003) Determination of the cleavage site of the presequence by mitochondrial processing peptidase on the substrate binding scaffold and the multiple subsites inside a molecular cavity. (Translated from eng) *J Biol Chem* 278(3):1879-1885 (in eng).
29. McAda PC & Douglas MG (1982) A neutral metallo endoprotease involved in the processing of an F1-ATPase subunit precursor in mitochondria. (Translated from eng) *J Biol Chem* 257(6):3177-3182 (in eng).
30. Miura S, Mori M, Amaya Y, & Tatibana M (1982) A mitochondrial protease that cleaves the precursor of ornithine carbamoyltransferase. Purification and properties. (Translated from eng) *Eur J Biochem* 122(3):641-647 (in eng).
31. Conboy JG, Fenton WA, & Rosenberg LE (1982) Processing of pre-ornithine transcarbamylase requires a zinc-dependent protease localized to the mitochondrial matrix. (Translated from eng) *Biochem Biophys Res Commun* 105(1):1-7 (in eng).
32. Schmidt B, Wachter E, Sebald W, & Neupert W (1984) Processing peptidase of *Neurospora* mitochondria. Two-step cleavage of imported ATPase subunit 9. (Translated from eng) *Eur J Biochem* 144(3):581-588 (in eng).
33. Luciano P, Tokatlidis K, Chambre I, Germanique JC, & Geli V (1998) The mitochondrial processing peptidase behaves as a zinc-metallopeptidase. (Translated from eng) *J Mol Biol* 280(2):193-199 (in eng).
34. Auld DS (1995) Removal and replacement of metal ions in metallopeptidases. (Translated from eng) *Methods Enzymol* 248:228-242 (in eng).
35. von Heijne G, Steppuhn J, & Herrmann RG (1989) Domain structure of mitochondrial and chloroplast targeting peptides. (Translated from eng) *Eur J Biochem* 180(3):535-545 (in eng).
36. Allison DS & Schatz G (1986) Artificial mitochondrial presequences. (Translated from eng) *Proc Natl Acad Sci U S A* 83(23):9011-9015 (in eng).
37. Roise D & Schatz G (1988) Mitochondrial presequences. (Translated from eng) *J Biol Chem* 263(10):4509-4511 (in eng).

38. Hendrick JP, Hodges PE, & Rosenberg LE (1989) Survey of amino-terminal proteolytic cleavage sites in mitochondrial precursor proteins: leader peptides cleaved by two matrix proteases share a three-amino acid motif. (Translated from eng) *Proc Natl Acad Sci U S A* 86(11):4056-4060 (in eng).
39. Gavel Y & von Heijne G (1990) Cleavage-site motifs in mitochondrial targeting peptides. (Translated from eng) *Protein Eng* 4(1):33-37 (in eng).
40. Song MC, Ogishima T, & Ito A (1998) Importance of residues carboxyl terminal relative to the cleavage site in substrates of mitochondrial processing peptidase for their specific recognition and cleavage. (Translated from eng) *J Biochem* 124(5):1045-1049 (in eng).
41. Moriwaki K, Ogishima T, & Ito A (1999) Analysis of recognition elements for mitochondrial processing peptidase using artificial amino acids: roles of the intervening portion and proximal arginine. (Translated from eng) *J Biochem* 126(5):874-878 (in eng).
42. Causton HC, *et al.* (2001) Remodeling of yeast genome expression in response to environmental changes. (Translated from eng) *Mol Biol Cell* 12(2):323-337 (in eng).
43. Setoguchi K, Otera H, & Mihara K (2006) Cytosolic factor- and TOM-independent import of C-tail-anchored mitochondrial outer membrane proteins. (Translated from eng) *EMBO J* 25(24):5635-5647 (in eng).
44. Waizenegger T, *et al.* (2004) Tob38, a novel essential component in the biogenesis of beta-barrel proteins of mitochondria. (Translated from eng) *EMBO Rep* 5(7):704-709 (in eng).
45. Specht KM & Shokat KM (2002) The emerging power of chemical genetics. (Translated from eng) *Curr Opin Cell Biol* 14(2):155-159 (in eng).
46. Geli V (1993) Functional reconstitution in *Escherichia coli* of the yeast mitochondrial matrix peptidase from its two inactive subunits. (Translated from eng) *Proc Natl Acad Sci U S A* 90(13):6247-6251 (in eng).
47. Wang G, *et al.* (2010) PNPASE regulates RNA import into mitochondria. *Cell* 142(3):456-467.
48. Farrelly E, Amaral MC, Marshall L, & Huang SG (2001) A high-throughput assay for mitochondrial membrane potential in permeabilized yeast cells. *Analytical biochemistry* 293(2):269-276.
49. Gaskova D, *et al.* (1998) Fluorescent probing of membrane potential in walled cells: diS-C3(3) assay in *Saccharomyces cerevisiae*. *Yeast* 14(13):1189-1197.
50. Zhang H, *et al.* (2001) Assessment of membrane potentials of mitochondrial populations in living cells. *Analytical biochemistry* 298(2):170-180.

51. Zara V, Ferramosca A, Papatheodorou P, Palmieri F, & Rassow J (2005) Import of rat mitochondrial citrate carrier (CIC) at increasing salt concentrations promotes presequence binding to import receptor Tom20 and inhibits membrane translocation. *Journal of cell science* 118(Pt 17):3985-3995.
52. Khalimonchuk O, *et al.* (2006) Sequential processing of a mitochondrial tandem protein: insights into protein import in *Schizosaccharomyces pombe*. *Eukaryotic cell* 5(7):997-1006.
53. Rainey RN, *et al.* (2006) A new function in translocation for the mitochondrial i-AAA protease Yme1: import of polynucleotide phosphorylase into the intermembrane space. *Molecular and cellular biology* 26(22):8488-8497.
54. Lithgow T & Schatz G (1995) Import of the cytochrome oxidase subunit Va precursor into yeast mitochondria is mediated by the outer membrane receptor Mas20p. *J Biol Chem* 270(24):14267-14269.
55. Steger HF, *et al.* (1990) Import of ADP/ATP carrier into mitochondria: two receptors act in parallel. *J Cell Biol* 111(6 Pt 1):2353-2363.
56. Truscott KN, *et al.* (2002) Mitochondrial import of the ADP/ATP carrier: the essential TIM complex of the intermembrane space is required for precursor release from the TOM complex. *Molecular and cellular biology* 22(22):7780-7789.
57. Smagula C & Douglas MG (1988) Mitochondrial import of the ADP/ATP carrier protein in *Saccharomyces cerevisiae*. Sequences required for receptor binding and membrane translocation. *J Biol Chem* 263(14):6783-6790.
58. Zhou C, *et al.* (2008) The kinase domain of mitochondrial PINK1 faces the cytoplasm. *Proc Natl Acad Sci U S A* 105(33):12022-12027.
59. Geisler S, *et al.* (2010) The PINK1/Parkin-mediated mitophagy is compromised by PD-associated mutations. *Autophagy* 6(7):871-878.
60. Matsuda N, *et al.* (2010) PINK1 stabilized by mitochondrial depolarization recruits Parkin to damaged mitochondria and activates latent Parkin for mitophagy. *J Cell Biol* 189(2):211-221.
61. Vives-Bauza C, *et al.* (2010) PINK1-dependent recruitment of Parkin to mitochondria in mitophagy. *Proc Natl Acad Sci U S A* 107(1):378-383.
62. Koyano F, *et al.* (2014) Ubiquitin is phosphorylated by PINK1 to activate parkin. *Nature* 510(7503):162-166.

63. McLelland GL, Soubannier V, Chen CX, McBride HM, & Fon EA (2014) Parkin and PINK1 function in a vesicular trafficking pathway regulating mitochondrial quality control. *EMBO J* 33(4):282-295.
64. Chen Y & Dorn GW, 2nd (2013) PINK1-phosphorylated mitofusin 2 is a Parkin receptor for culling damaged mitochondria. *Science* 340(6131):471-475.
65. Samii A, Nutt JG, & Ransom BR (2004) Parkinson's disease. *Lancet* 363(9423):1783-1793.
66. Clark IE, *et al.* (2006) *Drosophila pink1* is required for mitochondrial function and interacts genetically with parkin. *Nature* 441(7097):1162-1166.
67. Park J, *et al.* (2006) Mitochondrial dysfunction in *Drosophila* PINK1 mutants is complemented by parkin. *Nature* 441(7097):1157-1161.
68. Yang Y, *et al.* (2006) Mitochondrial pathology and muscle and dopaminergic neuron degeneration caused by inactivation of *Drosophila Pink1* is rescued by Parkin. *Proc Natl Acad Sci U S A* 103(28):10793-10798.
69. Greene AW, *et al.* (2012) Mitochondrial processing peptidase regulates PINK1 processing, import and Parkin recruitment. *EMBO Rep* 13(4):378-385.
70. Claypool SM, Boontheung P, McCaffery JM, Loo JA, & Koehler CM (2008) The cardiolipin transacylase, tafazzin, associates with two distinct respiratory components providing insight into Barth syndrome. *Mol Biol Cell* 19(12):5143-5155.
71. Dabir DV, *et al.* (2013) A small molecule inhibitor of redox-regulated protein translocation into mitochondria. *Dev Cell* 25(1):81-92.
72. Glick BS & Pon LA (1995) Isolation of highly purified mitochondria from *Saccharomyces cerevisiae*. *Methods Enzymol* 260:213-223.
73. Miyata N, *et al.* (in submission) Adaptation of a genetic screen reveals an inhibitor for mitochondrial protein import component Tim44. (EMBO).
74. Hasson SA, *et al.* (2010) Substrate specificity of the TIM22 mitochondrial import pathway revealed with small molecule inhibitor of protein translocation. *Proc Natl Acad Sci U S A* 107(21):9578-9583.
75. Koehler CM, *et al.* (1998) Tim9p, an essential partner subunit of Tim10p for the import of mitochondrial carrier proteins. (Translated from eng) *EMBO J* 17(22):6477-6486 (in eng).



# Chapter 3: Characterization of MitoBloCK-50

## Abstract

In the high-throughput screen conducted with purified MPP, 88 hit compounds were identified and confirmed as inhibitors of MPP activity. From this list, 28 compounds were ordered and characterized to identify those most promising for further study. MitoBloCK-50 (MB 50) was one of these promising candidates identified through these initial assays. Through the use of *in vitro* techniques such as radiolabeled cleavage assays and import experiments, MB 50 was shown to affect the import and processing of a variety of mitochondrial precursors, including proteins of interest frataxin, Cpn10, and Pink1. Additionally, MB 50 provoked Parkin recruitment when co-treated with CCCP in HeLa cells and induced body morphology and cardiac defects in zebrafish embryos upon treatment. Taken together, these results provide evidence as to the direct and indirect roles MPP may play in cellular pathways and organism development.

# Introduction

## Mitochondrial Structure & Function

Mitochondria consist of four separate compartments including the outer membrane, the intermembrane space, the inner membrane and the matrix. The primary role of the mitochondrion is energy production in the form of ATP; though the organelle also plays a central role in other cellular functions including signaling, cellular differentiation, cell death, cell cycle and cell growth. (1-5) The mitochondrial genome is approximately 16,000 base pairs and encodes 37 genes: 22 tRNAs, 2 rRNAs, 13 proteins, and 1 untranslated region. (6) A majority of the proteins that are utilized in the mitochondria are encoded by the nuclear genome, translated in the cytosol and must be imported into the mitochondria. Imported proteins functioning within the mitochondrial matrix typically possess a positively charged N-terminal mitochondrial targeting sequence (MTS) that directs it through the mitochondrial translocase machinery and into the mitochondrial matrix. (7)

Precursor proteins destined for the mitochondrial matrix first interact with the translocase of the outer membrane (TOM) complex, which is comprised of 7 integral membrane proteins (Tom70p, Tom40p, Tom22p, Tom20p, Tom7p, Tom6p, and Tom5p). (8-11) Following the traverse across the intermembrane space, precursors possessing an MTS encounter the translocase of the inner membrane 23 (TIM23), which is made up of 3 integral membrane proteins (Tim50p, Tim17p, and Tim23p). (8, 9, 12) Regarding the TIM23 complex, Tim17p and Tim23p make-up the pore of the complex, Tim50p acts as a guide for precursor proteins and Tim44p, Tim14p, mHsp70, and mGrpE function as the motor to attract the MTS to the complex and draw the precursor protein into the matrix for processing. (13-15) For precursor proteins

imported into the mitochondrial matrix to fold and function properly, their MTS must first be cleaved off. This cleavage is accomplished by the matrix protease, mitochondrial processing peptidase (MPP). (16, 17)

### *Mitochondrial Processing Peptidase*

MPP is a 100 kDa metalloendopeptidase and is a member of the pepsin family that includes pepsin and 3 members of the insulin-degrading enzyme group. (18) All members of this family possess an inverted zinc-binding motif with the structure; H-x-x-E-H-x<sub>76</sub>-E. Coordination of the zinc ion is accomplished with both His residues and the downstream Glu residue; the up stream Glu residue is responsible for the activation of water necessary for substrate cleavage. (19-21) The optimal pH range for purified MPP activity is pH 7-8, with inactivation at lower pH. MPP is inhibited by EDTA and *o*-phenanthroline and activated by divalent cations (Co<sup>2+</sup>, Mn<sup>2+</sup>, Zn<sup>2+</sup> and Mg<sup>2+</sup>). (22-25) At low levels of metal concentration the degree of MPP activation follows the following trend: Zn<sup>2+</sup> > Mn<sup>2+</sup> > Co<sup>2+</sup>, though unlike cobalt and manganese excess zinc inhibits MPP activity. (26, 27)

MPP is formed as a heterodimer complex that consists of an  $\alpha$  and a  $\beta$  subunit. Both subunits are necessary for the proper functioning of MPP. The MTS of precursor proteins is typically 20-60 amino acids and carries a global positive charge. (7) The MTS is both necessary and sufficient to target precursor proteins to their correct location within the mitochondrion. A number of non-mitochondrial molecules, including cytosolic proteins and nucleic acids have been successfully targeted to the mitochondrion through the use of only an N-terminal matrix targeting sequence. (28, 29)

For MPP to function properly both subunits ( $\alpha$  and  $\beta$ ) are necessary, but the two subunits perform different needs for cleavage of MPP substrates. (30) The zinc-binding domain resides on the  $\beta$  subunit. While  $\alpha$ -MPP has no catalytic activity, it does appear to play a role in substrate specificity and recognition via a highly conserved glycine-rich loop and a negative region that faces towards the active site cavity. (18) The crystal structure of yeast MPP suggests the active site is located in a central, negatively charged cavity and the glycine-rich loop appears to block accessibility to the cavity. When this loop is deleted, both the enzyme's substrate affinity and catalytic activity are decreased. (31, 32) Both subunits of MPP cooperatively form the substrate-binding pocket and each subunit is responsible for recognizing different aspects of precursor. The subunits alone were found to have low affinity towards elements of presequence but a native conformation was necessary for high substrate binding affinity. (33) The crystal structures of MPP with synthetic signal peptides suggests the presequence interacts with the polar cavity of MPP in an extended conformation, suggesting the helical conformation mitochondrial targeting sequences are capable of taking is important for recognition by the mitochondrial import machinery and must take on an extended conformation for the cleavage by MPP. (31) Through the use of mutagenesis, the zinc-binding domain (HxxEHx<sub>76</sub>H) of  $\beta$ -MPP is vital for the proper active formation, and may be in contact with  $\alpha$ -MPP. Additionally, the central region around Lys215 of  $\beta$ -MPP, which is not highly conserved, plays a role in interacting with  $\alpha$ -MPP. Finally, the C-terminal region that surrounds Ser314 of  $\beta$ -MPP is needed for catalytic activity. (34) Using both cross-linking analysis and surface plasmon resonance,  $\alpha$ -MPP was found to bind a precursor protein in the absence of  $\beta$ -MPP and was able to bind the precursor as effectively as MPP. From this, it appears  $\alpha$ -MPP is responsible for binding the mitochondrial targeting

sequence before it is presented to the catalytic domain. (34) All of these factors come together to provide strict specificity and high affinity for MPP and its substrates.

### *MitoBloCK-50*

MitoBloCK-50 (MB 50) also known as [2-(2-Hydroxybenzylidene)amino]-4-*tert*-butylphenol can be synthesized from the condensation of 2-amino-4-(*tert*-butyl)phenol and salicylaldehyde. (35) This compound has been utilized in the following types of synthetic organic chemistry: formation of hexacoordinated phosphorus (V) compounds, production of 2,3-dihydroquinolines via boronate complexes, formation of dioxaboracyclononenes, use of palladium(II) catalyzed oxidative cyclization to produce benzoxazoles, and in kinetic substitution reaction of tridentate ligands. (35-39) MB 50 has a molecular weight of 269.343 Da and its CAS registration number is 292167-53-4. (35) As of yet this compound has no known biological use.

### *Structure-Activity Relationships (SARs)*

Along with the characterization of the original hit compound from the HTS, SARs studies are usually conducted. The SAR describes the relationship between the compound of interest and its biological effect. These studies allow for the dissection and potential identification of essential moieties on the small molecule, along with building a library of both positive and negative analogs that can further enhance the characterization of the hit compound and effect on the protein pathway. Within this project, a SAR study was conducted by data mining the original HTS against a structural homology search for non-hit compounds or compounds not originally screened.

After the determination of MB 50 as a potential candidate for the inhibition of MPP our goal was to characterize this compound, along with building and characterizing potential positive and negative analogs for MB 50. This work was done using purified recombinant MPP, purified wild-type and MAS1ts mitochondria, mammalian cell culture, and zebrafish assays.

# Results

We focused on compound 819 (MitoBloCK-50; MB 50) for further characterization because it was one of the more promising compounds in the group from which we had the most hits. Additionally, when treated in conjugation with CCCP, we saw Parkin recruitment on the surface of EGFP-Parkin expressing HeLa cells (Figure 3.1). From the data presented in Chapter 2 concerning general mitochondrial dysfunction caused by the small molecules, MB 50 did not disrupt the integrity of the outer mitochondrial membrane, cause depolarization of the outer membrane, cause dysfunction of the ETC, or block the import of AAC. Similarly, MB 50 was also examined for its MIC<sub>50</sub> in HEK cells and its effect on mitochondrial morphology in HeLa cells (Figure 3.2). The MIC<sub>50</sub> of MB 50 was between 100 and 200  $\mu$ M and it did not appear to cause changes in mitochondrial morphology. Figure 3.3 shows the structure of MB 50 along with its positive and negative controls (determined from their ability to inhibit the MPP/JPT fluorogenic peptide assay).

The negative controls were found by data mining the HTS data for compounds that did not inhibit MPP activity and that possessed a greater than 60% homology with MB 50 based on structure analysis. This figure only shows the positive and negative control compounds that were ordered and tested along with MB 50; for a full list of all the compounds that fell into either of these groups refer to the appendices. The positive MB 50 analogs all contained the *para*-*t*-Butyl phenol connected to a substituted benzene ring via a methyl imine moiety. Within this structure we assumed that due to high degree of similarity with all the compounds, the combination of the *para*-*t*-butyl phenol and imine were likely to be the important substituents for this group of molecules. From this, we wanted our negative analogs to systematically substitute these groups

to assess if our hypothesis was correct about MB 50. Compound 013 lacked the hydroxyl group on the *para*-*t*-butyl phenol of MB 50 and the trifluoromethyl group adequately substitutes for the *t*-Butyl group based on size and geometry. Compound 302 lacked only the *para*-*t*-butyl group as compared the core structure of MB 50 and compound 247 exchanged the *para*-*t*-butyl group for an ethyl moiety, as compared with the core structure of MB 50.

MB 50 exhibited the ability inhibit the in-vitro cleavage of [<sup>35</sup>S] Su9-DHFR and its import into purified GA74 mitochondria (Figures 3.4 and 3.5). A titration of MB 50's ability to inhibit Su9-DHFR into mitochondria was also examined (Figure 3.6). These results suggested the IC<sub>50</sub> for Su9-DHFR import was approximately 12 μM. MB 50 was also tested against the import of Cytochrome C<sub>1</sub> (CytC<sub>1</sub>), Cytochrome B<sub>2</sub>-DHFR (1-167) (CytB<sub>2</sub>-DHFR (1-167)), and Cytochrome B<sub>2</sub>-DHFR (A63P) (CytB<sub>2</sub>-DHFR (A63P)). CytC<sub>1</sub> is targeted towards the inner membrane of the mitochondria and is one of the constituents of Complex III of the ETC. (40) CytB<sub>2</sub> is synthesized as a precursor in the cytosol and imported into the mitochondria. It contains a tightly folded heme-binding domain; the TIM23 complex sorts its transport across the outer membrane, which requires ATP. The 1-167 version of this construct is typically not processed by MPP since it is directed towards the intermembrane space due to a stop transfer sequence. (41-43) Conversely, the A63P mutant of this construct is targeted towards the matrix and is processed by MPP. (44-46) MB 50 showed the ability to inhibit both the import CytB<sub>2</sub>-DHFR (1-167) and CytB<sub>2</sub>-DHFR (A63P), but it did not appear to inhibit the import CytC<sub>1</sub> (Figure 3.7).

Frataxin is a 210 amino acid protein encoded by the nuclear DNA and is imported into the mitochondrion. Frataxin appears to be involved in the assembly of iron-sulfur clusters and has been proposed to be either an iron chaperone or an iron storage protein. The mRNA of frataxin is predominantly expressed in tissues with a high metabolic rate such as the liver,



kidney, brown adipose tissue and heart. (47, 48) Frataxin has been implicated in the etiology of FRDA, which is an autosomal recessive degenerative disease. Upon import into the mitochondria, frataxin is processed twice (in 2 sequential cleavages) by MPP, the first of the cleavages happens very rapidly, while the second cleavage is much slower and is the rate-limiting step for the formation of mature frataxin. A reduction in this second cleavage has been directly linked to the cause of FRDA and mutations in both MPP and frataxin have been shown to inhibit the cleavage of frataxin by MPP. The yeast and human frataxin presequence is 51 and 55 amino acids, respectively, and the presequence of yeast frataxin is cleaved between residues 20-21 and 51-52, while the human frataxin presequence is cleaved between 41-42 and 55-56. (47-53) MB 50 appears to inhibit the second cleavage of frataxin to a more significant extent than the first cleavage, while CCCP treatment completely blocks the import of frataxin (Figure 3.8).

Chaperonin 10 (Cpn10) along with chaperonin 60 aids in the stabilization and protection of disassembled proteins. Cpn10 exists as a ring-shape oligomer of 6–8 identical subunits that are self-assembled by the presence of  $Mg^{2+}$ -ATP. The central cavity of the cylindrical Cpn60 tetradecamer provides an isolated environment for protein folding, while Cpn10 binds to Cpn60 and synchronizes the release of the folded protein in a  $Mg^{2+}$ -ATP dependent manner. (54) Cpn10 does not have a known MTS that is cleaved by MPP, but MB 50 was found to completely inhibit the import of [ $^{35}S$ ] Cpn10 into purified mitochondria (Figure 3.8).

PTEN induced putative kinase 1 (Pink1), is synthesized as a 63 kDa protein and is cleaved by PARL between residues Ala103 and Phe104 resulting in a 43 kDa fragment. Within the topology of PINK1 there is a N-terminal mitochondrial localization sequence, a putative transmembrane sequence, a Ser/Thr kinase domain, and a C-terminal regulatory sequence. The

protein has been found to localize to the outer membrane of mitochondria, but is found primarily in the cytosol. Experiments suggest the Ser/Thr kinase domain faces outward toward the cytosol, indicating a possible point of interaction with Parkin, which is believed to play a role in the clearance of dysfunctional mitochondria. (55-61) MB 50 was found to inhibit the import of hPink1 into GA74 mitochondria. A titration against hPink1 import determined this to occur at approximately 25  $\mu$ M (Figure 3.9).

Parkin recruitment was also assessed using EGFP-Parkin expressing MTS dsRed HeLa cells and treatment with either 1% DMSO, CCCP alone, MB 50 alone, or CCCP with MB 50 (Figure 3.10). 5  $\mu$ M of CCCP recruits some Parkin to the surface of mitochondria, while 10  $\mu$ M of CCCP recruits substantially more Parkin to the surface of mitochondria as evidenced by the yellow merged panel in the figure. 40  $\mu$ M of MB 50 alone does not recruit Parkin to mitochondria. Conversely, the combination of 2.5 or 5  $\mu$ M CCCP with either 20  $\mu$ M or 40  $\mu$ M MB 50 is capable of recruiting a significant amount of Parkin to mitochondria and this recruitment appears to be greater than 10  $\mu$ M of CCCP alone. The quantification showed that when 40  $\mu$ M of MB 50 was combined with either 2.5 or 5  $\mu$ M CCCP, it exhibited a greater amount of Parkin recruitment than CCCP alone.

The genes that encode for MPP are MAS1 (MPP  $\beta$ ) & MAS2 (MPP  $\alpha$ ). The temperature-sensitive mutant for yeast MPP  $\beta$  (MAS1) at incubation temperatures of 37°C exhibits signs of MPP knockdown. It is apparent that MB 50 and the MAS1 ts mutant affect the import of Su9-DHFR in a different manner (Figure 3.11). The MAS1ts yeast mutant shows an accumulation of unprocessed, and trypsin protected, Su9-DHFR, while MB 50 in both wild-type and MAS1 ts mitochondria exhibits a decrease in overall import of Su9-DHFR.

MB 50 was examined using zebrafish expressing cardiac myocyte light chain 2 (cmlc2), which only express DsRed in heart cells (Figure 3.12). Zebrafish are useful for these types of studies because they are fertilized externally, the embryos are optically clear, and the embryos are osmotically permeable. Additionally, the parent fish can be crossed weekly to produce hundreds of embryos. By 3 days post-fertilization the nervous and cardiac systems have started to develop. At 20  $\mu$ M MB 50 the zebrafish start showing a change in body curvature, and at 50  $\mu$ M the body curvature is more severe and there was a slight loss of pigmentation. At 20  $\mu$ M MB 50 the heart also starts to exhibit severe atrial distension and does not appear to flip. Zebrafish pigmentation is initiated during embryogenesis and begins in the retinal epithelium and in the melanophores. The pigment cells develop rapidly, and within hours they constitute a prominent feature of the embryo. (62, 63) One common method for zebrafish depigmentation is through the treatment with N-phenylthiourea (PTU), which is capable of completely blanching the zebrafish, but can also be washed-out. PTU works by inhibiting melanogenesis by blocking all tyrosinase-dependent steps in the melanin pathway. (64) Another method for causing depigmentation of zebrafish is through the chelation of copper with compounds such as neocuproine and bathocuproine. (65, 66) Using both bathocuproine and PTU as controls, MB 50 was examined for its ability to be washed-out following 3 days of treatment. After 3 days of treatment with 40  $\mu$ M MB 50, bathocuproine, or PTU we saw a severe body curvature effect with MB 50, a slight decrease in pigmentation with bathocuproine and a significant loss of pigmentation with PTU. Following 2 days where all compounds have been washed-out and the zebrafish have been allowed to develop normally we see that the pigmentation has returned completely in all three-drug conditions and that the body curvature issue with MB 50 is not as severe as seen after 3 days of MB 50 treatment (Figure 3.13).

To show justification for our data mining method for a SAR study, the *in-vitro* cleavage of Su9-DHFR was investigated with the analogs (Figure 3.4). EDTA and MB 50 significantly inhibited the formation of mature Su9-DHFR, while the negative MB 50 analogs (247, 302, and 013) do exhibit some accumulation of the second cleavage by MPP of Su9-DHFR, but a majority of the mature Su9-DHFR by 5 minutes is formed as compared to the 1% DMSO control. The positive analogs (238, 515, 340, 700, 051, and 067) as referenced in Chapter 2 showed similar results in the inhibition of MPP cleavage activity as MB 50 (data not shown). It appears that the selection of the key moieties in MB 50 are plausible and that these negative analogs for the MB 50 group can be carried on further.

The analogs were also tested for their ability to inhibit the import [<sup>35</sup>S] Su9-DHFR into GA74 mitochondria (Figure 3.5). Out of the negative MB 50 analogs, compound 302 showed little to no inhibition of Su9-DHFR import, compound 013 showed moderate inhibition and compound 247 exhibited comparable inhibition of Su9-DHFR as MB 50. As for the positive MB 50 analogs, compounds 515 and 700 exhibited significant inhibition to Su9-DHFR import, 238 and 340 appeared to have some inhibitory affect, while compounds 067 and 051 showed little to no degree of inhibition of Su9-DHFR import into GA74 mitochondria.

Lastly, the analogs were tested to determine their effects on zebrafish development (Figure 3.14). At 3 days post fertilization, MB 50 and its positive analogs (515 & 700) all exhibit changes in body curvature that get more severe with increasing drug concentration as compared to the control zebrafish (Figure 3.14: Top). When comparing the negative controls (013 & 302) and MB 50, the negative controls showed some signs of malformation and changes in body curvature, but at similar concentrations MB 50 appeared to be more severe than both negative

analogs (Figure 3.14: Bottom). Drug 247 was left out of this table because at all concentrations tested all of the zebrafish were severely mutilated and none of them were alive.

# Discussion

Through the analysis of the data for MB 50 and both its positive and negative analogs it appears the key structural component of MB 50 is the *para*-*t*-butyl phenol connected to a substituted benzene ring via a methyl imine moiety. Within this sub-structure of MB 50 the likely moieties responsible for activity are likely to be the hydroxyl group of the phenol, the imine, or some combination/coordination of the two groups. The substituents seen on the benzene ring of MB 50 and its positive analogs likely aid in the specificity of the compounds, but it can not be ruled out that they play some role in the chemistry these compounds are capable of exhibiting. One of the rather interesting positive analogs for MB 50 is compound 515, which is known as 3-bromo-5-(*tert*-butyl)benzene-1,2-diol. With some synthetic manipulations this compound could act as a precursor to the imine moiety seen in the rest of the compounds within the MB 50 group. The fact this compound shows activity towards MPP, though not to the same extent as MB 50, gives some credence to which part of MB 50 is required for the inhibition of MPP, and which part could potentially increase potency, binding efficiency, or alter binding specificity.

MB 50 was capable of inhibiting the import of Su9-DHFR, CytB<sub>2</sub>-DHRF (1-167) and CytB<sub>2</sub>-DHFR (A63P), frataxin, Cpn10, and hPink1, while it did not inhibit the import of CytC<sub>1</sub> or AAC. Both CytB<sub>2</sub>-DHFR (1-167) and CytB<sub>2</sub>-DHFR (A63P) are initially processed MPP, the difference between them is CytB<sub>2</sub>-DHFR (1-167) possesses a stop transfer sequence after the MTS, which directs it towards the intermembrane space. IMP cleaves off the stop transfer sequence of CytB<sub>2</sub>-DHFR (1-167). CytB<sub>2</sub>-DHFR (A63P) is directed to the matrix via the A63P mutation, therefore it is only processed by MPP. (41) The fact that MPP inhibits the import of

both CytB<sub>2</sub>-DHFR (1-167) and CytB<sub>2</sub>-DHFR (A63P) is not unexpected since MPP has to process them before they can take their mature form. On the other hand, MB 50 was not capable of inhibiting CytC<sub>1</sub>, though this was expected. Though the exact mechanism for CytC<sub>1</sub> is not completely resolved, the general consensus is CytC<sub>1</sub> import requires a membrane potential, ATP, and the precursor is first processed by MPP and then IMP2. (25, 67-71) The discrepancy between our work and data showing that MPP processes CytC<sub>1</sub> could signify a difference between how MPP interacts with CytB<sub>2</sub> and CytC<sub>1</sub>.

From the crystal structures of MPP with synthetic signal peptides, it appears the presequence interacts with the polar cavity of MPP in an extended conformation, suggesting the helical conformation taken mitochondrial targeting sequences is important for recognition by the mitochondrial import machinery and cleavage by MPP (Figure 1.5). (31) It appears that electrostatic interactions are capable of capturing the positively-charged MTS and bringing it into the negatively-charged MPP cavity. MPP is capable of scanning the presequence as it threads through the cavity along the negatively-charged walls of both subunits and determine the correct site of cleavage. With this model in mind, MPP would be capable of distinguishing different length presequences as they travel from the  $\beta$  subunit to the  $\alpha$  subunit, and thereby effectively, and reproducibly, cleave the correct site and release the mature protein. If MB 50 is exerting an effect in the active site or an ancillary site that affects precursor recognition, this could potentially explain the difference in import inhibition for CytB<sub>2</sub> and CytC<sub>1</sub>. Perhaps MPP recognizes these two presequences differently, and MB 50 is only able to affect the recognition of CytB<sub>2</sub>.

Frataxin, which has been linked to FRDA, is cleaved in two sequential steps by MPP. The first of these cleavages happens very rapidly, while the second cleavage is much slower and is the rate-determining step for the formation of mature frataxin. A reduced rate and ability to

conduct the second cleavage of frataxin is believed to be a major factor in the etiology of FRDA. (72-76) MB 50 showed the ability to inhibit the two-step processing of frataxin differently when import into mitochondria. Though there was some reduction of the intermediate product when compared to the amount of intermediate product to DMSO treated mitochondria, the majority of the difference was seen when comparing the amount of mature product. Treatment with MB 50 resulted in approximately a 70-75% reduction in the amount of mature frataxin at the final time point, while CCCP treatment appeared to block both processed forms equally. MB 50, therefore, could be an interesting agent to study the cleavage process of frataxin and its link to FRDA.

Cpn10 resides within the mitochondrial matrix and with the aid of Cpn60 helps precursor proteins fold into their native state. (77) Cpn10 does not contain a known MTS and its mechanism for import into the mitochondrial matrix is not completely understood. (54, 78) MB 50 appears to completely inhibit the import of Cpn10 in GA74 mitochondria, therefore, even though Cpn10 does not contain a known MTS for MPP, our data suggest MPP is involved in the import of Cpn10 and its maturation into a functional mitochondrial matrix protein. This could mean Cpn10 does in fact possess a presquence recognized by MPP, or un-inhibited MPP is necessary for import of Cpn10 import even though it does not cleave the Cpn10 precursor.

Parkinson's disease is a neurodegenerative disorder of the central nervous system, which is typified by movement-related symptoms resulting from the loss of dopamine-generating cells in the substantia nigra. (79) Recently two genes have been linked to familial forms of this disease, Pink1 and Parkin. (57) Drosophila studies revealed the two proteins function in the same pathway and that Pink1 is upstream of Parkin. (80-82) Under normal conditions Pink1 is quickly degraded, but under conditions where the mitochondrial membrane is depolarized Pink1 is stabilized. Once stabilized, Pink1 goes to the outer mitochondrial membrane where it recruits



Parkin via its Ser/Thr kinase domain and results in the ubiquitination and degradation of senescent or damaged mitochondria. (57, 61) Previous work using RNAi also showed decreasing the amount of MPP caused an increase in the accumulation of Pink1 on the mitochondrial surface. This increase in Pink1 accumulation also caused an increase in Parkin recruitment and mitochondrial degradation. (83) We were able to show MB 50 was able to inhibit the import of Pink1 and, in conjunction with CCCP treatment; it was capable of recruiting Parkin to the surface of mitochondria. MB 50 has the potential to be used as a stimulant for the activation of the Pink1-Parkin mitochondrial mitophagy pathway. MB 50 needs to be investigated further for its ability to up-regulate this pathway and for its ability to direct damaged or dysfunctional mitochondria to be degraded.

When zebrafish were treated with MB 50 they exhibited a change in body curvature, an atrial heart distension (the heart also failed to flip), and loss of pigmentation at high concentrations compared to DMSO treatment. Additionally, we found MB 50 could be washed-out after 3 days post-fertilization with return of pigmentation and the body change was not as severe. Organismal development and muscular systems (i.e., the cardiac system) are extremely prone to mitochondrial abnormalities due to their reliance on ATP production. Using zebrafish as a model organism to simulate human diseases is becoming fairly commonplace; as is their use in replicating mitochondrial disorders. (84) During early stages of zebrafish development mitochondria are paramount to proper growth, development, and cardiac function; therefore, the body curvature, notochord abnormalities, and cardiac malformation seen with MB 50 and its inhibition of MPP make complete sense due to the high demand of functional mitochondria. This data mirrors much of the data we have collected with other MitoBloCK compounds. (85, 86)

This could signify that MPP is upstream to many of the other pathway we have investigated in the lab or that the individual pathways are separate but result in similar phenotypes.

# Materials and Methods

**Reagents.** Chemical libraries and investigated compounds were obtained from Chembridge Corporation (San Diego, CA), Asinex Ltd (Moscow, Russia) and Life Chemicals (Burlington, Canada). All other reagents were purchased from Sigma-Aldrich, EMD Biosciences, MB Biomedicals, US Biological and JPT Innovative Peptide Solutions. For trypan blue assays, cultured HeLa cells were grown in DMEM high glucose medium (Invitrogen) with glutamine, sodium pyruvate, 10% FBS, and penicillin-streptomycin (complete medium).

***In-vitro* Su9-DHFR Cleavage Assay.** Before the cleavage assay with purified recombinant MPP, [<sup>35</sup>S]-methionine and cysteine labeled Su9-DHFR was made with the TNT Quick Coupled Transcription/Translation kit (Promega). Each sample consisted of 8 μL of Su9-DHFR/[<sup>35</sup>S] added to 12 μL of MPP solution (solution included purified recombinant MPP at 128 nM final concentration, drug at 100 μM final concentration (if added), 4 mM EDTA with 0.04 mM *o*-phenanthroline [final concentration; negative control], 1% DMSO [final concentration], and 1 mM MnCl<sub>2</sub> [final concentration]). DMSO only, drugs, or EDTA/*o*-phenanthroline were incubated with MPP for an hour at room temperature before the addition of Su9-DHFR. 20 μL aliquots were taken at 2, 5, and 10-minute time points; the reactions were quenched with the addition of Laemmli sample buffer and all samples were analyzed by SDS-PAGE and autoradiography.

**Mitochondria Purification.** Mitochondria were purified from GA74 or MAS1 ts yeast cells grown in YPEG as described in previous studies. (85, 87) After purification, the concentration was measured by bicinchoninic acid (BCA) assay and mitochondria were stored at -80°C. Mammalian mitochondria were purified from HeLa cells grown in DMEM as previously

described in studies. (86) After purification, the concentration was measured by bicinchoninic acid (BCA) assay and the mitochondria were purified and used fresh for each import assay.

**Import of radiolabeled proteins into mitochondria.** Before import into purified mitochondria, [<sup>35</sup>S]-methionine and cysteine labeled precursor proteins were using the TNT Quick Coupled Transcription/Translation kit (Promega). Imports of precursor proteins into purified yeast mitochondria were conducted based on established protocol. (85, 88) Due to the fact that the drug compounds were primarily only soluble in DMSO a final concentration in each import reaction of 1% was used. Drugs in DMSO or DMSO vehicle only was added to the mitochondria (25-50 µg/mL) in import buffer and incubated for 15 min at 25°C. Imports were initiated with the addition of radio-labeled precursor and aliquots were removed at intervals during the reaction time-course. Import was terminated with the addition of 25 µg/mL of trypsin or just placed on ice for those import reactions where carbonate extraction was performed. After 15 min, 200 µg/mL of soybean trypsin inhibitor was added to deactivate trypsin. Mitochondria were pelleted by centrifugation at 8,000 x g for 5 min. To investigate proteins not inserted into the membrane, a carbonate extraction step was performed without the use of trypsin as described previously. (89)

Imports into purified mammalian mitochondria were conducted using a similar method as the one described for yeast mitochondria except that the mammalian mitochondria were diluted to a final concentration of 200 µg/mL in a different import buffer consisting of 20 mM Hepes-KOH pH 7.4, 70 mM sucrose, 220 mM mannitol, 0.5 mM MgCl<sub>2</sub>, 1 mM ATP, 20 mM sodium succinate, and 5 mM NADH.

For all imports, the mitochondria were disrupted in Laemmli sample buffer after the final

centrifugation and analyzed by SDS-PAGE and autoradiography .

**Cell manipulations.** For microscopy experiments, HeLa cells treated with DMSO, MB 50, or CCCP for 24 or 48 hrs, were fixed with 4% formaldehyde. Cells were visualized with a microscope 9 Axiovert200M (Carl Zeiss) using a Plan-Fluor 63x oil objective. Images were acquired at room temperature with a charge-coupled device camera (ORCA ER, Hamamatus Photonics) controlled by Axiovision software (Carl Zeiss). Images were resized to 300 dpi without resampling using Photoshop software (Adobe).

**Trypan blue cell integrity assay.** A modified version of previously described protocols was used to assess cell integrity. (90, 91) Starting material for each experiment was 1-2 plates (10 cm) of HeLa cell culture. Confluent cultures of HeLa cells were first washed with phosphate-buffered saline (PBS) solution (Invitrogen) and then detached from plates with a solution of 0.05% trypsin/EDTA (Invitrogen). Cells were then collected in DMEM high glucose medium +10% FBS medium to quench trypsin reaction and then pelleted at 125 x g for 5 minutes. Cell pellet was subsequently resuspended in PBS and then centrifuged as before. Washed pellet was resuspended in 2-4 ml DMEM high glucose medium +10% FBS and cell density was quantified using a hemocytometer. A 0.25 ml aliquot containing approximately 625,000 cells was diluted 1:1 into DMEM high glucose medium +10% FBS containing DMSO, drug, or CCCP at 2X of the final assay concentration. After gentle mixing by inversion, the 0.5 ml reaction was incubated for 24 hours. Next, a 0.25 ml aliquot of trypan blue solution (0.4% w/v trypan blue in Hank's balanced salt solution [Invitrogen]) was added to each reaction and incubated for 5 minutes at RT. Cell integrity was assessed by counting blocks of 100 cells from each reaction with a hemocytometer. HeLa cells with a blue center were counted as permeabilized and those with a clear center were counted as being intact.

**Zebrafish Lines.** Zebrafish displaying fluorescent hearts were derived from transgenic TL fish expressing a mitochondrially targeted dsRed regulated by a cardiac myocyte light chain 2 (*cm1c2*) promoter to make it heart-specific. O-dianisidine staining was conducted in *cm1c2* lines.

**Zebrafish Husbandry.** Zebrafish lines were maintained in a 14-hour-light/10-hour-dark cycle and mated for 1 hour to obtain synchronized embryonic development. Embryos were grown in E3 buffer (5 mM sodium chloride, 0.17 mM potassium chloride, 0.33 mM calcium chloride, 0.33 mM magnesium sulfate) at 28.5°C.

**Zebrafish Drug Treatment Assay.** Zebrafish were mated for 1 hour to obtain synchronized embryonic development. Embryos were grown to 3 hpf in E3 buffer (5 mM sodium chloride, 0.17 mM potassium chloride, 0.33 mM calcium chloride, 0.33 mM magnesium sulfate) and then incubated with buffer, 1% DMSO, or drug for 3 days at 28.5°C. Following treatment, embryos were imaged using a Leica S8APO microscope at 1.575x magnification or Leica MZ16F fluorescent stereoscope (TexasRed filter set) at 5x magnification. *Cm1c2* embryos were stained with o-dianisidine (40% (v/v) ethanol, 0.01 M sodium acetate, 0.65% hydrogen peroxide, 0.6 mg/mL o-dianisidine) and incubated for 15 minutes in complete darkness. Embryos were then washed with E3 buffer to remove residual stain and stereoscopically imaged under white light using a Leica S8APO microscope at 1.575x magnification. Images were resized to 300 dpi without resampling using Adobe Photoshop.

**Analysis and Statistics.** Unless otherwise stated, all results reported are representative of three experimental replicates. Quantitative analysis was performed in GraphPad Prism 5 software (GraphPad Software, Inc.) unless otherwise stated.

**Miscellaneous.** Western blotting was performed using standard protocols with polyclonal antibodies raised towards highly purified antigens. The PDI antibody was a mouse monoclonal antibody purchased from Abcam Inc. (Cambridge, MA). Proteins were transferred to nitrocellulose membranes and immune complexes were visualized with HRP labeled Protein A in a chemiluminescence assay (Pierce). Chemiluminescent imaging was performed on an Alpha Innotech (Santa Clara, CA) FluorChem FC2 workstation unless otherwise noted. Autoradiographic imaging was performed on film.

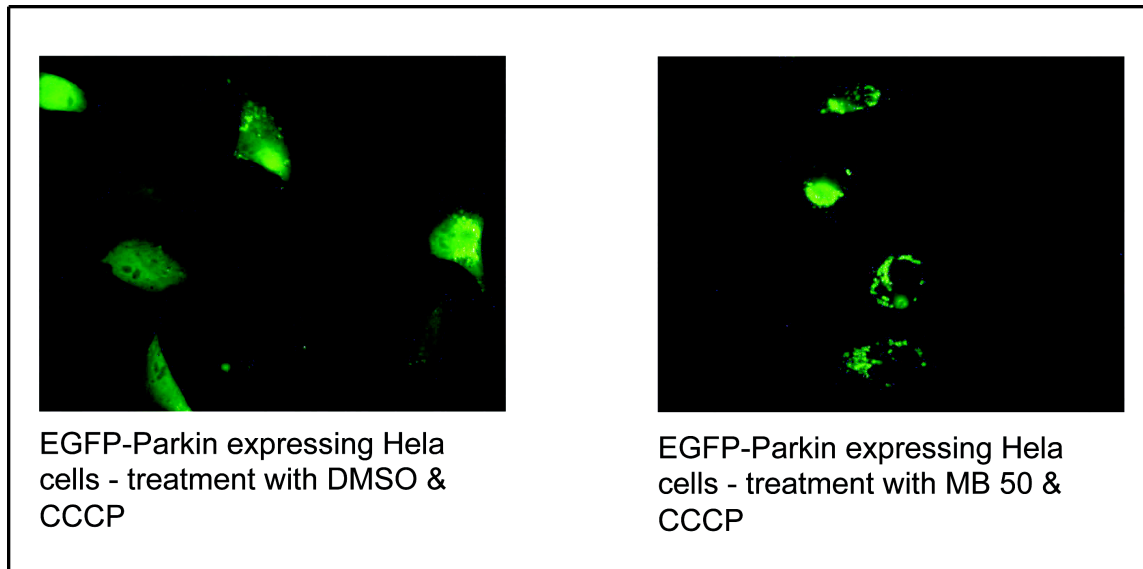


**Figure 3.1 Parkin recruitment on the surface of EGFP-Parkin Expressing HeLa Cells.**

EGFP-Parkin expressing HeLa cells were treated with either 10  $\mu$ M CCCP and 1% DMSO or 10  $\mu$ M CCCP and 40  $\mu$ M of MB 50. EGFP Parkin is more diffuse throughout the cell in the CCCP only condition, whereas EGFP appears to become more localized when CCCP and MB 50 are added concurrently. This localization appears to be on mitochondria. *Figured included with permission from Non Miyata.*



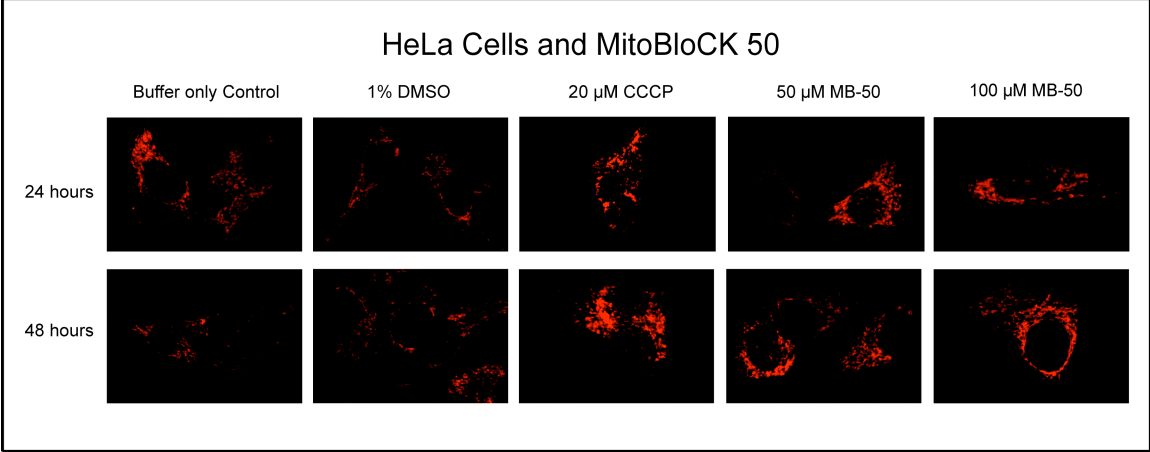
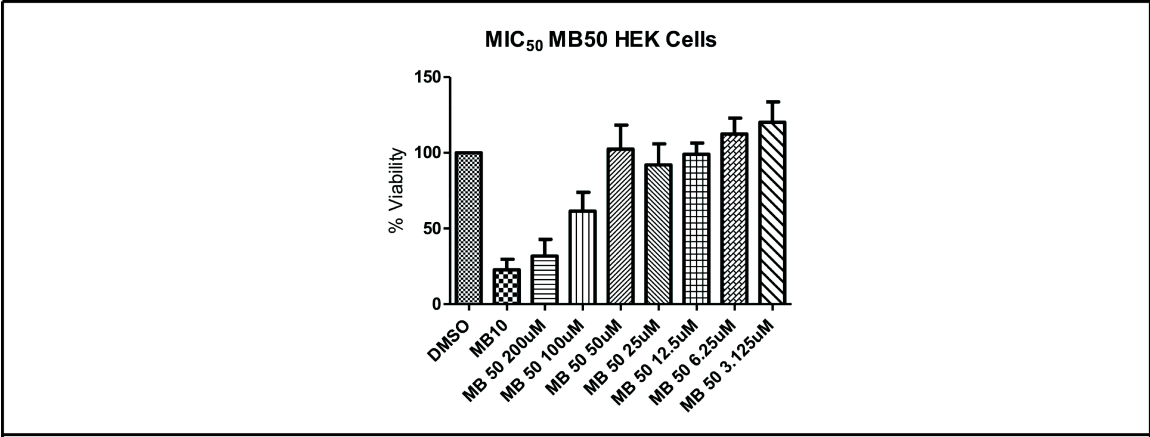
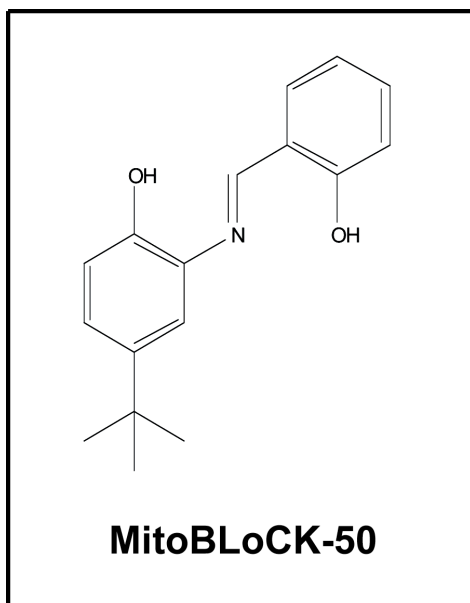


**Figure 3.2 MIC<sub>50</sub> of MB 50 in HEK Cells and Mitochondrial Morphology in HeLa Cells.**

Treating the cells for 24 hours with varying concentrations of MB 50 and conducting a cell count for each condition using the hemocytometer determined the MIC<sub>50</sub> in HEK cells (done in triplicate for each condition). The MIC<sub>50</sub> for MB 50 in HEK cells is 100–200  $\mu$ M. HeLa cells expressing MLS dsRed were used to determine if MB 50 caused changes in mitochondrial morphology as compared to 1% DMSO or 20  $\mu$ M CCCP for 24 and 48 hours of treatment. MB 50 at 50  $\mu$ M (24 & 48 hrs) did not appear to cause the mitochondria to become punctate unlike the mitochondria seen in the CCCP treatment. MB 50 at 100  $\mu$ M did appear to cause some degree of punctate mitochondria but it was not as severe as CCCP treatment. MB 50 treatment on HeLa cells did not seem to cause adverse effects to mitochondrial morphology.



Type of Control	Structure	Structure	Structure
+	<p style="text-align: right;">238</p>	<p style="text-align: right;">515</p>	<p style="text-align: right;">340</p>
+	<p style="text-align: right;">700</p>	<p style="text-align: right;">051</p>	<p style="text-align: right;">067</p>

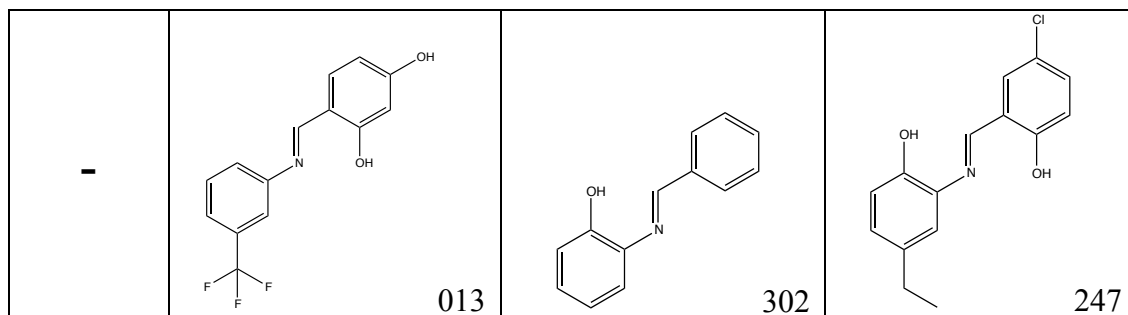


**Figure 3.3 Structures of MB 50 and a Selection of its Analogs.**

All of the MB 50 analogs were determined either directly from the MPP primary and secondary screens or by data mining the screen for compounds that did not inhibit MPP but had a greater than 60% homology with MB 50 based on structural analysis. Compound 013, lacked the hydroxyl group on the *para*-*t*-butyl phenol of MB 50 and the trifluoromethyl group adequately substitutes for the *t*-butyl group based on size and geometry. Compound 302, lacked only the *para*-*t*-butyl group as compared the core structure of MB 50 and compound 247 exchanged the *para*-*t*-butyl group for an ethyl moiety as compared with the core structure of MB 50.

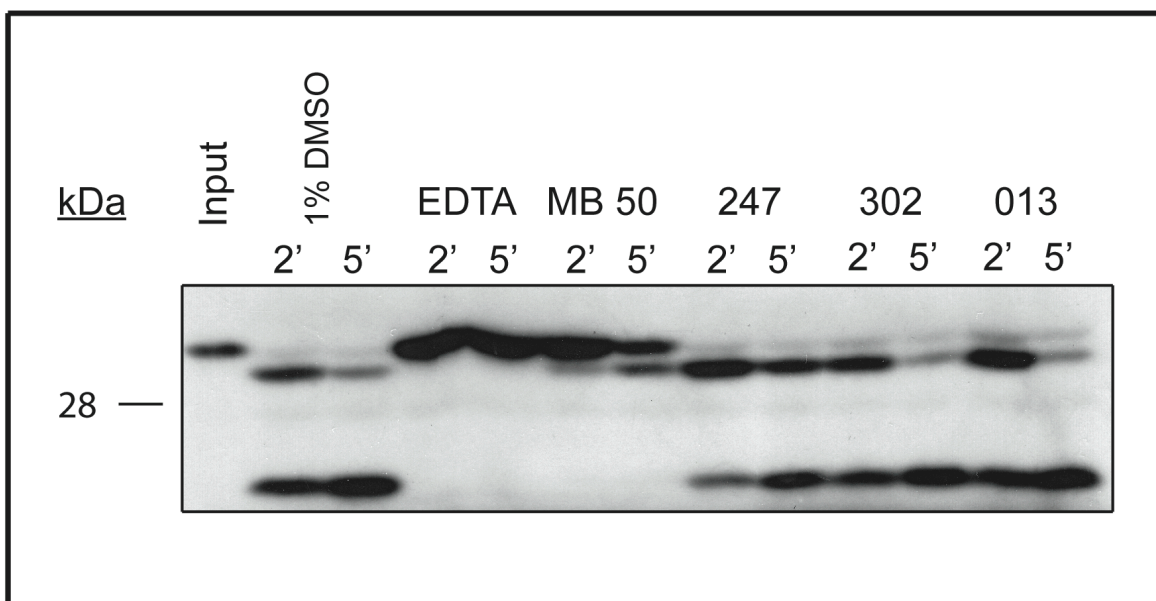


**Figure 3.4 *In-Vitro* Cleavage of [<sup>35</sup>S] Su9-DHFR by Recombinant MPP with MB 50 and Negative Analogs.**

[<sup>35</sup>S] Su9-DHFR was synthesized using a TNT Quick Coupled Transcription/Translation kit. GA74 yeast mitochondria were treated with either 1% DMSO, 50 μM CCCP & 1 mg/mL valinomycin, or 100 μM of Drug for 15 minutes at 25°C. 10 μL of [<sup>35</sup>S] Su9-DHFR solution/reaction time point was added to each condition and 250 μL aliquots were taken at each of 2 time points (2 and 5-minutes). Reactions were quenched on ice by adding 50 μg/mL of trypsin. All imports were disrupted in Laemmli sample buffer and analyzed by SDS-PAGE and autoradiography. EDTA and MB 50 significantly inhibited the formation of mature Su9-DHFR, while the negative MB 50 analogs (247, 302, and 013) did exhibit some accumulation of the second cleavage by MPP of Su9-DHFR, but a majority of the mature Su9-DHFR by 5 minutes is formed as compared with the 1% DMSO control.

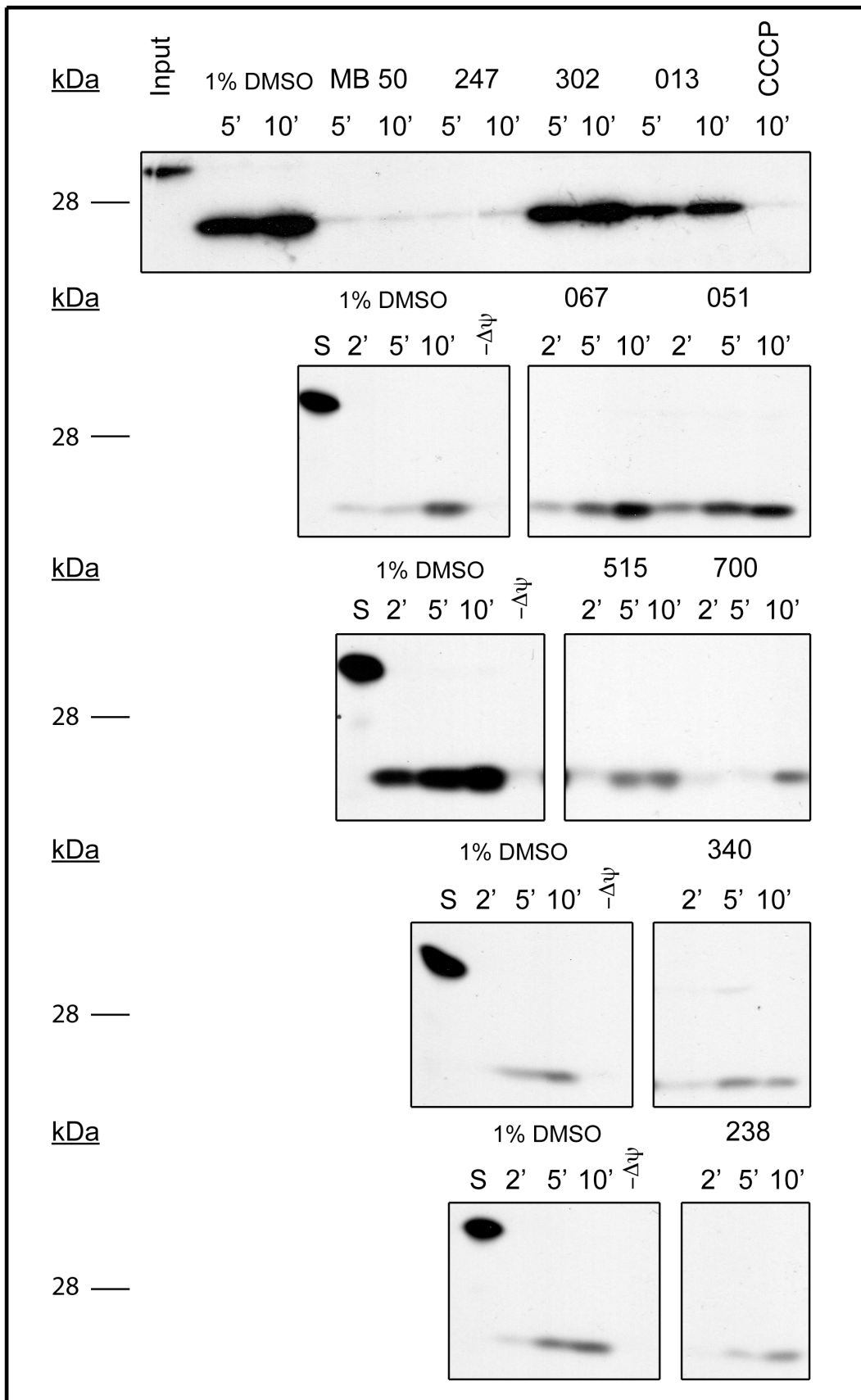


**Figure 3.5 [<sup>35</sup>S] Su9-DHFR import into GA74 Mitochondria with MB 50 and Analogs.**

[<sup>35</sup>S] Su9-DHFR was synthesized using a TNT Quick Coupled Transcription/Translation kit. GA74 yeast mitochondria were treated with either 1% DMSO, 50 μM CCCP & 1 mg/mL valinomycin, or 100 μM of Drug for 15 minutes at 25°C. 10 μL of [<sup>35</sup>S] Su9-DHFR solution/reaction time point was added to each condition and 250 μL aliquots were taken at each of 3 time points (2, 5, and 10-minutes). Reactions were quenched on ice by adding 50 μg/mL of trypsin. All imports were disrupted in Laemmli sample buffer and analyzed by SDS-PAGE and autoradiography. Out of the negative MB 50 analogs, compound 302 showed little to no inhibition of Su9-DHFR import, compound 013 showed moderate inhibition and compound 247 exhibited comparable inhibition of Su9-DHFR as MB 50. As for the positive MB 50 analogs, compounds 515 and 700 exhibited significant inhibition to Su9-DHFR import, 238 and 340 appeared to have some inhibitory affect, while compounds 067 and 051 showed little to no degree of inhibition of Su9-DHFR import into GA74 mitochondria.

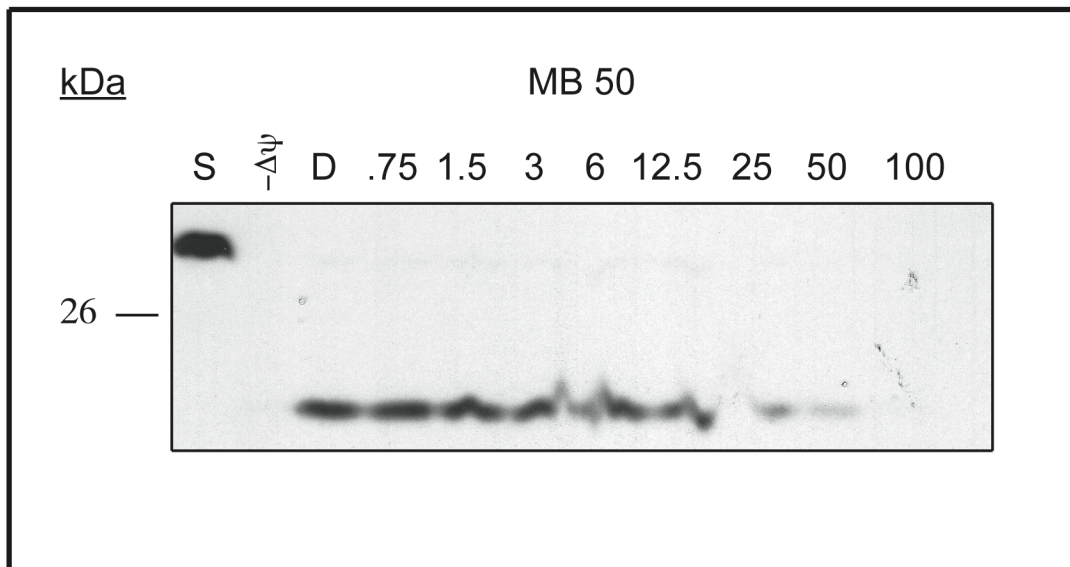


**Figure 3.6 Titration of MB 50 with the Import of [<sup>35</sup>S] Su9-DHFR into GA74 Mitochondria.**

[<sup>35</sup>S] Su9-DHFR was synthesized using a TNT Quick Coupled Transcription/Translation kit.

GA74 yeast mitochondria were treated with either 1% DMSO, 50  $\mu$ M CCCP & 1 mg/mL valinomycin, or varying concentrations of MB 50 for 15 minutes at 25°C. 10  $\mu$ L of [<sup>35</sup>S] Su9-DHFR solution was added to each condition and 250  $\mu$ L aliquots were taken after 5-minutes.

Reactions were quenched on ice by adding 50  $\mu$ g/mL of trypsin. All imports were disrupted in Laemmli sample buffer and analyzed by SDS-PAGE and autoradiography. The IC<sub>50</sub> of MB 50 was approximately 12-15  $\mu$ M with regard to the import of Su9-DHFR into GA74 mitochondria.



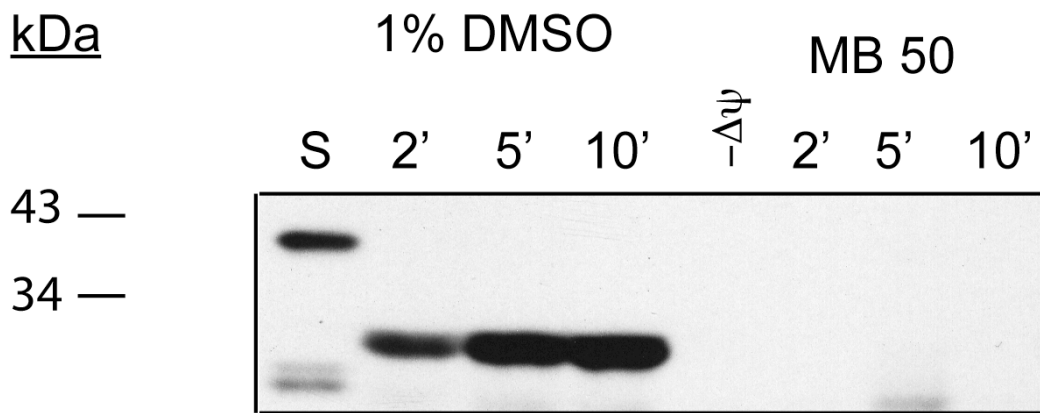
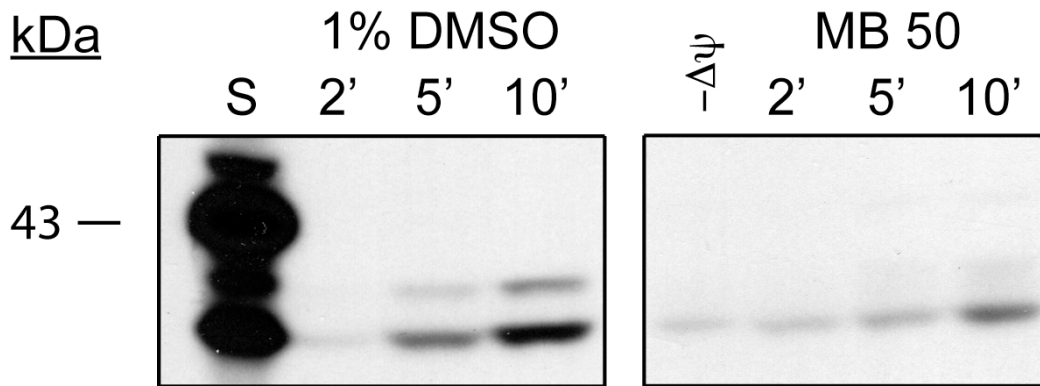
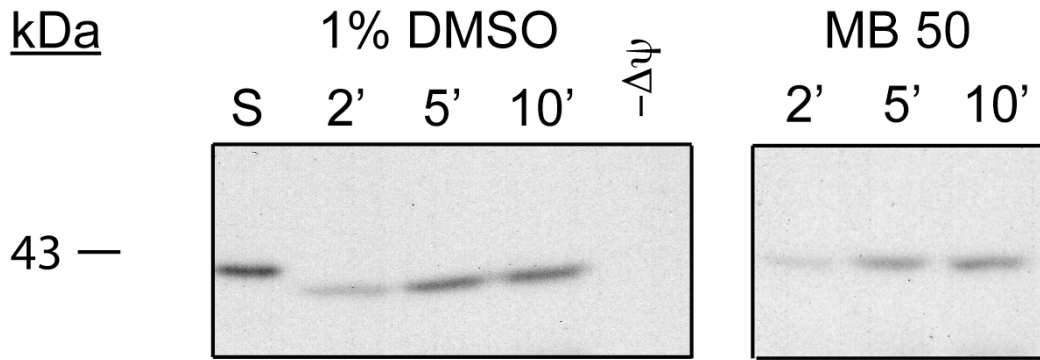
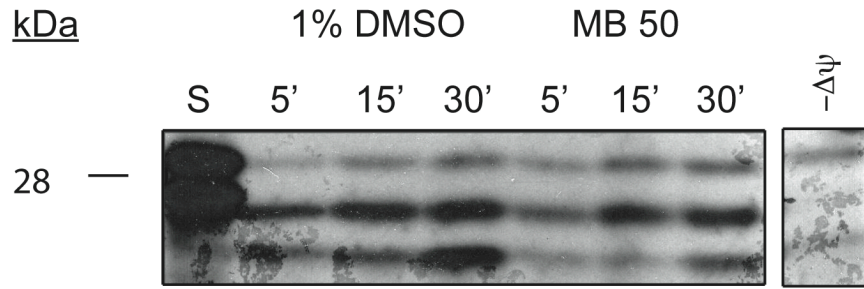


**Figure 3.7 CytC<sub>1</sub>, CytB<sub>2</sub>-DHFR (1-167), and CytB<sub>2</sub>-DHFR (A63P) import into GA74 Mitochondria with MB 50.**

[<sup>35</sup>S] CytC<sub>1</sub>, CytB<sub>2</sub>-DHFR (1-167) and CytB<sub>2</sub>-DHFR (A63P) were synthesized using a TNT Quick Coupled Transcription/Translation kit. GA74 yeast mitochondria were treated with either 1% DMSO, 50 μM CCCP & 1 mg/mL valinomycin, or 100 μM of MB 50 for 15 minutes at 25°C. 10 μL of [<sup>35</sup>S] transcript solutions/reaction time point was added to each condition and 250 μL aliquots were taken at each of 3 time points (2, 5, and 10-minutes). Reactions were quenched on ice by adding 50 μg/mL of trypsin. All imports were disrupted in Laemmli sample buffer and analyzed by SDS-PAGE and autoradiography. According to the data, MB 50 inhibited CytB<sub>2</sub>-DHFR (1-167) and CytB<sub>2</sub>-DHFR (A63P), while CytC<sub>1</sub> did not appear to be inhibited by treatment of MB 50.

**Frataxin Import into GA74 Mitochondria**



**Cpn10 Import into GA74 Mitochondria**

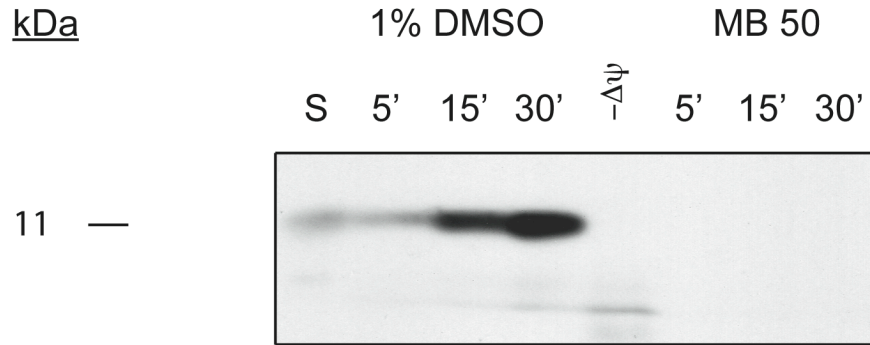
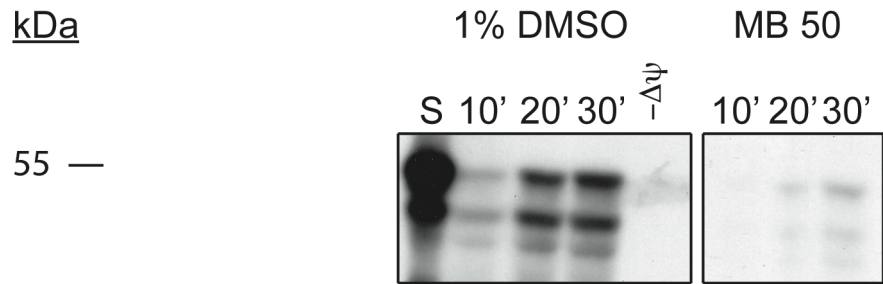


**Figure 3.8 Frataxin and Cpn10 Import into GA74 Mitochondria with MB 50 Treatment.**

[<sup>35</sup>S] Frataxin and Cpn10 were synthesized using a TNT Quick Coupled Transcription/Translation kit. GA74 yeast mitochondria were treated with either 1% DMSO, 50 μM CCCP & 1 mg/mL valinomycin, or 100 μM of MB 50 for 15 minutes at 25°C. 10 μL of [<sup>35</sup>S] transcript solutions/reaction time point was added to each condition and 250 μL aliquots were taken at each of 3 time points (5, 15, and 30-minutes). Reactions were quenched on ice by adding 50 μg/mL of trypsin. All imports were disrupted in Laemmli sample buffer and analyzed by SDS-PAGE and autoradiography. Once frataxin is imported it is processed twice by MPP, the first cleavage happens very rapidly, while the second cleavage occurs at a much slower rate and is the rate-limiting step for the formation of mature frataxin. MB 50 appears to inhibit the second cleavage of frataxin to a more significant extent than the first cleavage, while CCCP treatment completely blocks the import of frataxin. Cpn10 does not contain a known MPP cleavage site, but MB 50 is capable of completely inhibiting the import of Cpn 10 in purified mitochondria.

*Figure included with permission from Eric Torres.*

### Pink1 Import into GA74 Mitochondria



### MB 50 Titration - Pink1 Import

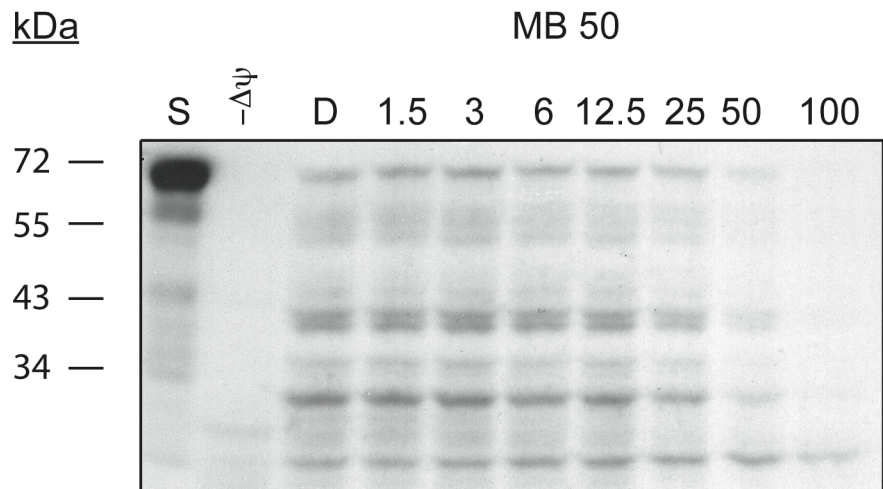


**Figure 3.9 Import and Titration of hPink1 into GA74 Mitochondria and MB 50.**

[<sup>35</sup>S] hPink was synthesized using a TNT Quick Coupled Transcription/Translation kit. For the import of hPink1, GA74 yeast mitochondria were treated with either 1% DMSO, 50 μM CCCP & 1 mg/mL valinomycin, or 100 μM of MB 50 for 15 minutes at 25°C. 10 μL of [<sup>35</sup>S] hPink1 solution/reaction time point was added to each condition and 250 μL aliquots were taken at each of 3 time points (10, 20, and 30-minutes). For the titration of MB 50, GA74 yeast mitochondria were treated with either 1% DMSO, 50 μM CCCP & 1 mg/mL valinomycin, or varying concentrations of MB 50 for 15 minutes at 25°C. 10 μL of [<sup>35</sup>S] hPink1 solution was added to each condition and 250 μL aliquots were taken after 30-minutes. All reactions for both experiments were quenched on ice by adding 50 μg/mL of trypsin. All imports were disrupted in Laemmli sample buffer and analyzed by SDS-PAGE and autoradiography. MB 50 was capable of significantly inhibiting the import of hPink1 into mitochondria and had an IC<sub>50</sub> of approximately 25 μM.

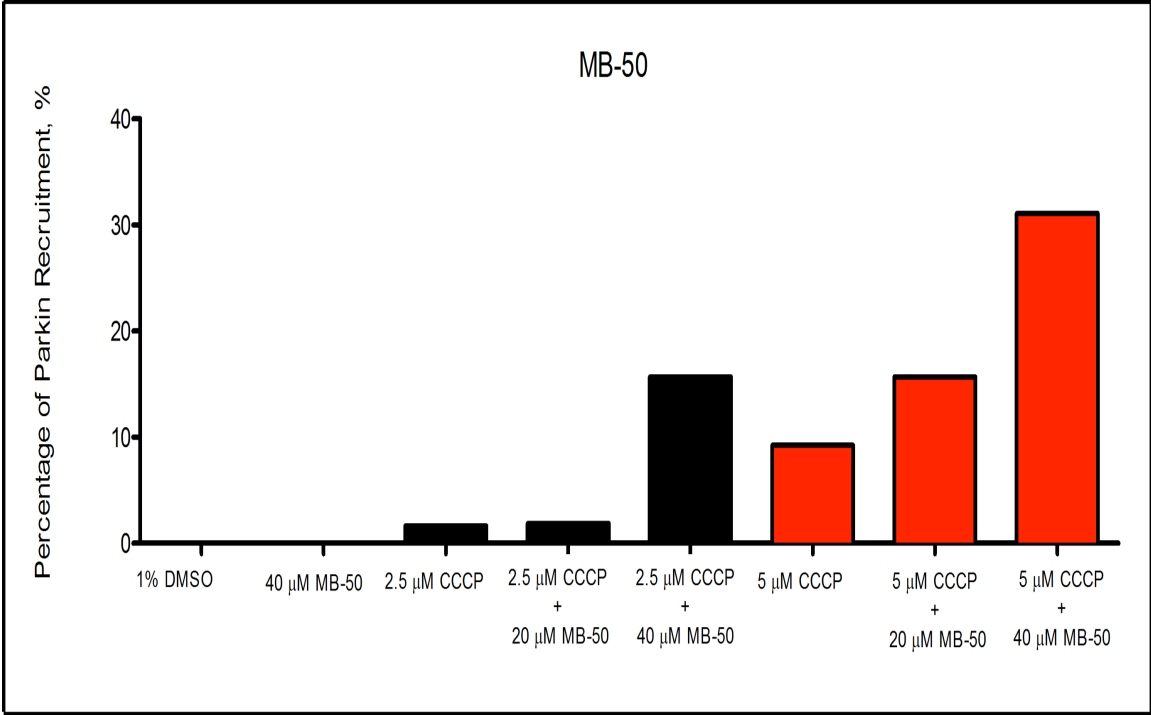
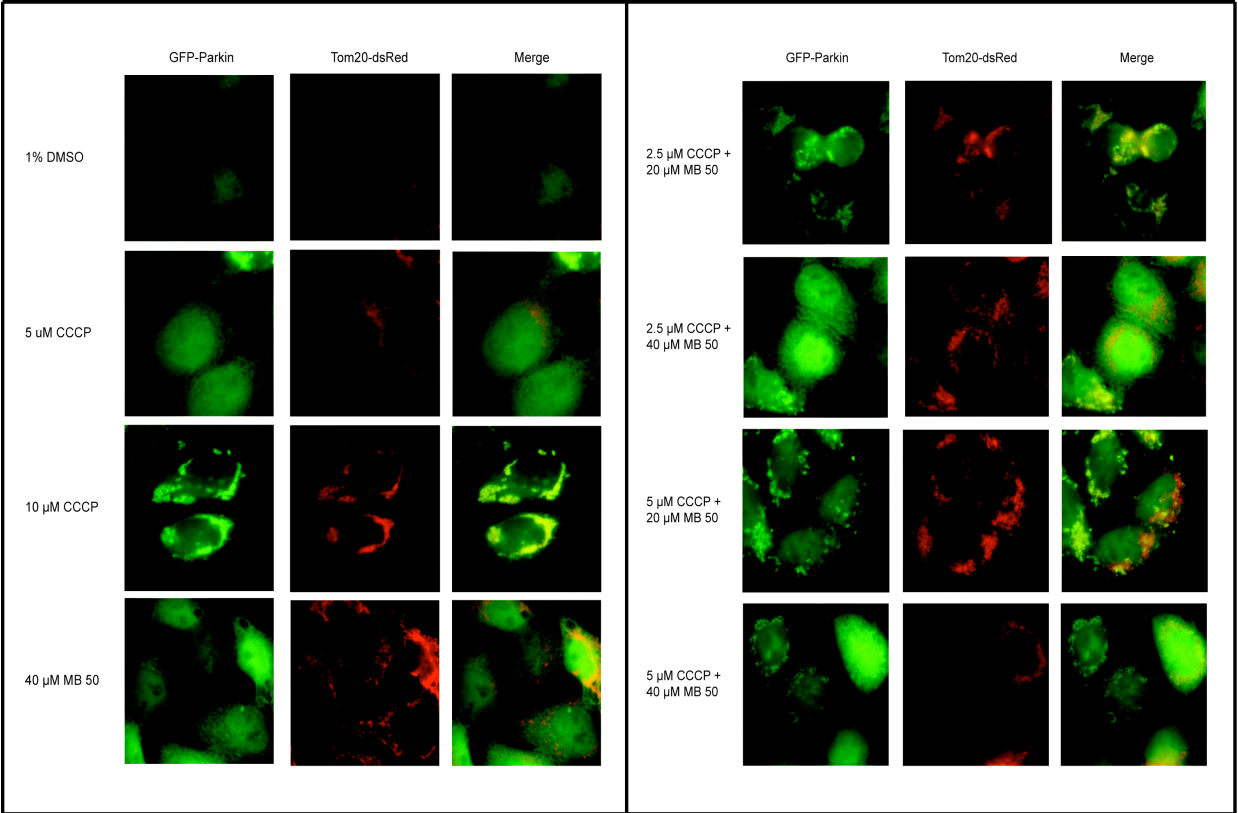


**Figure 3.10 Parkin Recruitment in EGFP-Parkin Expressing MTS dsRed HeLa MTS with Quantification.**

EGFP-Parkin expressing MTS dsRed HeLa cells were treated with either 5 or 10  $\mu\text{M}$  CCCP, 1% DMSO, 40  $\mu\text{M}$  MB 50 or 4 different combinations of CCCP and MB 50. 5  $\mu\text{M}$  of CCCP recruited some Parkin to the surface of mitochondria, while 10  $\mu\text{M}$  of CCCP recruited substantially more Parkin to the surface of mitochondria as evidenced by the yellow merged panel in the figure above. 40  $\mu\text{M}$  of MB 50 alone did not recruit Parkin to mitochondria. The combination of 2.5 or 5  $\mu\text{M}$  CCCP with either 20  $\mu\text{M}$  or 40  $\mu\text{M}$  MB 50 was capable of recruiting a significant amount of Parkin to mitochondria and this recruitment appeared to be greater than 10  $\mu\text{M}$  of CCCP alone. The quantification was done by counting 100 cells/condition and showed that when 40  $\mu\text{M}$  of MB 50 was combined with either 2.5 or 5  $\mu\text{M}$  CCCP it exhibited a greater amount of Parkin recruitment than CCCP alone. *Figure included with permission from Juwina Wijaya.*



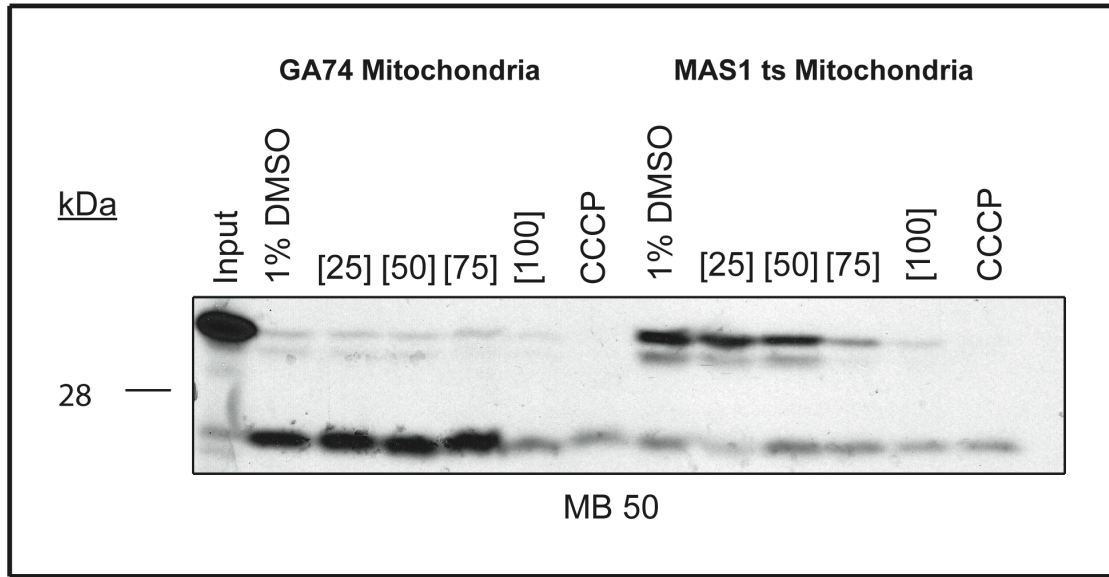


**Figure 3.11 Comparison of  $[^{35}\text{S}]$  Su9-DHFR in GA74 and MAS1 ts Mitochondria with MB 50 Treatment.**

$[^{35}\text{S}]$  Su9-DHFR was synthesized using a TNT Quick Coupled Transcription/Translation kit.

GA74 or MAS1 ts yeast mitochondria were treated with either 1% DMSO, 50  $\mu\text{M}$  CCCP & 1

mg/mL valinomycin, or varying concentrations of MB 50 for 15 minutes at 25°C. 10  $\mu\text{L}$  of  $[^{35}\text{S}]$

Su9-DHFR solution was added to each condition and 250  $\mu\text{L}$  aliquots were taken after 5-

minutes. Reactions were quenched on ice by adding 50  $\mu\text{g}/\text{mL}$  of trypsin. All imports were

disrupted in Laemmli sample buffer and analyzed by SDS-PAGE and autoradiography. The

MAS1 ts mutant Su9-DHFR was arrested in its import and protected from trypsin shaving, as

compared with DMSO treatment. Similarly, when the concentration of MB 50 was increased, the

total amount of Su9-DHFR import was decreased for both types of mitochondria and the amount

of un-processed Su9-DHFR for the MAS1 ts was significantly decreased.

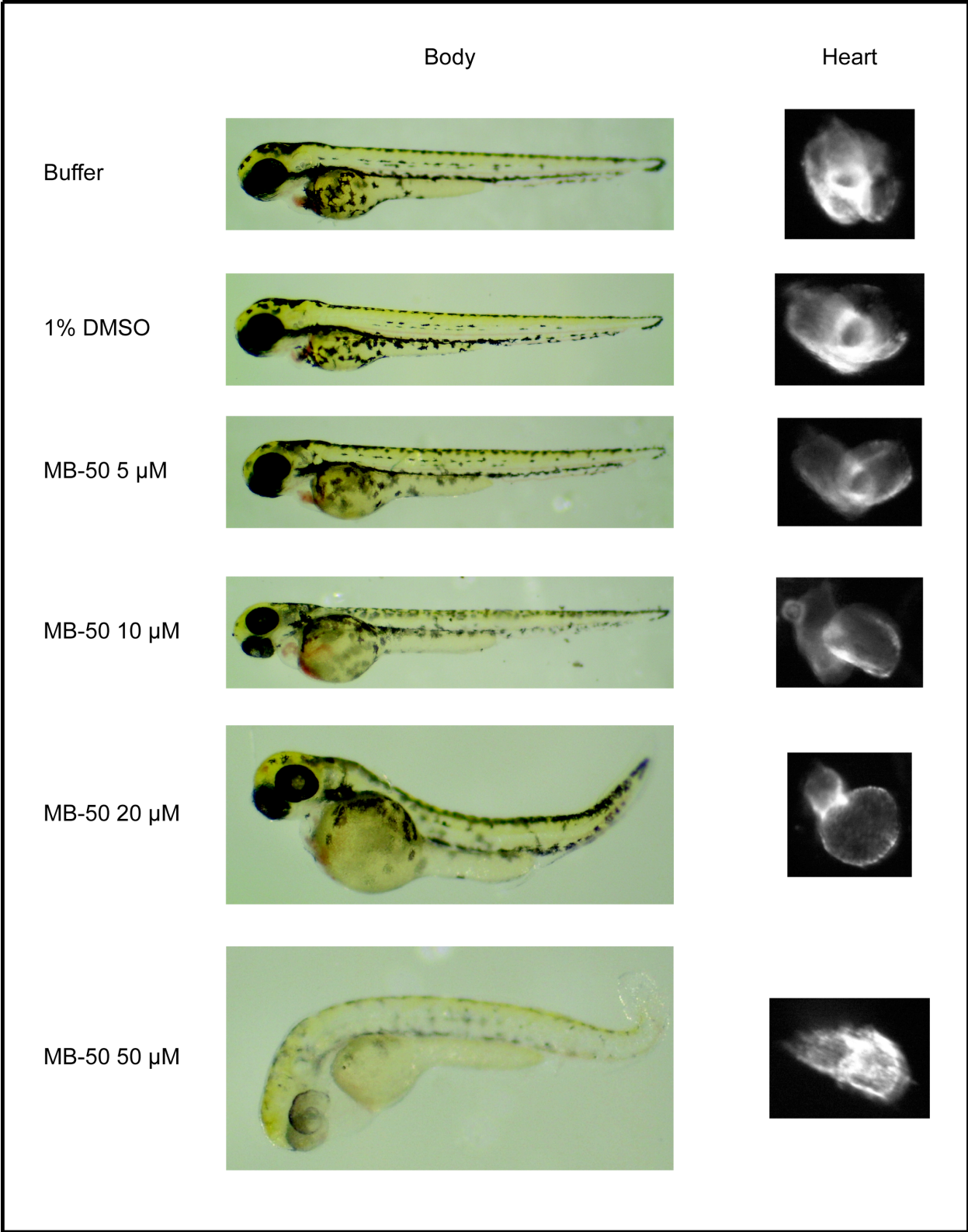


**Figure 3.12 Zebrafish Treatment with MB 50.**

Cmlc2 DsRed zebrafish were allowed to develop for 3 hours post-fertilization and then treated with 1% DMSO or the varying concentrations of MB 50. After 3 day post-fertilization the embryos were imaged using a Leica S8APO microscope at 1.575x magnification or Leica MZ16F fluorescent stereoscope (TexasRed filter set) at 5x magnification. At 20  $\mu$ M of MB 50 the zebrafish start showing a change in body curvature and at 50  $\mu$ M the body curvature was more severe and there was a loss in pigmentation. At 20  $\mu$ M MB 50 the heart also started to exhibit severe atrial distension and does not appear to flip.

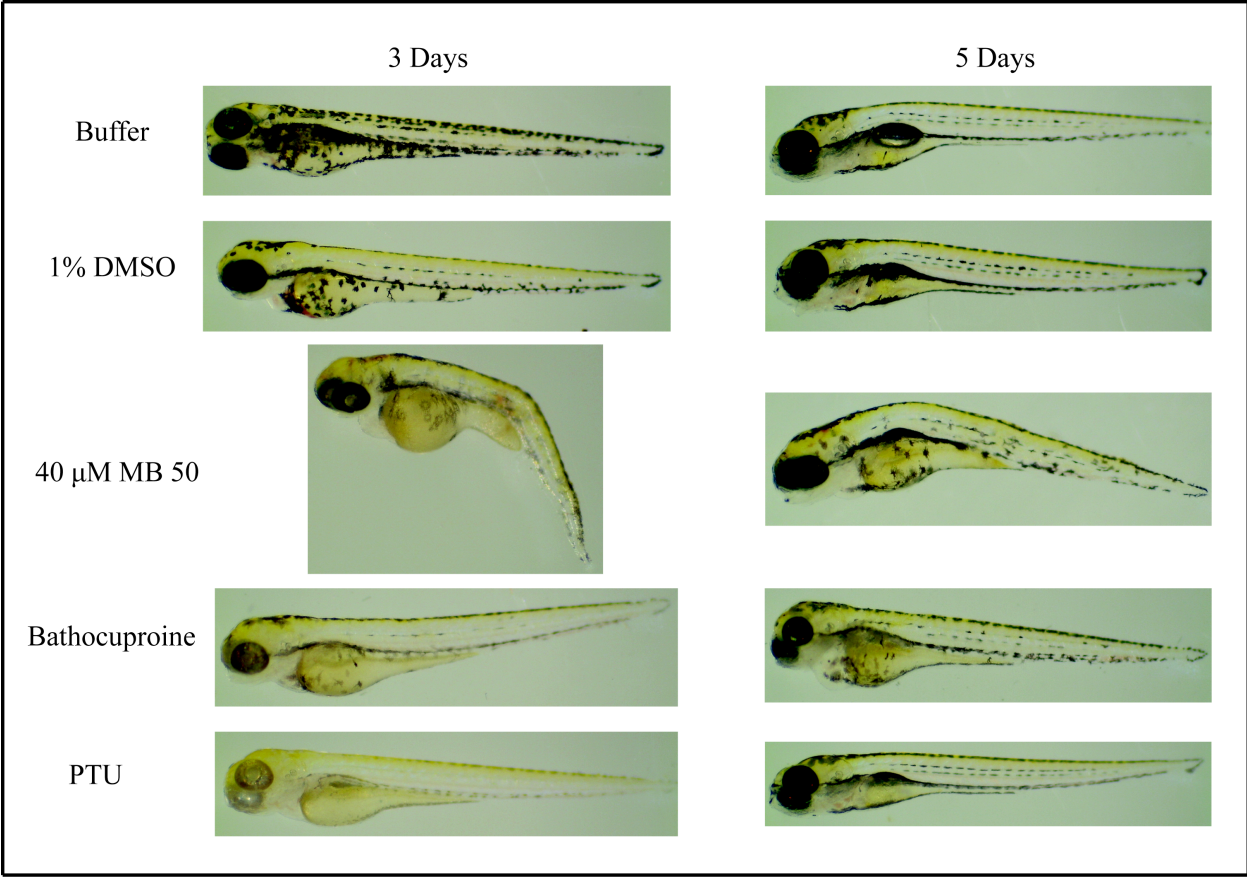


**Figure 3.13 Zebrafish Treated with MB 50, Bathocuproine, and PTU for 3 Days and then Wash-out for 2 Days.**

Cmlc2 DsRed Zebrafish were allowed to develop for 3 hours post-fertilization and treated with 1% DMSO, 40  $\mu$ M MB 50, 10  $\mu$ M Bathocuproine, or 0.003% PTU. After 3 day post-fertilization the embryos were imaged using a Leica S8APO microscope at 1.575x magnification, washed with E3 buffer and allowed to develop for an additional 2 day with no treatment. Following 5 day post-fertilization the embryos were imaged using a Leica S8APO microscope at 1.575x magnification. After 3 days of treatment with 40  $\mu$ M MB 50, bathocuproine, or PTU we saw a severe body curvature effect with MB 50, a slight decrease in pigmentation with bathocuproine and a significant loss of pigmentation with PTU. Following a 2-day washout period and the zebrafish were allowed to develop undisturbed, we saw the pigmentation had returned completely in all 3 drug conditions and the body curvature issue with MB 50 was not as severe.

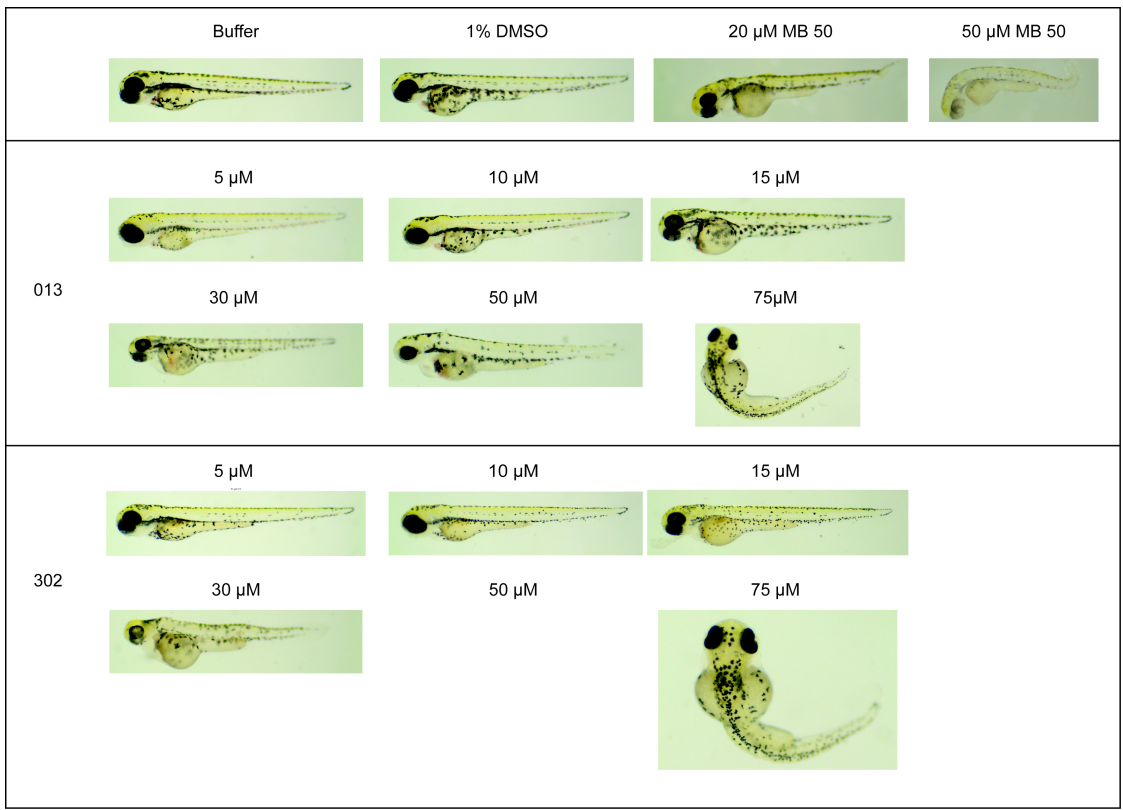
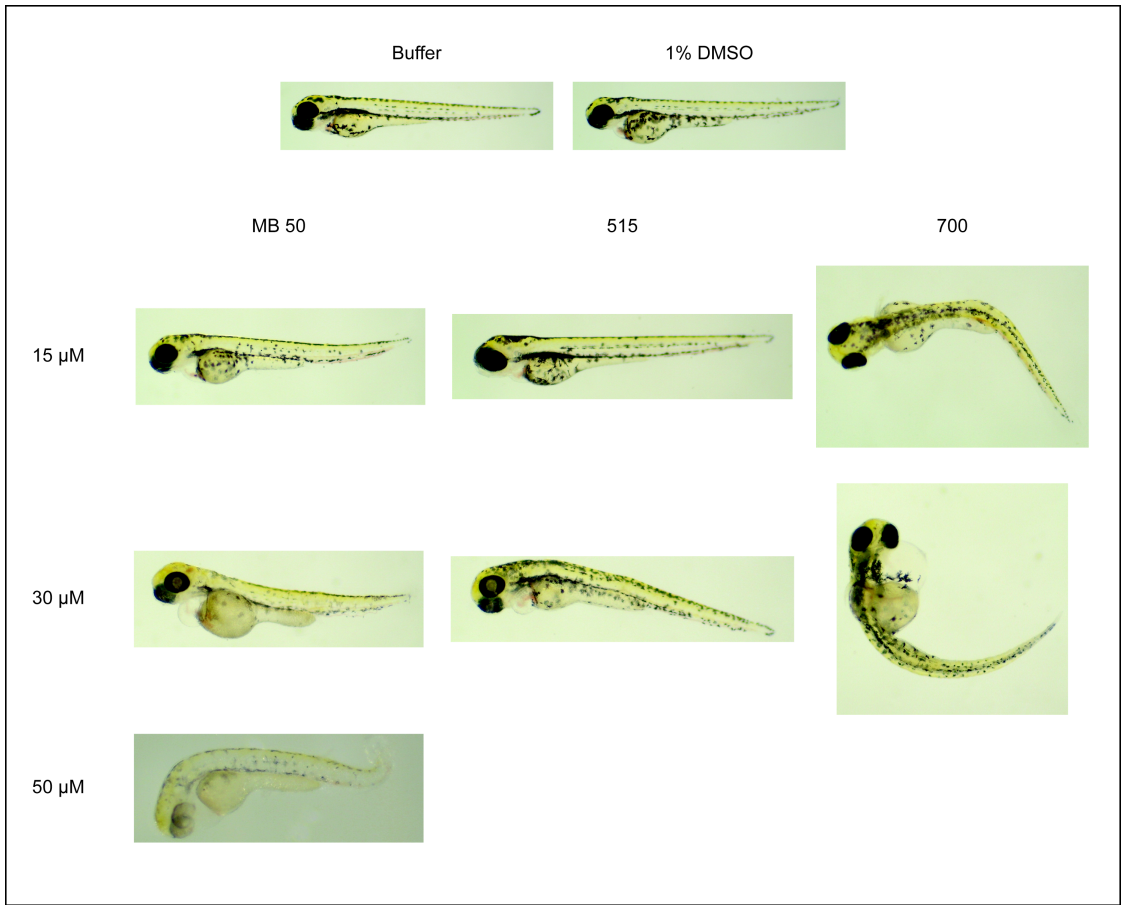


**Figure 3.14 Zebrafish Treated with MB 50 and its analogs.**

Cmlc2 dsRed Zebrafish were allowed to develop for 3 hours post-fertilization and were treated with 1% DMSO or the varying concentrations of MB 50 and its analogs. After 3 day post-fertilization the embryos were imaged using a Leica S8APO microscope at 1.575x magnification or Leica MZ16F fluorescent stereoscope (TexasRed filter set) at 5x magnification. MB 50 and its positive analogs (515 & 700) are in the top panel and all exhibited changes in body curvature that get more severe with increasing drug concentration as compared with the control zebrafish. The bottom panel shows MB 50 along with its negative controls (013 & 302). Drug 247 was left out of this table because at all concentrations tested all of the zebrafish were severely mutilated and none were alive. When comparing the negative controls to MB 50, the negative controls showed some signs of malformation and changes in body curvature, but at similar concentrations MB 50 appeared to be more severe than both negative analogs.

# References

1. Daum G, Bohni PC, & Schatz G (1982) Import of proteins into mitochondria. Cytochrome b2 and cytochrome c peroxidase are located in the intermembrane space of yeast mitochondria. *J Biol Chem* 257(21):13028-13033.
2. Jensen MB & Jasper H (2014) Mitochondrial Proteostasis in the Control of Aging and Longevity. *Cell Metab.*
3. Chi X, Kale J, Leber B, & Andrews DW (2014) Regulating cell death at, on, and in membranes. *Biochim Biophys Acta.*
4. Qi QR & Yang ZM (2014) Regulation and function of signal transducer and activator of transcription 3. *World J Biol Chem* 5(2):231-239.
5. Kianian PM & Kianian SF (2014) Mitochondrial dynamics and the cell cycle. *Front Plant Sci* 5:222.
6. Sickmann A, *et al.* (2003) The proteome of *Saccharomyces cerevisiae* mitochondria. *Proc Natl Acad Sci U S A* 100(23):13207-13212.
7. von Heijne G, Steppuhn J, & Herrmann RG (1989) Domain structure of mitochondrial and chloroplast targeting peptides. *Eur J Biochem* 180(3):535-545.
8. Pfanner N, Craig EA, & Honlinger A (1997) Mitochondrial preprotein translocase. *Annu Rev Cell Dev Biol* 13:25-51.
9. Neupert W (1997) Protein import into mitochondria. *Annu Rev Biochem* 66:863-917.
10. Honlinger A, *et al.* (1996) Tom7 modulates the dynamics of the mitochondrial outer membrane translocase and plays a pathway-related role in protein import. *EMBO J* 15(9):2125-2137.
11. Dietmeier K, *et al.* (1997) Tom5 functionally links mitochondrial preprotein receptors to the general import pore. *Nature* 388(6638):195-200.
12. Yamamoto H, *et al.* (2002) Tim50 is a subunit of the TIM23 complex that links protein translocation across the outer and inner mitochondrial membranes. *Cell* 111(4):519-528.
13. Geissler A, *et al.* (2002) The mitochondrial presequence translocase: an essential role of Tim50 in directing preproteins to the import channel. *Cell* 111(4):507-518.
14. Gaume B, *et al.* (1998) Unfolding of preproteins upon import into mitochondria. *EMBO J* 17(22):6497-6507.



15. Geissler A, *et al.* (2000) Membrane potential-driven protein import into mitochondria. The sorting sequence of cytochrome b(2) modulates the deltappsi-dependence of translocation of the matrix-targeting sequence. *Mol Biol Cell* 11(11):3977-3991.
16. Gakh O, Cavadini P, & Isaya G (2002) Mitochondrial processing peptidases. *Biochim Biophys Acta* 1592(1):63-77.
17. Endo T & Yamano K (2009) Multiple pathways for mitochondrial protein traffic. *Biol Chem* 390(8):723-730.
18. Ito A (1999) Mitochondrial processing peptidase: multiple-site recognition of precursor proteins. *Biochem Biophys Res Commun* 265(3):611-616.
19. Paces V, Rosenberg LE, Fenton WA, & Kalousek F (1993) The beta subunit of the mitochondrial processing peptidase from rat liver: cloning and sequencing of a cDNA and comparison with a proposed family of metallopeptidases. *Proc Natl Acad Sci U S A* 90(11):5355-5358.
20. Kitada S, Shimokata K, Niidome T, Ogishima T, & Ito A (1995) A putative metal-binding site in the beta subunit of rat mitochondrial processing peptidase is essential for its catalytic activity. *J Biochem* 117(6):1148-1150.
21. Kitada S, Yamasaki E, Kojima K, & Ito A (2003) Determination of the cleavage site of the presequence by mitochondrial processing peptidase on the substrate binding scaffold and the multiple subsites inside a molecular cavity. *J Biol Chem* 278(3):1879-1885.
22. McAda PC & Douglas MG (1982) A neutral metallo endoprotease involved in the processing of an F1-ATPase subunit precursor in mitochondria. *J Biol Chem* 257(6):3177-3182.
23. Miura S, Mori M, Amaya Y, & Tatibana M (1982) A mitochondrial protease that cleaves the precursor of ornithine carbamoyltransferase. Purification and properties. *Eur J Biochem* 122(3):641-647.
24. Conboy JG, Fenton WA, & Rosenberg LE (1982) Processing of pre-ornithine transcarbamylase requires a zinc-dependent protease localized to the mitochondrial matrix. *Biochem Biophys Res Commun* 105(1):1-7.
25. Schmidt B, Wachter E, Sebald W, & Neupert W (1984) Processing peptidase of *Neurospora* mitochondria. Two-step cleavage of imported ATPase subunit 9. *Eur J Biochem* 144(3):581-588.
26. Luciano P, Tokatlidis K, Chambre I, Germanique JC, & Geli V (1998) The mitochondrial processing peptidase behaves as a zinc-metallopeptidase. *J Mol Biol* 280(2):193-199.

27. Auld DS (1995) Removal and replacement of metal ions in metallopeptidases. *Methods Enzymol* 248:228-242.
28. Hurt EC, Allison DS, Muller U, & Schatz G (1987) Amino-terminal deletions in the presequence of an imported mitochondrial protein block the targeting function and proteolytic cleavage of the presequence at the carboxy terminus. *J Biol Chem* 262(3):1420-1424.
29. Vestweber D, Brunner J, Baker A, & Schatz G (1989) A 42K outer-membrane protein is a component of the yeast mitochondrial protein import site. *Nature* 341(6239):205-209.
30. Shimokata K, Kitada S, Ogishima T, & Ito A (1998) Role of alpha-subunit of mitochondrial processing peptidase in substrate recognition. *J Biol Chem* 273(39):25158-25163.
31. Taylor AB, *et al.* (2001) Crystal structures of mitochondrial processing peptidase reveal the mode for specific cleavage of import signal sequences. *Structure* 9(7):615-625.
32. Nagao Y, *et al.* (2000) Glycine-rich region of mitochondrial processing peptidase alpha-subunit is essential for binding and cleavage of the precursor proteins. *J Biol Chem* 275(44):34552-34556.
33. Kojima K, Kitada S, Shimokata K, Ogishima T, & Ito A (1998) Cooperative formation of a substrate binding pocket by alpha- and beta-subunits of mitochondrial processing peptidase. *J Biol Chem* 273(49):32542-32546.
34. Luciano P, Geoffroy S, Brandt A, Hernandez JF, & Geli V (1997) Functional cooperation of the mitochondrial processing peptidase subunits. *J Mol Biol* 272(2):213-225.
35. Rodriguez M, Ochoa ME, Santillan R, Farfan N, & Barba V (2005) Imino Diels-Alder reaction of boronates: A new route to 3,4-dihydroquinolines. *Journal of Organometallic Chemistry* 690(12):2975-2988.
36. Lopez-Ruiz H, Mera-Moreno I, Rojas-Lima S, Santillan R, & Farfan N (2008) Stereoselective addition of allylmagnesium chloride to the C=N bond of [4.3.0] boron heterobicycles. *Tetrahedron Lett* 49(10):1674-1677.
37. Wong CY, McDonald R, & Cavell RG (1996) Hexacoordinate phosphorus .7. Synthesis and characterization of neutral phosphorus(V) compounds containing divalent tridentate diphenol imine, azo, and thio ligands. *Inorg Chem* 35(2):325-334.
38. Chen WH & Pang Y (2009) Efficient synthesis of 2-(2'-hydroxyphenyl)benzoxazole by palladium(II)-catalyzed oxidative cyclization. *Tetrahedron Lett* 50(48):6680-6683.

39. Kim JS, Kim SY, Park YY, Tomiyasu H, & Ikeda Y (2000) A kinetic study on substitution reactions of tridentate ligands for acetylacetonate in bis(acetylacetonato)(tetrahydrofuran)dioxouranium(VI). *Inorg Chim Acta* 304(2):199-203.
40. Priest JW & Hajduk SL (2003) Trypanosoma brucei cytochrome c1 is imported into mitochondria along an unusual pathway. *J Biol Chem* 278(17):15084-15094.
41. Popov-Celeketic D, Waegemann K, Mapa K, Neupert W, & Mokranjac D (2011) Role of the import motor in insertion of transmembrane segments by the mitochondrial TIM23 complex. *EMBO Rep* 12(6):542-548.
42. Curran SP, Leuenberger D, Oppliger W, & Koehler CM (2002) The Tim9p-Tim10p complex binds to the transmembrane domains of the ADP/ATP carrier. *EMBO J* 21(5):942-953.
43. Curran SP, *et al.* (2004) The role of Hot13p and redox chemistry in the mitochondrial TIM22 import pathway. *J Biol Chem* 279(42):43744-43751.
44. Goswami AV, Samaddar M, Sinha D, Purushotham J, & D'Silva P (2012) Enhanced J-protein interaction and compromised protein stability of mtHsp70 variants lead to mitochondrial dysfunction in Parkinsons disease. *Human Molecular Genetics* 21(15):3317-3332.
45. Popov-Celeketic D, Waegemann K, Mapa K, Neupert W, & Mokranjac D (2011) Role of the import motor in insertion of transmembrane segments by the mitochondrial TIM23 complex. *Embo Reports* 12(6):542-548.
46. Beasley EM, Muller S, & Schatz G (1993) The Signal That Sorts Yeast Cytochrome-B2 to the Mitochondrial Intermembrane Space Contains 3 Distinct Functional Regions. *Embo Journal* 12(6):2303-2311.
47. Huynen MA, Snel B, Bork P, & Gibson TJ (2001) The phylogenetic distribution of frataxin indicates a role in iron-sulfur cluster protein assembly. *Hum Mol Genet* 10(21):2463-2468.
48. Pandey A, *et al.* (2013) Frataxin directly stimulates mitochondrial cysteine desulfurase by exposing substrate-binding sites, and a mutant Fe-S cluster scaffold protein with frataxin-bypassing ability acts similarly. *J Biol Chem* 288(52):36773-36786.
49. Bencze KZ, *et al.* (2006) The structure and function of frataxin. *Critical reviews in biochemistry and molecular biology* 41(5):269-291.
50. Campuzano V, *et al.* (1996) Friedreich's ataxia: autosomal recessive disease caused by an intronic GAA triplet repeat expansion. *Science* 271(5254):1423-1427.

51. Durr A, *et al.* (1996) Clinical and genetic abnormalities in patients with Friedreich's ataxia. *N Engl J Med* 335(16):1169-1175.
52. Kirches E, *et al.* (2011) Dual role of the mitochondrial protein frataxin in astrocytic tumors. *Laboratory investigation; a journal of technical methods and pathology* 91(12):1766-1776.
53. Koutnikova H, *et al.* (1997) Studies of human, mouse and yeast homologues indicate a mitochondrial function for frataxin. *Nat Genet* 16(4):345-351.
54. van der Giezen M, Leon-Avila G, & Tovar J (2005) Characterization of chaperonin 10 (Cpn10) from the intestinal human pathogen *Entamoeba histolytica*. *Microbiology* 151(Pt 9):3107-3115.
55. Zhou C, *et al.* (2008) The kinase domain of mitochondrial PINK1 faces the cytoplasm. *Proc Natl Acad Sci U S A* 105(33):12022-12027.
56. Geisler S, *et al.* (2010) The PINK1/Parkin-mediated mitophagy is compromised by PD-associated mutations. *Autophagy* 6(7):871-878.
57. Matsuda N, *et al.* (2010) PINK1 stabilized by mitochondrial depolarization recruits Parkin to damaged mitochondria and activates latent Parkin for mitophagy. *J Cell Biol* 189(2):211-221.
58. Vives-Bauza C, *et al.* (2010) PINK1-dependent recruitment of Parkin to mitochondria in mitophagy. *Proc Natl Acad Sci U S A* 107(1):378-383.
59. Koyano F, *et al.* (2014) Ubiquitin is phosphorylated by PINK1 to activate parkin. *Nature* 510(7503):162-166.
60. McLelland GL, Soubannier V, Chen CX, McBride HM, & Fon EA (2014) Parkin and PINK1 function in a vesicular trafficking pathway regulating mitochondrial quality control. *EMBO J* 33(4):282-295.
61. Chen Y & Dorn GW, 2nd (2013) PINK1-phosphorylated mitofusin 2 is a Parkin receptor for culling damaged mitochondria. *Science* 340(6131):471-475.
62. Lister JA (2002) Development of pigment cells in the zebrafish embryo. *Microscopy research and technique* 58(6):435-441.
63. Logan DW, Burn SF, & Jackson IJ (2006) Regulation of pigmentation in zebrafish melanophores. *Pigment cell research / sponsored by the European Society for Pigment Cell Research and the International Pigment Cell Society* 19(3):206-213.

64. Karlsson J, von Hofsten J, & Olsson PE (2001) Generating transparent zebrafish: a refined method to improve detection of gene expression during embryonic development. *Marine biotechnology* 3(6):522-527.
65. O'Reilly-Pol T & Johnson SL (2008) Neocuproine ablates melanocytes in adult zebrafish. *Zebrafish* 5(4):257-264.
66. Ishizaki H, *et al.* (2010) Combined zebrafish-yeast chemical-genetic screens reveal gene-copper-nutrition interactions that modulate melanocyte pigmentation. *Disease models & mechanisms* 3(9-10):639-651.
67. Nicholson DW, Stuart RA, & Neupert W (1989) Biogenesis of cytochrome c1. Role of cytochrome c1 heme lyase and of the two proteolytic processing steps during import into mitochondria. *J Biol Chem* 264(17):10156-10168.
68. Wachter C, Schatz G, & Glick BS (1992) Role of ATP in the intramitochondrial sorting of cytochrome c1 and the adenine nucleotide translocator. *EMBO J* 11(13):4787-4794.
69. Martin J, Mahlke K, & Pfanner N (1991) Role of an energized inner membrane in mitochondrial protein import. Delta psi drives the movement of presequences. *J Biol Chem* 266(27):18051-18057.
70. Nunnari J, Fox TD, & Walter P (1993) A mitochondrial protease with two catalytic subunits of nonoverlapping specificities. *Science* 262(5142):1997-2004.
71. Schleyer M & Neupert W (1985) Transport of proteins into mitochondria: translocational intermediates spanning contact sites between outer and inner membranes. *Cell* 43(1):339-350.
72. Knight SA, Sepuri NB, Pain D, & Dancis A (1998) Mt-Hsp70 homolog, Ssc2p, required for maturation of yeast frataxin and mitochondrial iron homeostasis. *J Biol Chem* 273(29):18389-18393.
73. Branda SS, *et al.* (1999) Yeast and human frataxin are processed to mature form in two sequential steps by the mitochondrial processing peptidase. *J Biol Chem* 274(32):22763-22769.
74. Gordon DM, Kogan M, Knight SA, Dancis A, & Pain D (2001) Distinct roles for two N-terminal cleaved domains in mitochondrial import of the yeast frataxin homolog, Yfh1p. *Hum Mol Genet* 10(3):259-269.
75. Adamec J, *et al.* (2000) Iron-dependent self-assembly of recombinant yeast frataxin: implications for Friedreich ataxia. *Am J Hum Genet* 67(3):549-562.

76. Cavadini P, Adamec J, Taroni F, Gakh O, & Isaya G (2000) Two-step processing of human frataxin by mitochondrial processing peptidase. Precursor and intermediate forms are cleaved at different rates. *J Biol Chem* 275(52):41469-41475.
77. Irrcher I, Adhietty PJ, Joseph AM, Ljubicic V, & Hood DA (2003) Regulation of mitochondrial biogenesis in muscle by endurance exercise. *Sports medicine* 33(11):783-793.
78. Ryan MT, Naylor DJ, Hoogenraad NJ, & Hoj PB (1995) Affinity purification, overexpression, and characterization of chaperonin 10 homologues synthesized with and without N-terminal acetylation. *J Biol Chem* 270(37):22037-22043.
79. Samii A, Nutt JG, & Ransom BR (2004) Parkinson's disease. *Lancet* 363(9423):1783-1793.
80. Clark IE, *et al.* (2006) *Drosophila pink1* is required for mitochondrial function and interacts genetically with parkin. *Nature* 441(7097):1162-1166.
81. Park J, *et al.* (2006) Mitochondrial dysfunction in *Drosophila* PINK1 mutants is complemented by parkin. *Nature* 441(7097):1157-1161.
82. Yang Y, *et al.* (2006) Mitochondrial pathology and muscle and dopaminergic neuron degeneration caused by inactivation of *Drosophila* Pink1 is rescued by Parkin. *Proc Natl Acad Sci U S A* 103(28):10793-10798.
83. Greene AW, *et al.* (2012) Mitochondrial processing peptidase regulates PINK1 processing, import and Parkin recruitment. *EMBO Rep* 13(4):378-385.
84. Steele SL, Prykhozhiy SV, & Berman JN (2014) Zebrafish as a model system for mitochondrial biology and diseases. *Translational research : the journal of laboratory and clinical medicine* 163(2):79-98.
85. Dabir DV, *et al.* (2013) A small molecule inhibitor of redox-regulated protein translocation into mitochondria. *Dev Cell* 25(1):81-92.
86. Miyata N, *et al.* (in submission) Adaptation of a genetic screen reveals an inhibitor for mitochondrial protein import component Tim44. (EMBO).
87. Glick BS & Pon LA (1995) Isolation of highly purified mitochondria from *Saccharomyces cerevisiae*. *Methods Enzymol* 260:213-223.
88. Hasson SA, *et al.* (2010) Substrate specificity of the TIM22 mitochondrial import pathway revealed with small molecule inhibitor of protein translocation. *Proc Natl Acad Sci U S A* 107(21):9578-9583.

89. Koehler CM, *et al.* (1998) Tim9p, an essential partner subunit of Tim10p for the import of mitochondrial carrier proteins. *EMBO J* 17(22):6477-6486.
90. Freshney RI (2000) *Culture of animal cells : a manual of basic technique* (Wiley, New York) 4th Ed pp xxvi, 577.
91. Strober W (2001) Trypan blue exclusion test of cell viability. *Current protocols in immunology / edited by John E. Coligan ... [et al.]* Appendix 3:Appendix 3B.

# Chapter 4: Characterization of MitoBloCK-51

## Abstract

A second compound, MitoBloCK-51 (MB 51) was identified as a promising inhibitor of mitochondrial processing peptidase (MPP) from the high-throughput screen and subsequent characterization assays. Experiments conducted to characterize MB 51 *in vitro* showed inhibition of the processing of known MPP substrates including fraxtin, and Pink1. Interestingly, when the import of Pink1 was conducted in the presence of MB 51 utilizing carbonate extraction, a high molecular weight aggregate formed that was not present with the vehicle control alone or with CCCP treatment. Parkin recruitment in HeLa cells was not greatly affected with MB 51 treatment, however when zebrafish were treated with MB 51, developmental abnormalities were observed. Additionally, MB 51 treatment resulted in a lack of pigmentation of the embryos, an effect similar to that observed with bathocuprione or PTU treatment, known inhibitors of melanin formation. These results illustrate potential interactions of MPP in copper metabolism or mitophagy; functions not usually assumed for import proteases.



# Introduction

## Mitochondrial Structure & Function

Mitochondria consist of four separate compartments including the outer membrane, the intermembrane space, the inner membrane and the matrix. The primary role of the mitochondrion is energy production in the form of ATP, though the organelle also plays a central role in other cellular functions that include signaling, cellular differentiation, cell death, cell cycle and cell growth. (1-5) The mitochondrial genome is approximately 16,000 base pairs and encodes for 37 genes, which include: 22 tRNAs, 2 rRNAs, 13 proteins, and 1 untranslated region. (6) A majority of the proteins utilized in the mitochondria are encoded by the nuclear genome, translated in the cytosol and must be imported into the mitochondria. Imported proteins that function in the mitochondrial matrix typically possess a positively charged N-terminal mitochondrial targeting sequence (MTS) that directs them through the mitochondrial translocase machinery and into the mitochondrial matrix. (7)

Precursor proteins that are destined for the mitochondrial matrix first interact with the translocase of the outer membrane (TOM) complex, which is comprised of 7 integral membrane proteins (Tom70p, Tom40p, Tom22p, Tom20p, Tom7p, Tom6p, and Tom5p). (8-11) Following the traverse across the intermembrane space, precursors that possess an MTS encounter the translocase of the inner membrane 23 (TIM23), which is comprised of 3 integral membrane proteins (Tim50p, Tim17p, and Tim23p). (8, 9, 12) Tim17p and Tim23p make-up the pore of the complex, Tim50p acts as a guide for precursor proteins and Tim44p, Tim14p, mHsp70, and mGrpE function as the motor to attract the MTS to the complex and draw the precursor protein into the matrix for processing. (13-15) For precursor proteins imported into the mitochondrial

matrix to fold and function properly, their MTS must first be cleaved off. This cleavage is accomplished by the matrix protease, mitochondrial processing peptidase (MPP). (16, 17)

### *Mitochondrial Processing Peptidase*

MPP is a 100 kDa metalloendopeptidase and is a member of the pitrilysin family that includes pitrilysin and 3 members of the insulin-degrading enzyme family. (18) All members of this family possess an inverted zinc-binding motif with the structure: H-x-x-E-H-x<sub>76</sub>-E. Coordination of the zinc ion is accomplished by both His residues and the downstream Glu residue; the upstream Glu residue is responsible for the activation of water required for substrate cleavage. (19-21) The optimal pH range for purified MPP activity is pH 7-8, with inactivation at lower pH. MPP is inhibited by EDTA and *o*-phenanthroline and activated by divalent cations (Co<sup>2+</sup>, Mn<sup>2+</sup>, Zn<sup>2+</sup> and Mg<sup>2+</sup>). (22-25) At low concentrations of metals, the degree of MPP activation follows the following trend, Zn<sup>2+</sup> > Mn<sup>2+</sup> > Co<sup>2+</sup>; though unlike cobalt and manganese, excess of zinc inhibits MPP activity. (26, 27)

MPP is formed as a heterodimer complex that consists of an  $\alpha$  and a  $\beta$  subunit. Both subunits are necessary for the proper functioning of MPP. The MTS of precursor proteins is typically 20-60 amino acids and carries a global positive charge. (7) The MTS is both necessary and sufficient to target precursor proteins to their correct location within the mitochondrion. A number of non-mitochondrial molecules, including cytosolic proteins and nucleic acids have been successfully targeted to the mitochondrion through the use of only an N-terminal matrix targeting sequence. (28, 29)

For MPP to function properly both subunits ( $\alpha$  and  $\beta$ ) are necessary, but the two subunits perform different needs for cleavage of MPP substrates. (30) The zinc-binding domain resides on

the  $\beta$  subunit. The  $\alpha$ -MPP subunit has no catalytic activity but appears to play a role in substrate specificity and recognition, via a highly conserved glycine-rich loop and a negative region that faces towards the active site cavity. (18) The crystal structure of yeast MPP suggests the active site is located in a central, negatively charged cavity and the glycine-rich loop appears to block accessibility to the cavity. When this loop is deleted both the enzyme's substrate affinity and catalytic activity are decreased. (31, 32) Both subunits of MPP cooperatively form the substrate-binding pocket and each subunit is responsible for recognizing different aspects of precursor. The subunits alone were found to have low affinity towards elements of presequence however the native conformation was necessary for high substrate binding affinity. (33) From crystal structures of MPP with synthetic signal peptides, it appears the presequence interacts with the polar cavity of MPP in an extended conformation, suggesting the helical conformation mitochondrial targeting sequences take on is important for recognition by the mitochondrial import machinery and for cleavage by MPP. (31) Through the use of mutagenesis, the zinc-binding domain (HxxEHx<sub>7</sub>H) of  $\beta$ -MPP was shown to be vital for the proper formation of active and may be in contact with  $\alpha$ -MPP. Additionally, the central region around Lys215 of  $\beta$ -MPP, which is not highly conserved, plays a role in interacting with  $\alpha$ -MPP. Finally, the C-terminal region that surrounds Ser314 of  $\beta$ -MPP is needed for catalytic activity. (34) Using both cross-linking analysis and surface plasmon resonance  $\alpha$ -MPP was found to bind a precursor protein in the absence of  $\beta$ -MPP and was able to bind the precursor as effectively as MPP. It appears  $\alpha$ -MPP is responsible for binding the mitochondrial targeting sequence before it is presented to the catalytic domain. (34) All of these factors come together to provide strict specificity and high affinity for MPP and its substrates.

## *MitoBloCK-51*

MitoBloCK-51 (MB 51) also known as 2-(1-methyl,1,10b-dihydrospiro[benzo[e]pyrazolo[1,5-c][1,3]oxazine-5,4'-piperidin]-2-yl)benzene-1,4-diol. This compound was purchased from Life Chemicals and so far has no published method for synthesis, nor has it been utilized in any other schemes of organic synthesis. MB 51 has a molecular weight of 365.431 Da and a CAS registration number of 899972-20-4. As of yet this compound has no known biological use.

## *Structure-Activity Relationships (SARs)*

In addition to the characterization of the original hit compound from the HTS, a SARs study is usually conducted. The SAR describes the relationship between the compound of interest and its biological effect. These studies allow for the dissection and potential identification of essential moieties on the small molecule, along with building a library of both positive and negative analogs that can further enhance the characterization of the hit compound and effect on the protein pathway. Within this project, a SAR study was conducted by data mining the original HTS against a structural homology search for non-hit compounds or compounds that were not originally screened.

After the determination of MB 51 as a potential candidate for the inhibition of MPP our goal was to characterize this compound, along with building and characterizing potential positive and negative analogs for MB 51. This work was done using purified recombinant MPP, purified wild-type and MAS1ts mitochondria, mammalian cell culture, and zebrafish assays.

# Results

One of the compounds we focused on for further characterization was compound 199 (MitoBloCK-51; MB 51) because it was one of the more promising compounds resulting from a group with a number of hits. Its core structure of a quinone/hydroquinone is interesting due to its similarity to coenzyme Q and when treated in conjugation with CCCP we saw Pink1 accumulation (Figure 4.1). According to the data presented in chapter 2 concerning general mitochondrial dysfunction caused by the small molecules, MB 51 did not disrupt the integrity of the outer mitochondrial membrane, cause depolarization of the outer membrane, cause dysfunction of the ETC, or block the import of AAC. Similarly, MB 51 was also examined for its MIC<sub>50</sub> in HEK cells and its effect on mitochondrial morphology in HeLa cells (Figure 4.2). The MIC<sub>50</sub> of MB 51 is approximately 200  $\mu$ M and it did not appear to cause changes in mitochondrial morphology. Figure 3.3 shows the structure of MB 51 along with its positive and negative controls regarding their ability to inhibit the MPP/JPT fluorogenic peptide assay.

The negative controls were found by data mining the HTS data for compounds that did not inhibit MPP activity and possessed a greater than 60% homology with MB 51 based on structure analysis. This figure only shows the positive and negative controls compounds that were ordered and tested along with MB 51; for a full list of all the compounds that fell into either of these groups refer to the appendices. Based on the similarities with all the positive MB 51 analogs and the fact they all contain the quinone/hydroquinone moiety we assumed this group was the important substituent for this group of molecules. As such, we wanted our negative analogs to systematically substitute substituents from this group to assess if our hypothesis was correct about MB 51. Compound 001, completely substitutes the quinone moiety for a benzene

ring, thereby getting rid of both hydroxyl groups on the ring. Compound 082, changes the quinone moiety for a phenol one, which causes the loss of one of the hydroxyl groups. Compound 102, replaces on the hydroxyl groups in the quinone for a methyl, which allows for some similarity in geometry to the original quinone but a loss of the reactivity that the original group possessed.

MB 51 exhibits the ability to not only inhibit the in-vitro cleavage of [<sup>35</sup>S] Su9-DHFR but also its import into purified GA74 mitochondria (Figures 4.4 and 4.5). A titration of MB 51's ability to inhibit Su9-DHFR into mitochondria was also examined (Figure 4.6). The IC<sub>50</sub> for Su9-DHFR import was approximately 50 μM. MB 51 was also tested against the import of Cytochrome C<sub>1</sub> (CytC<sub>1</sub>), Cytochrome B<sub>2</sub>-DHFR (1-167) (CytB<sub>2</sub>-DHFR (1-167)), and Cytochrome B<sub>2</sub>-DHFR (A63P) (CytB<sub>2</sub>-DHFR (A63P)). CytC<sub>1</sub> is targeted towards the inner membrane of the mitochondria and is one of the constituents of Complex III of the ETC. (35) CytB<sub>2</sub> is synthesized as a precursor in the cytosol and imported into the mitochondria. It contains a tightly folded heme-binding domain; the TIM23 complex sorts its transport across the outer membrane, which requires ATP. The 1-167 version of this construct is typically not processed by MPP since it is directed towards the intermembrane space due to a stop transfer sequence. (36-38) Conversely, the A63P mutant of this construct is targeted towards the matrix and is processed by MPP. (38-40) MB 51 showed the ability to inhibit both the import CytB<sub>2</sub>-DHFR (1-167) and CytC<sub>1</sub>, but it did not appear to inhibit the import of CytB<sub>2</sub>-DHFR (A63P), (Figure 4.7).

Frataxin is a 210 amino acid protein encoded by the nuclear DNA that is imported into the mitochondrion. Frataxin appears to be involved in the assembly of iron-sulfur clusters and has been proposed to be either an iron chaperone or an iron storage protein. The mRNA of frataxin is predominantly expressed in tissues with a high metabolic rate such as the liver,

kidney, brown adipose tissue and heart. (41, 42) Frataxin has been implicated in the etiology of FRDA, which is an autosomal recessive degenerative disease. Upon import into the mitochondria, frataxin is processed twice (in 2 sequential cleavages) by MPP, the first of the cleavages happens very rapidly, while the second cleavage is much slower and is the rate-limiting step for the formation of mature frataxin. A reduction in this second cleavage has been directly linked to the cause of FRDA and mutations in both MPP and frataxin have been shown to inhibit the cleavage of frataxin by MPP. The yeast and human frataxin presequence is 51 and 55 amino acids, respectively, and the presequence of yeast frataxin is cleaved between residues 20-21 and 51-52, while the human frataxin presequence is cleaved between 41-42 and 55-56. (41-47) MB 51 appears to cause an overall inhibition of frataxin, while CCCP treatment completely blocks the import of frataxin (Figure 4.8).

Chaperonin 10 (Cpn10) along with chaperonin 60 aids in the stabilization and protection of disassembled proteins. Cpn10 exists as a ring-shape oligomer of between six to eight identical subunits that are self-assembled by the presence of  $Mg^{2+}$ -ATP. The central cavity of the cylindrical Cpn60 tetradecamer provides an isolated environment for protein folding, while Cpn10 binds to Cpn60 and synchronizes the release of the folded protein in a  $Mg^{2+}$ -ATP dependent manner. (48) Cpn10 does not contain a known MPP cleavage site, but MB 51 is capable of significantly inhibiting the import of Cpn10 in purified mitochondria (Figure 4.8).

PTEN induced putative kinase 1 (Pink1), which is synthesized as a 63 kDa protein that is cleaved by PARL, between residues Ala103 and Phe104, resulting in a 43 kDa fragment. Within the topology of PINK1 there is a N-terminal mitochondrial localization sequence, a putative transmembrane sequence, a Ser/Thr kinase domain, and a C-terminal regulatory sequence. The protein has been found to localize to the outer membrane of mitochondria, but is found primarily

in the cytosol. Experiments suggest the Ser/Thr kinase domain faces outward toward the cytosol, indicating a possible point of interaction with Parkin, which is believed to play a role in the clearance of dysfunctional mitochondria. (49-55) MB 51 was found to inhibit the import of hPink1 into GA74 mitochondria and from the titration, hPink1 import was determined to occur between 50 and 100  $\mu\text{M}$  (Figure 4.9: A, B). hPink1 was also imported into GA74 mitochondria in the presence of MB 51, but instead of trypsin treatment, the samples were quenched on ice and proteins embedded in the membrane were extracted with carbonate extraction. Under these conditions, MB 51 caused the formation of a higher molecular weight aggregate that was not observed in either treatment with 1% DMSO or CCCP (Figure 4.9: C).

Parkin recruitment was assessed using EGFP-Parkin expressing MTS dsRed HeLa cells and treatment with either 1% DMSO, CCCP alone, MB 51 alone, or CCCP with MB 51 (Figure 4.10). 5  $\mu\text{M}$  of CCCP recruits some Parkin to the surface of mitochondria, while 10  $\mu\text{M}$  of CCCP recruited substantially more Parkin to the surface of mitochondria as evidenced by the yellow merged panel in the figure. 40  $\mu\text{M}$  of MB 51 alone did not recruit Parkin to mitochondria. According to the quantification, which was done by counting 100 cells/condition it showed that concurrent treatment with MB 51 and CCCP did not exhibit a significant amount of Parkin recruitment than CCCP alone.

The genes that encode MPP are MAS1 (MPP  $\beta$ ) & MAS2 (MPP  $\alpha$ ). The temperature-sensitive mutant for yeast MPP  $\beta$  (MAS1) at incubation temperatures of 37°C exhibits signs of MPP knockdown. It is apparent that MB 51 and the MAS1 ts mutant affect the import of Su9-DHFR in a different manner (Figure 4.11). The MAS1ts yeast mutant showed an accumulation of unprocessed, and trypsin protected, Su9-DHFR, while MB 51 in both wild-type and MAS1 ts mitochondria exhibited a decrease in overall import of Su9-DHFR.



Following the test with radio-labeled precursors, MB 51 was tested against zebrafish expressing cardiac myocyte light chain 2 (cmlc2), which only express DsRed protein in heart cells (Figure 4.12). Zebrafish are useful for these types of studies because they are fertilized externally, the embryos are optically clear, and the embryos are osmotically permeable. The parent strain can also be crossed weekly to produce hundreds of embryos, and by 3 day post-fertilization the nervous and cardiac systems have started to develop. At 20  $\mu$ M MB 51, the zebrafish started showing a loss of pigmentation and at 50  $\mu$ M the zebrafish exhibited a severe loss in pigmentation. At 20  $\mu$ M MB 51 the heart also started to exhibit severe atrial distension and appeared to no flip. Zebrafish pigmentation is initiated during embryogenesis and begins in the retinal epithelium and in the melanophores. The pigment cells develop rapidly, and within hours they constitute a prominent feature of the embryo. (56, 57) One common method for zebrafish depigmentation is through the treatment with N-phenylthiourea (PTU), which is capable of completely blanching the zebrafish, but can also be washed-out. PTU works by inhibiting melanogenesis by blocking all tyrosinase-dependent steps in the melanin pathway. (58) Another method for causing depigmentation of zebrafish is through the chelation of copper with compounds such as neocuproine and bathocuproine. (59, 60) Using both bathocuproine and PTU as controls, MB 51 was examined for its ability to be washed-out following 3 days of treatment. After 3 days of treatment with 40  $\mu$ M MB 51, bathocuproine, or PTU we saw a severe loss of pigmentation and a slight change in body curvature with MB 51, a slight decrease in pigmentation with bathocuproine and a significant loss of pigmentation with PTU. Following 2 days where all compounds have been washed-out, and the zebrafish have been allowed to develop normally, we saw pigmentation had returned completely in all three drug conditions, but

the MB 51 treated zebrafish still exhibited a body curvature issue and a defect around the heart sac (Figure 4.13).

We wanted to investigate the MB 51 analogs, simply to show justification for our data mining method for a structure-activity relationship (SAR) study, using *in-vitro* cleavage of Su9-DHFR (Figure 4.4). EDTA, MB 50, and the positive analogs (329 & 321) significantly inhibited the formation of mature Su9-DHFR, while the negative MB 51 analogs (102, 082, and 001) did exhibit inhibition of the cleavage of Su9-DHFR by MPP as compared with the 1% DMSO control. The positive analogs (325, 184, and 172), as referenced in Chapter 2, showed similar results in the inhibition of MPP cleavage activity as MB 51 (data not shown). According to these results it appeared that the selection of the key moieties in MB 51 are plausible and that these negative analogs for the MB 51 group could be carried on further.

MB 51 and its analogs were then tested for their ability to inhibit the import [<sup>35</sup>S] Su9-DHFR into GA74 mitochondria (Figure 4.5). Out of the negative MB 51 analogs, compound 102 showed little to no inhibition of Su9-DHFR import, while compounds 082 and 001 showed severe inhibition of Su9-DHFR. For the positive MB 51 analogs, compounds 325 and 184 exhibited significant inhibition to Su9-DHFR import, 329 and 321 appeared to have some inhibitory affect on the import of Su9-DHFR import into GA74 mitochondria.

The analogs were also tested for their effects on zebrafish (Figure 4.14). MB 51 and its positive analogs (321 & 329) all exhibited a loss in pigmentation (Figure 4.14: Top). Depigmentation for MB 51 started at 15 μM and steadily got more severe with increasing concentration of drug. After 30 μM the fish also started exhibiting other defects in body shape and around the heart. Depigmentation for 321 started earlier than MB 51 (10 μM), but did not get as severe at higher concentrations and the body defects were also not as prevalent as with MB

51. Depigmentation for 329 started at 15  $\mu\text{M}$  and steadily got more severe with increasing concentration of drug. We were unable to examine any fish beyond 30  $\mu\text{M}$  because none of them survived, but based on trends compound 329 appears to exhibit similar results as MB 51. When comparing the negative controls (102, 001, & 082) to MB 51 (Figure 4.14: Bottom), 102 and 001 did not exhibit the same signs of depigmentation as MB 51, but at higher concentrations they presented changes in body shape and heart malformations. When comparing 082 to MB 51, 082 did show signs of depigmentation but they were not consistent as the concentration of 082 increases. This was also true for body defects that were present at low concentrations but not at higher concentrations.

# Discussion

Through the analysis of the data for MB 51 and both its positive and negative analogs it appears the key structural component of MB 51 is the 2-(5,10b-dihydro-1*H*-benzo[*e*]pyrazolo[1,5-*c*][1,3]oxazin-2-yl)benzene-1,4-diol. Within the sub-structure of all the MB 51 relevant compounds the active moiety is most likely the quinone/hydroquinone group that is capable of conducting a multitude of reactions, along with be a center for both oxidation and reduction chemistry similar to coenzyme Q. When examining the group attached to the quinone group this could aid in specificity or reactive chemistry, but based on the analysis of the SARs compounds, the quinone moiety is the key reactive group and any other reactive group simply provide an ancillary role.

MB 51 was capable of inhibiting the import of Su9-DHFR, CytC<sub>1</sub>, CytB<sub>2</sub>-DHFR (1-167), frataxin, Cpn10, hPink1, and to some extent CytB<sub>2</sub>-DHFR (A63P) before the final time point, while it did not inhibit the import of AAC. Both CytB<sub>2</sub>-DHFR (1-167) and CytB<sub>2</sub>-DHFR (A63P) are initially processed by MPP, the difference between them is CytB<sub>2</sub>-DHFR (1-167) possess a stop transfer sequence after the MTS, which directs it towards the intermembrane space. IMP cleaves off the stop transfer sequence of CytB<sub>2</sub>-DHFR (1-167). CytB<sub>2</sub>-DHFR (A63P) is directed to the matrix via the A63P mutation, therefore it is only processed by MPP. (38) MB51 appears to predominantly inhibit the import of CytB<sub>2</sub>-DHFR (1-167) compared to CytB<sub>2</sub>-DHFR (A63P). Though the exact mechanism for CytC<sub>1</sub> is not completely resolved, the general consensus is that CytC<sub>1</sub> import requires a membrane potential, ATP, and the precursor is first processed by MPP and then IMP2. (25, 61-65) The discrepancy between our work and data showing that MPP

processes CytB<sub>2</sub>-DHFR (A63P) could signify a difference between how MPP interacts with CytB<sub>2</sub>-DHFR (1-167) and CytB<sub>2</sub>-DHFR (A63P).

Crystal structures of MPP with synthetic signal peptides suggest the presequence interacts with the polar cavity of MPP in an extended conformation, suggesting the importance of this feature for both recognition by import machinery and cleavage by MPP (Figure 1.5). (31) It appears that electrostatic interactions are capable of capturing the positively-charged MTS and bringing it into the negatively-charged MPP cavity. MPP can scan the presequence as it threads through the cavity along the negatively-charged walls of both subunits and determine the correct site of cleavage. From this model, MPP would be capable of distinguishing different length presequences as they travel from the  $\beta$  subunit to the  $\alpha$  and thereby effectively and reproducibly cleave the correct site and release the mature protein. If MB 51 is exerting an effect in the active site, or an ancillary site that affects precursor recognition, this could potentially explain the difference in import inhibition for CytB<sub>2</sub>-DHFR (1-167) and CytB<sub>2</sub>-DHFR (A63P). Perhaps MPP recognizes these two presequences differently and MB 51 is only able to affect the recognition of CytB<sub>2</sub>-DHFR (A63P).

Cpn10 resides within the mitochondrial matrix and with the aid of Cpn60 helps precursor proteins fold into their native state. (66) Cpn10 does not contain a known MTS and its mechanism for import into the mitochondrial matrix is not completely understood. (48, 67) MB 51 appears to completely inhibit the import of Cpn10 in GA74 mitochondria, therefore, even though Cpn10 does not contain a known MTS for MPP our data suggests that MPP is involved in the import of Cpn10 and its maturation into a functional mitochondrial matrix protein. This could mean that Cpn10 does in fact possess a presequence that MPP recognizes or that un-inhibited

MPP is necessary for import of Cpn10 import even though it does not cleave the Cpn10 precursor.

Parkinson's disease is a neurodegenerative disorder of the central nervous system, which is typified by movement-related symptoms that are the result of loss of dopamine-generating cells in the substantia nigra. (68) Recently two genes have been linked to familial forms of this disease, Pink1 and Parkin. (51) Drosophila studies revealed the two proteins function in the same pathway and that Pink1 is upstream of Parkin. (69-71) Under normal conditions Pink1 is quickly degraded, but under conditions where the mitochondrial membrane is depolarized Pink1 is stabilized. Once stabilized, Pink1 goes to the outer mitochondrial membrane where it recruits Parkin via its Ser/Thr kinase domain and results in the ubiquitination and degradation of senescent or damaged mitochondria. (51, 55) Previous work using RNAi showed that decreasing the amount of MPP caused an increase in the accumulation of Pink1 on the mitochondrial surface. This increase in Pink1 accumulation also caused an increase in Parkin recruitment and mitochondrial degradation. (72) We were able to show that MB 51 was able to inhibit the import of Pink1, but in conjunction with CCCP treatment it was not capable of recruiting Parkin to the surface of mitochondria. This could be due to the fact that MB 51 is not capable of inducing the recruitment of Parkin or that our assay is simply not sensitive enough to estimate the change in Parkin recruitment to the surface of mitochondria under native conditions.

When zebrafish were treated with MB 51 they exhibited a loss of pigmentation, an atrial heart distension (the heart also failed to flip), and some change in body curvature compared with DMSO treatment. In addition, we found MB 51 could be washed-out after 3 days post-fertilization with return of pigmentation and the body change was not as severe. Organismal development and muscular systems (i.e., the cardiac system) are extremely prone to

mitochondrial abnormalities due to their reliance on ATP production. Using zebrafish as a model organism to simulate human diseases is becoming fairly commonplace, along with their use to replicate mitochondrial disorders. (73) During early stages of zebrafish development mitochondria are paramount to proper growth, development, and cardiac function; therefore, the body curvature, notochord abnormalities, and cardiac malformation seen with MB 51 and its inhibition of MPP make complete sense due to the high demand of functional mitochondria. This data mirrors much of the data we have collected with other MitoBloCK compounds. (74, 75) This could signify that MPP is upstream to many of the other pathway we have investigated in the lab or that the individual pathways are separate but result in similar phenotypes. A striking difference with MB 51 is the depigmentation at relatively low concentrations. Previous studies with zebrafish have linked copper metabolism with the loss of pigmentation. (76) This could signify that MPP plays some role in copper metabolism and that MB 51 is capable of specifically disrupting this interaction; however further work is required to elucidate this connection.

# Material and Methods

**Reagents.** Chemical libraries and investigated compounds were obtained from Chembridge Corporation (San Diego, CA), Asinex Ltd (Moscow, Russia) and Life Chemicals (Burlington, Canada). All other reagents were purchased from Sigma-Aldrich, EMD Biosciences, MB Biomedicals, US Biological and JPT Innovative Peptide Solutions. For trypan blue assays, cultured HeLa cells were grown in DMEM high glucose medium (Invitrogen) with glutamine, sodium pyruvate, 10% FBS, and penicillin-streptomycin (complete medium).

***In-vitro* Su9-DHFR Cleavage Assay.** Before the cleavage assay with purified recombinant MPP, [<sup>35</sup>S]-methionine and cysteine labeled Su9-DHFR was made with the TNT Quick Coupled Transcription/Translation kit (Promega). Each sample consisted of 8 μL of Su9-DHFR/[<sup>35</sup>S] added to 12 μL of MPP solution (solution included purified recombinant MPP at 128 nM final concentration, drug at 100 μM final concentration (if added), 4 mM EDTA with 0.04 mM *o*-phenanthroline [final concentration; negative control], 1% DMSO [final concentration], and 1 mM MnCl<sub>2</sub> [final concentration]). DMSO only, drugs, or EDTA/*o*-phenanthroline were incubated with MPP for an hour at room temperature before the addition of Su9-DHFR. 20 μL aliquots were taken at 2, 5, and 10-minute time points; the reactions were quenched with the addition of Laemmli sample buffer and all samples were analyzed by SDS-PAGE and autoradiography.

**Mitochondria Purification.** Mitochondria were purified from GA74 or MAS1 ts yeast cells grown in YPEG as described in previous studies. (74, 77) After purification, the concentration was measured by bicinchoninic acid (BCA) assay and mitochondria were stored at -80°C. Mammalian mitochondria were purified from HeLa cells grown in DMEM as previously



described in studies. (75) After purification, the concentration was measured by bicinchoninic acid (BCA) assay and the mitochondria were purified and used fresh for each import assay.

**Import of radiolabeled proteins into mitochondria.** Before import into purified mitochondria, [<sup>35</sup>S]-methionine and cysteine labeled precursor proteins were using the TNT Quick Coupled Transcription/Translation kit (Promega). Imports of precursor proteins into purified yeast mitochondria were conducted based on established protocol. (74, 78) Due to the fact that the drug compounds were primarily only soluble in DMSO a final concentration in each import reaction of 1% was used. Drugs in DMSO or DMSO vehicle only was added to the mitochondria (25-50 µg/mL) in import buffer and incubated for 15 min at 25°C. Imports were initiated with the addition of radio-labeled precursor and aliquots were removed at intervals during the reaction time-course. Import was terminated with the addition of 25 µg/mL of trypsin or just placed on ice for those import reactions where carbonate extraction was performed. After 15 min, 200 µg/mL of soybean trypsin inhibitor was added to deactivate trypsin. Mitochondria were pelleted by centrifugation at 8,000 x g for 5 min. To investigate proteins not inserted into the membrane, a carbonate extraction step was performed without the use of trypsin as described previously. (79)

Imports into purified mammalian mitochondria were conducted using a similar method as the one described for yeast mitochondria except that the mammalian mitochondria were diluted to a final concentration of 200 µg/mL in a different import buffer consisting of 20 mM Hepes-KOH pH 7.4, 70 mM sucrose, 220 mM mannitol, 0.5 mM MgCl<sub>2</sub>, 1 mM ATP, 20 mM sodium succinate, and 5 mM NADH.

For all imports, the mitochondria were disrupted in Laemmli sample buffer after the final

centrifugation and analyzed by SDS-PAGE and autoradiography .

**Cell manipulations.** For microscopy experiments, HeLa cells treated with DMSO, MB 50, or CCCP for 24 or 48 hrs, were fixed with 4% formaldehyde. Cells were visualized with a microscope 9 Axiovert200M (Carl Zeiss) using a Plan-Fluor 63x oil objective. Images were acquired at room temperature with a charge-coupled device camera (ORCA ER, Hamamatus Photonics) controlled by Axiovision software (Carl Zeiss). Images were resized to 300 dpi without resampling using Photoshop software (Adobe).

**Trypan blue cell integrity assay.** A modified version of previously described protocols was used to assess cell integrity. (80, 81) Starting material for each experiment was 1-2 plates (10 cm) of HeLa cell culture. Confluent cultures of HeLa cells were first washed with phosphate-buffered saline (PBS) solution (Invitrogen) and then detached from plates with a solution of 0.05% trypsin/EDTA (Invitrogen). Cells were then collected in DMEM high glucose medium +10% FBS medium to quench trypsin reaction and then pelleted at 125 x g for 5 minutes. Cell pellet was subsequently resuspended in PBS and then centrifuged as before. Washed pellet was resuspended in 2-4 ml DMEM high glucose medium +10% FBS and cell density was quantified using a hemocytometer. A 0.25 ml aliquot containing approximately 625,000 cells was diluted 1:1 into DMEM high glucose medium +10% FBS containing DMSO, drug, or CCCP at 2X of the final assay concentration. After gentle mixing by inversion, the 0.5 ml reaction was incubated for 24 hours. Next, a 0.25 ml aliquot of trypan blue solution (0.4% w/v trypan blue in Hank's balanced salt solution [Invitrogen]) was added to each reaction and incubated for 5 minutes at RT. Cell integrity was assessed by counting blocks of 100 cells from each reaction with a hemocytometer. HeLa cells with a blue center were counted as permeabilized and those with a clear center were counted as being intact.

**Zebrafish Lines.** Zebrafish displaying fluorescent hearts were derived from transgenic TL fish expressing a mitochondrially targeted dsRed regulated by a cardiac myocyte light chain 2 (*cmhc2*) promoter to make it heart-specific. O-dianisidine staining was conducted in *cmhc2* lines.

**Zebrafish Husbandry.** Zebrafish lines were maintained in a 14-hour-light/10-hour-dark cycle and mated for 1 hour to obtain synchronized embryonic development. Embryos were grown in E3 buffer (5 mM sodium chloride, 0.17 mM potassium chloride, 0.33 mM calcium chloride, 0.33 mM magnesium sulfate) at 28.5°C.

**Zebrafish Drug Treatment Assay.** Zebrafish were mated for 1 hour to obtain synchronized embryonic development. Embryos were grown to 3 hpf in E3 buffer (5 mM sodium chloride, 0.17 mM potassium chloride, 0.33 mM calcium chloride, 0.33 mM magnesium sulfate) and then incubated with buffer, 1% DMSO, or drug for 3 days at 28.5°C. Following treatment, embryos were imaged using a Leica S8APO microscope at 1.575x magnification or Leica MZ16F fluorescent stereoscope (TexasRed filter set) at 5x magnification. *Cmhc2* embryos were stained with o-dianisidine (40% (v/v) ethanol, 0.01 M sodium acetate, 0.65% hydrogen peroxide, 0.6 mg/mL o-dianisidine) and incubated for 15 minutes in complete darkness. Embryos were then washed with E3 buffer to remove residual stain and stereoscopically imaged under white light using a Leica S8APO microscope at 1.575x magnification. Images were resized to 300 dpi without resampling using Adobe Photoshop.

**Analysis and Statistics.** Unless otherwise stated, all results reported are representative of three experimental replicates. Quantitative analysis was performed in GraphPad Prism 5 software (GraphPad Software, Inc.) unless otherwise stated.

**Miscellaneous.** Western blotting was performed using standard protocols with polyclonal antibodies raised towards highly purified antigens. The PDI antibody was a mouse monoclonal antibody purchased from Abcam Inc. (Cambridge, MA). Proteins were transferred to nitrocellulose membranes and immune complexes were visualized with HRP labeled Protein A in a chemiluminescence assay (Pierce). Chemiluminescent imaging was performed on an Alpha Innotech (Santa Clara, CA) FluorChem FC2 workstation unless otherwise noted. Autoradiographic imaging was performed on film.

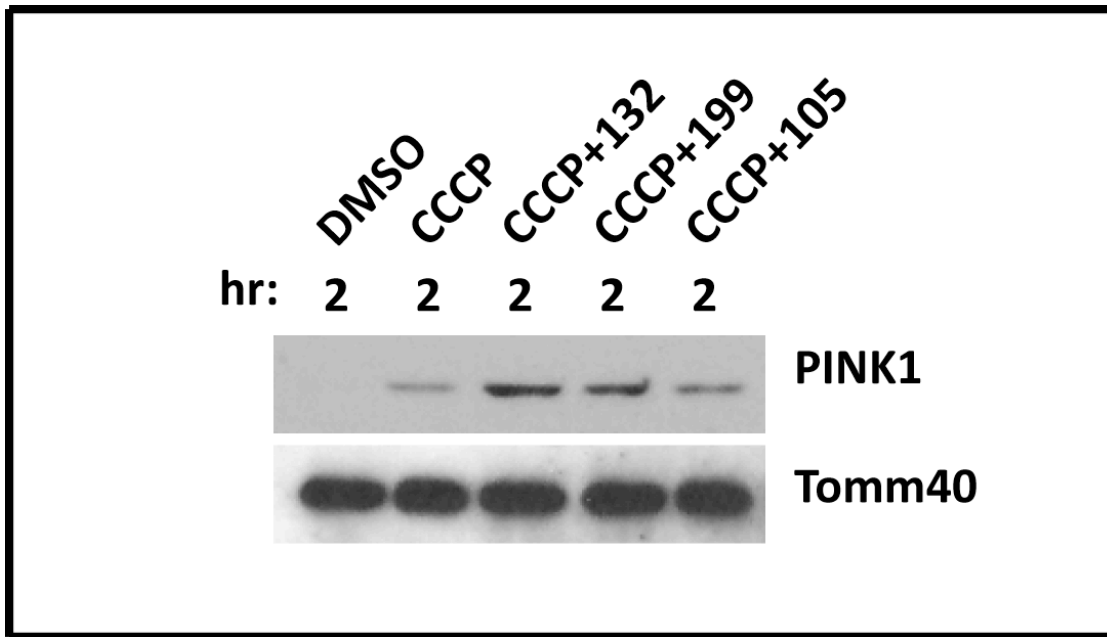


**Figure 4.1 Pink1 Accumulation with Concurrent Treatment of CCCP and MB 51.**

HeLa cells were treated with DMSO, 10  $\mu$ M CCCP, 40  $\mu$ M of MB 51 (199), or CCCP & MB 51. Gels were blotted for antibodies for Pink1 and Tomm40 (loading control). Comparing CCCP treatment and CCCP plus MB 51 after 2 hours of treatment, it appears the concurrent treatment of CCCP and MB 51 causes more accumulation of Pink1 than CCCP alone. *Figure included with permission from Non Miyata.*

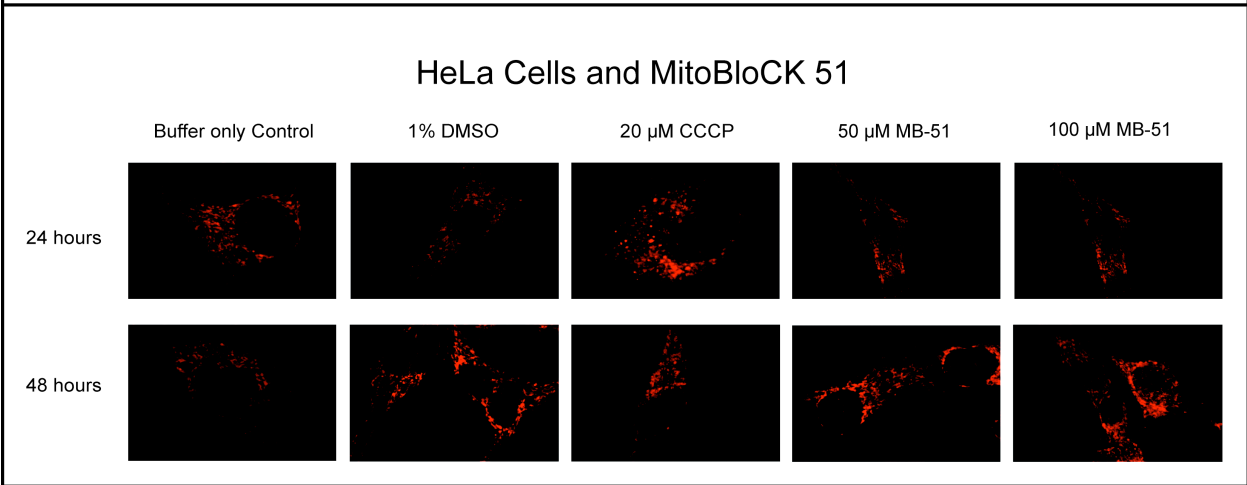
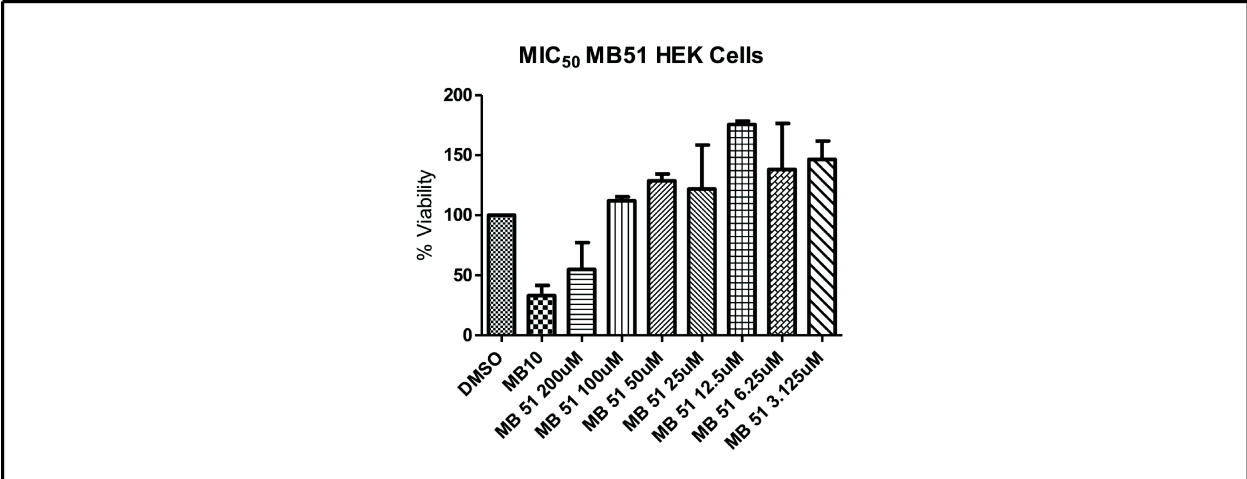
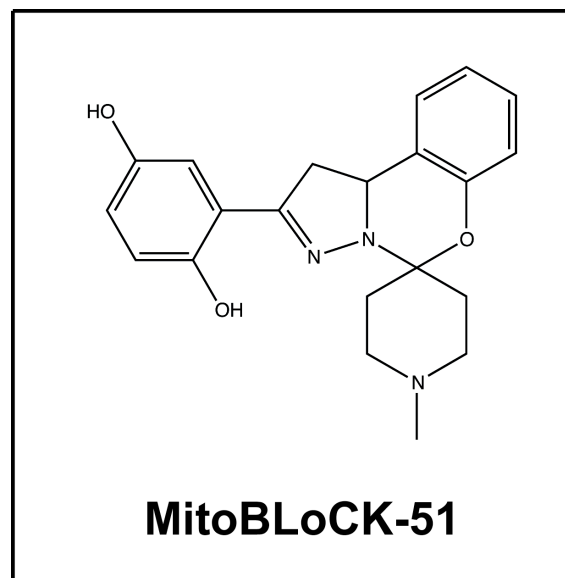


**Figure 4.2 MIC<sub>50</sub> of MB 51 in HEK Cells and Mitochondrial Morphology in HeLa Cells.**

Treating the cells for 24 hours with the varying concentrations of MB 51 and then conducting a cell count for each condition using the hemocytometer determined the MIC<sub>50</sub> in HEK cells (done in triplicate for each condition). The MIC<sub>50</sub> for MB 51 in HEK cells was approximately 200  $\mu$ M. HeLa cells expressing MLS DsRed were used to determine if MB 51 caused changes in mitochondrial morphology as compared with 1% DMSO or 20  $\mu$ M CCCP for 24 and 48 hours of treatment. MB 51 at 50 and 100  $\mu$ M (24 & 48 hrs) did not appear to cause the mitochondria to become punctate unlike the mitochondria seen in the CCCP treatment. MB 51 treatment on HeLa cells did not seem to cause adverse effects to mitochondrial morphology.



Type of Control	Structure	Structure	Structure
+	<p style="text-align: right;">325</p>	<p style="text-align: right;">184</p>	<p style="text-align: right;">172</p>
+	<p style="text-align: right;">321</p>	<p style="text-align: right;">329</p>	
-	<p style="text-align: right;">001</p>	<p style="text-align: right;">082</p>	<p style="text-align: right;">102</p>



### **Figure 4.3 Structures of MB 51 and a Selection of its Analogs.**

All of the MB 51 analogs were determined either directly from the MPP primary and secondary screens or by data mining the screen for compounds that did not inhibit MPP but had a greater than 60% homology with MB 51 based on structural analysis. Based on the similarities with all the positive MB 51 analogs, and the fact they all contain the quinone/hydroquinone moiety, we assumed this group to be the important substituent for this group of molecules. We wanted our negative analogs to systematically substitute substituents from this group to assess if our hypothesis was correct about MB 51. Compound 001, completely substitutes the quinone moiety for a benzene ring, thereby getting rid of both hydroxyl groups on the ring. Compound 082, changes the quinone moiety for a phenol one, which causes the loss of one of the hydroxyl groups. Compound 102, replaces one of the hydroxyl groups in the quinone for a methyl, which allows for some similarity in geometry to the original quinone but a loss of the reactivity that the original group possessed.

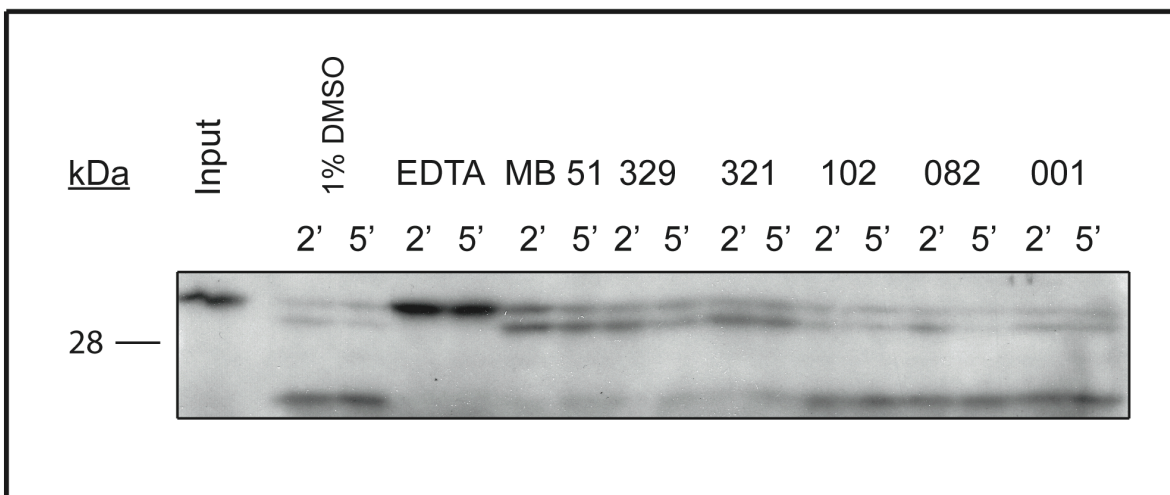


**Figure 4.4 In-Vitro Cleavage of [<sup>35</sup>S] Su9-DHFR by Recombinant MPP with MB 51 and analogs.**

[<sup>35</sup>S] Su9-DHFR was synthesized using a TNT Quick Coupled Transcription/Translation kit. GA74 yeast mitochondria were treated with either 1% DMSO, 50 μM CCCP & 1 mg/mL valinomycin, or 100 μM of Drug for 15 minutes at 25°C. 10 μL of [<sup>35</sup>S] Su9-DHFR solution/reaction time point was added to each condition and 250 μL aliquots were taken at each of 2 time points (2 and 5-minutes). Reactions were quenched on ice by adding 50 μg/mL of trypsin. All imports were disrupted in Laemmli sample buffer and analyzed by SDS-PAGE and autoradiography. EDTA, MB 51, and the positive analogs (329 & 321) significantly inhibited the formation of mature Su9-DHFR, while the negative MB 51 analogs (102, 082, and 001) did exhibit inhibition of the cleavage of Su9-DHFR by MPP as compared with the 1% DMSO control.

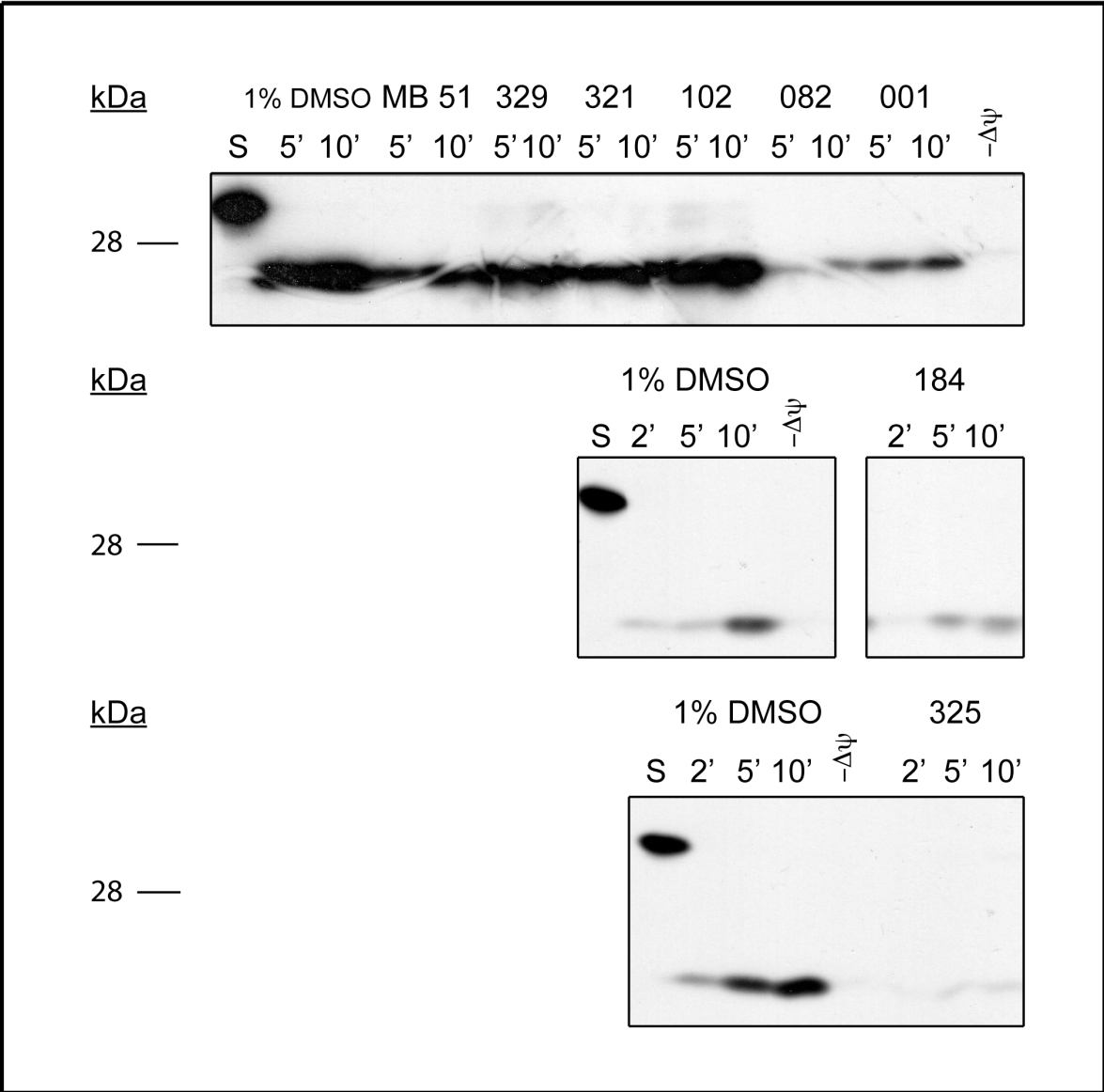


**Figure 4.5 [<sup>35</sup>S] Su9-DHFR import into GA74 Mitochondria with MB 51 and Analogs.**

[<sup>35</sup>S] Su9-DHFR was synthesized using a TNT Quick Coupled Transcription/Translation kit. GA74 yeast mitochondria were treated with either 1% DMSO, 50 μM CCCP & 1 mg/mL valinomycin, or 100 μM of Drug for 15 minutes at 25°C. 10 μL of [<sup>35</sup>S] Su9-DHFR solution/reaction time point was added to each condition and 250 μL aliquots were taken at each of 3 time points (2, 5, and 10-minutes). Reactions were quenched on ice by adding 50 μg/mL of trypsin. All imports were disrupted in Laemmli sample buffer and analyzed by SDS-PAGE and autoradiography. Out of the negative MB 51 analogs, compound 102 showed little to no inhibition of Su9-DHFR import, while compounds 082 and 001 showed severe inhibition of Su9-DHFR. For the positive MB 51 analogs, compounds 325 and 184 exhibited significant inhibition to Su9-DHFR import, and 329 and 321 appeared to have some inhibitory affect on the import of Su9-DHFR import into GA74 mitochondria.

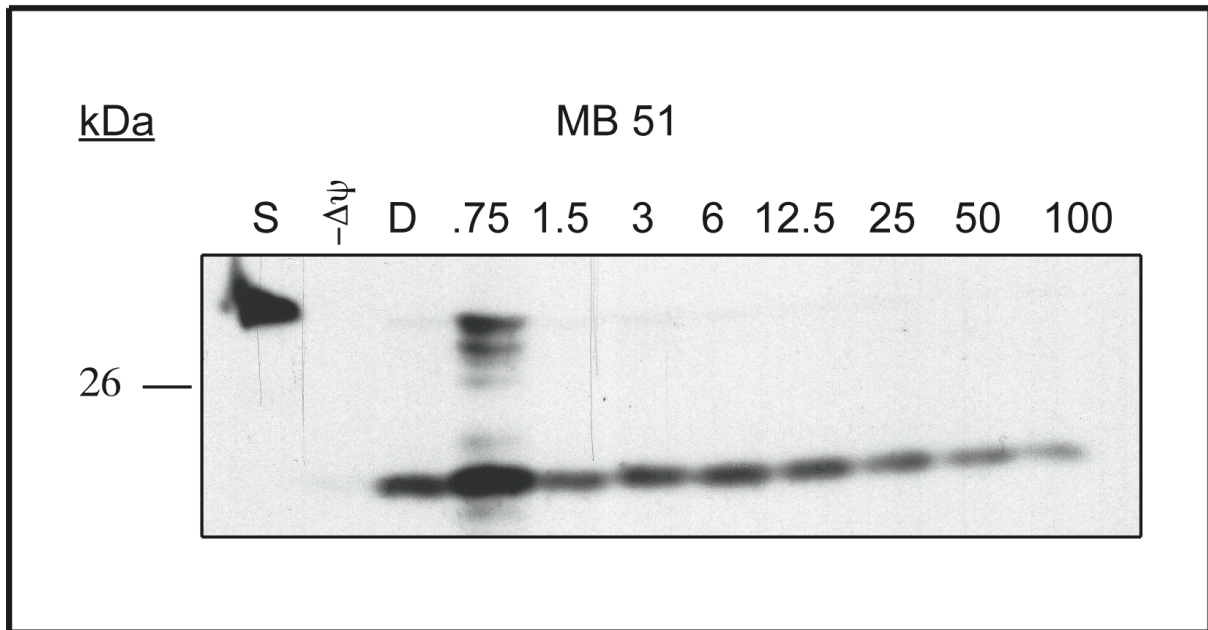


**Figure 4.6 Titration of MB 51 with the Import of [<sup>35</sup>S] Su9-DHFR into GA74 Mitochondria.**

[<sup>35</sup>S] Su9-DHFR was synthesized using a TNT Quick Coupled Transcription/Translation kit.

GA74 yeast mitochondria were treated with either 1% DMSO, 50 μM CCCP & 1 mg/mL valinomycin, or varying concentrations of MB 51 for 15 minutes at 25°C. 10 μL of [<sup>35</sup>S] Su9-DHFR solution was added to each condition and 250 μL aliquots were taken after 5-minutes.

Reactions were quenched on ice by adding 50 μg/mL of trypsin. All imports were disrupted in Laemmli sample buffer and analyzed by SDS-PAGE and autoradiography. The IC<sub>50</sub> of MB 51 was approximately 50 μM with regard to the import of Su9-DHFR into GA74 mitochondria.

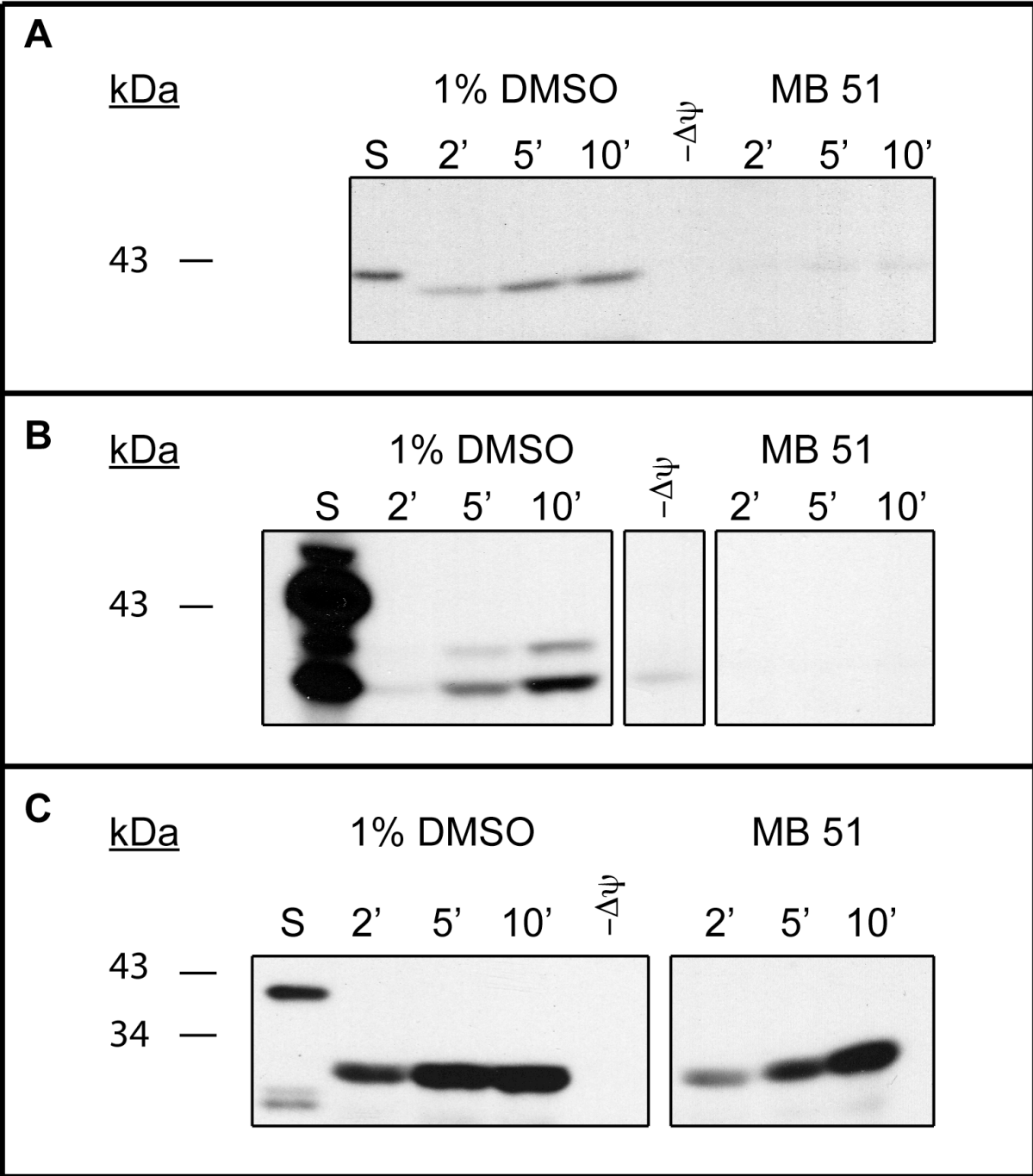
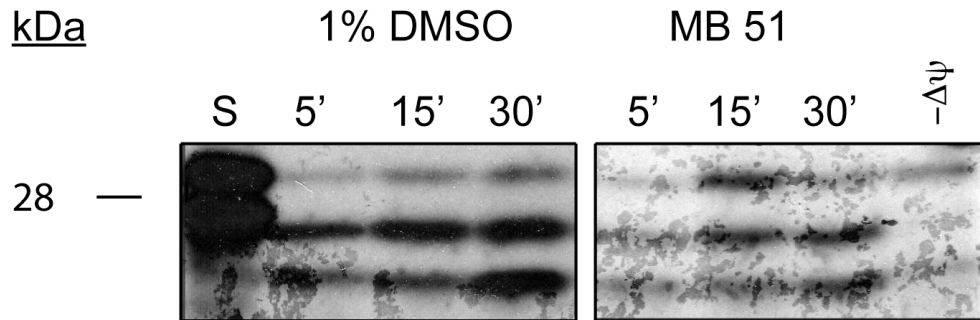


**Figure 4.7 CytC<sub>1</sub>, CytB<sub>2</sub>-DHFR (1-167), and CytB<sub>2</sub>-DHFR (A63P) import into GA74 Mitochondria with MB 51.**

[<sup>35</sup>S] CytC<sub>1</sub>, CytB<sub>2</sub>-DHFR (1-167) and CytB<sub>2</sub>-DHFR (A63P) were synthesized using a TNT Quick Coupled Transcription/Translation kit. GA74 yeast mitochondria were treated with either 1% DMSO, 50 μM CCCP & 1 mg/mL valinomycin, or 100 μM of MB 51 for 15 minutes at 25°C. 10 μL of [<sup>35</sup>S] transcript solutions/reaction time point was added to each condition and 250 μL aliquots were taken at each of 3 time points (2, 5, and 10-minutes). Reactions were quenched on ice by adding 50 μg/mL of trypsin. All imports were disrupted in Laemmli sample buffer and analyzed by SDS-PAGE and autoradiography. According to the data, MB 51 inhibited CytB<sub>2</sub>-DHFR (1-167) (B panel) and CytC<sub>1</sub> (A panel), while CytB<sub>2</sub>-DHFR (A63P) (C panel) did not appear to be inhibited by treatment of MB 51.

### Frataxin Import into GA74 Mitochondria



### Cpn10 Import into GA74 Mitochondria

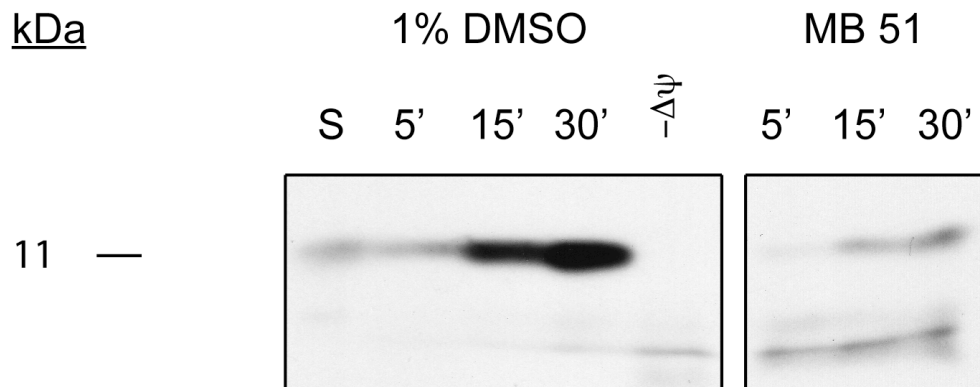




**Figure 4.8 Frataxin and Cpn10 Import into GA74 Mitochondria with MB 51 Treatment.**

[<sup>35</sup>S] Frataxin and Cpn10 were synthesized using a TNT Quick Coupled Transcription/Translation kit. GA74 yeast mitochondria were treated with either 1% DMSO, 50 μM CCCP & 1 mg/mL valinomycin, or 100 μM of MB 51 for 15 minutes at 25°C. 10 μL of [<sup>35</sup>S] transcript solutions/reaction time point was added to each condition and 250 μL aliquots were taken at each of 3 time points (5, 15, and 30-minutes). Reactions were quenched on ice by adding 50 μg/mL of trypsin. All imports were disrupted in Laemmli sample buffer and analyzed by SDS-PAGE and autoradiography. MB 51 appeared to cause an overall inhibition of frataxin, while CCCP treatment completely blocked the import of frataxin. Cpn10 does not contain a known MPP cleavage site, but MB 51 was capable of significantly inhibiting the import of Cpn10 in purified mitochondria. *Figure included with permission from Eric Torres.*

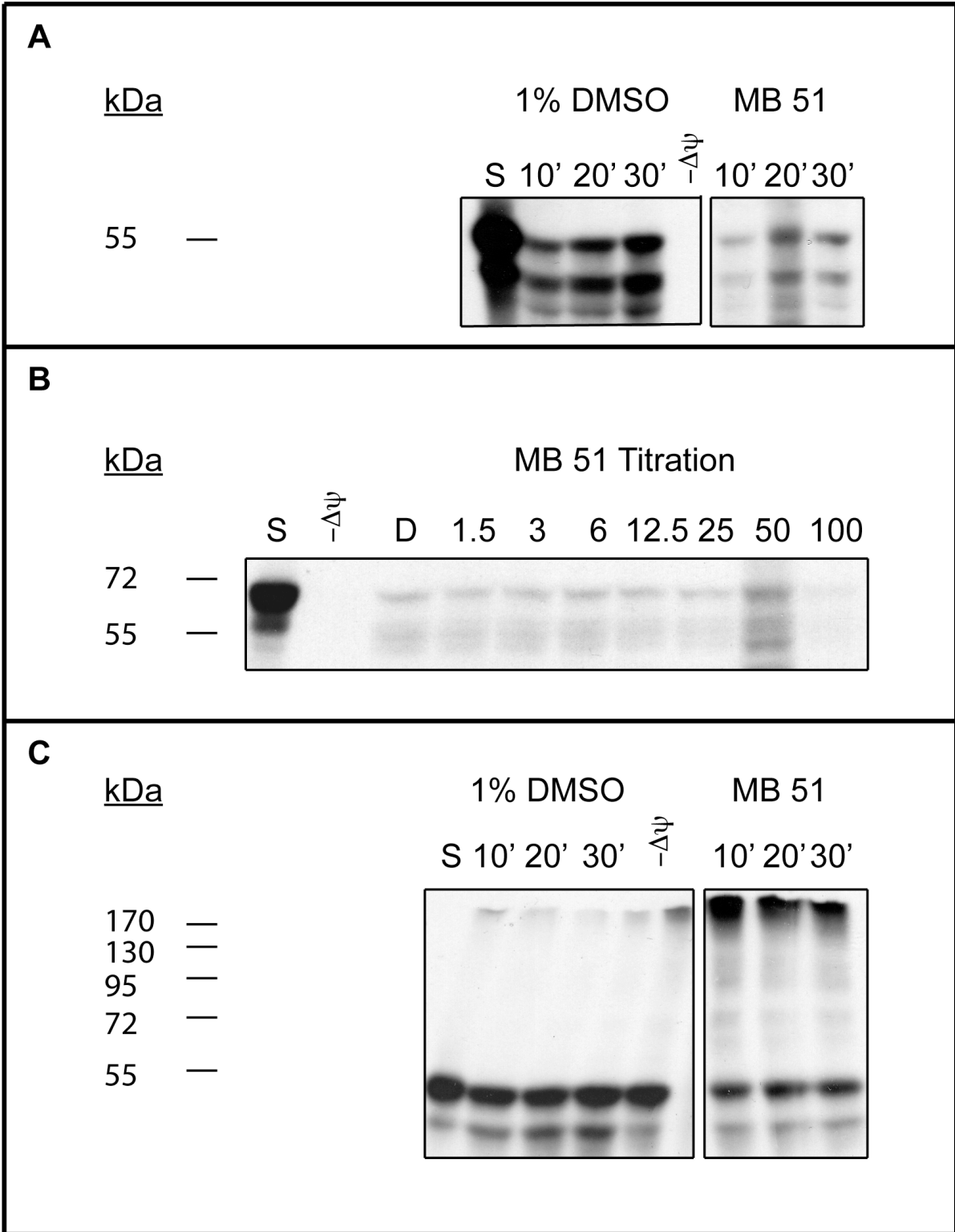


**Figure 4.9 Import and Titration of hPink1 into GA74 Mitochondria and MB 51.**

[<sup>35</sup>S] hPink was synthesized using a TNT Quick Coupled Transcription/Translation kit. For the import of hPink1, GA74 yeast mitochondria were treated with either 1% DMSO, 50 μM CCCP & 1 mg/mL valinomycin, or 100 μM of MB 51 for 15 minutes at 25°C. 10 μL of [<sup>35</sup>S] hPink1 solution/reaction time point was added to each condition and 250 μL aliquots were taken at each of 3 time points (10, 20, and 30-minutes). For the titration of MB 51, GA74 yeast mitochondria were treated with either 1% DMSO, 50 μM CCCP & 1 mg/mL valinomycin, or varying concentrations of MB 51 for 15 minutes at 25°C. 10 μL of [<sup>35</sup>S] hPink1 solution was added to each condition and 250 μL aliquots were taken after 30-minutes. Reactions for both panel A and B experiments were quenched on ice by adding 50 μg/mL of trypsin. All imports were disrupted in Laemmli sample buffer and analyzed by SDS-PAGE and autoradiography. MB 51 was capable of significantly inhibiting the import of hPink1 into mitochondria (panel A) and had an IC<sub>50</sub> between 50–100 μM (panel B). hPink1 was also imported into GA74 mitochondria in the presence of MB 51, but instead of trypsin treatment, the samples were quenched on ice and proteins embedded in the membrane were extracted with carbonate extraction (panel C). Under these conditions, MB 51 caused the formation of a higher molecular weight aggregate that was not observed in either treatment with 1% DMSO or CCCP.

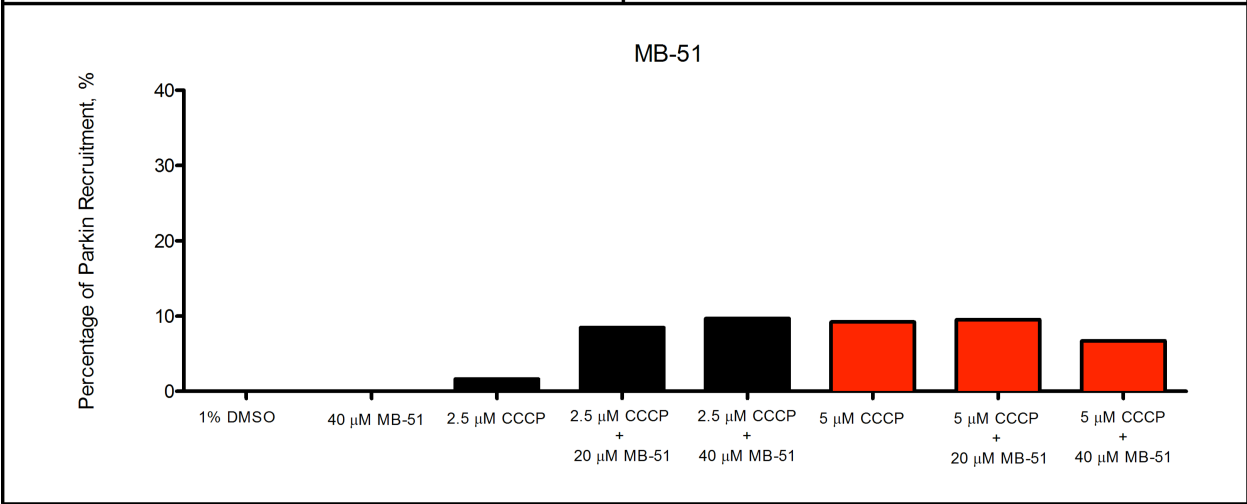
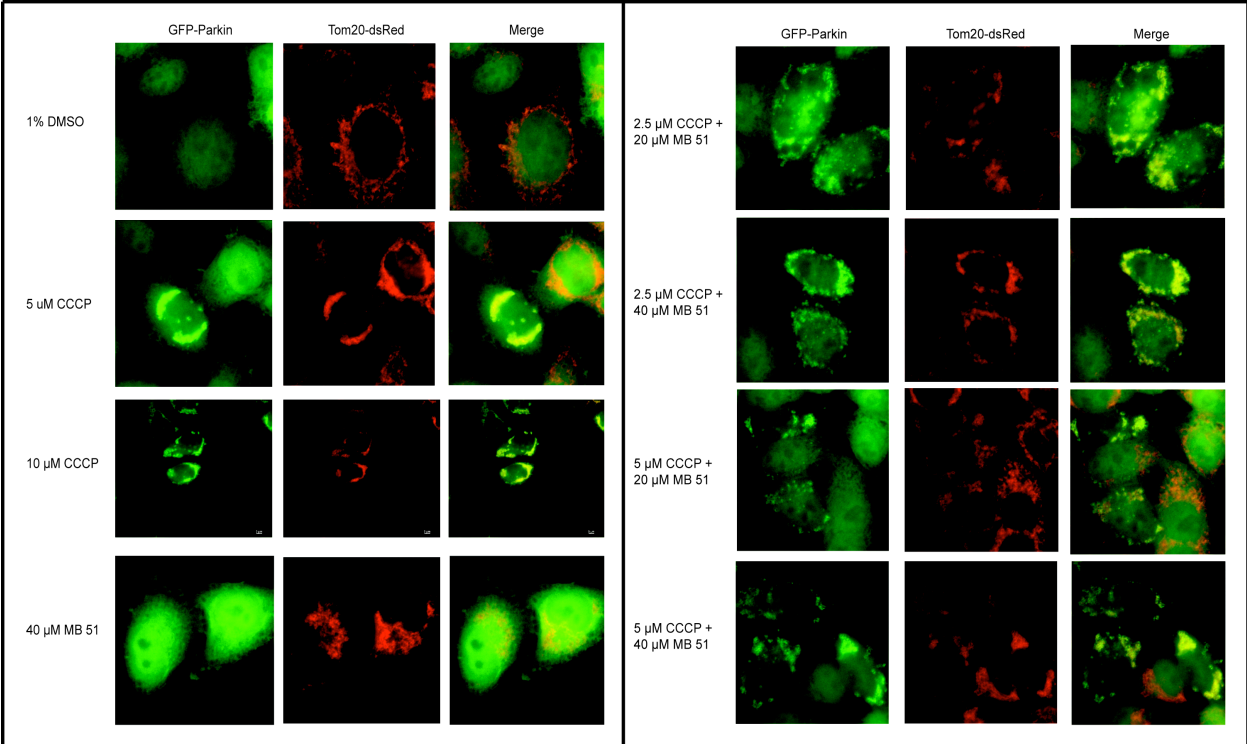


**Figure 4.10 Parkin Recruitment in EGFP-Parkin Expressing MTS dsRed HeLa MTS with Quantification.**

EGFP-Parkin expressing MTS DsRed HeLa cells were treated with either 5 or 10  $\mu\text{M}$  CCCP, 1% DMSO, 40  $\mu\text{M}$  MB 51 or 4 different combinations of CCCP and MB 51. 5  $\mu\text{M}$  of CCCP recruited some Parkin to the surface of mitochondria, while 10  $\mu\text{M}$  of CCCP recruited substantially more Parkin to the surface of mitochondria as evidenced by the yellow merged panel in the figure above. 40  $\mu\text{M}$  of MB 51 alone did not recruit Parkin to mitochondria. According to the quantification, which was done by counting 100 cells/condition it showed that concurrent treatment with MB 51 and CCCP did not exhibited a significant amount of Parkin recruitment than CCCP alone. *Figure included with permission from Juwina Wijaya.*

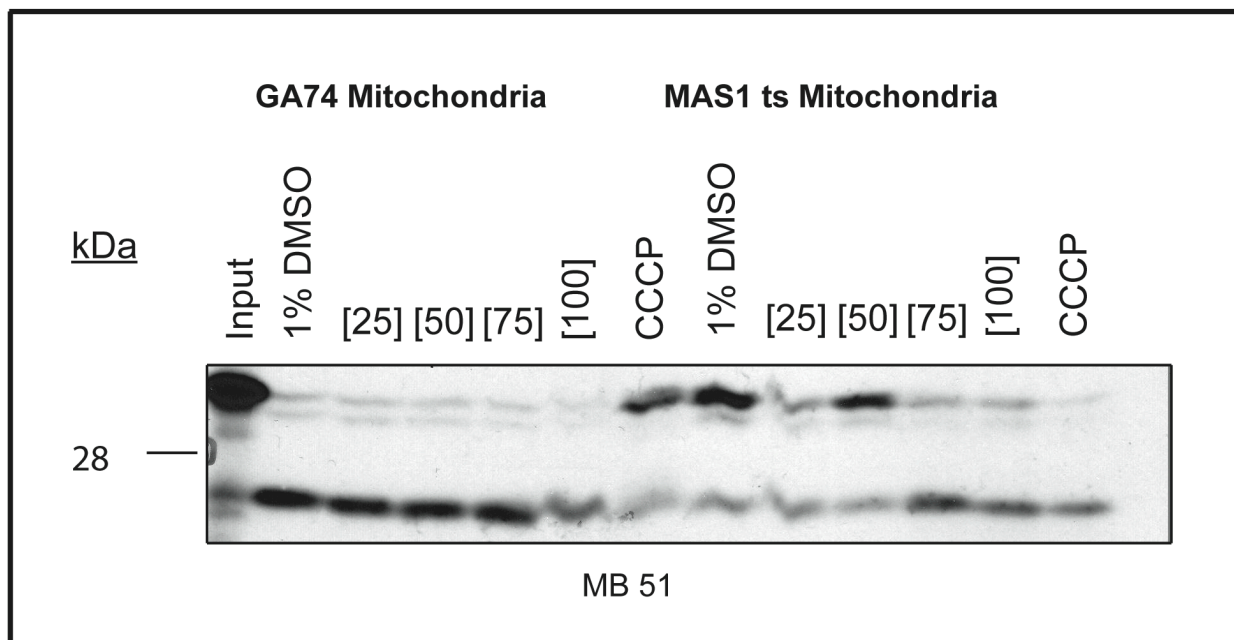


**Figure 4.11 Comparison of [<sup>35</sup>S] Su9-DHFR in GA74 and MAS1 ts Mitochondria with MB 51 Treatment.**

[<sup>35</sup>S] Su9-DHFR was synthesized using a TNT Quick Coupled Transcription/Translation kit. GA74 or MAS1 ts yeast mitochondria were treated with either 1% DMSO, 50  $\mu$ M CCCP & 1 mg/mL valinomycin, or varying concentrations of MB 51 for 15 minutes at 25°C. 10  $\mu$ L of [<sup>35</sup>S] Su9-DHFR solution was added to each condition and 250  $\mu$ L aliquots were taken after 5-minutes. Reactions were quenched on ice by adding 50  $\mu$ g/mL of trypsin. All imports were disrupted in Laemmli sample buffer and analyzed by SDS-PAGE and autoradiography. When comparing 1% DMSO GA74 and MAS1 ts mitochondria it is apparent that Su9-DHFR is arrested in its import and protected from trypsin shaving in the MAS1 ts mutant. Similarly, when the concentration of MB 51 is increased, the total amount of Su9-DHFR import is decreased in both instances. In addition, the amount of un-processed Su9-DHFR for the MAS1 ts is significantly decreased. *Figure included with permission from Eric Torres.*

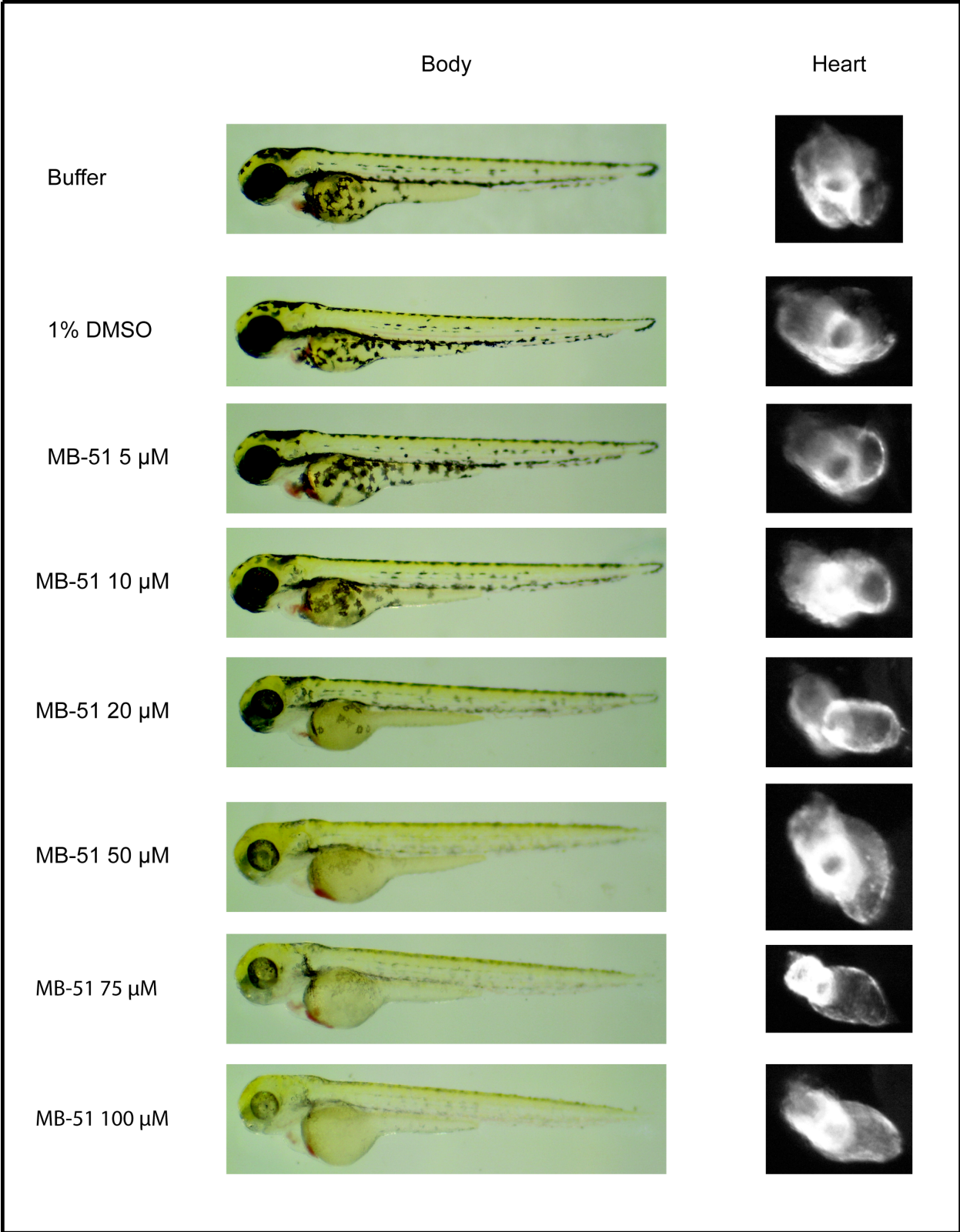


**Figure 4.12 Zebrafish Treatment with MB 50.**

Cmcl2 DsRed zebrafish were allowed to develop for 3 hours post-fertilization and then treated with 1% DMSO or the varying concentrations of MB 51. After 3 day post-fertilization the embryos were imaged using a Leica S8APO microscope at 1.575x magnification or Leica MZ16F fluorescent stereoscope (TexasRed filter set) at 5x magnification. At 20  $\mu$ M of MB 51 the zebrafish started showing a loss of pigmentation and from 50  $\mu$ M onward there was a significant loss in pigmentation. At 20  $\mu$ M MB 51 the heart also started to exhibit severe atrial distension and appeared to not have flipped.



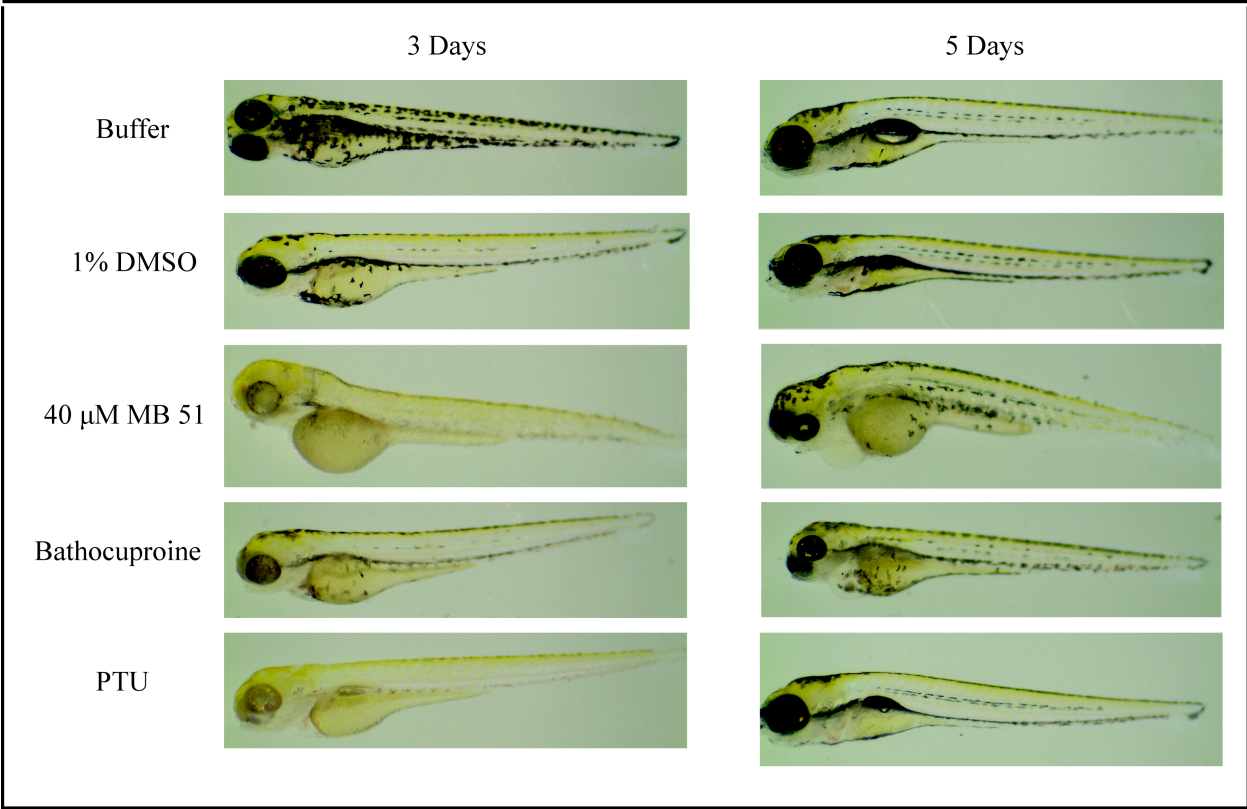


**Figure 4.13 Zebrafish Treated with MB 50, Bathocuproine, and PTU for 3 Days and then Wash-out for 2 Days.**

Cmcl2 DsRed zebrafish were allowed to develop for 3 hours post-fertilization and then treated with 1% DMSO, 40  $\mu$ M MB 51, 10  $\mu$ M Bathocuproine, or 0.003% PTU. After 3 day post-fertilization the embryos were imaged using a Leica S8APO microscope at 1.575x magnification, washed with E3 buffer and allowed to develop for an additional 2 day with no treatment.

Following 5 day post-fertilization the embryos were imaged using a Leica S8APO microscope at 1.575x magnification. After 3 days of treatment with 40  $\mu$ M MB 51, bathocuproine, or PTU we saw a severe loss of pigmentation and a slight change in body curvature with MB 51, a slight decrease in pigmentation with bathocuproine and a significant loss of pigmentation with PTU.

Following 2 days where all compounds have been washed-out and the zebrafish have been allowed to develop normally, we saw the pigmentation has returned completely in all 3 drug conditions, but the MB 51 treated zebrafish still exhibited a body curvature issue and a defect around the heart sac.

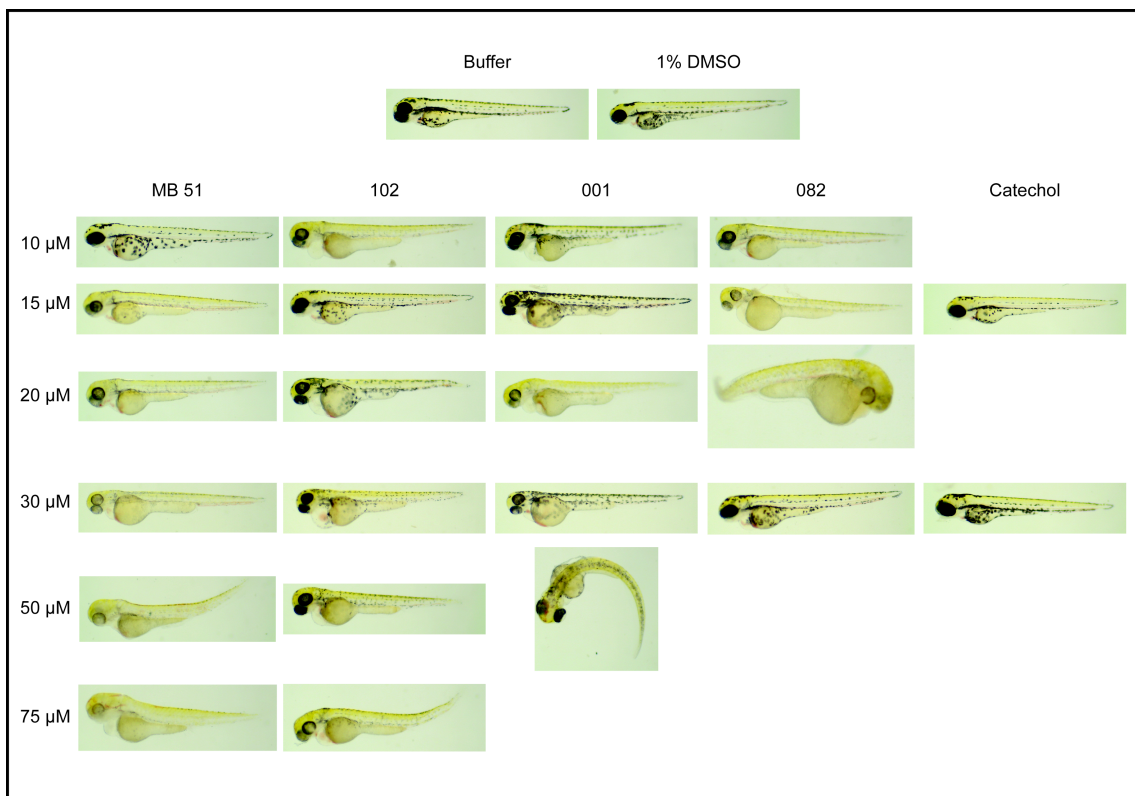
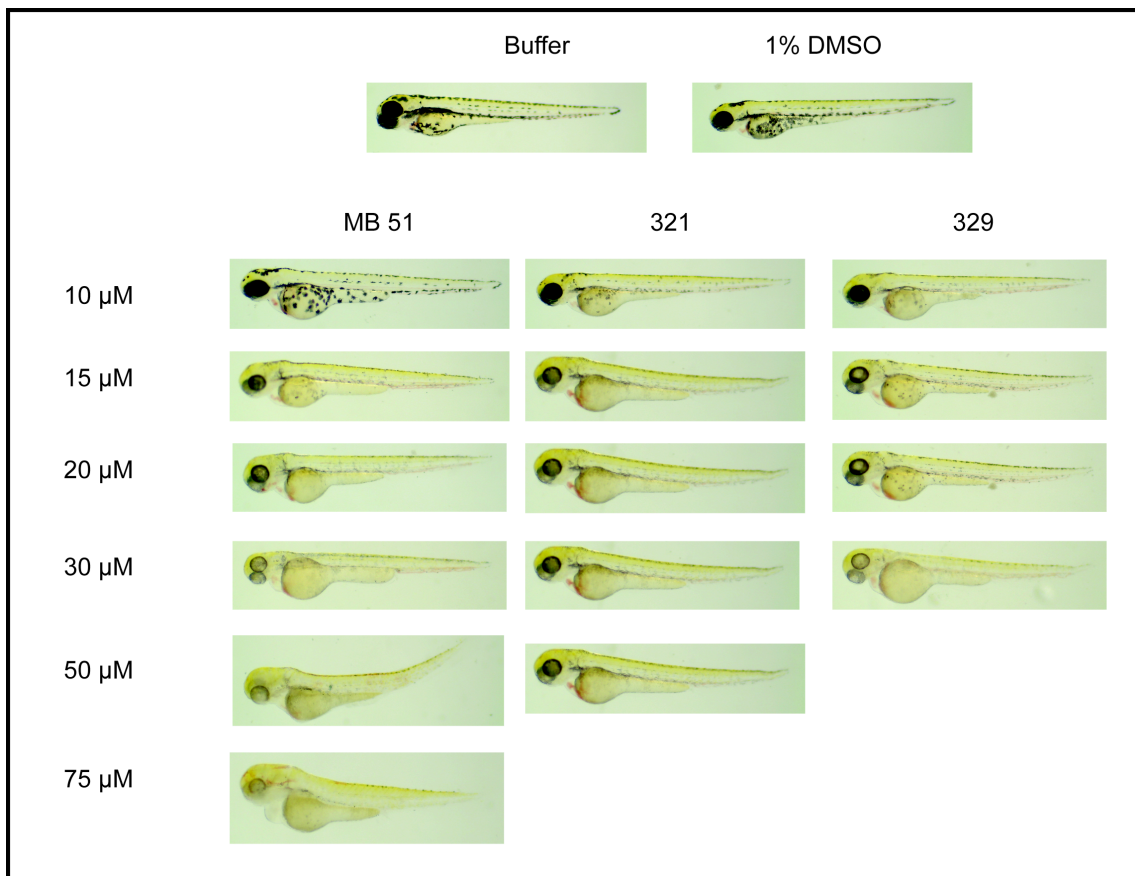


**Figure 4.14 Zebrafish Treated with MB 50 and its analogs.**

Cmcl2 DsRed zebrafish were allowed to develop for 3 hours post-fertilization and then treated with 1% DMSO or the varying concentrations of MB 51 and its analogs. After 3 day post-fertilization the embryos were imaged using a Leica S8APO microscope at 1.575x magnification. MB 51 and its positive analogs (321 & 329) are in the top panel and all exhibited a loss in pigmentation. Depigmentation for MB 51 started at 15  $\mu$ M and steadily got more severe with increasing concentration of drug. After 30  $\mu$ M the fish also started exhibiting other defects in body shape and around the heart. Depigmentation for 321 started earlier than MB 51 (10  $\mu$ M), but did not get as severe at higher concentrations and the body defects were also not as prevalent as with MB 51. Depigmentation for 329 started at 15  $\mu$ M and steadily got more severe with increasing concentration of drug. We were unable to examine any fish beyond 30  $\mu$ M because none of them survived, but from trends, compound 329 appeared to exhibit similar results as MB 51. The bottom panel shows MB 51 along with its negative controls (102, 001 & 082). When comparing the negative controls to MB 51, 102 and 001 did not exhibit the same signs of depigmentation as MB 51, but at higher concentrations they presented with changes in body shape and heart malformations. When comparing 082 to MB 51, 082 did show signs of depigmentation but they were not consistent as the concentrations of 082 increases. This was also true for body defects that were present at low concentrations but not at higher ones.

# References

1. Daum G, Bohni PC, & Schatz G (1982) Import of proteins into mitochondria. Cytochrome b2 and cytochrome c peroxidase are located in the intermembrane space of yeast mitochondria. (Translated from eng) *J Biol Chem* 257(21):13028-13033 (in eng).
2. Jensen MB & Jasper H (2014) Mitochondrial Proteostasis in the Control of Aging and Longevity. (Translated from Eng) *Cell Metab* (in Eng).
3. Chi X, Kale J, Leber B, & Andrews DW (2014) Regulating cell death at, on, and in membranes. (Translated from Eng) *Biochim Biophys Acta* (in Eng).
4. Qi QR & Yang ZM (2014) Regulation and function of signal transducer and activator of transcription 3. (Translated from Eng) *World J Biol Chem* 5(2):231-239 (in Eng).
5. Kianian PM & Kianian SF (2014) Mitochondrial dynamics and the cell cycle. (Translated from Eng) *Front Plant Sci* 5:222 (in Eng).
6. Sickmann A, et al. (2003) The proteome of *Saccharomyces cerevisiae* mitochondria. (Translated from eng) *Proc Natl Acad Sci U S A* 100(23):13207-13212 (in eng).
7. von Heijne G, Steppuhn J, & Herrmann RG (1989) Domain structure of mitochondrial and chloroplast targeting peptides. (Translated from eng) *Eur J Biochem* 180(3):535-545 (in eng).
8. Pfanner N, Craig EA, & Honlinger A (1997) Mitochondrial preprotein translocase. (Translated from eng) *Annu Rev Cell Dev Biol* 13:25-51 (in eng).
9. Neupert W (1997) Protein import into mitochondria. (Translated from eng) *Annu Rev Biochem* 66:863-917 (in eng).
10. Honlinger A, et al. (1996) Tom7 modulates the dynamics of the mitochondrial outer membrane translocase and plays a pathway-related role in protein import. (Translated from eng) *EMBO J* 15(9):2125-2137 (in eng).
11. Dietmeier K, et al. (1997) Tom5 functionally links mitochondrial preprotein receptors to the general import pore. (Translated from eng) *Nature* 388(6638):195-200 (in eng).
12. Yamamoto H, et al. (2002) Tim50 is a subunit of the TIM23 complex that links protein translocation across the outer and inner mitochondrial membranes. (Translated from eng) *Cell* 111(4):519-528 (in eng).

13. Geissler A, et al. (2002) The mitochondrial presequence translocase: an essential role of Tim50 in directing preproteins to the import channel. (Translated from eng) *Cell* 111(4):507-518 (in eng).
14. Gaume B, et al. (1998) Unfolding of preproteins upon import into mitochondria. (Translated from eng) *EMBO J* 17(22):6497-6507 (in eng).
15. Geissler A, et al. (2000) Membrane potential-driven protein import into mitochondria. The sorting sequence of cytochrome b(2) modulates the  $\Delta\psi$ -dependence of translocation of the matrix-targeting sequence. (Translated from eng) *Mol Biol Cell* 11(11):3977-3991 (in eng).
16. Gakh O, Cavadini P, & Isaya G (2002) Mitochondrial processing peptidases. (Translated from eng) *Biochim Biophys Acta* 1592(1):63-77 (in eng).
17. Endo T & Yamano K (2009) Multiple pathways for mitochondrial protein traffic. (Translated from eng) *Biol Chem* 390(8):723-730 (in eng).
18. Ito A (1999) Mitochondrial processing peptidase: multiple-site recognition of precursor proteins. (Translated from eng) *Biochem Biophys Res Commun* 265(3):611-616 (in eng).
19. Paces V, Rosenberg LE, Fenton WA, & Kalousek F (1993) The beta subunit of the mitochondrial processing peptidase from rat liver: cloning and sequencing of a cDNA and comparison with a proposed family of metallopeptidases. (Translated from eng) *Proc Natl Acad Sci U S A* 90(11):5355-5358 (in eng).
20. Kitada S, Shimokata K, Niidome T, Ogishima T, & Ito A (1995) A putative metal-binding site in the beta subunit of rat mitochondrial processing peptidase is essential for its catalytic activity. (Translated from eng) *J Biochem* 117(6):1148-1150 (in eng).
21. Kitada S, Yamasaki E, Kojima K, & Ito A (2003) Determination of the cleavage site of the presequence by mitochondrial processing peptidase on the substrate binding scaffold and the multiple subsites inside a molecular cavity. (Translated from eng) *J Biol Chem* 278(3):1879-1885 (in eng).
22. McAda PC & Douglas MG (1982) A neutral metallo endoprotease involved in the processing of an F1-ATPase subunit precursor in mitochondria. (Translated from eng) *J Biol Chem* 257(6):3177-3182 (in eng).
23. Miura S, Mori M, Amaya Y, & Tatibana M (1982) A mitochondrial protease that cleaves the precursor of ornithine carbamoyltransferase. Purification and properties. (Translated from eng) *Eur J Biochem* 122(3):641-647 (in eng).
24. Conboy JG, Fenton WA, & Rosenberg LE (1982) Processing of pre-ornithine transcarbamylase requires a zinc-dependent protease localized to the mitochondrial matrix. (Translated from eng) *Biochem Biophys Res Commun* 105(1):1-7 (in eng).

25. Schmidt B, Wachter E, Sebald W, & Neupert W (1984) Processing peptidase of *Neurospora* mitochondria. Two-step cleavage of imported ATPase subunit 9. (Translated from eng) *Eur J Biochem* 144(3):581-588 (in eng).
26. Luciano P, Tokatlidis K, Chambre I, Germanique JC, & Geli V (1998) The mitochondrial processing peptidase behaves as a zinc-metallopeptidase. (Translated from eng) *J Mol Biol* 280(2):193-199 (in eng).
27. Auld DS (1995) Removal and replacement of metal ions in metallopeptidases. (Translated from eng) *Methods Enzymol* 248:228-242 (in eng).
28. Hurt EC, Allison DS, Muller U, & Schatz G (1987) Amino-terminal deletions in the presequence of an imported mitochondrial protein block the targeting function and proteolytic cleavage of the presequence at the carboxy terminus. (Translated from eng) *J Biol Chem* 262(3):1420-1424 (in eng).
29. Vestweber D, Brunner J, Baker A, & Schatz G (1989) A 42K outer-membrane protein is a component of the yeast mitochondrial protein import site. (Translated from eng) *Nature* 341(6239):205-209 (in eng).
30. Shimokata K, Kitada S, Ogishima T, & Ito A (1998) Role of alpha-subunit of mitochondrial processing peptidase in substrate recognition. (Translated from eng) *J Biol Chem* 273(39):25158-25163 (in eng).
31. Taylor AB, et al. (2001) Crystal structures of mitochondrial processing peptidase reveal the mode for specific cleavage of import signal sequences. (Translated from eng) *Structure* 9(7):615-625 (in eng).
32. Nagao Y, et al. (2000) Glycine-rich region of mitochondrial processing peptidase alpha-subunit is essential for binding and cleavage of the precursor proteins. (Translated from eng) *J Biol Chem* 275(44):34552-34556 (in eng).
33. Kojima K, Kitada S, Shimokata K, Ogishima T, & Ito A (1998) Cooperative formation of a substrate binding pocket by alpha- and beta-subunits of mitochondrial processing peptidase. (Translated from eng) *J Biol Chem* 273(49):32542-32546 (in eng).
34. Luciano P, Geoffroy S, Brandt A, Hernandez JF, & Geli V (1997) Functional cooperation of the mitochondrial processing peptidase subunits. (Translated from eng) *J Mol Biol* 272(2):213-225 (in eng).
35. Priest JW & Hajduk SL (2003) *Trypanosoma brucei* cytochrome c1 is imported into mitochondria along an unusual pathway. *J Biol Chem* 278(17):15084-15094.
36. Curran SP, et al. (2004) The role of Hot13p and redox chemistry in the mitochondrial TIM22 import pathway. *J Biol Chem* 279(42):43744-43751.

37. Curran SP, Leuenberger D, Oppliger W, & Koehler CM (2002) The Tim9p-Tim10p complex binds to the transmembrane domains of the ADP/ATP carrier. *EMBO J* 21(5):942-953.
38. Popov-Celeketic D, Waegemann K, Mapa K, Neupert W, & Mokranjac D (2011) Role of the import motor in insertion of transmembrane segments by the mitochondrial TIM23 complex. *EMBO Rep* 12(6):542-548.
39. Goswami AV, Samaddar M, Sinha D, Purushotham J, & D'Silva P (2012) Enhanced J-protein interaction and compromised protein stability of mtHsp70 variants lead to mitochondrial dysfunction in Parkinsons disease. (Translated from English) *Human Molecular Genetics* 21(15):3317-3332 (in English).
40. Beasley EM, Muller S, & Schatz G (1993) The Signal That Sorts Yeast Cytochrome-B2 to the Mitochondrial Intermembrane Space Contains 3 Distinct Functional Regions. (Translated from English) *Embo Journal* 12(6):2303-2311 (in English).
41. Huynen MA, Snel B, Bork P, & Gibson TJ (2001) The phylogenetic distribution of frataxin indicates a role in iron-sulfur cluster protein assembly. *Hum Mol Genet* 10(21):2463-2468.
42. Pandey A, et al. (2013) Frataxin directly stimulates mitochondrial cysteine desulfurase by exposing substrate-binding sites, and a mutant Fe-S cluster scaffold protein with frataxin-bypassing ability acts similarly. *J Biol Chem* 288(52):36773-36786.
43. Bencze KZ, et al. (2006) The structure and function of frataxin. *Critical reviews in biochemistry and molecular biology* 41(5):269-291.
44. Campuzano V, et al. (1996) Friedreich's ataxia: autosomal recessive disease caused by an intronic GAA triplet repeat expansion. *Science* 271(5254):1423-1427.
45. Durr A, et al. (1996) Clinical and genetic abnormalities in patients with Friedreich's ataxia. *N Engl J Med* 335(16):1169-1175.
46. Kirches E, et al. (2011) Dual role of the mitochondrial protein frataxin in astrocytic tumors. *Laboratory investigation; a journal of technical methods and pathology* 91(12):1766-1776.
47. Koutnikova H, et al. (1997) Studies of human, mouse and yeast homologues indicate a mitochondrial function for frataxin. *Nat Genet* 16(4):345-351.
48. van der Giezen M, Leon-Avila G, & Tovar J (2005) Characterization of chaperonin 10 (Cpn10) from the intestinal human pathogen *Entamoeba histolytica*. *Microbiology* 151(Pt 9):3107-3115.
49. Zhou C, et al. (2008) The kinase domain of mitochondrial PINK1 faces the cytoplasm. *Proc Natl Acad Sci U S A* 105(33):12022-12027.



50. Geisler S, et al. (2010) The PINK1/Parkin-mediated mitophagy is compromised by PD-associated mutations. *Autophagy* 6(7):871-878.
51. Matsuda N, et al. (2010) PINK1 stabilized by mitochondrial depolarization recruits Parkin to damaged mitochondria and activates latent Parkin for mitophagy. *J Cell Biol* 189(2):211-221.
52. Vives-Bauza C, et al. (2010) PINK1-dependent recruitment of Parkin to mitochondria in mitophagy. *Proc Natl Acad Sci U S A* 107(1):378-383.
53. Koyano F, et al. (2014) Ubiquitin is phosphorylated by PINK1 to activate parkin. *Nature* 510(7503):162-166.
54. McLelland GL, Soubannier V, Chen CX, McBride HM, & Fon EA (2014) Parkin and PINK1 function in a vesicular trafficking pathway regulating mitochondrial quality control. *EMBO J* 33(4):282-295.
55. Chen Y & Dorn GW, 2nd (2013) PINK1-phosphorylated mitofusin 2 is a Parkin receptor for culling damaged mitochondria. *Science* 340(6131):471-475.
56. Lister JA (2002) Development of pigment cells in the zebrafish embryo. *Microscopy research and technique* 58(6):435-441.
57. Logan DW, Burn SF, & Jackson IJ (2006) Regulation of pigmentation in zebrafish melanophores. *Pigment cell research / sponsored by the European Society for Pigment Cell Research and the International Pigment Cell Society* 19(3):206-213.
58. Karlsson J, von Hofsten J, & Olsson PE (2001) Generating transparent zebrafish: a refined method to improve detection of gene expression during embryonic development. *Marine biotechnology* 3(6):522-527.
59. O'Reilly-Pol T & Johnson SL (2008) Neocuproine ablates melanocytes in adult zebrafish. *Zebrafish* 5(4):257-264.
60. Ishizaki H, et al. (2010) Combined zebrafish-yeast chemical-genetic screens reveal gene-copper-nutrition interactions that modulate melanocyte pigmentation. *Disease models & mechanisms* 3(9-10):639-651.
61. Nicholson DW, Stuart RA, & Neupert W (1989) Biogenesis of cytochrome c1. Role of cytochrome c1 heme lyase and of the two proteolytic processing steps during import into mitochondria. *J Biol Chem* 264(17):10156-10168.
62. Wachter C, Schatz G, & Glick BS (1992) Role of ATP in the intramitochondrial sorting of cytochrome c1 and the adenine nucleotide translocator. *EMBO J* 11(13):4787-4794.

63. Martin J, Mahlke K, & Pfanner N (1991) Role of an energized inner membrane in mitochondrial protein import. Delta psi drives the movement of presequences. *J Biol Chem* 266(27):18051-18057.
64. Nunnari J, Fox TD, & Walter P (1993) A mitochondrial protease with two catalytic subunits of nonoverlapping specificities. *Science* 262(5142):1997-2004.
65. Schleyer M & Neupert W (1985) Transport of proteins into mitochondria: translocational intermediates spanning contact sites between outer and inner membranes. *Cell* 43(1):339-350.
66. Irrcher I, Adhihetty PJ, Joseph AM, Ljubicic V, & Hood DA (2003) Regulation of mitochondrial biogenesis in muscle by endurance exercise. *Sports medicine* 33(11):783-793.
67. Ryan MT, Naylor DJ, Hoogenraad NJ, & Hoj PB (1995) Affinity purification, overexpression, and characterization of chaperonin 10 homologues synthesized with and without N-terminal acetylation. *J Biol Chem* 270(37):22037-22043.
68. Samii A, Nutt JG, & Ransom BR (2004) Parkinson's disease. *Lancet* 363(9423):1783-1793.
69. Clark IE, et al. (2006) *Drosophila* pink1 is required for mitochondrial function and interacts genetically with parkin. *Nature* 441(7097):1162-1166.
70. Park J, et al. (2006) Mitochondrial dysfunction in *Drosophila* PINK1 mutants is complemented by parkin. *Nature* 441(7097):1157-1161.
71. Yang Y, et al. (2006) Mitochondrial pathology and muscle and dopaminergic neuron degeneration caused by inactivation of *Drosophila* Pink1 is rescued by Parkin. *Proc Natl Acad Sci U S A* 103(28):10793-10798.
72. Greene AW, et al. (2012) Mitochondrial processing peptidase regulates PINK1 processing, import and Parkin recruitment. *EMBO Rep* 13(4):378-385.
73. Steele SL, Prykhodzhiy SV, & Berman JN (2014) Zebrafish as a model system for mitochondrial biology and diseases. *Translational research : the journal of laboratory and clinical medicine* 163(2):79-98.
74. Dabir DV, et al. (2013) A small molecule inhibitor of redox-regulated protein translocation into mitochondria. *Dev Cell* 25(1):81-92.
75. Miyata N, et al. (in submission) Adaptation of a genetic screen reveals an inhibitor for mitochondrial protein import component Tim44. (EMBO).
76. Mendelsohn BA, et al. (2006) Atp7a determines a hierarchy of copper metabolism essential for notochord development. *Cell Metab* 4(2):155-162.

77. Glick BS & Pon LA (1995) Isolation of highly purified mitochondria from *Saccharomyces cerevisiae*. *Methods Enzymol* 260:213-223.
78. Hasson SA, et al. (2010) Substrate specificity of the TIM22 mitochondrial import pathway revealed with small molecule inhibitor of protein translocation. *Proc Natl Acad Sci U S A* 107(21):9578-9583.
79. Koehler CM, et al. (1998) Tim9p, an essential partner subunit of Tim10p for the import of mitochondrial carrier proteins. (Translated from eng) *EMBO J* 17(22):6477-6486 (in eng).
80. Freshney RI (2000) *Culture of animal cells : a manual of basic technique* (Wiley, New York) 4th Ed pp xxvi, 577.
81. Strober W (2001) Trypan blue exclusion test of cell viability. *Current protocols in immunology* / edited by John E. Coligan ... [et al.] Appendix 3:Appendix 3B.

## Chapter 5: Comparison of MitoBloCK-50 and MitoBloCK-51

Small molecules can potentially affect their target protein in a number of different ways, from binding directly to portions of the active site to binding to an ancillary site that indirectly affects the protein's active site. All of these actions have the potential to cause varying downstream changes in the cellular environment. By studying the differences that each small molecule causes for the same target we can gather more information on how the protein of interest functions. Comparing the data of MB 50 and MB 51 much of their effects against MPP are fairly similar, but we did observe some glaring differences. The major differences seen between the two inhibitors of MPP involved import of CytC<sub>1</sub> and CytB<sub>2</sub>, Pink1 import when coupled with carbonate extraction, Parkin recruitment, and zebrafish treatment.

MB 50 was capable of inhibiting the import of CytB<sub>2</sub>-DHFR (1-167) and CytB<sub>2</sub>-DHFR (A63P), while it did not inhibit the import of CytC<sub>1</sub>. On the other hand, MB 51 was able to inhibit the import of CytC<sub>1</sub> and CytB<sub>2</sub>-DHFR (1-167), while the inhibition of CytB<sub>2</sub>-DHFR (A63P) was not as robust (Figure 5.1). Both drugs were capable of inhibiting the import of CytB<sub>2</sub>-DHFR (1-167), but they showed opposite effects for CytC<sub>1</sub> and CytB<sub>2</sub>-DHFR (A63P). MPP is able to cleave an extremely diverse set of substrates with varying lengths, amino acid sequence, and overall charge, but its cleavage site for each of its substrates is specific and accurate. The active cavity of MPP is believed to be capable of scanning its substrates for the correct site of processing, therefore the differences we are observing between MB 50 and 51

could signify the two drugs are binding in a different region within MPP. A difference in binding site might have a different effect on MPP's ability to recognize different substrates.

We also saw different effects between MB 50 and 51 for Pink1 import and Parkin recruitment (Figure 5.2 & 5.3). When analyzing the import of Pink1 with carbonate extraction we observed a high molecular weight Pink1 aggregate that formed after treatment with MB 51, but not MB 50. On the other hand, when we looked at Parkin recruitment on the surface of mitochondria following drug treatment, we saw that MB 50 in conjunction with CCCP was capable of inducing the Parkin recruitment, but MB 51 failed to show similar results. The current model for Parkin recruitment is that Pink1, which is normally degraded quickly upon import into mitochondria becomes stabilized due mitochondrial dysfunction. Pink1 is then directed towards the outer membrane where it presents a Ser/Thr kinase domain towards the cytosol, which is capable of directing the recruitment of Parkin. Once Parkin is recruited, the damaged mitochondria then degraded via autophagy. With this in mind, our data regarding MB 50 and 51 appears to be conflicting. MB 51 is capable of causing Pink1 aggregation, which could signify that it has the potential to cause Pink1 mitochondrial accumulation and direction towards the outer membrane. This should then cause the recruitment of Parkin, but when we tested MB 51 for Parkin recruitment in HeLa cells it failed to show significant recruitment. On the other hand, MB 50 did not exhibit Pink1 aggregation, but did recruit Parkin to the surface of mitochondria. This could mean that the aggregation seen with MB 51 does not correlate with Pink1 accumulation on the surface of mitochondria or we require a different method for detecting Parkin recruitment.

MB 50 and 51 also exhibited significant differences when zebrafish were exposed to the two drugs (Figure 5.4). MB 50 caused the zebrafish to have severe developmental problems with

body curvature and cardiac abnormalities after 3 days of drug exposure. Once MB 50 was washed out and the zebrafish were allowed to grow for an additional 2 days, they still exhibited some changes in body curvature and cardiac development, but these issues were not as drastic as before MB 50 was washed out. This could signify that MB 50 has some long lasting effects on zebrafish development even after the drug is removed. MB 51 caused the zebrafish to have some changes in body shape and cardiac development, but the most striking affect was a complete depigmentation after 3 days of drug exposure. Once MB 51 was washed out the pigmentation came back completely, but the changes in body shape and cardiac development appeared to be more severe at 5 days post-fertilization then at 3 days. Comparing this outcome to MB 50 it could suggest that the effect of MB 51 after it has been removed is more long lasting and pervasive than the lasting effects of MB 50. Taking all the data reexamined in this comparison chapter into account it appears MB 50 and 51 may act on MPP in a different manner and/or a different binding site, which causes different downstream affects.

# Future Directions

Further work needs to be done to determine the binding sites of both MB 50 and 51 with MPP. One method for this is via computational modeling and docking experiments with MPP and the MitoBLoCK drugs. Another method capable of showing where the MitoBLoCK drugs bind to MPP is through x-ray crystallography. Once this data is acquired we would then narrow regions of possible drug-protein interactions, which could be further tested with site-directed mutagenesis on MPP to determine what mutations were capable of altering drug binding. This work would further help us determine if the differences we observed between MB 50 and 51 were due to differing interactions with MPP or they were caused by different off-target effects. Docking experiments with MB 50 and 51 analogs could also help us determine if our hypothesis regarding the key structural features of each drug group are correct and if more effective drug candidates can be developed.

Zebrafish depigmentation seen with exposure to MB 51 also needs to be further tested. We compared treatment of MB 51 with a copper chelator and PTU, which inhibits melanogenesis by blocking all tyrosine-dependent steps in the melanin pathway. All three compounds caused the fish to lose pigmentation and all three compounds could be washed out allowing the fish pigmentation to completely return. This led us to the idea that MB 51 inhibition of MPP could be involved in copper metabolism, melanogenesis, and/or the production of melanin. An experiment that could shed light on the involvement of copper metabolism is to add increasing amounts of copper during treatment with MB 51 to see if by adding copper we can block depigmentation. We could also utilize both CRISPR (germ-line knockdown) and morpholino (transient protein

knockdown) technology to test whether we observe the same effects when we knockdown MPP as compared MB 51 drug treatment.

Using zebrafish its possible to specifically label certain populations of neurons with fluorescent proteins. Previous work in this area has produced a line of zebrafish where the dopaminergic neurons are tagged with GFP. (1-3) Using this line or ones similar to it we could test MB 50 and 51's ability to affect dopaminergic neurons, thereby gaining more insight into whether our small molecules and their capability to alter Pink1 import and induce Parkin recruitment can be linked to Parkinson's disease or other dopamine-related diseases. There are also known morpholinos for Pink1, Parkin, and Mitofusin, which could be used in conjunction with our small molecules to learn more about the Pink-Parkin mitochondrial degradation pathway and its link to disease. (4-6)

Lastly, while compiling the data for this thesis I discovered a hit compound that has the potential to be an interesting MPP inhibitor, apomorphine (its structure can be seen in the appendix). Apomorphine is known by the following commercial names: Apokyn, Ixense, Spontane, and Uprima. It is a non-selective dopamine agonist capable of activating both D<sub>1</sub>-like and D<sub>2</sub>-like dopamine receptors; it also exhibits antagonistic affects on 5-HT and  $\alpha$ -adrenergic receptors. (7-10) Historically, apomorphine has been used as a treatment for alcoholism, Parkinson's disease, erectile dysfunction, Alzheimer's disease, and opioid addiction. (11-17) The ability of apomorphine to inhibit the function of MPP needs to be investigated in our entire preliminary assays; cleavage of the JPT fluorogenic peptide, Su9-DHFR cleavage, and Su9-DHFR import. Once these test are completed and apomorphine is confirmed to be a MPP inhibitor it needs to be modeled along with the rest of the compounds, characterized further for specific import inhibition, and treated on zebrafish.



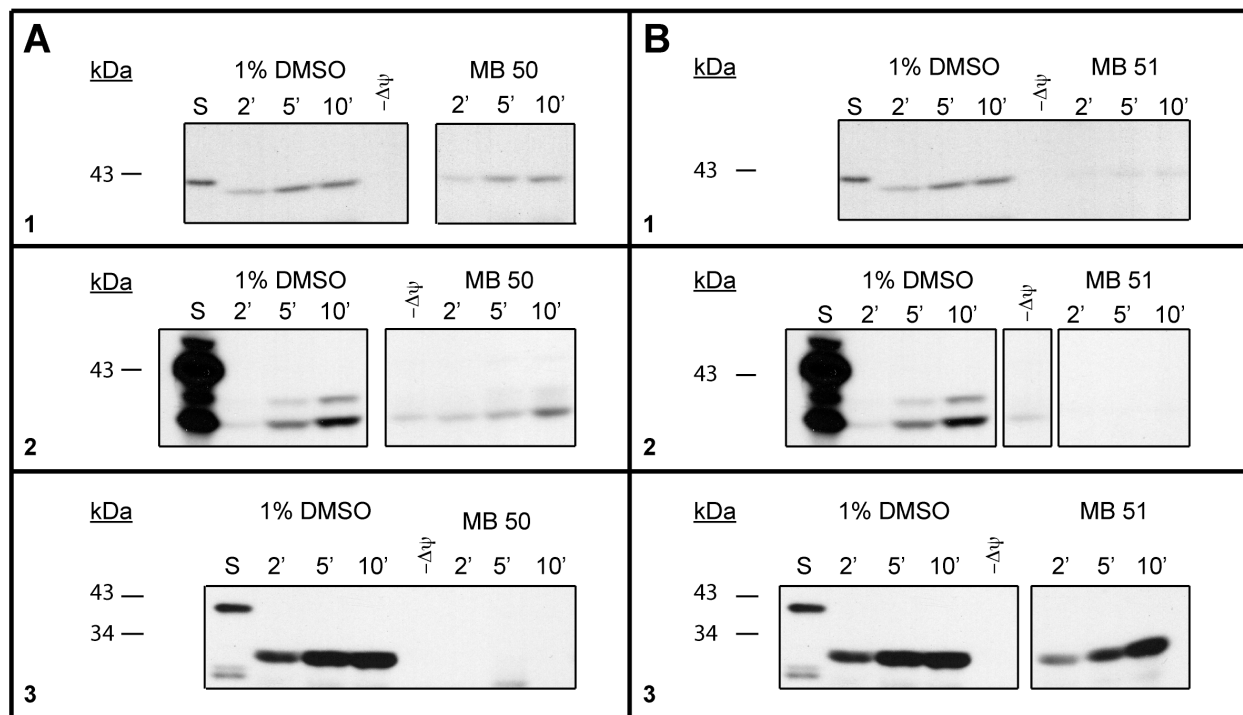


**Figure 5.1 Comparison of MB 50 and 51 with import of CytC<sub>1</sub>, CyB<sub>2</sub>-DHRF (1-167) and CytB<sub>2</sub>-DHFR (A63P).**

The aim of this figure is to show the comparison of MB 50 and MB 51 treatment on the import of CytC<sub>1</sub>, CyB<sub>2</sub>-DHRF (1-167) and CytB<sub>2</sub>-DHFR (A63P). Panel A shows import with MB 50 treatment, while panel B is MB 51 treatment. CytC<sub>1</sub> import is in both panels A1 and B1. CyB<sub>2</sub>-DHRF (1-167) import is in both panels A2 and B2. CytB<sub>2</sub>-DHFR (A63P) import is in both panels A3 and B3. For additional details about these experiments see Chapter 3 for MB 50 experiments and Chapter 4 for MB 51 experiments.

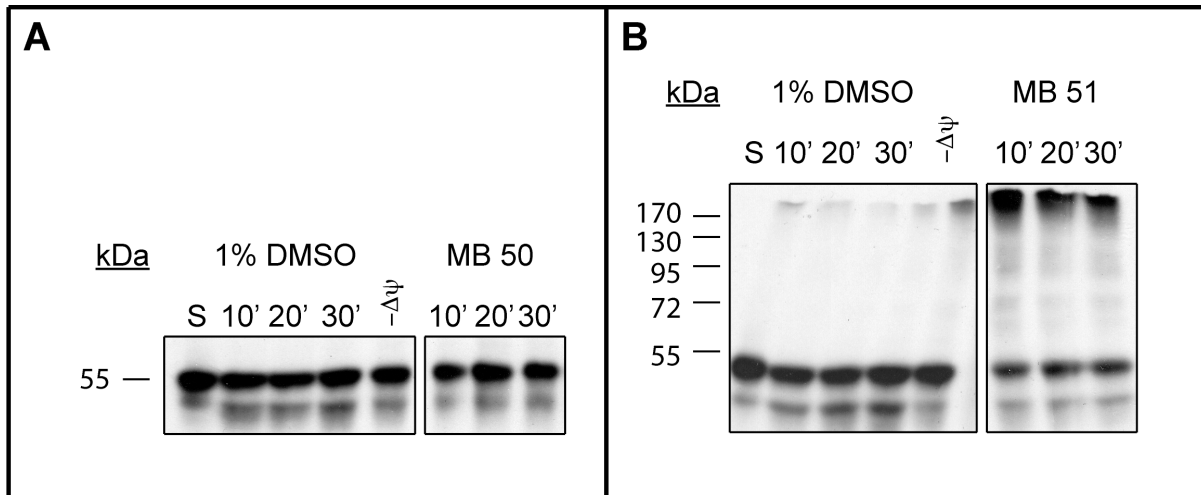


**Figure 5.2 Comparison of MB 50 and MB 51 with Pink1 Import in Conjunction with Carbonate Extraction.**

Panel A looks at MB 50 treatment with the import of hPink1 with carbonate extraction and Panel B shows the treatment of MB 51 with import of hPink1 in conjunction with carbonate extraction. MB 51 treatment exhibits a high molecular weight aggregate as compared to DMSO, CCCP, and MB 50 treatment.

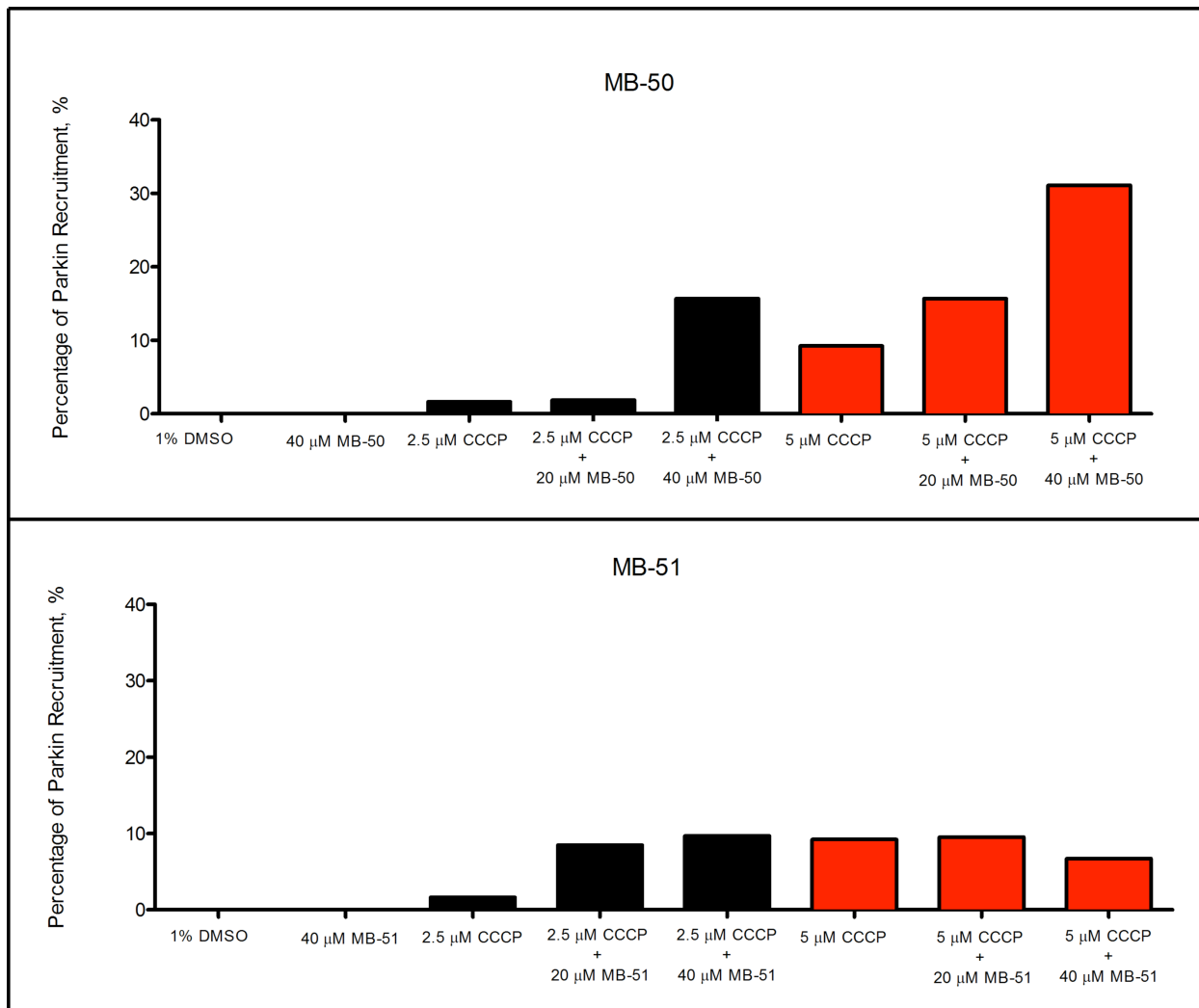


**Figure 5.3 Comparison of MB 50 and MB 51 with Parkin Recruitment on EGFP Parkin Expressing HeLa Cells.**

Both upper and lower panels are quantifications of the number of HeLa cells showing recruitment of Parkin on the surface of mitochondria (upper – MB 50, lower – MB 51). MB 50 treatment (40  $\mu$ M) with concurrent treatment of CCCP (5  $\mu$ M) exhibited significantly more Parkin recruitment than MB 51 treatment (40  $\mu$ M) with concurrent treatment of CCCP (5  $\mu$ M).

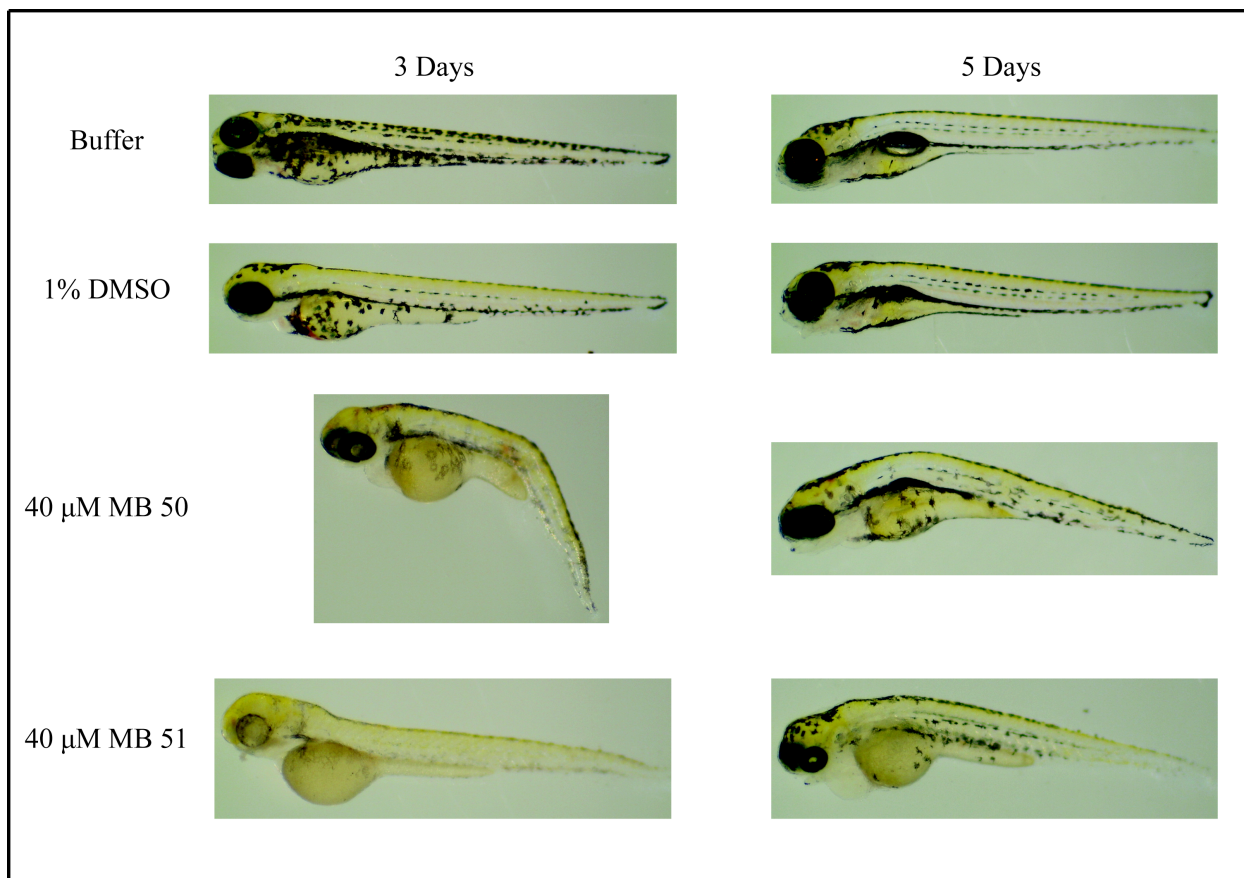


**Figure 5.4 Comparison of MB 50 & 51 Treatment with Zebrafish.**

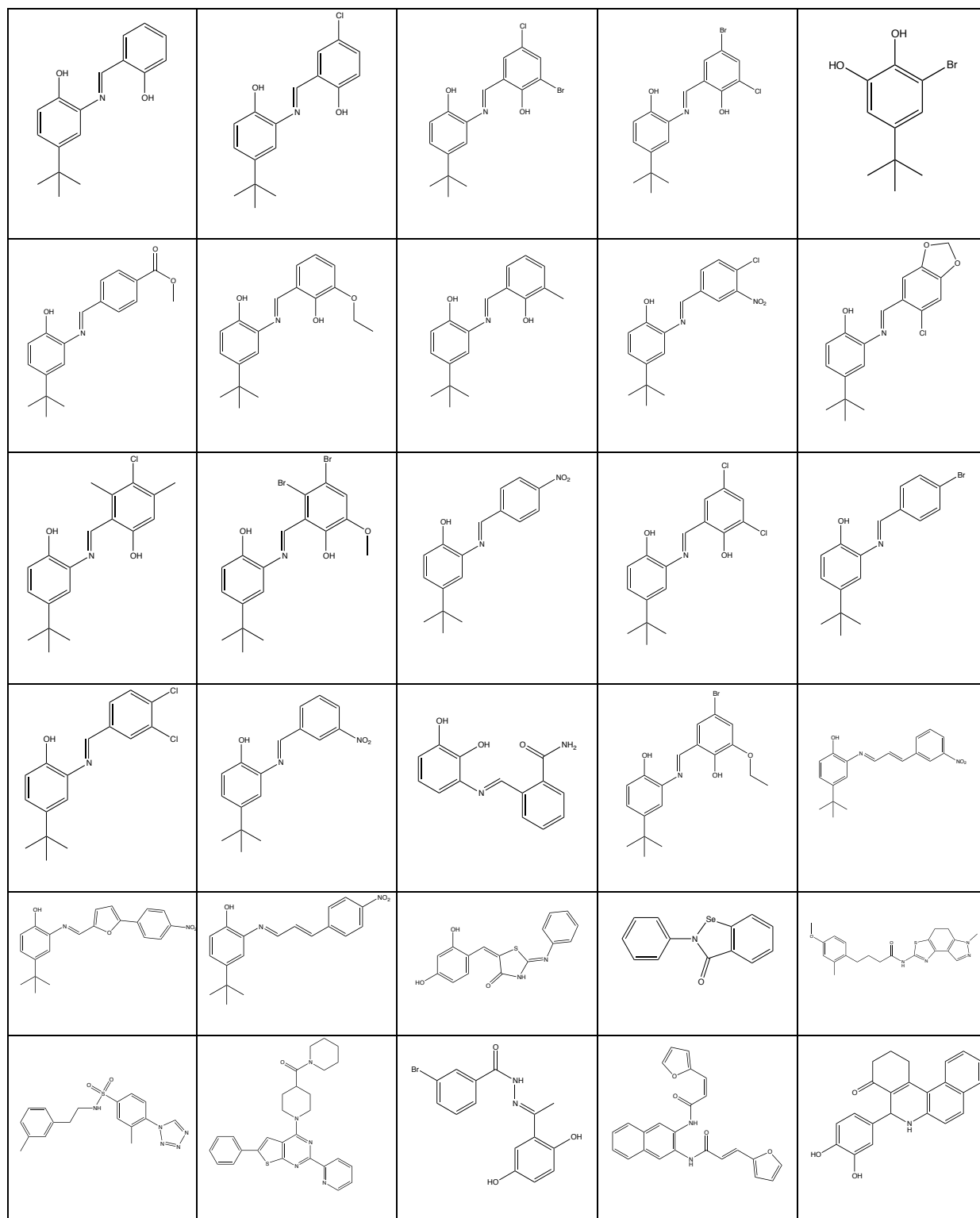
Cmcl2 DsRed zebrafish were allowed to develop for 3 hour post-fertilization and then they were treated with 1% DMSO or 40  $\mu$ M of either MB 50 or MB 51. After 3 days the drugs were washed out the zebrafish were allowed develop for an additional 2 days. MB 50 treatment exhibits a severe change in body and cardiac development after 3 days of exposure. Once MB 50 is washed out the development problems still exist but they are as severe. MB 51 treatment exhibits a severe loss of pigmentation and some defects with body shape and cardiac development. After MB 51 is washed out the pigmentation returns completely, but changes in body and cardiac development appear to be fairly similar if not a bit worse when comparing day 3 to day 5.

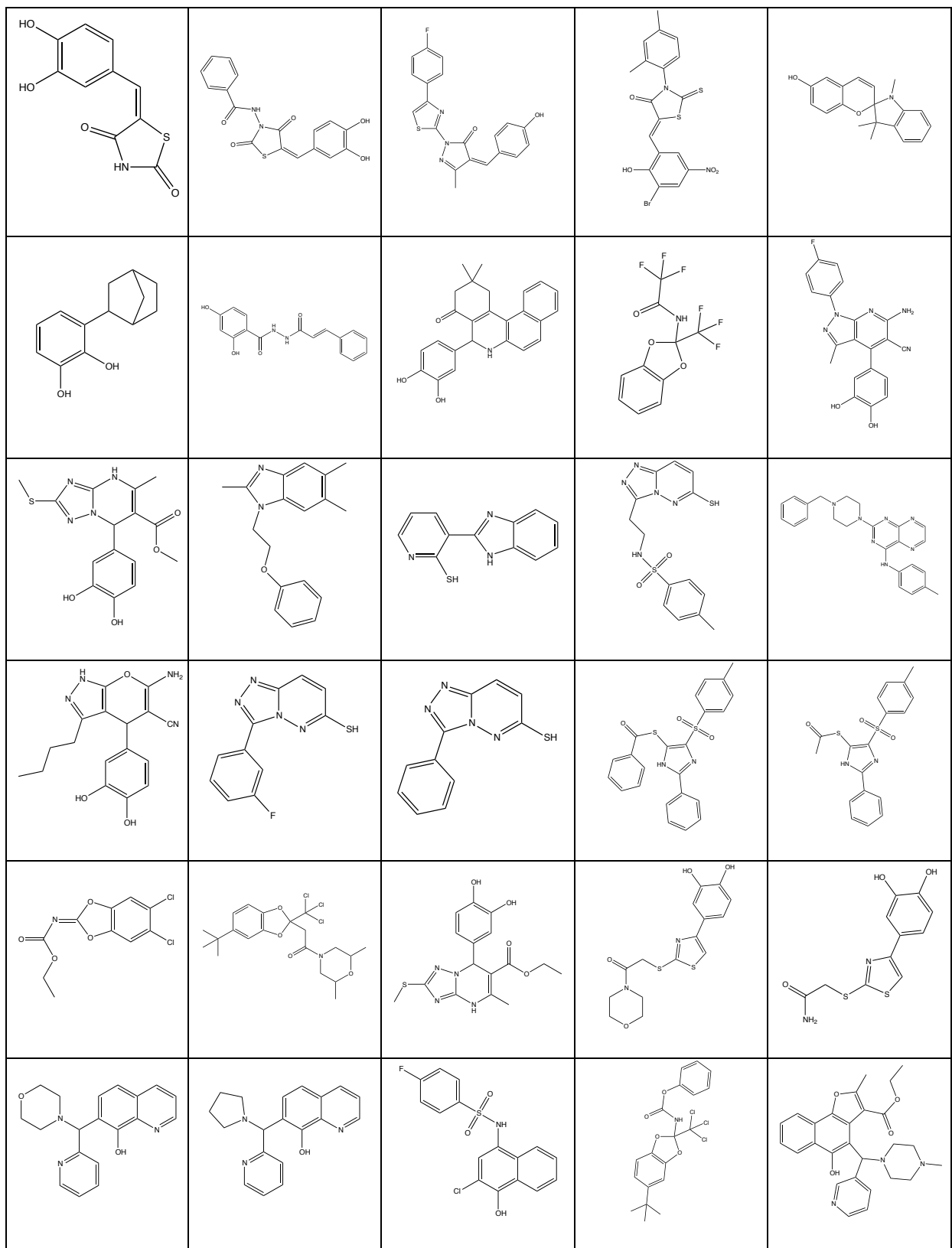
# References

1. Sager JJ, Bai Q, & Burton EA (2010) Transgenic zebrafish models of neurodegenerative diseases. *Brain structure & function* 214(2-3):285-302.
2. Xi Y, *et al.* (2011) Transgenic zebrafish expressing green fluorescent protein in dopaminergic neurons of the ventral diencephalon. *Dev Dyn* 240(11):2539-2547.
3. Sallinen V, *et al.* (2010) Dopaminergic cell damage and vulnerability to MPTP in Pink1 knockdown zebrafish. *Neurobiology of disease* 40(1):93-101.
4. Mortiboys H, *et al.* (2008) Mitochondrial function and morphology are impaired in parkin-mutant fibroblasts. *Annals of neurology* 64(5):555-565.
5. Grunewald A, *et al.* (2010) Mutant Parkin impairs mitochondrial function and morphology in human fibroblasts. *PLoS One* 5(9):e12962.
6. Yokota T, *et al.* (2003) Down regulation of DJ-1 enhances cell death by oxidative stress, ER stress, and proteasome inhibition. *Biochem Biophys Res Commun* 312(4):1342-1348.
7. Millan MJ, *et al.* (2002) Differential actions of antiparkinson agents at multiple classes of monoaminergic receptor. I. A multivariate analysis of the binding profiles of 14 drugs at 21 native and cloned human receptor subtypes. *The Journal of pharmacology and experimental therapeutics* 303(2):791-804.
8. Newman-Tancredi A, *et al.* (2002) Differential actions of antiparkinson agents at multiple classes of monoaminergic receptor. III. Agonist and antagonist properties at serotonin, 5-HT(1) and 5-HT(2), receptor subtypes. *The Journal of pharmacology and experimental therapeutics* 303(2):815-822.
9. Newman-Tancredi A, *et al.* (2002) Differential actions of antiparkinson agents at multiple classes of monoaminergic receptor. II. Agonist and antagonist properties at subtypes of dopamine D(2)-like receptor and alpha(1)/alpha(2)-adrenoceptor. *The Journal of pharmacology and experimental therapeutics* 303(2):805-814.
10. Hsieh GC, *et al.* (2004) Central mechanisms regulating penile erection in conscious rats: the dopaminergic systems related to the proerectile effect of apomorphine. *The Journal of pharmacology and experimental therapeutics* 308(1):330-338.
11. Dent JY (1949) Apomorphine Treatment of Addiction. *British Journal of Addiction to Alcohol & Other Drugs* 46(1):15-28.

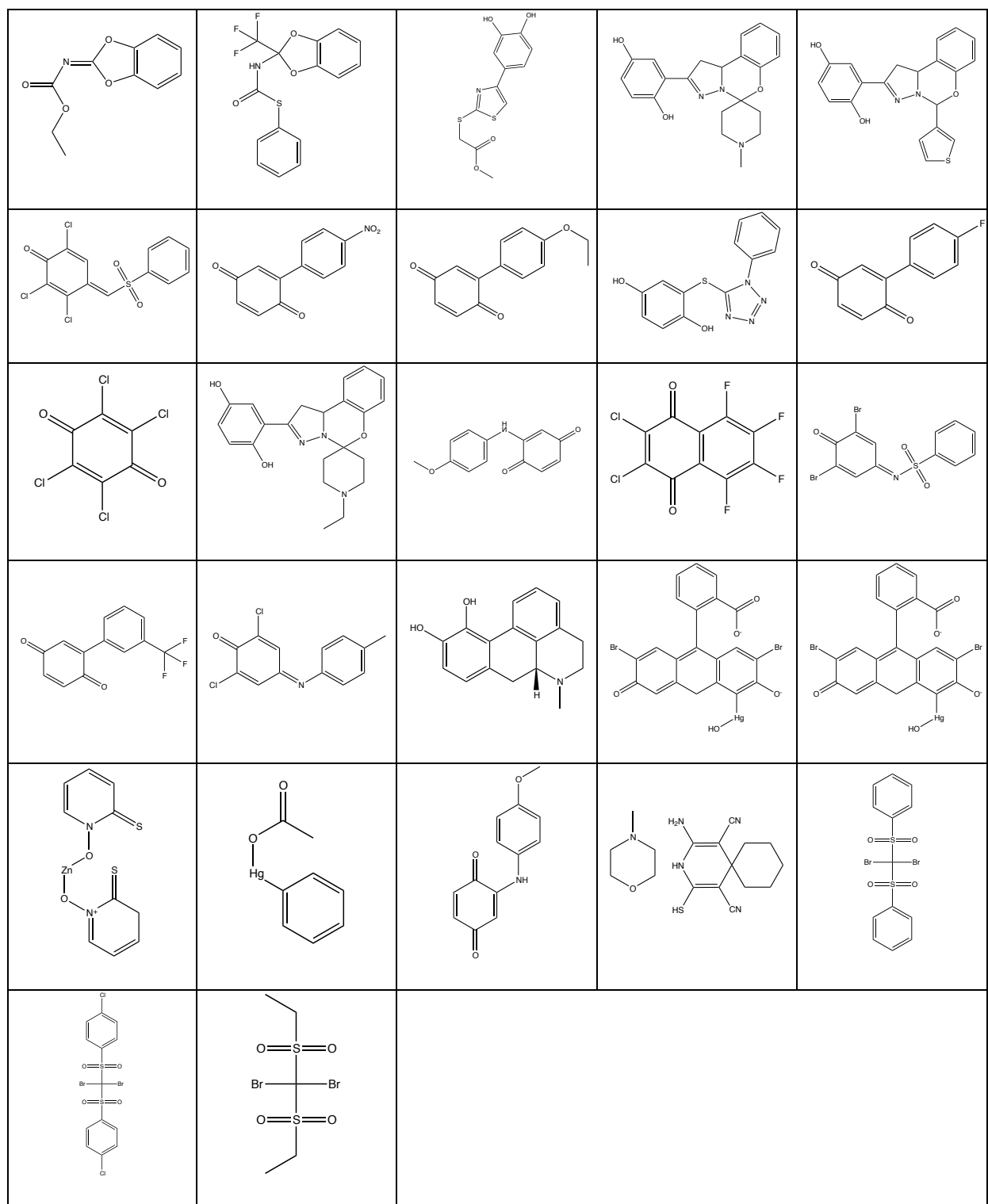
12. Barcroft H & Schwab RS (1951) The effect of apomorphine and that of adrenalin, on the tremor of Parkinson's disease. *The Journal of nervous and mental disease* 114(6):541-542.
13. Schwab RS, Amador LV, & Lettvin JY (1951) Apomorphine in Parkinson's disease. *Transactions of the American Neurological Association* 56:251-253.
14. Cotzias GC, Papavasiliou PS, Fehling C, Kaufman B, & Mena I (1970) Similarities between neurologic effects of L-dopa and of apomorphine. *N Engl J Med* 282(1):31-33.
15. Corsini GU, Del Zompo M, Gessa GL, & Mangoni A (1979) Therapeutic efficacy of apomorphine combined with an extracerebral inhibitor of dopamine receptors in Parkinson's disease. *Lancet* 1(8123):954-956.
16. Chaudhuri KR & Clough C (1998) Subcutaneous apomorphine in Parkinson's disease. *Bmj* 316(7132):641.
17. Lashuel HA, *et al.* (2002) New class of inhibitors of amyloid-beta fibril formation. Implications for the mechanism of pathogenesis in Alzheimer's disease. *J Biol Chem* 277(45):42881-42890.

# Appendix A: Hit Compounds from HTS

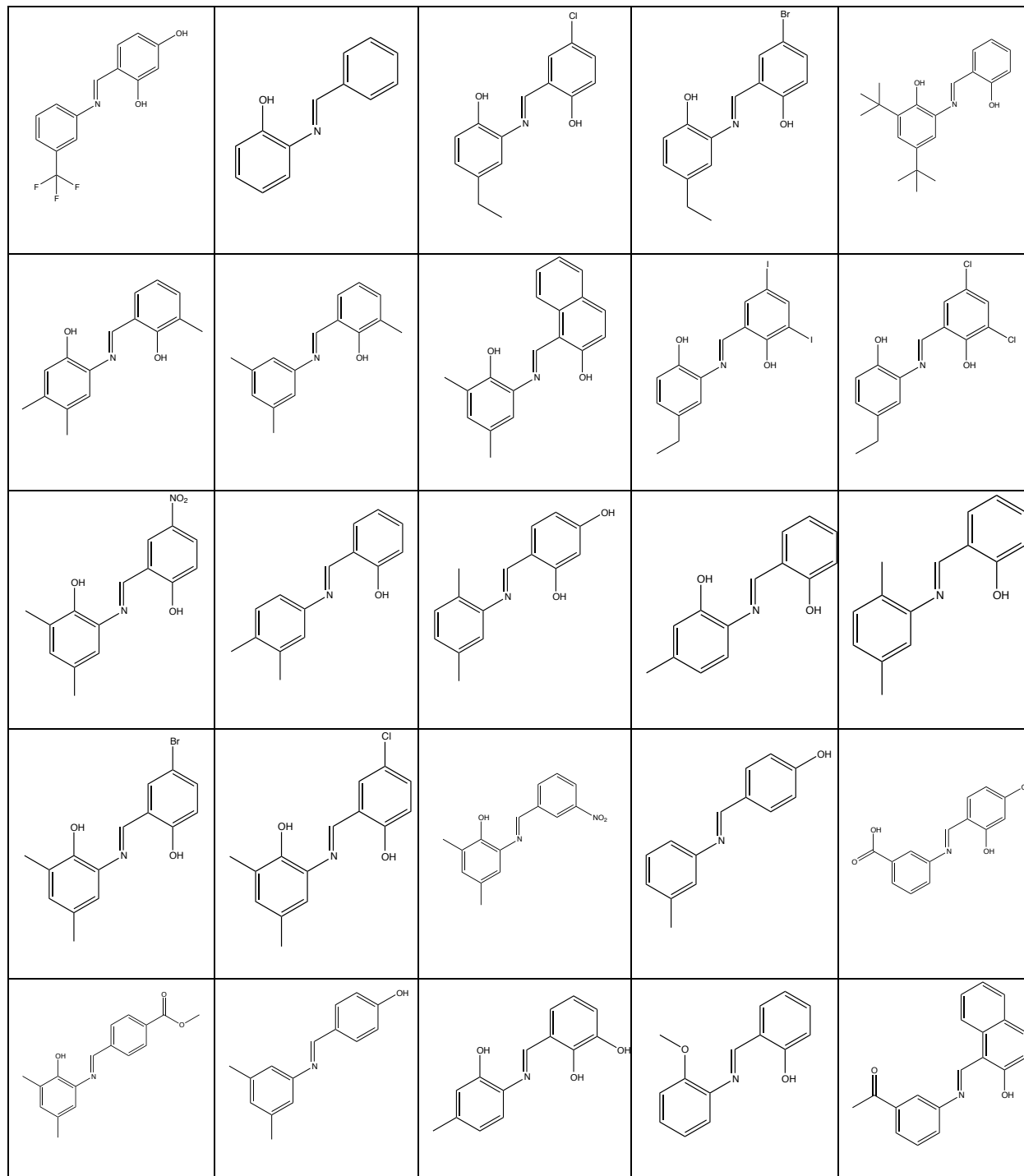


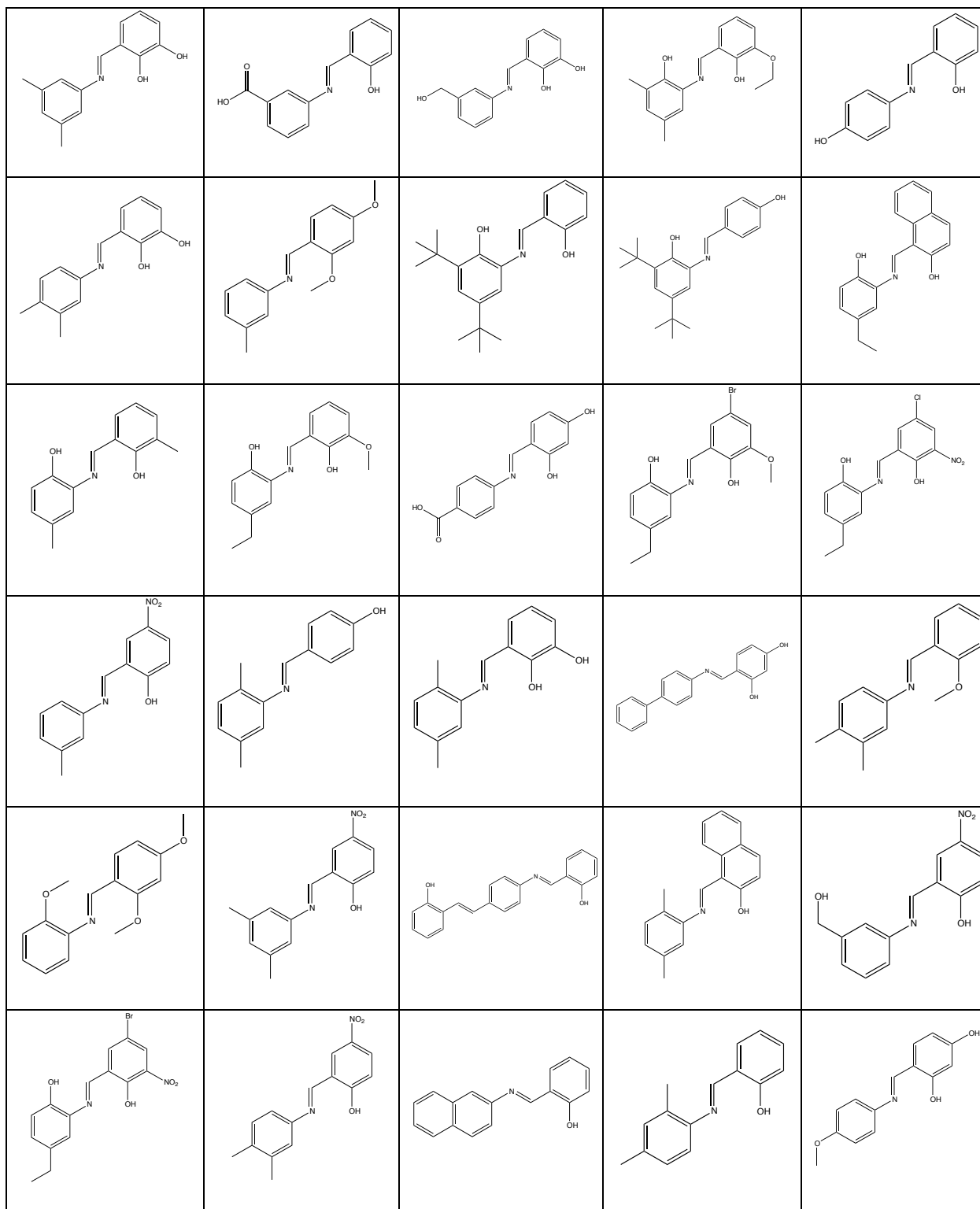


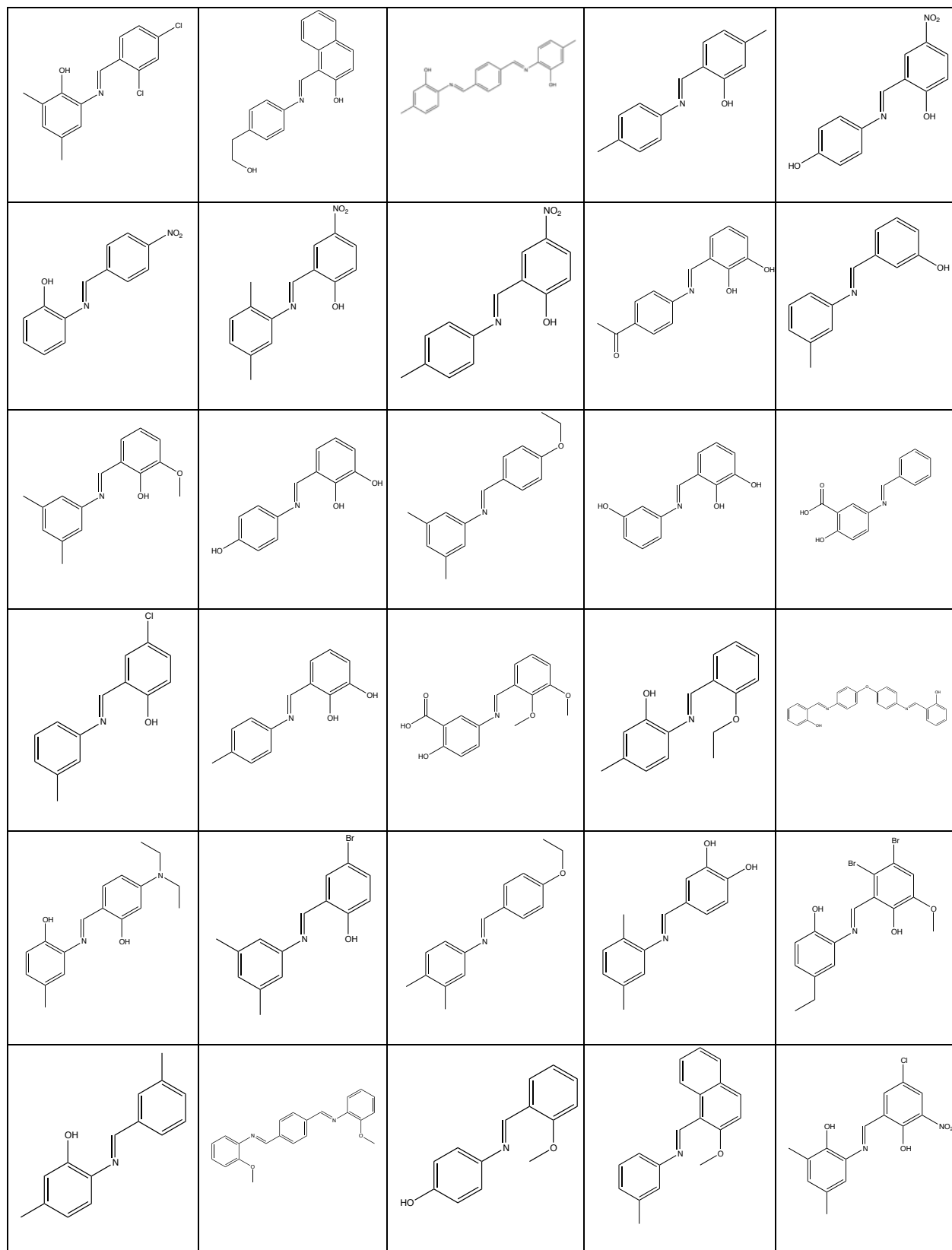


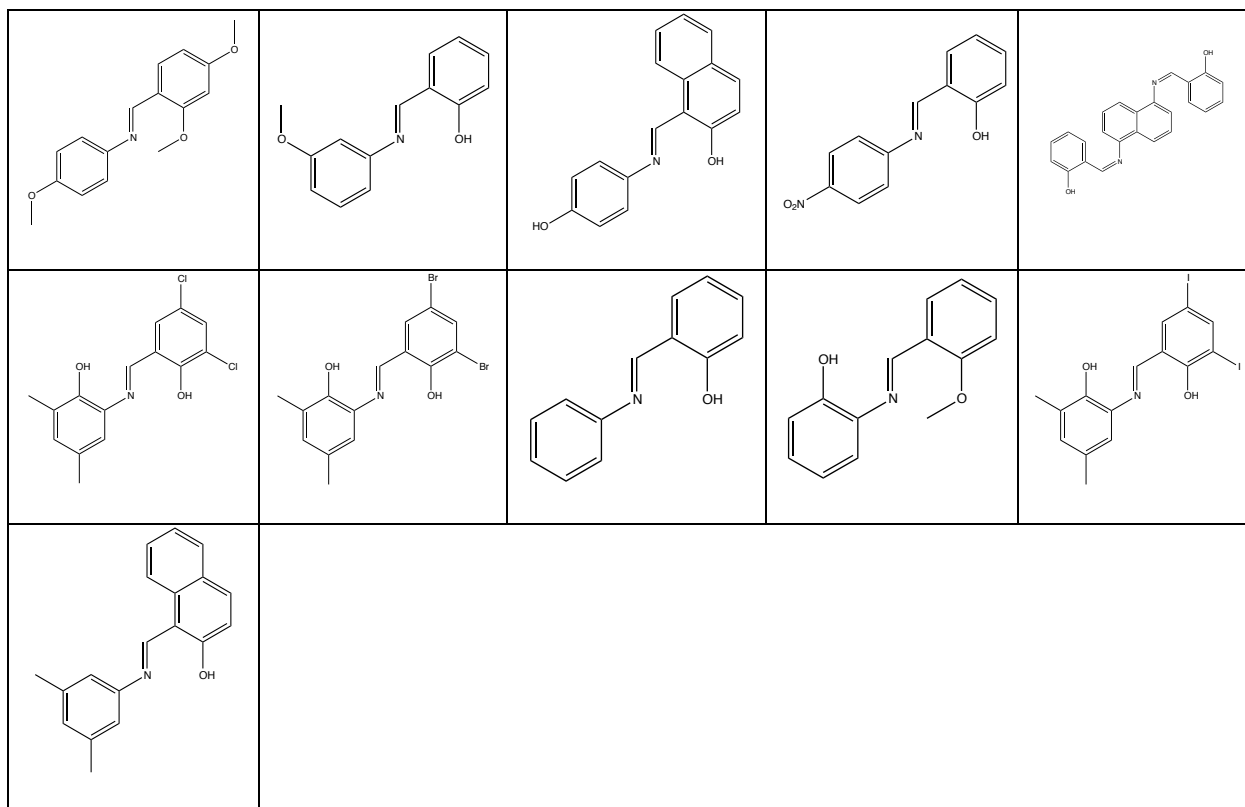


# Appendix B: Data Mined Negative SARS For MitoBloCK-50

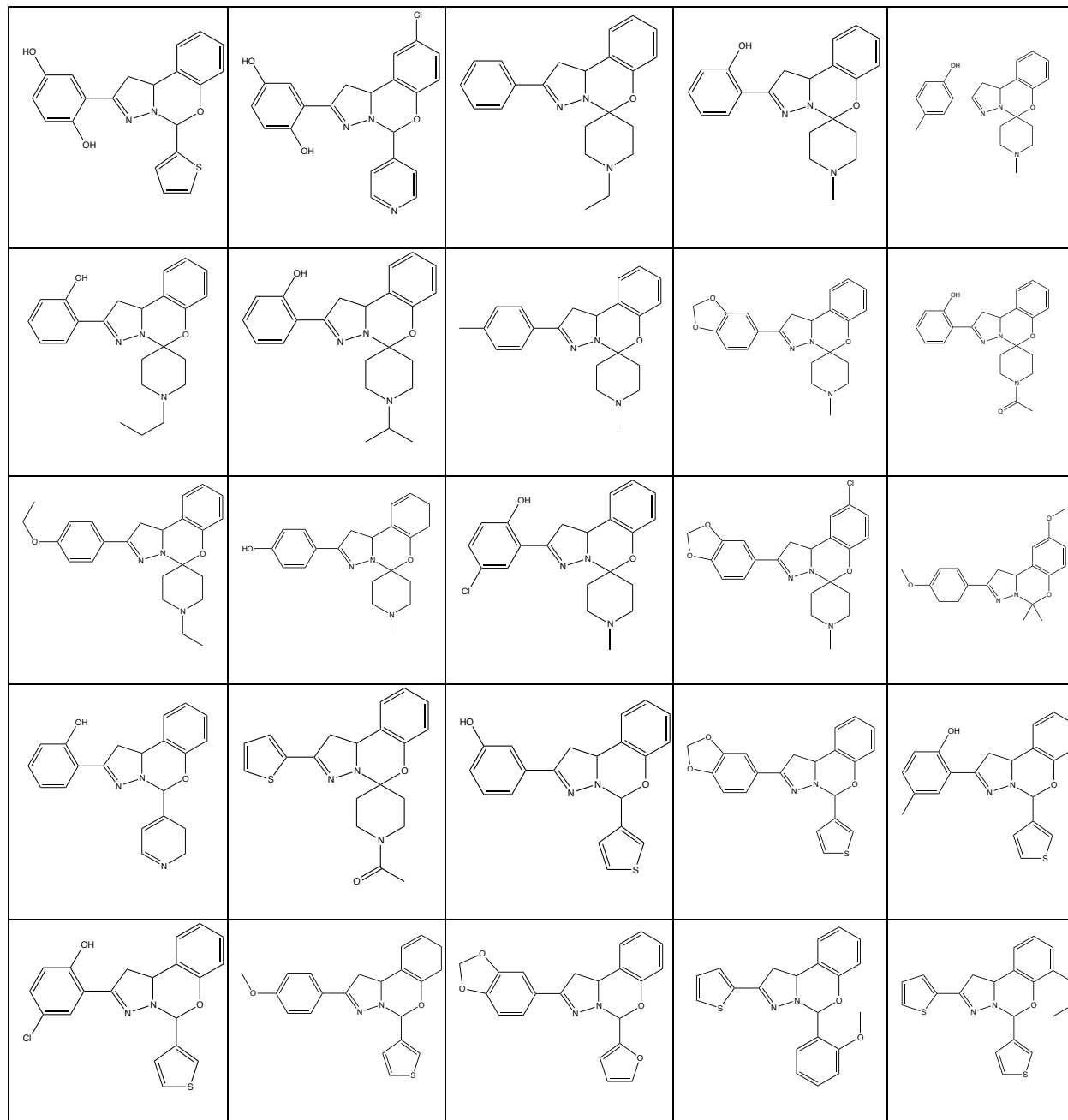


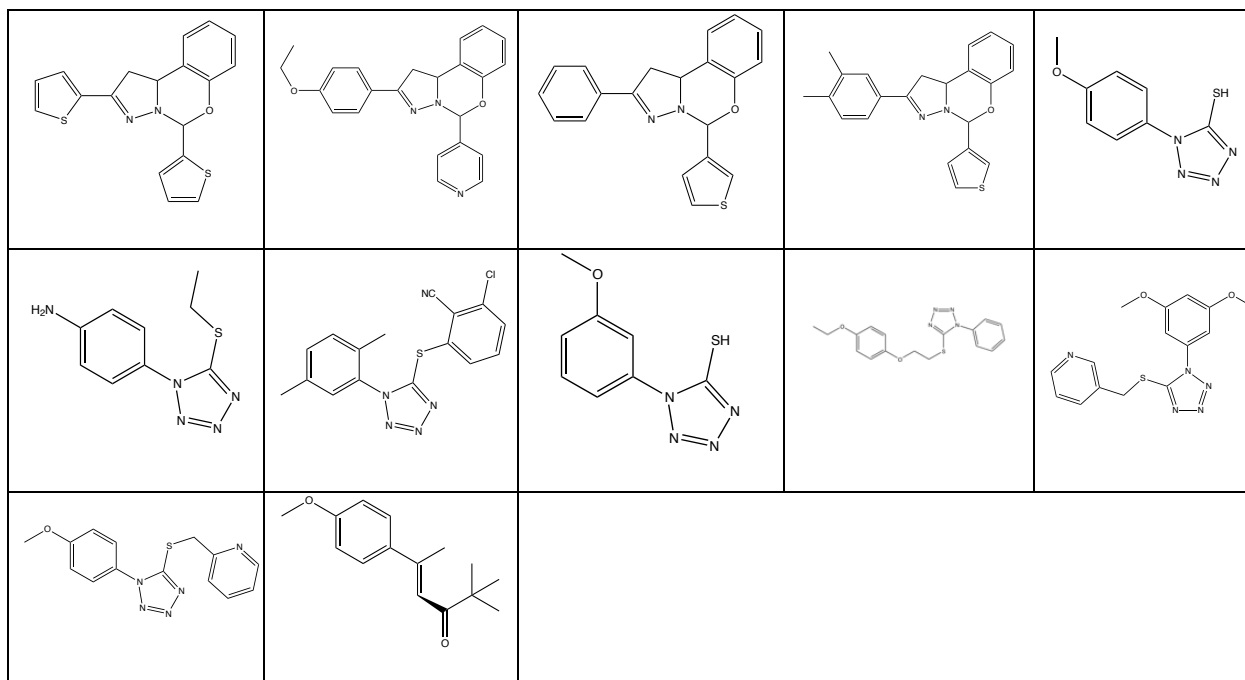




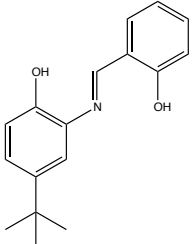
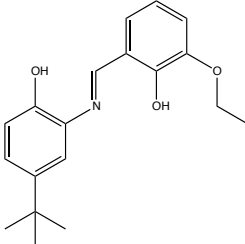
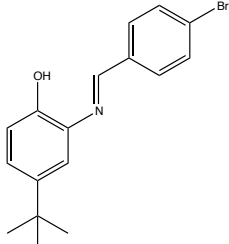
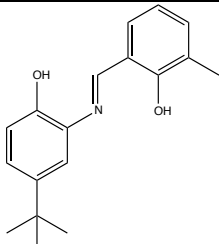
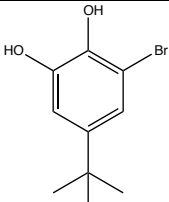


# Appendix C: Data Mined Negative SARS For MitoBloCK-51

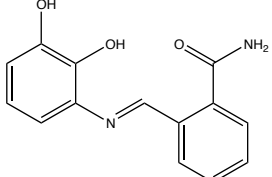
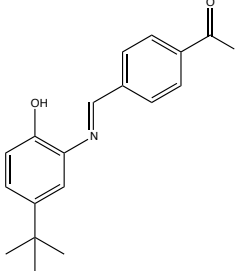
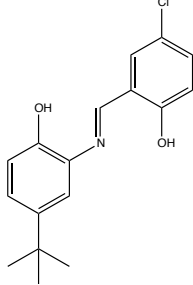
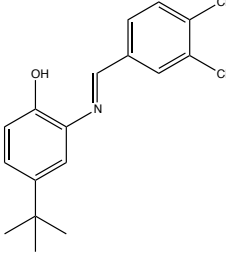
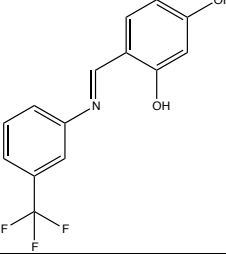
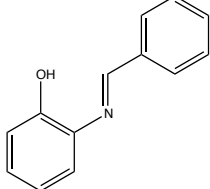


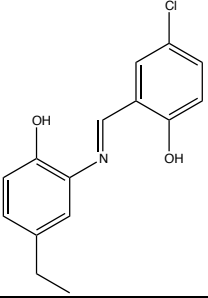


## Appendix D: MB 50 Nomenclature for Published Data

Thesis Name	Published Nomenclature	Structure
MB 50	MitoBloCK-50.1	
238	MitoBloCK-50.2	
051	MitoBloCK-50.3	
067	MitoBloCK-50.4	
515	MitoBloCK-50.5	

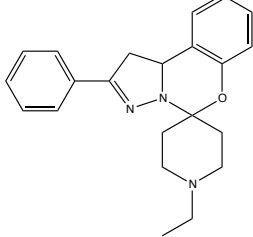
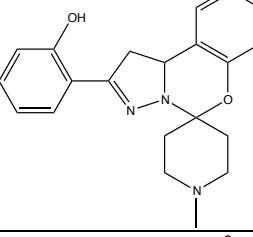


340	MitoBloCK-50.6	
700	MitoBloCK-50.7	
993	MitoBloCK-50.8	
930	MitoBloCK-50.9	
013	MitoBloCK-50n-1	
302	MitoBloCK-50n-2	

247	MitoBloCK-50n-3	 <p>The chemical structure of MitoBloCK-50n-3 is a bisphenol derivative. It consists of two phenolic rings connected by a central imine bridge (-N=CH-). The left phenolic ring is substituted with a hydroxyl group (-OH) at the 3-position and an ethyl group (-CH<sub>2</sub>CH<sub>3</sub>) at the 4-position. The right phenolic ring is substituted with a hydroxyl group (-OH) at the 3-position and a chlorine atom (-Cl) at the 4-position.</p>
-----	-----------------	---

## Appendix E: MB 51 Nomenclature for Published Data

Thesis Name	Published Nomenclature	Structure
MB 51	MitoBloCK-51.1	
325	MitoBloCK-51.2	
184	MitoBloCK-51.3	
172	MitoBloCK-51.4	
321	MitoBloCK-51.5	
329	MitoBloCK-51.6	

001	MitoBloCK-51n-1	
082	MitoBloCK-51n-2	
102	MitoBloCK-51n-3	